U.S. Department
of Commerce

Volume 115
Number 4
October 2017

Fishery Bulletin

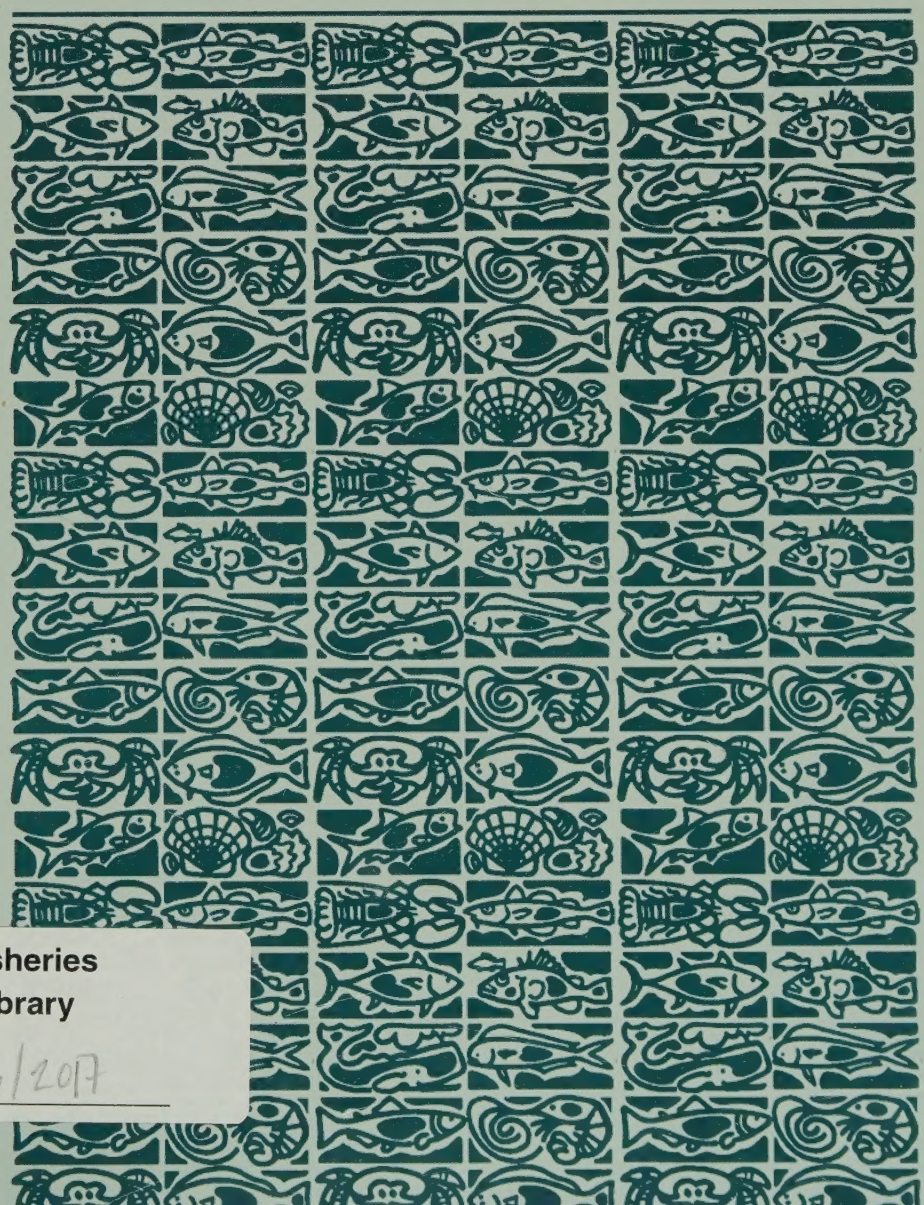

Pacific Islands Fisheries
Science Center Library

Received on: 11/6/2017

U.S. Department of Commerce

Wilbur Ross
Secretary

National Oceanic and Atmospheric Administration

Benjamin Friedman
Acting NOAA Administrator

National Marine Fisheries Service

Chris Oliver
Assistant Administrator
for Fisheries

The *Fishery Bulletin* (ISSN 0090-0656) is published quarterly by the Scientific Publications Office, National Marine Fisheries Service, NOAA, 7600 Sand Point Way NE, Seattle, WA 98115-0070.

Although the contents of this publication have not been copyrighted and may be reprinted entirely, reference to source is appreciated.

The Secretary of Commerce has determined that the publication of this periodical is necessary according to law for the transaction of public business of this Department. Use of funds for printing of this periodical has been approved by the Director of the Office of Management and Budget.

For Sale by the Superintendent of Documents, U.S. Government Printing Office, Washington, DC 20402. Subscription price per year: $32.00 domestic and $44.80 foreign. Cost per single issue: $19.00 domestic and $26.60 foreign. **See back for order form.**

Fishery Bulletin

Scientific Editor
Richard Langton

National Marine Fisheries Service
Northeast Fisheries Science Center
Maine Field Station
17 Godfrey Drive, Suite 1
Orono, ME 04473

Managing Editor
Sharyn Matriotti

National Marine Fisheries Service
Scientific Publications Office
7600 Sand Point Way NE
Seattle, Washington 98115-0070

Associate Editor
Kathryn Dennis

National Marine Fisheries Service
Office of Science and Technology
1845 Wasp Blvd., Bldg. 176
Honolulu, Hawaii 96818

Editorial Committee

Richard Brodeur	National Marine Fisheries Service, Newport, Oregon
John Carlson	National Marine Fisheries Service, Panama City, Florida
Kevin Craig	National Marine Fisheries Service, Beaufort, North Carolina
John Graves	Virginia Institute of Marine Science, Gloucester Point, Virginia
Rich McBride	National Marine Fisheries Service, Woods Hole, Massachusetts
Rick Methot	National Marine Fisheries Service, Seattle, Washington
Bruce Mundy	National Marine Fisheries Service, Honolulu, Hawaii
David Sampson	Oregon State University, Newport, Oregon
Michael Simpkins	National Marine Fisheries Service, Woods Hole, Massachusetts
Dave Somerton	National Marine Fisheries Service, Seattle, Washington
Mary Yoklavich	National Marine Fisheries Service, Santa Cruz, California

***Fishery Bulletin* web site: www.fisherybulletin.noaa.gov**

The *Fishery Bulletin* carries original research reports on investigations in fishery science, engineering, and economics. It began as the Bulletin of the United States Fish Commission in 1881; it became the Bulletin of the Bureau of Fisheries in 1904 and the *Fishery Bulletin* of the Fish and Wildlife Service in 1941. Separates were issued as documents through volume 46; the last document was no. 1103. Beginning with volume 47 in 1931 and continuing through volume 62 in 1963, each separate appeared as a numbered bulletin. A new system began in 1963 with volume 63 in which papers are bound together in a single issue. Beginning with volume 70, number 1, January 1972, *Fishery Bulletin* became a periodical, issued quarterly. In this form, it is available by subscription from the Superintendent of Documents, U.S. Government Printing Office, Washington, DC 20402. It is also available free in limited numbers to libraries, research institutions, state and federal agencies, and in exchange for other scientific publications.

U.S. Department of Commerce
Seattle, Washington

Volume 115
Number 4
October 2017

Fishery Bulletin

Contents

Articles

437–450 **Harvey J. Walsh and Vince G. Guida**

Spring occurrence of fish and macro-invertebrate assemblages near designated wind energy areas on the northeast U.S. continental shelf

451–459 **Adriana Gonzalez-Pestana, Nicolas Acuña-Perales, Javier Coasaca-Cespedes, Francisco Cordova-Zavaleta, Joanna Alfaro-Shigueto, Jeffrey C. Mangel, and Pepe Espinoza**

Trophic ecology of the smooth hammerhead shark (*Sphyrna zygaena*) off the coast of northern Peru

460–472 **David A. Dippold, Robert T. Leaf, James S. Franks, and J. Read Hendon**

Growth, mortality, and movement of cobia (*Rachycentron canadum*)

473–483 **Lisa J. Natanson, Camilla T. McCandless, Kelsey James, and John Hoey**

Gestation period and pupping seasonality of female spiny dogfish (*Squalus acanthias*) off southern New England

484–495 **Serge Aucoin, Steve Weege, Max Toebe, Jeff Guertin, Jonathan Gorham, and Michael Bresette**

A new underwater shark capture method used by divers to catch and release nurse sharks (*Ginglymostoma cirratum*)

Short contribution

496–503 **Paul G. von Szalay and David A. Somerton**

A method for predicting trawlability in the Gulf of Alaska with the use of calibrated, split-beam, echosounder backscatter

The National Marine Fisheries Service (NMFS) does not approve, recommend, or endorse any proprietary product or proprietary material mentioned in this publication. No reference shall be made to NMFS, or to this publication furnished by NMFS, in any advertising or sales promotion which would indicate or imply that NMFS approves, recommends, or endorses any proprietary product or proprietary material mentioned herein, or which has as its purpose an intent to cause directly or indirectly the advertised product to be used or purchased because of this NMFS publication.

The NMFS Scientific Publications Office is not responsible for the contents of the articles.

Articles

504–516 **Rebecca Peters and Paulinus Chigbu**

Spatial and temporal patterns of abundance of juvenile black sea bass (*Centropristis striata*) in Maryland coastal bays

517–531 **Jana M. del Favero, Mario Katsuragawa, Fabricio S. C. Oliveira, Nayara C. Tannure, M. L. Zani-Teixeira, and Jefferson T. Turner**

Seasonal and regional variation in egg size of the Argentine anchoita (*Engraulis anchoita*) in the southeastern Brazilian Bight

532–543 **Nicholas M. Whitney, Connor F. White, Paul A. Anderson, Robert E. Hueter, and Gregory B. Skomal**

The physiological stress response, postrelease behavior, and mortality of blacktip sharks (*Carcharhinus limbatus*) caught on circle and J-hooks in the Florida recreational fishery

544–555 **Anna N. Kagley, Joseph M. Smith, Kurt L. Fresh, Kinsey E. Frick, and Thomas P. Quinn**

Residency, partial migration, and late egress of subadult Chinook salmon (*Oncorhynchus tshawytscha*) and coho salmon (*O. kisutch*) in Puget Sound, Washington

Short contribution

556–565 **Michael P. Torre, Danielle M. Lifavi, and Timothy E. Targett**

Diel differences in abundance and diversity of fish species and blue crab (*Callinectes sapidus*) in the sandy beach shore zone of lower Delaware Bay

Article

566–575 **Christopher Magel, Clifford Ryer, and Richard Brill**

Recovery of visual function in Pacific halibut (*Hippoglossus stenolepis*) after exposure to bright light

Acknowledgment of reviewers

Guidelines for authors

National Marine Fisheries Service
NOAA

Fishery Bulletin
established in 1881

Spencer F. Baird
First U.S. Commissioner of Fisheries and founder of *Fishery Bulletin*

Spring occurrence of fish and macro-invertebrate assemblages near designated wind energy areas on the northeast U.S. continental shelf

Harvey J. Walsh (contact author)[1]
Vince G. Guida[2]

Email address for contact author: harvey.walsh@noaa.gov

[1] Northeast Fisheries Science Center
National Marine Fisheries Service, NOAA
28 Tarzwell Drive
Narragansett, Rhode Island 02882

[2] Northeast Fisheries Science Center
National Marine Fisheries Service, NOAA
74 Magruder Road
Highlands, New Jersey 07732

Abstract—Fish and macro-invertebrate assemblages were examined in the vicinity of 5 wind energy areas on the northeast U.S. continental shelf by using 2 sampling gears. Collections of fish and macro-invertebrates during the spring of 2014 with a 2-m beam trawl and a standard bottom trawl were compared. Correspondence analysis of proportions of taxa in the catch at sampling stations and estimated individual weights, averaged by taxon, were used to describe the composition of assemblages, and composition of the catch was compared between collections made with the 2 different gears and among different wind energy areas. These comparisons indicated that the 2 gears collected different fish and macro-invertebrate communities. Analysis of the collections by gear type indicated that assemblages varied across several spatial scales. Canonical correspondence analysis was used to examine the relationship between assemblages, sampling programs, and environmental variables to determine which variables and Correspondence analysis dimensions were aligned with stations and were related to the assemblages. Environmental variables explained 20.5% of the variation for the beam trawl stations and assemblages and 28.8% of variation for the bottom trawl stations and assemblages. Our results indicate that assessments of wind energy areas on the northeast U.S. shelf should be conducted by using multiple gear types across multiple spatial and temporal scales.

Manuscript submitted 7 March 2016.
Manuscript accepted 29 June 2017.
Fish. Bull. 115:437–450 (2017).
Online publication date: 26 July 2017.
doi: 10.7755/FB.115.4.1.

The views and opinions expressed or implied in this article are those of the author (or authors) and do not necessarily reflect the position of the National Marine Fisheries Service, NOAA.

Offshore wind farms have been gaining increased interest as a potential source of renewable energy (Wilson et al., 2010; Tabassum-Abbasi et al., 2014). The Bureau of Ocean Energy Management (BOEM) has designated 8 wind energy areas (WEAs) on the northeast U.S. continental shelf between North Carolina and Massachusetts (Bailey et al., 2014). These wind energy areas comprise lease blocks that will be made available for commercial leases and limited research leases (BOEM[1]). Commercial leases allow the leaseholder to ask BOEM for the right to develop wind energy production facilities on the leasehold and undertake a 4-step process of planning and analysis, lease issuance, site assessment, and construction and operations. Limited research leases allow the leaseholder to conduct technological testing and gather data for 5 years. Assessing the environmental impact of offshore wind production is part of the permitting process and is led by BOEM (Federal Register, 2014).

Assessment of the impacts of the location, construction, and energy production of offshore wind farms on fish and macro-invertebrates on the northeast U.S. shelf is in the early stages. However, European countries have been conducting environmental assessments since the early 1990s that have resulted in review articles on the general impacts of, and long-term research needs for, offshore wind farms (Wilson et al., 2010; Lindeboom et al., 2011; Bailey et al., 2014; Bergstrom et al., 2014; Dai et al., 2015; Lindeboom et al., 2015). The reviews have generally concluded there are potentially minor to moderate effects on fish and macro-invertebrate communities. These effects may result from increased anthropogenic noise and electromagnetic fields, increased turbidity, loss or degradation of existing bottom habitats, gains in hard bottom and structural habitats, and the limitation or exclusion of fisheries (Wilson et al., 2010; Bergstrom et al., 2014; Dai et al., 2015;

[1] BOEM (Bureau of Ocean Energy Management). 2017. Renewable energy on the Outer Continental Shelf, 1 p. [Fact sheet; available from website.]

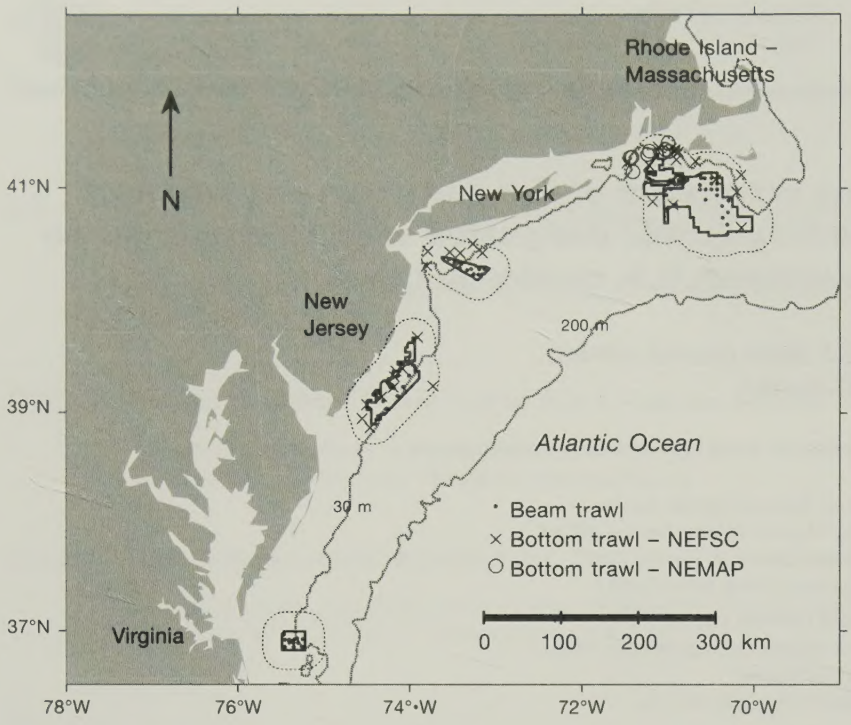

Figure 1

Map of the northeast U.S. continental shelf showing 5 wind energy areas (WEAs) off Virginia, New Jersey, New York, Rhode Island, and Massachusetts where sampling of fish and macro-invertebrates was conducted in the spring of 2014. The Rhode Island–Massachusetts and Massachusetts WEAs were combined because of their close proximity to one another. Collections were made with a beam trawl within lease blocks of each WEA (solid black lines), and collections made with a bottom trawl were selected from inside a 20-km buffer around each WEA (dashed black lines) on the basis of data from surveys conducted by the Northeast Fisheries Science Center (NEFSC) and Northeast Monitoring and Assessment Program (NEAMAP). The 30-m and 200-m isobaths also are shown (dotted black lines).

Lindeboom et al., 2015). These effects all have the potential to modify community structure, including changes in species composition, diversity, and productivity (Bergstrom et al., 2014; Lindeboom et al., 2015).

The reviews highlight the need for before, during, and after construction monitoring to examine ecosystem level effects and the need to continue to track effects over the long term (Lindeboom et al., 2011; Lindenboom et al., 2015). Recommendations also include the use of multiple gear types to examine the entire ecosystem (Wilson et al., 2010), the examination of population-level effects (Bergstrom et al., 2014; Lindeboom et al., 2015), and the implementation of sampling across large spatial scales (Dai et al., 2015; Lindeboom et al., 2015).

Annual trawl surveys of the northeast U.S. shelf by the Northeast Fisheries Science Center (NEFSC), with the use of standardized bottom trawl gear (ICES[2]; Politis et al.[3]) designed to catch juvenile and adult demersal and semipelagic species, provide broad-scale and long-term distribution and abundance patterns of numerous fish and macro-invertebrates (Gabriel, 1992; Lucey and Nye, 2010). However, assessments of smaller noncommercial organisms and prerecruitment stages of fish and macro-invertebrates with the use of smaller research gear, which have smaller mesh sizes for retaining smaller (younger) juveniles, have been conducted only on limited spatial and temporal scales (Steves et al., 1999; Steves and Cowen, 2000; Sullivan et al., 2000; Diaz et al., 2003). The objective for our study was to examine the fish and macro-invertebrate assemblages in the vicinity of BOEM WEAs on the northeast U.S. shelf by comparing the composition of collections made with small-mesh gear and the standardized bottom trawl gear that are routinely used in the 2 long-term annual fish and macro-invertebrate bottom trawl surveys conducted under the NEFSC (Azarovitz, 1981) and Northeast Area Monitoring and Assessment Program (NEAMAP) (Bonzek et al.[4]). Specifically, we examined the proportion of a taxon in catch per station and average weight of individuals collected with 2 types of trawl gear: a 2-m beam trawl and a 4-seam, 3-bridle survey trawl (Bonzek et al.[4]; Politis et al.[3]). We also describe the relationships between the fish and macro-invertebrate assemblages and the explanatory environmental variables.

Materials and methods

Collection of data

Sampling was conducted in the vicinity of 5 WEAs on the northeast U.S. shelf during the spring of 2014 (Fig. 1). Collections were made at night with a 2-m beam

[2] ICES (International Council for the Exploration of the Sea). 2005. Report of the study group on survey trawl standardisation (SGSTS), 16–18 April 2005, Rome, Italy. ICES CM 2005/B:02, 67 p, [Available from website.]

[3] Politis, P. J., J. K. Galbraith, P. Kostovick, and R. W. Brown. 2014. Northeast Fisheries Science Center bottom trawl survey protocols for the NOAA Ship *Henry B. Bigelow*. Northeast Fish. Sci. Cent. Ref. Doc, 14-06, 138 p. [Available from website.]

[4] Bonzek, C. F., J. Gartland, D. J. Gauthier, and R. J. Latour. 2012. Data collection and analysis in support of single and multispecies stock assessments in the Mid-Atlantic: Northeast Area Monitoring and Assessment Program Near Shore Trawl Survey (NEAMAP), 280 p. [Avaliable from website.]

trawl (Kuipers, 1975) with a 0.63-cm-mesh net from 11 March to 12 April 2014. This sampling was restricted to the time of night because the research vessel was used to conduct visual transect surveys of marine mammals and precluded any fishing during daylight hours. Bottom trawl collections were made with a 4-seam, 3-bridle otter trawl net with a dimension of 400×12 cm and with a 2.5-cm-mesh liner (Bonzek et al.[4]; Politis et al.[3]). The nets used by NEFSC and NEAMAP for bottom trawl surveys are not identical, and differences include the sweeps, headline floats, number of both top and belly panels, and the mesh size of some panels (Bonzek et al.[4]; Politis et al.[3]). Samples were collected both day and night from 2 to 20 April 2014 during the NEFSC survey and during the day from 7 to 20 May 2014 during the NEAMAP survey.

Samples were collected with the beam trawl within the BOEM-designated lease blocks of 5 WEAs: Virginia (VA, n=12); New Jersey (NJ, n=13); New York (NY, n=10); Rhode Island–Massachusetts (RIMA); and Massachusetts (MA). Data from 2 BOEM WEAs, RIMA and MA, were combined into a single WEA (RIMA–MA, n=23) because of their close proximity to one another (Fig. 1). Lease blocks were chosen haphazardly to best coincide with visual transect surveys of marine mammals that occurred during daylight hours, and preference was given to those lease blocks that had been sampled during previous surveys with various gears. Both the NEFSC and NEAMAP surveys use a stratified random sampling design. Therefore, samples from within a 20-km buffer around each WEA with the same depth range as that of beam trawl stations (20–60 m) were used for comparison with beam trawl collections. This procedure resulted in bottom trawl samples being available for 3 WEAs: NJ (n=10); NY (n=6); and RIMA–MA (n=23). Unfortunately, no bottom trawl samples were available for comparison with the VA WEA because of a lack of sampling during the NEFSC survey and because the WEA was deeper than the NEAMAP survey area.

Trawl samples were processed on board, and processing was similar for the surveys at the NJ, NY, and RIMA–MA WEAs. Samples were sorted to the lowest practicable taxon, which varied by survey (Suppl. Table). We compared taxa sampled with the beam trawl with taxa sampled with the bottom trawl (Table 1) and found that shrimp were identified to lower taxonomic levels in the beam trawl collections (e.g., caridean shrimp and the white shrimp, *Penaeus setiferus*; Suppl. Table) (online only) than in NEFSC bottom trawl collections (e.g., unclassified shrimp; Suppl. Table) (online only). These finer taxonomic levels combined for the comparisons by gear type, and those comparisons were made at the highest level of identification (e.g., unclassified shrimp). The total numbers and aggregate weights (measured in kilograms) were available for each taxon and each station. Percent frequency of occurrence was calculated for each taxon, by gear type. The proportion of a taxon in the catch at a sampling station was calculated by dividing the aggregate weight of a taxon by the total weight of all taxa captured at a station. The estimated average individual weight for each taxon (measured in grams) was calculated by dividing the total weight (measured in grams) by the total count for each taxon.

Environmental and habitat sampling was conducted concurrently with trawl sampling. Water temperature and salinity were measured at each trawl station by using either a Sea-Bird Scientific[5] SBE 19 SeaCAT conductivity, temperature, and depth profiler (Sea-Bird Scientific, Bellevue, WA) or Hydrolab MS5 sonde (OTT Hydromet, Kempten, Germany). Bottom water temperature (measured in degrees Celsius) and salinity measurements were taken within 5 m of the bottom. Sediment samples were collected at beam trawl stations by using a 0.04-m^2 or 0.10-m^2 Young-modified Van Veen grab sampler. The Folk (1954) sediment classification system was used to classify beam trawl station sediments into the following categories: 1=muddy sand; 2=sand; 3=sand–slightly gravelly sand; 4=slightly gravelly sand; 5=slightly gravelly sand–gravelly sand; 6=gravelly sand; 7=gravelly sand–sandy gravel.

Statistical analyses

Several statistical analyses were undertaken in order to compare catches across gear types and across WEAs. Correspondence analysis (CA) was used to compare the fish and macro-invertebrate assemblages in relation to gear type and WEA and canonical correspondence analysis (CCA) was used to examine the relationship between assemblages and sampling program and environmental variables. A Student's t-test was used to examine whether the beam and bottom trawls collected individuals of significantly different sizes.

The software package "FactoMineR" (Le et al., 2008) in R, vers. 3.2.2 (R Core Team, 2015) was used to perform CA on average proportions and individual weights by a taxon per station to describe proportion of fish and macro-invertebrates and individual size, by station. We conducted 3 analyses: beam and bottom trawl collections combined; beam trawl only collections; and bottom trawl only collections. Beam and bottom trawl stations were analyzed together to examine differences among the collections, by gear type. Assemblage composition in relation to WEA was examined by analyzing beam trawl and bottom trawl samples separately. The inclusion of rare taxa in CA and CCA often leads to assemblage patterns similar to those in data where rare taxa have been removed (Marancik et al., 2005; Walsh et al. 2006) and rare taxa often increase species richness of some assemblages (Marancik et al., 2005) or appear as outliers separate from larger assemblages (Walsh et al., 2006). To simplify our analyses, however, only taxa that had at least a 10% frequency of occurrence were used in the analyses. Percent frequency of occurrence was based on all stations sampled for the

[5] Mention of trade names or commercial companies is for identification purposes only and does not imply endorsement by the National Marine Fisheries Service, NOAA.

Table 1

Percent frequency of occurrence (PFO) and percent contribution of average proportions and average individual weights per station to the first 2 dimensions of correspondence analysis (CA1 and CA2) for fish and macroinvertebrate taxa that had at least a 10% frequency of occurrence in beam trawl and bottom trawl samples collected in the vicinity of wind energy areas on the northeast U.S. continental shelf in the spring of 2014. The *t*-statistics, *P*-values, and degrees of freedom (df) are reported for Student's *t*-tests conducted for 11 taxa that had at least 5% frequency of occurrence in collections made with both gear types. Sizes of individuals sampled were significantly different for the collections made with the 2 gear types (*P*-values≤0.0045). For the ordination plot of the analysis, see Figure 3.

			Percent contribution of CA1 and CA2		Student's *t*-test		
Classification	Taxon	PFO	Average proportion of taxon per station	Average individual weight per station	*P*-value	*t*-statistic	df
Mollusca	*Placopecten magellanicus*	23.5	1.2	0.3	0.2025	−1.28	83
	Decapodiformes	27.1	0.1	0.1			
Crustacea	Unclassified shrimp	20.0	83.4	0.0	0.1502	−1.45	83
	Homarus americanus	15.3	0.7	0.4			
	Brachyura	47.1	1.1	4.2	0.0404	−2.08	83
Pelagic fish	*Alosa* spp.	30.6	1.1	0.6			
	Clupea harengus	43.5	0.5	0.3			
	Merluccius bilinearis	56.5	1.7	0.2	0.0003	−3.74	83
Demersal fish	*Squalus acanthias*	61.2	9.1	56.8			
	Leucoraja spp.	70.6	6.2	2.1	<0.0001	−6.74	83
	Melanogrammus aeglefinus	14.1	0.7	0.5			
	Urophycis chuss	47.1	2.2	1.2	0.0001	−4.02	83
	Urophycis regia	23.5	0.5	0.8	0.0468	−2.02	83
	Prionotus spp.	27.1	0.0	1.6			
	Myoxocephalus octodecemspinosus	25.9	0.7	3.7	<0.0001	−5.79	83
	Centropristis striata	14.1	0.6	2.0			
	Zoarces americanus	21.2	0.5	4.8	0.0001	−4.14	83
	Ammodytes spp.	10.6	0.6	0.2			
	Scophthalmus aquosus	45.9	0.4	0.6	<0.0001	−7.46	83
	Etropus spp.	38.8	2.2	0.0	0.2847	−1.08	83
	Paralichthys oblongus	11.8	0.1	0.5			
	Paralichthys dentatus	24.7	0.1	1.3			
	Limanda ferruginea	12.9	0.2	1.7			
	Pseudopleuronectes americanus	34.1	0.5	1.9			

combined beam and bottom trawl analyses (Table 1). When the collections made with each gear type were analyzed separately, the percent frequency of occurrence was calculated on the basis of stations sampled with an individual gear (Tables 2 and 3). Therefore, the total number and composition of the taxa used differed in the 3 analyses: comparison by gear type (n=24; Table 1); comparison by WEA of collections made with the beam trawl (n=28; Table 2); and comparison by WEA of collections made with a bottom trawl (n=28; Table 3). Taxa that contributed significantly to the beam trawl (>1%) and bottom trawl (>3%) ordinations were used to describe the different communities that were collected, and the percentage contribution of these taxa to the ordination, which varied by analysis, allowed a clear graphic representation of their relationships.

The R package "vegan" (Oksanen et al., 2015) was used to perform CCA on average proportion of taxa per station, estimated average individual weights for each taxon per station, and 6 explanatory variables for the 2 types of WEA sampling: beam trawl only and bottom trawl only. Both categorical variables (sediment [1 to 7], light [day or night]), and continuous (latitude, longitude, depth, bottom water temperature and salinity) explanatory variables were used, and they differed for each analysis. Continuous variables were standardized to a mean of zero and a standard deviation of one. For the beam trawl analysis, latitude, longitude, depth, sediment, bottom water temperature, and salinity were the categorical variables used. Light was not examined for beam trawl catches because all sampling was done during hours of darkness. For the bottom trawl analysis, latitude, longitude, depth, light, bottom water temperature, and salinity were used. Day-of-year was used in both analyses as a covariable to compensate for seasonality in sample collections. Program (NEFSC or NEAMAP),

Table 2

Percent frequency of occurrence (PFO) and percent contribution of average proportions and average individual weights per station to the first 2 dimensions of correspondence analysis (CA1 and CA2) for fish and macroinvertebrate taxa that had at least a 10% frequency of occurrence in beam trawl samples collected in the vicinity of wind energy areas on the northeast U.S. continental shelf in the spring of 2014. For the ordination plot of the analysis, see Figure 4.

			Percent contribution of CA1 and CA2	
Classification	Taxon	PFO	Average proportion of taxon per station	Average individual weight per station
Porifera	Porifera	19.0	52.1926	
Ctenophora	Ctenophora	19.0	0.2471	
Polychaeta	Polychaeta	13.8	0.1387	0.0804
Mollusca	Gastropoda	55.2	2.4551	0.0425
	Pleurobranchomorpha	70.7	2.2524	0.0036
	Bivalvia	39.7	6.5778	0.0838
	Placopecten magellanicus	17.2	0.3847	0.1179
Crustacea	Peracarida	29.3	0.4728	0.0140
	Caridea	100.0	11.1031	0.0049
	Penaeus setiferus	10.3	0.5125	0.0332
	Pagurus spp.	46.6	2.1334	0.0332
	Brachyura	37.9	1.3297	11.8286
Echinodermata	*Echinarachnius parma*	58.6	5.7585	0.0084
	Asteriidae	10.3	0.0967	0.0987
Pelagic fish	*Merluccius bilinearis*	24.1	0.3033	0.0032
Demersal fish	*Leucoraja* spp.	41.4	27.4802	37.5870
	Urophycis chuss	25.9	0.4356	0.0004
	Urophycis regia	32.8	25.7295	0.1852
	Prionotus spp.	24.1	4.6438	0.0342
	Centropristis striata	15.5	0.8081	0.1016
	Ammodytes spp.	25.9	0.0737	0.0147
	Gobiidae	20.7	0.1470	0.0194
	Scophthalmus aquosus	17.2	0.2820	0.6746
	Etropus spp.	60.3	3.4550	0.0174

coded as a categorical variable, was also used as a covariable to compensate for the difference among trawl nets used for the bottom trawl collections. For each analysis, forward selection of the explanatory variables and analysis of variance (R Core Team, 2015) were used to determine which explanatory variables and dimensions were aligned with groups of stations and were related to the fish and macro-invertebrate assemblages.

Eleven taxa had at least a 5% frequency of occurrence in collections made with the 2 types of gears and the average individual weight per station was analyzed with R (R Core Team, 2015) to determine whether the gears caught significantly different sizes for individual weight. A difference in individual weight among collections, by gear type, was considered significant at Bonferroni corrected P-values of ≤ 0.0045.

Results

Beam trawl samples were dominated by a variety of benthic organisms; the top 5 taxa determined on the basis of their average proportion per station were caridean shrimp, common sand dollar (*Echinarachnius parma*), *Leucoraja* spp., poriferan sponges, and bivalves (Suppl. Table) (online only). Demersal and pelagic fish dominated bottom trawl samples; the top 5 were *Leucoraja* spp., spiny dogfish (*Squalus acanthias*), Atlantic herring (*Clupea harengus*), haddock (*Melanogrammus aeglefinus*), and *Peprilus* spp. (Suppl. Table) (online only).

Comparison of assemblages by gear type

The analyses for comparison by gear type indicated that the beam and bottom trawl sampled different fish and macro-invertebrate communities. The beam trawl caught significantly smaller individuals, by weight, than the bottom trawl for 6 of the 11 taxa that were tested (Table 1; Fig. 2). The collection of significantly smaller individuals of 6 fish species, *Leucoraja* spp., silver hake (*Merluccius bilinearis*), longhorn sculpin (*Myoxocephalus octodecemspinosus*), windowpane (*Scophthalmus aquosus*), red hake (*Urophycis chuss*), and ocean pout (*Zoarces americanus*), indicated that the beam trawl was more efficient than the bottom

Table 3

Percent frequency of occurrence (PFO) and percent contribution of average proportions and average individual weights per station to the first 2 dimensions of correspondence analysis (CA1 and CA2) for fish and macroinvertebrate taxa that had at least a 10% frequency of occurrence in bottom trawl samples collected in the vicinity of wind energy areas on the northeast U.S. continental shelf during the spring of 2014. For the ordination plot of the analysis, see Figure 5.

			Percent contribution of CA1 and CA2	
Classification	Taxon	PFO	Average proportion of taxon per station	Average individual weight per station
Mollusca	*Placopecten magellanicus*	28.2	0.0011	0.2433
	Decapodiformes	53.8	0.2941	1.0434
Merostomata	*Limulus polyphemus*	12.8	1.5450	22.7470
Crustacea	Unclassified shrimp	15.4	0.0004	0.0554
	Homarus americanus	33.3	1.6580	0.9347
	Brachyura	74.4	0.6235	1.4495
Pelagic fish	*Alosa* spp.	66.7	3.0492	1.3781
	Clupea harengus	94.9	11.7095	0.6319
	Merluccius bilinearis	89.7	0.5675	0.1974
	Stenotomus chrysops	20.5	3.9466	7.2997
	Scomber scombrus	17.9	0.0001	0.0162
	Peprilus spp.	20.5	2.2370	1.0757
Demersal fish	*Squalus acanthias*	43.6	5.2427	33.3815
	Leucoraja spp.	100.0	19.1962	3.1704
	Melanogrammus aeglefinus	28.2	3.1472	1.5533
	Urophycis chuss	64.1	0.2408	2.9577
	Urophycis regia	33.3	0.2033	3.1282
	Prionotus spp.	53.8	0.0293	2.7215
	Myoxocephalus octodecemspinosus	48.7	1.6763	3.9863
	Hemitripterus americanus	15.4	0.0857	14.4757
	Centropristis striata	30.8	2.1206	9.3053
	Zoarces americanus	33.3	1.3455	5.5046
	Scophthalmus aquosus	74.4	0.7544	1.8307
	Etropus spp.	25.6	0.0028	0.0687
	Paralichthys oblongus	25.6	0.4396	3.5277
	Paralichthys dentatus	53.8	0.3313	8.4038
	Limanda ferruginea	28.2	0.3330	3.0043
	Pseudopleuronectes americanus	74.4	0.9314	4.1960

trawl at collecting juveniles (or younger age classes, <2 years old) for some taxa. Conversely, the lack of collections of other abundant demersal fish (e.g., spiny dogfish; haddock; yellowtail flounder (*Limanda ferruginea*); winter flounder (*Pseudopleuronectes americanus*); and summer flounder (*Paralichthys dentatus*)) and a lack of pelagic fish (e.g., *Alosa* spp.; Atlantic herring; Atlantic mackerel (*Scomber scombrus*); and *Peprilus* spp.), regardless of size, indicate that the bottom trawl was more efficient in collecting a number of fish taxa (Suppl. Table) (online only).

The variation in catch composition by gear type indicated that CA assemblage structures separated by gear type. Visualization of the first 2 dimensions of the CA ordination described the overall pattern of assemblages associated with each gear type (Fig. 3). The first 2 dimensions explained 30.8% of the variance in assemblages, with eigenvalues of 0.81 and 0.41 respectively. Taxa that contributed significantly (>1%; Table 1) to the ordination highlight the different communities collected by each gear (Fig. 3). The collections made with the 2 gear types separated from each other along the first dimension (Fig. 3A) and average proportion of taxa per station (90.7%) contributed most to the separation of assemblages (Fig. 3B). The beam trawl was stretched along the first dimension and had higher station proportions of unclassified shrimp, brachyuran crabs, sea scallop (*Placopecten magellanicus*), *Etropus* spp., and red hake. The close association of sea scallop and red hake in ordination space may be related to their inquiline relationship, where benthic juvenile red hake live in the mantle of live sea scallop (Able and Fahay, 1998). The collections made with the bottom trawl appear to the left of the origin and had a higher proportion of *Leucoraja* spp., and the bottom trawl was the only gear to sample *Alosa* spp. and spiny dogfish (Fig. 3B). The second dimension aligned with the WEA location, particularly for the collections made with the

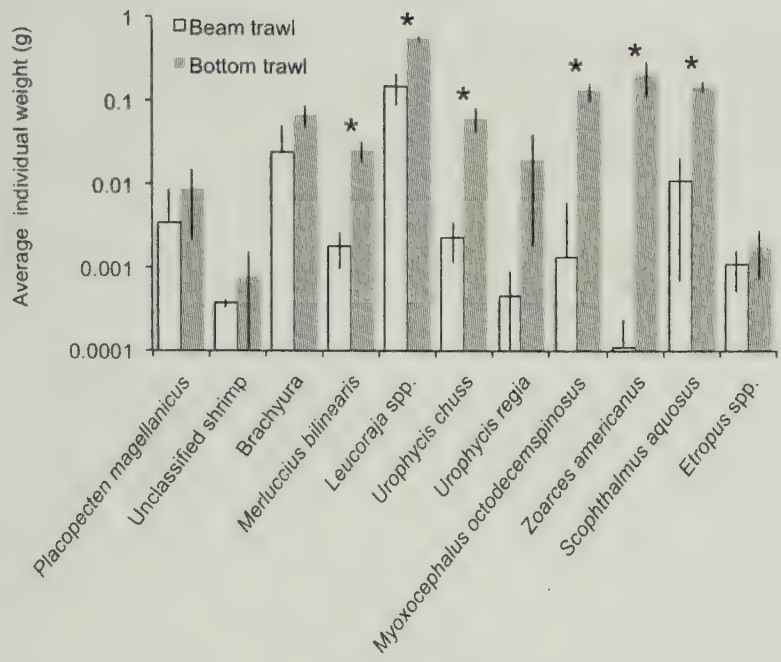

Figure 2

Average individual weight (g) of taxa that had at least a 5% frequency of occurrence in collections made with the beam and bottom trawls on the northeast U.S. continental shelf in 2014. A Student's *t*-test was used to examine whether the sizes of individuals were significantly different between the collections made with the 2 gear types. An asterisk (*) indicates a taxa for which a difference in individual size between collections by gear type was considered significant (Bonferroni corrected *P*-value: ≤0.0045). Error bars indicate standard errors of the means.

bottom trawl (Fig. 3A). Both average proportion of taxa per station (76.6%) and average individual weights by taxon (23.4%) contributed to assemblage variation (Fig. 3, B and C). The beam trawl collected significantly smaller individuals of most taxa, and the bottom trawl stations in the NJ WEA had spiny dogfish with larger average individual weights (Fig. 3C).

Comparison of assemblages by wind energy area

The separate analyses of collections made with each gear type indicated that the fish and macro-invertebrate communities varied across several spatial scales and that assemblage varied among and within WEAs. Four CA dimensions explained at least 50% of the variation in average proportion of a taxon per station and estimated average individual weight of a taxon per station for analyses of both the beam and bottom trawl collections. Again, the first 2 dimensions described the overall pattern of assemblages associated with each gear type (Figs. 4 and 5).

The first 2 dimensions of the CA for the beam trawl described 30.2% of the variance in assemblages with eigenvalues of 0.72 and 0.64 respectively. Taxa that contributed significantly (>1%; Table 2) to the ordination highlight the different communities across the large spatial scale (north to south) and within WEAs (Fig. 4). The 3 northern WEAs (RIMA–MA, NY, NJ) were distinct from the VA WEA, and separated along the second dimension (Fig. 4A), and average proportion of taxa per station (85.3%) contributed most to the separation in assemblage structure (Fig. 4B). The VA WEA had higher proportions of spotted hake (*Urophycis regia*), *Prionotus* spp., *Etropus* spp., *Pagrus* spp., gastropods, bivalves, and brachyuran crabs (Fig. 4B). The northern WEAs overlapped each other, but did show some separation along both dimensions, particularly for the RIMA–MA WEA (Fig. 4A), indicating variation of communities at smaller spatial scales (e.g., within WEAs). Both average proportion of taxa per station (63.7%) and average individual weights of taxa per station (36.3%) contributed to the variation (Fig. 4, B and C). Stations in the lower left quadrant (Fig. 4A) had higher proportions and larger average individual weight of *Leucoraja* spp. (Fig. 4, B and C). The stations on the lower right quadrant of the ordination, located mostly in the RIMA–MA WEA (Fig. 4A), had higher proportions of poriferan sponges and larger average individual weight of brachyuran crabs (Fig. 4, B and C). Stations near the origin (Fig. 4A) had higher proportions of caridean shrimp, common sand dollar, and species of the order Pleurobranchomorpha (Fig. 4B). Both the sea scallop and the red hake are close in ordination space near the origin, but are not labeled.

The first 2 dimensions of the CA for the bottom trawl explained 32.5% of the variance in assemblages, with eigenvalues of 0.47 and 0.27, respectively. Taxa that contributed significantly (>3%; Table 3) to the ordination highlight the differences among the assemblages (Fig. 5). The NY and NJ WEAs were distinct from the RIMA–MA WEA, and separated along the first dimension (Fig. 5A). Average individual weight of a taxon per station (85.8%) contributed most to the separation in assemblage structure along the first dimension (Fig. 5C). Larger individuals of horseshoe crab (*Limulus Polyphemus*), and spiny dogfish were caught in the NY and NJ WEAs, and larger individuals of longhorn sculpin, ocean pout, sea raven (*Hemitripterus americanus*), and yellowtail flounder were caught in the RIMA–MA WEA (Fig. 5C). Additionally, the RIMA–MA WEA had higher station proportions of scup (*Stenotomus chrysops*) and haddock than the NY and NJ WEAs (Fig. 5B). Variability in assemblage structure also occurred

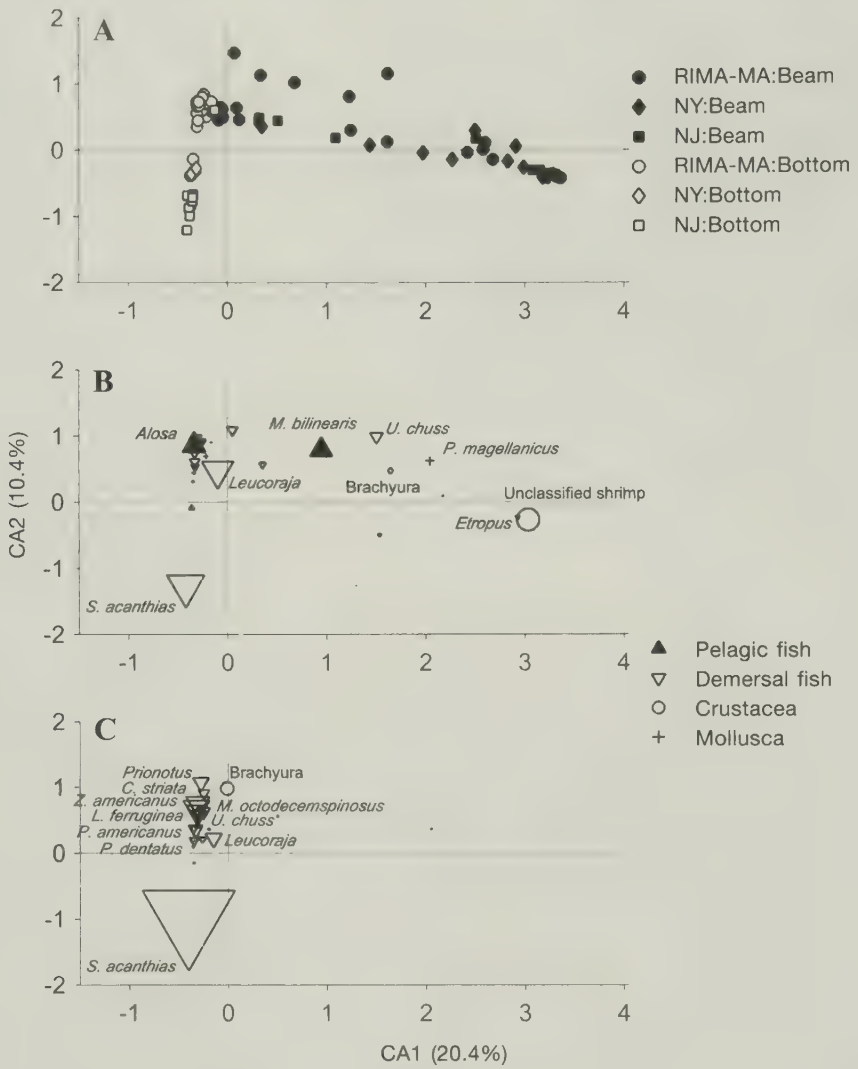

Figure 3

(**A**) Correspondence analysis ordination plots, showing the scores and variance explained for the first and second dimensions (CA1 and CA2), of the sampling stations at 3 wind energy areas, Rhode Island–Massachusetts and Massachusetts (RIMA-MA), New York (NY), and New Jersey (NJ), by using fish and macroinvertebrate taxa that occurred in at least 10% of the collections made in 2014. Beam trawl is represented by a solid symbol and bottom trawl by an open symbol. The size of the symbols are scaled to the contribution of each taxon to the ordination and are shown by taxon classification for (**B**) average proportion of a taxon per station and (**C**) average individual weight of a taxon per station. Taxa that contributed more than 1% to the ordination are labeled (For names of taxa, see Table 1).

within the RIMA–MA WEA (Fig. 5A). The stations of the RIMA–MA WEA separated along the second dimension (Fig. 5A), and both the average proportion of taxa per station (47.5%) and average individual weights of taxa per station (52.5%) contributed to the variation in assemblage structure (Fig. 5, B and C). Stations in the upper right quadrant (Fig. 5A) had higher proportions of scup and haddock (Fig. 5B), and larger individuals of numerous taxa, such as scup, sea raven, spotted hake, fourspot flounder (*Paralichthys oblongus*), black sea bass (*Centropristis striata*), and summer flounder (Fig. 5C). The other assemblage (in the lower right quadrant) had higher proportions of *Leucoraja* spp., Atlantic herring, and *Alosa* spp. (Fig. 5B), and larger individuals of longhorn sculpin, ocean pout, yellowtail flounder, winter flounder, and *Leucoraja* spp. (Fig. 5C).

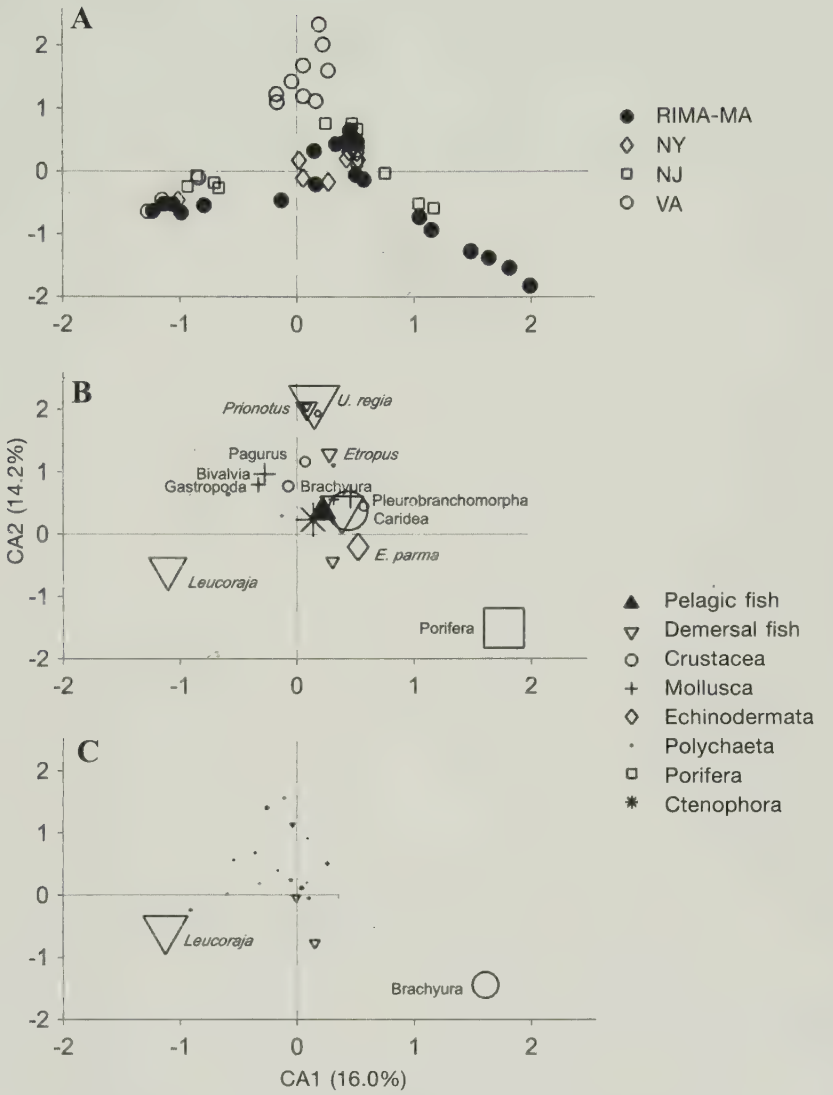

Figure 4

(**A**) Correspondence analysis ordination plots, showing the scores and variance explained for the first and second dimensions (CA1 and CA2), of the sampling stations at 4 wind energy areas, Rhode Island-Massachusetts and Massachusetts (RIMA–MA), New York (NY), New Jersey (NJ), and Virginia (VA) by using fish and macro-invertebrate taxa that occurred in at least 10% of the collections made by beam trawl in 2014. The size of the symbols are scaled to the contribution of each taxon to the ordination and are shown by taxon classification for (**B**) average proportion of a taxon per station and (**C**) average individual weight of a taxon per station. Taxa that contributed more than 1% to the ordination are labeled (For names of taxa, see Table 2).

Environmental relationships

Environmental variables were related to the station groups and associated fish and macro-invertebrate assemblages for both beam and bottom trawls. Forward selection of the explanatory environmental variables indicated bottom salinity was not significantly related to the assemblages sampled by either gear and was removed from the analyses. The 5 remaining environmental variables, which differed among gears used for sampling, resulted in the first 2 CCA dimensions significantly aligning with the station groups (Fig. 6). The unconstrained variance explained the most variability of each ordination, 75.8% and 56.0% for the beam and bottom trawls, respectively. The environmental variables explained 20.5% of the variation for the beam

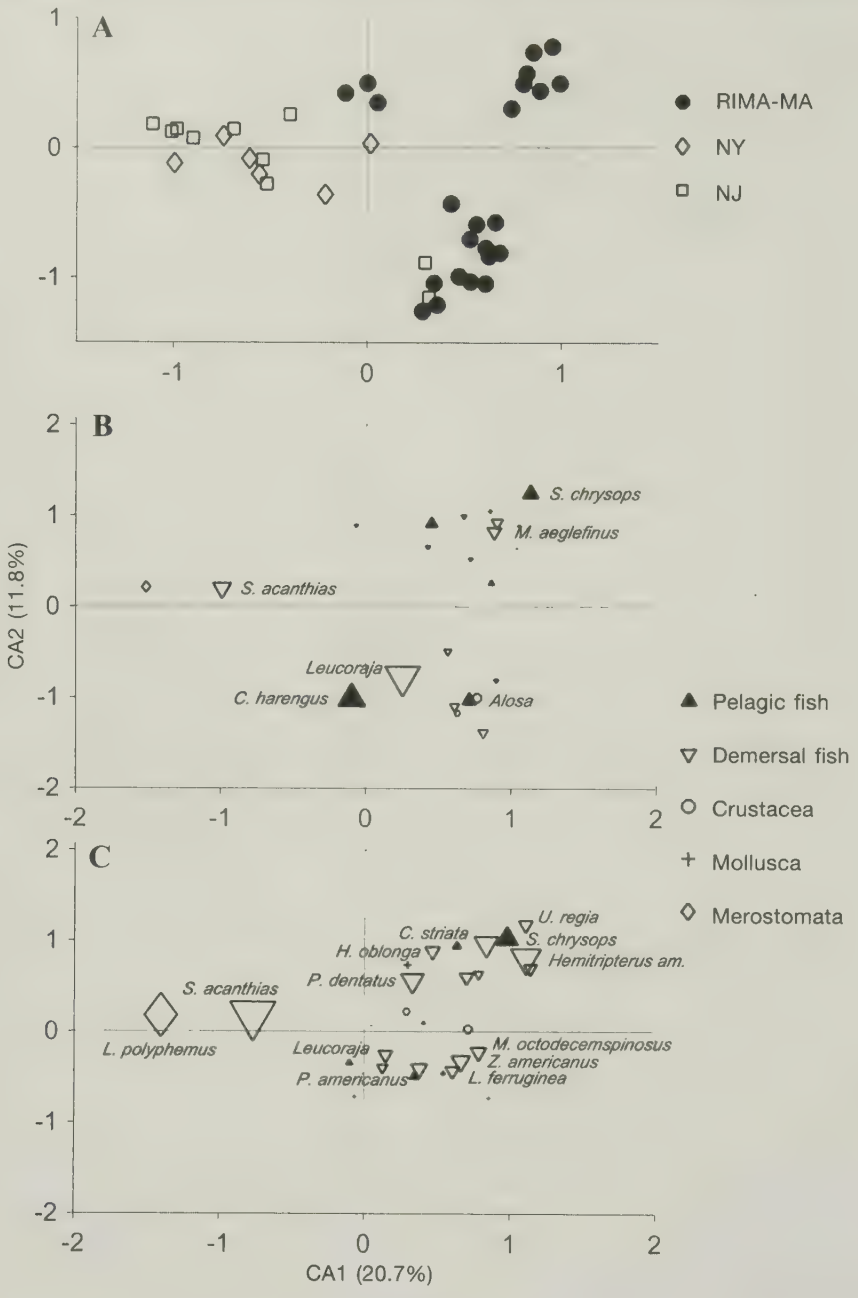

Figure 5

(**A**) Correspondence analysis ordination plots, showing the scores and variance explained for the first and second dimensions (CA1 and CA2), of the sampling stations at 3 wind energy areas, Rhode Island–Massachusetts and Massachusetts (RIMA–MA), New York (NY), and New Jersey (NJ), by using fish and macro-invertebrate taxa that occurred in at least 10% of the collections made with a bottom trawl in 2014. The size of the symbols are scaled to the contribution of each taxon to the ordination and are shown by taxon classification for (**B**) average proportion of a taxon per station and (**C**) average individual weight of a taxon per station. Taxa that contributed more than 3% to the ordination are labeled (For names of taxa, see Table 3).

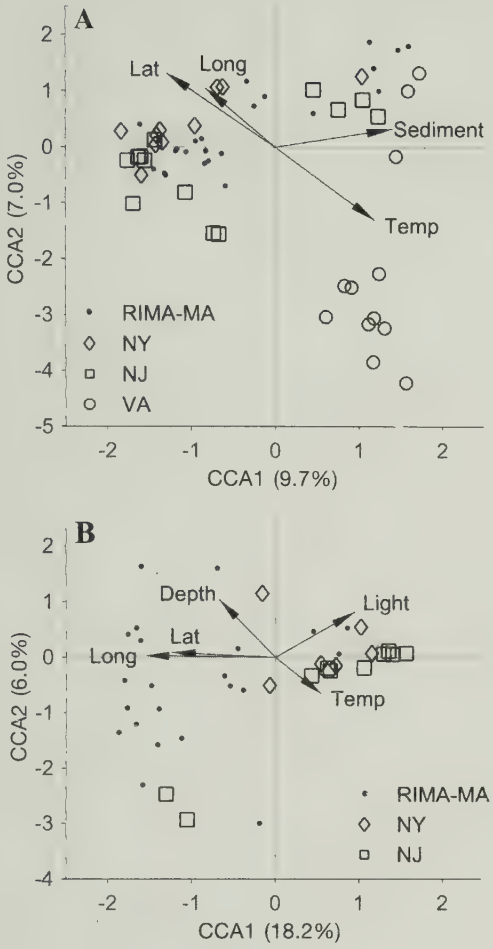

Figure 6

Canonical correspondence analysis (CCA) ordination plots, showing the scores and variance explained for the first and second dimensions (CCA1 and CCA2), of the sampling stations for each wind energy area, Rhode Island–Massachusetts and Massachusetts (RIMA–MA), New York (NY), New Jersey (NJ), and Virginia (VA), by using fish and macro-invertebrate taxa that occurred in at least 10% of the collections made in 2014 with a (**A**) beam trawl and (**B**) bottom trawl. The arrows depict the gradient of each explanatory variable.

trawl station groups and assemblages and 28.8% for the bottom trawl station groups and assemblages. Finally, covariables explained smaller proportions of the variance, with day of year explaining 3.7% and 3.1% for the beam trawl and bottom trawl, respectively. For the bottom trawl analysis, program (i.e., NEFSC vs. NEAMAP) explained 12.0% of the variance. For beam trawl station groups and assemblages, latitude (F=2.57, df=1, P≤0.006), longitude (F=3.94, df=1, P≤0.001), sediment (F=4.10, df=1, P≤0.001), and bottom water temperature (F=1.94, df=1, P≤0.040) were significantly correlated for the beam trawl station groups and assemblages (Fig. 6A). For the bottom trawl station groups and assemblages, all 5 remaining variables—latitude (F=4.87, df=1, $P \leq 0.001$), longitude (F=2.92, df=1, P≤0.005), depth (F=2.25, df=1, P≤0.011), bottom water temperature (F=2.05, df=1, P≤0.019), and light (F=3.82, df=1, P≤0.001—were correlated (Fig. 6B). Thus, the station groups in ordination space were similar but not identical among the CAs and CCAs in the comparisons of the separation of WEAs in Figure 6 with those in Figures 4 and 5.

The variable of location on the northeast U.S. shelf, defined by latitude and longitude, correlated most with station groups and assemblages for the beam and bottom trawl collections. Most VA WEA stations from the beam trawl collections separated from the northern WEAs along the first and second dimensions (Fig. 6A), and aligned with latitude and longitude, and explained 45.1% of the environmental correlation. Bottom water temperature explained 8.8% of correlation and aligned opposite latitude and longitude (Fig. 6A), indicating that the spring bottom temperature was lower in the northern WEAs. Sediment explained the final 31.4% of the environmental correlations for the beam trawl collection and aligned with the first dimension and variability in the northern WEAs stations (Fig. 6A).

Latitude and longitude combined explained most of the environmental variability (59.2%) for the bottom trawl station groups and assemblages, and aligned with the first dimension (Fig. 6B). The importance of the remaining 3 environmental variables (depth, light, and bottom water temperature) ranged from 14.4% to 12.9%. Bottom water temperature and depth opposed each other (Fig. 6B), with temperature decreasing with increasing depth. Light aligned near the middle of the 2 dimensions (Fig. 6B), and was related to day-night variability in bottom trawl collections. Daytime collections were spread throughout the ordination space, whereas nighttime collections were clustered in the lower left quadrant (data not shown).

Discussion

The differences in the identified fish and macro-invertebrate assemblages in the collections made with the 2 gear types highlight the importance of employing multiple types of gears for environmental assessments (Wilson et al., 2010). The beam trawl collected a higher proportion of juvenile fish, small noncommercial fish, and small macro-invertebrate prey species than the bottom trawl (Suppl. Table (online only); Figs. 2 and 3). The diversity of the beam trawl samples may be the reason why the ordinations for those stations were more variable than the bottom trawl stations. In contrast, the bottom trawl caught a higher average proportion of and larger (i.e., older) demersal and pelagic, commercially important fish and fewer macro-invertebrates per station (Suppl. Table; Figs. 2 and 3) and generally had lower variability in or-

dination space. Average proportion of taxa per station drove assemblage structure defined by the beam trawl samples (Fig. 4) because the beam trawl caught a smaller size range of individuals. Average individual weights by taxon per station were more important to assemblage structure for bottom trawl samples (Fig. 5).

Sampling season and variation in mesh sizes of nets may account for some of the differences in the comparisons of assemblages for the 2 gear types. Beam trawl sampling occurred earlier in the spring than bottom trawl sampling, and the beam trawl had a smaller mesh. Additionally, variability in sampling time of day (lack of day samples for beam trawl collections) may have influenced our analyses. Other research on the northeast U.S. shelf has shown that gear type and mesh size of nets influence species and size in composition of catch (Vasslides and Able, 2008; Slacum et al., 2010; Malek et al., 2014). Beam trawls often catch more demersal taxa and otter trawls catch more pelagic taxa (Vasslides and Able, 2008; Malek et al., 2014). Malek et al. (2014) also found that a beam trawl caught smaller individuals than an otter trawl equipped with a net of the same mesh size. Assessments of WEAs would clearly benefit from the use of gears, such as beam trawls, that collect smaller individuals of both fish and macro-invertebrates, allowing a more comprehensive understanding of the potential impact of developing wind farms, because the combination of beam trawls with bottom trawls provides a more complete view of demersal communities than bottom trawls alone.

Fish and macro-invertebrate assemblages varied spatially on the northeast U.S. shelf for both gear types, and latitude and longitude were important explanatory variables. The VA WEA is the farthest distance from the other WEAs and had the least overlap in assemblage composition for the beam trawl stations (Fig. 4). The NJ and NY WEAs were the closest to each other, and had the most overlap in assemblages for the bottom trawl stations (Fig. 4), and both also overlapped with portions of RIMA–MA for beam trawl stations (Fig. 3). Regional variation in assemblage structure on the northeast U.S. shelf, following a south to north gradient, has been described for both fish (Gabriel, 1992; Lucey and Nye, 2010) and macro-invertebrates (Wigely and Theroux, 1981; Theroux and Wigely, 1998; Hale, 2010). Consequently, impacts of WEAs spread along the shelf may become additive for assemblages that span large distances (i.e., 50–100 km). Therefore, impact assessments need to take a more holistic ecosystem-scale approach.

Assemblage structure varied within WEAs, and may be due to the effect of habitat conditions on species distributions. The explanatory habitat variables, sediment, depth, and bottom water temperature, correlated with assemblage structure in the beam trawl and bottom trawl collections (Fig. 6). The lack of daytime beam trawl sampling may have influenced our results because some species have been found to exhibit diel patterns of microhabitat use on the northeast U.S. shelf (Diaz et al., 2003); consequently additional round-the-clock sampling may lead to the discovery of different habitat relationships than those we report here. Nevertheless, taxon-specific relationships with habitat on the shelf have previously been shown for fish and macro-invertebrates and were most closely associated with sediment characteristics (Wigely and Theroux, 1981; Theroux and Wigely, 1998; Methratta and Link, 2006, 2007), depth (in both the cross-shelf and shoal formations) (Viscido et al., 1997; Steves et al., 1999; Methratta and Link, 2007; Vasslides and Able, 2008; Slacum et al., 2010), and bottom water temperature, particularly with seasonal temperature changes (Steves et al., 1999; Malek et al., 2014). Hale (2010), in examining estuarine and near shore sample locations, also showed that salinity was related to macro-invertebrate assemblages. The RIMA–MA WEA covered the largest area and had the most diverse assemblages for both beam and bottom trawl collections (Figs. 4 and 5). This finding may be related to greater heterogeneity in habitat types within this combined WEA. Impact assessments within and among WEAs need to take into account habitat variability.

Our study provides a "snapshot" of the springtime assemblages for the northeast U.S. shelf. Seasonality, as defined by day of year, explained a small proportion (<4%) of the variability in fish and macro-invertebrate assemblage structure for both the beam and bottom trawl collections. Other research on the northeast U.S. shelf has documented the existence of seasonal assemblages. Steves et al. (1999) identified 3 seasonal assemblages for recently settled juvenile fish: winter–spring, summer, and fall. Malek et al. (2014) identified summer and fall assemblages from beam trawl and otter trawl collections in Rhode Island Sound that remained stable across years. Therefore yearlong temporal sampling of WEAs will be needed to assess the entire assemblage structure, especially considering the complex life history (e.g., multiple life stages with various habitat needs) of many of the shelf species of both fish and macro-invertebrates.

Overall, our results and previous research indicate that effects of WEAs will need to be critically assessed for WEAs on an individual basis. Additionally, effects should be evaluated across multiple spatial and temporal scales to determine population-level effects on resident fish and macro-invertebrates (Bergstrom et al., 2014; Lindeboom et al., 2015). Many species use large areas during their life span (e.g., egg, larval, juvenile, adult stages), often make long-distance seasonal migrations (Secor, 2015), and therefore small-scale effects (on the scale of individual WEAs) may have additive effects (Bergstrom et al., 2014; Dai et al., 2015) on populations of commercially and ecologically important fish and macro-invertebrates.

Acknowledgments

Partial funding for this project was provided by the BOEM-NOAA Interagency Agreement #M13PG00019.

We thank the officers and crew of the NOAA Ship *Gordon Gunter*, P. Plantamura, M. Lowe, E. Broughton, J. Prezioso, and J. Rosendale for their assistance with beam trawl collections. We also thank the NEFSC Ecosystems Survey Branch and the Virginia Institute of Marine Science, especially D. Gauthier for the bottom trawl data. K. Marancik, D. Packer, and 3 anonymous reviewers provided comments on a previous version of the manuscript.

Literature cited

Able, K. W., and M. P. Fahay.
1998. The first year in the life of estuarine fishes in the Middle Atlantic Bight, 342 p. Rutgers Univ. Press, New Brunswick, NJ.

Azarovitz, T. R.
1981. A brief historical review of the Woods Hole Laboratory trawl survey time series. Can. Spec. Publ. Fish. Aquat. Sci. 58:62–67.

Bailey, H., K. L. Brookes, and P. M. Thompson.
2014. Assessing environmental impacts of offshore wind farms: lessons learned and recommendations for the future. Aquat. Biosyst. 10:8.

Bergstrom, L., L. Kautsky, T. Malm, R. Rosenberg, M. Wahlberg, N. Å. Capetillo, and D. Wilhelmsson.
2014. Effects of offshore wind farms on marine wildlife—a generalized impact assessment. Environ. Res. Lett. 9:034012.

Dai, K., A. Bergot, C. Liang W.-N.Xiang, and Z. Huang.
2015. Environmental issues associated with wind energy—a review. Renew. Energy 75:911–921.

Diaz, R. J., G. R. Cutter, and K. W. Able.
2003. The importance of physical and biogenic structure to juvenile fishes on the shallow inner continental shelf. Est. Coast. 26:12–20.

Federal Register.
2014. MMAA104000; Timing requirements for the submission of a site assessment plan (SAP) or general activities plan (GAP) for a renewable energy project on the Outer Continental Shelf (OCS). Fed. Regist. 79:21617–21626. [Available from website.]

Folk, R. L.
1954. The distinction between grain size and mineral composition in sedimentary-rock nomenclature. J. Geol. 62:344–359.

Gabriel, W. L.
1992. Persistence of demersal fish assemblages between Cape Hatteras and Nova Scotia, Northwest Atlantic. J. Northwest Atl. Fish. Soc. 14:29–46.

Hale, S. S.
2010. Biogeographical patterns of marine benthic macroinvertebrates along the Atlantic coast of the Northeastern USA. Est. Coast. 33:1039–1053.

Kuipers, B.
1975. On the efficiency of a two-metre beam trawl for juvenile plaice (*Pleuronectes platessa*). Neth. J. Sea Res. 9:69–85.

Le, S., J. Josse, and F. Husson.
2008. FactoMineR: an R package for multivariate analysis. J. Stat. Softw. 25(1):1–18.

Lindeboom, H. J., H. J. Kouwenhoven, M. J. N. Bergman, S. Bouma, S. Brasseur, R. Daan, R. C. Fijn, D. de Haan, S. Dirksen, R. van Hal, et al.
2011. Short-term ecological effects of an offshore wind farm in the Dutch coastal zone; a compilation. Environ. Res. Lett. 6:035101.

Lindeboom, H., S. Degraer, J. Dannheim, A. B. Gill, and D. Wilhelmsson.
2015. Offshore wind park monitoring programmes, lessons learned and recommendations for the future. Hydrobiologia 756:169–180.

Lucey, S. M., and J. A. Nye.
2010. Shifting species assemblages in the Northeast US Continental Shelf Large Marine Ecosystem. Mar. Ecol. Prog. Ser. 415:23–33.

Malek, A. J., J. S. Collie, and J. Gartland.
2014. Fine-scale spatial patterns in the demersal fish and invertebrate community in a northwest Atlantic ecosystem. Est. Coast. Shelf Sci. 147:1–10.

Marancik, K. E., L. M. Clough, and J. A. Hare.
2005. Cross-shelf and seasonal variation in larval fish assemblages on the southeast United States continental shelf off the coast of Georgia. Fish. Bull. 103:108–129.

Methratta, E. T., and J. S. Link.
2006. Associations between surficial sediments and groundfish distributions in the Gulf of Maine–Georges Bank region. North Am. J. Fish. Manage. 26:473–489.
2007. Ontogenetic variation in habitat associations for four flatfish species in the Gulf of Maine-Georges Bank region. J. Fish. Biol. 70:1669–1688.

Oksanen, J., F. Guillaume Blanchet, R. Kindt, P. Legendre, P. R. Minchin, R. B. O'Hara, G. L. Simpson, P. Solymos, M. H. H. Stevens, and H. Wagner.
2015. vegan: community ecology package. R package vers. 2.3-1. [Available from website.]

R Core Team.
2015. R: a language and environment for statistical computing. R Foundation for Statistical Computing, Vienna, Austria. [Available from website, accessed August 2015.]

Secor, D. H.
2015. Migration ecology of marine fish, 304 p. Johns Hopkins Univ. Press, Baltimore, MD.

Slacum, H. W. Jr., W. H. Burton, E. T. Methratta, E. D. Weber, R. J. Llansó, and J. Dew-Baxter.
2010. Assemblage structure in shoal and flat-bottom habitats on the inner continental shelf of the Middle Atlantic Bight, USA. Mar. Coast. Fish. 2:277–298.

Steves, B. P., and R. K. Cowen.
2000. Settlement, growth, and movement of silver hake *Merluccius bilinearis* in nursery habitat on the New York Bight continental shelf. Mar. Ecol. Prog. Ser. 196:279–290.

Steves, B. P., R. K. Cowen, and M. H. Malchoff.
1999. Settlement and nursery habitats for demersal fishes on the continental shelf of the New York Bight. Fish. Bull. 98:167–188.

Sullivan, M. C., R. K. Cowen, K. W. Able, and M. P. Fahay.
2000. Spatial scaling of recruitment in four continental shelf fishes. Mar. Ecol. Prog. Ser. 207:141–154.

Tabassum-Abbasi, M. P., T. Abbasi, and S. A. Abbasi.
2014. Wind energy: increasing deployment, rising environmental concerns. Renew. Sustain. Energy Rev. 31:270–288.

Theroux, R. B., and R. L. Wigely.
1998. Quantitative composition and distribution of the macrobenthic invertebrate fauna of the continental shelf ecosystems of the northeastern United States. NOAA Tech. Rep. NMFS 140, 240 p.

Vasslides, J. M., and K. W. Able.
2008. Importance of shoreface sand ridges as habitat for fishes off the northeast coast of the United States. Fish. Bull. 106:93–107.

Viscido, S. V., D. E. Stearns, and K. W. Able.
1997. Seasonal and spatial patterns of an epibenthic decapod crustacean assemblage in north-west Atlantic continental shelf waters. Est. Coast. Shelf Sci. 45:377–392. Article

Walsh, H. J., K. E. Marancik, and J. A. Hare.
2006. Juvenile fish assemblages collected on unconsolidated sediments of the southeast United States continental shelf. Fish. Bull. 104:256–277.

Wigely, R. L., and R. B. Theroux.
1981. Atlantic continental shelf and slope of the United States: macrobenthic invertebrate fauna of the Middle Atlantic Bight region—faunal composition and quantitative distribution. Geol. Surv. Prof. Pap. 529-N, 198 p.

Wilson, J. C., M. Elliott, N. D. Cutts, L. Mander, V. Mendão, R. Perez-Dominguez, and A. Phelps.
2010. Coastal and offshore wind energy generation: is it environmentally benign? Energies 3:1383.

National Marine Fisheries Service
NOAA

Fishery Bulletin
established in 1881

Spencer F. Baird
First U.S. Commissioner of Fisheries and founder of *Fishery Bulletin*

Trophic ecology of the smooth hammerhead shark (*Sphyrna zygaena*) off the coast of northern Peru

Adriana Gonzalez-Pestana (contact author)[1,2,3]
Nicolas Acuña-Perales[1,4]
Javier Coasaca-Cespedes[1,2]
Francisco Cordova-Zavaleta[1,5]
Joanna Alfaro-Shigueto[1,2,6]
Jeffrey C. Mangel[1,6]
Pepe Espinoza[2,7]

Email address for contact author: adriana@prodelphinus.org

[1] ProDelphinus
Calle Jose Galvez 780-e
Lima 18, Peru

[2] Universidad Científica del Sur
Panamericana Sur Km 19
Villa El Salvador, Lima 42, Peru

[3] James Cook University
1 James Cook Dr.
Townsville City, Queensland 4811, Australia

[4] Universidad Ricardo Palma
Avenida Alfredo Benavides 5440
Santiago de Surco, Lima 33, Peru

[5] Universidad Nacional Agraria La Molina
Avenida La Molina s/n
La Molina, Lima 12, Peru

[6] Center for Ecology and Conservation
College of Life and Environmental Sciences
University of Exeter. Penryn Campus
Penryn, Cornwall TR10 9FE, United Kingdom

[7] Instituto del Mar del Perú
Esquina Gamarra y General Valle s/n
Chucuito, Callao 05, Peru

Abstract—The smooth hammerhead (*Sphyrna zygaena*) is the third most captured shark species in Peru, a nation with one of the largest shark fisheries in the Pacific Ocean. We sought to better understand the trophic ecology of this shark in northern Peru by analyzing stomach contents. From 2013 through 2015, we collected 485 samples of gut contents from sharks measuring 53–294 cm in total length. Our results show that the smooth hammerhead is a top predator with a diet dominated by jumbo flying squid (*Dosidicus gigas*) and the Patagonian squid (*Doryteuthis* (*Amerigo*) *gahi*). Smooth hammerheads displayed different diets with different body size, and this finding indicates that sharks change their distribution and habitat during development. This study represents the most comprehensive investigation to date of the trophic ecology of smooth hammerhead in waters off Peru. We propose that these waters represent an important eastern Pacific Ocean feeding ground for smooth hammerhead. Because this species is commercially important and also preys upon other commercial species, these findings could contribute to the design and implementation of plans for ecosystem-based fisheries management.

Manuscript submitted 14 October 2016.
Manuscript accepted 7 June 2017.
Fish. Bull. 115:451–459 (2017).
Online publication date: 31 July 2017.
doi: 10.7755/FB.115.2

The views and opinions expressed or implied in this article are those of the author (or authors) and do not necessarily reflect the position of the National Marine Fisheries Service, NOAA.

The smooth hammerhead (*Sphyrna zygaena*) is distributed from California to Chile within the eastern Pacific Ocean. This species reaches a maximum size of 370–400 cm in total length (TL), and is one of the largest fishes in the southeast Pacific Ocean (Fowler et al., 2005). At birth, neonates measure 50–61 cm-TL (Fowler et al., 2005). Neonate and juvenile smooth hammerheads use shallow coastal waters as nursery grounds and as they grow larger they move to more offshore oceanic waters (Smale, 1991; Diemer et al., 2011; Francis, 2016). The distribution of adults worldwide, however, is still unknown (Francis, 2016).

Abundance of this species is decreasing and the species is classified as vulnerable in the IUCN Red List of Threatened Species (Casper et al., 2005). As of September 2014, the species has been included in Appendix II of the Convention on International Trade in Endangered Species of Wild Fauna and Flora (https://cites.org/eng/app/appendices.php). Smooth hammerhead fins are prized in Asian markets and sharks are increasingly targeted in some areas. Peru is one of the top 12 countries that supply shark fins to Asian markets (Cheung and Chang, 2011). The smooth hammerhead is commonly caught in the southeast Pacific Ocean but the impact of these fisheries on its population is unknown (Fowler et al., 2005). Peru also reports the highest accumulated historical shark landings in the Pacific Ocean and smooth hammerhead is identified as the third most captured shark species by the fisheries of Peru and the most frequently captured shark species off northern Peru (Gonzalez-Pestana et

al., 2016). However, the fisheries lack robust monitoring and management, and species biology and ecology remain poorly understood, both locally and worldwide (Fowler et al., 2005; Cortés et al., 2010).

There are limited studies from Mexico, Ecuador, and Peru on the diet of smooth hammerhead in the Pacific Ocean. Research shows that the diet of this shark in waters off Mexico is composed of fishes and cephalopods (e.g., California needlefish [*Strongylura exilis*]; common clubhook squid [*Onychoteuthis banksia*]) (Galvan-Magaña et al., 1989; Ochoa-Díaz, 2009; Galvan-Magaña et al., 2013). In waters off Ecuador, information suggests that the diet is composed mainly of cephalopods (e.g., jumbo flying squid [*Dosidicus gigas*]; purpleback flying squid [*Sthenoteuthis oualaniensis*]; whip-lash squid [*Mastigoteuthis dentata*]; and sharpear enope squid [*Ancistrocheirus lesueurii*]) (Castañeda and Sandoval, 2004; Estupiñan-Montaño and Cedeño-Figueroa, 2005; Bolaño Martínez, 2009). In one study in Peru, the diet of smooth hammerhead was analyzed and smooth hammerheads were found to feed primarily on fishes (Pacific sardine [*Sardinops sagax*]; Peruvian hake [*Merluccius gayi peruanus*]; and Peruvian anchoveta [*Engraulis ringens*]), as well as on cephalopods (*Loligo* spp., and jumbo squids) (Castañeda[1]). Although this study in Peru had an adequate sample size, time series, and size distribution for the smooth hammerhead, it is more descriptive than analytical and is limited to a seasonal comparison.

We sought to better understand the trophic ecology of smooth hammerhead off the coast of northern Peru by analyzing stomach contents. We assessed diet variability by sex, body size, location, season, year, and environmental conditions.

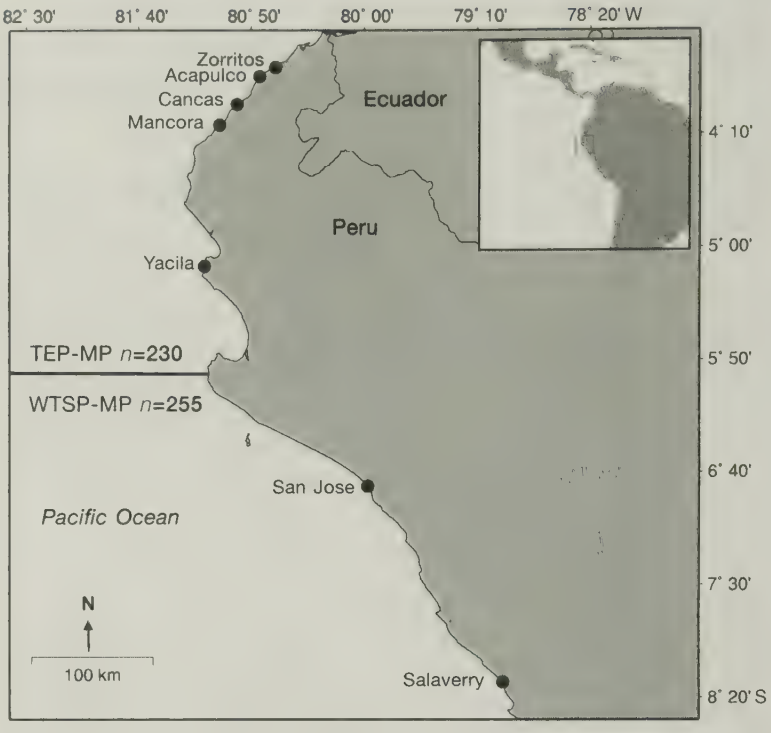

Figure 1

Map of the study area and the 7 landing sites where smooth hammerhead (*Sphyrna zygaena*) were collected off northern Peru from December 2012 through June 2015. The black line defines the division between the Tropical East Pacific Marine Province (TEP–MP) and the Warm Temperate Southeastern Pacific Marine Province (WTSP–MP), *n*=number of stomachs collected from each marine province. This map was created with Seaturtle.org Maptool (Seaturtle.org Inc. website, accessed January 2017).

Materials and methods

Collections, storage, and analysis of samples

Samples were collected from a small-scale driftnet fishery from December 2012 through June 2015 at 7 landing sites along the coast of northern Peru: Zorritos, Acapulco, Cancas, Mancora, Yacila, San Jose, and Salaverry (Fig. 1). Nets in this fishery are typically set at the time of sunset and retrieved the following morning for an average set length of ca. 14 h (Alfaro-Shigueto et al., 2010). Sharks were measured (total length) and sex was determined. Stomachs were extracted and preserved in 10% formalin solution.

Analysis of stomach contents

Prey items from stomach contents were analyzed at the Laboratorio de Ecología Trófica of the Instituto de Mar del Perú,[2] and identified to the lowest possible taxon, counted, and weighed (wet weight). For identification of fishes and cephalopods, and their hard parts (otoliths and beaks), the following identification guides were used: Iverson and Pinkas (1971); Wolff (1982, 1984); Clarke (1986); Chirichigno and Cornejo (2001); Garcia-Godos (2001); Lu and Ickeringill (2002); and Xavier and Cherel (2009). Cephalopod beaks were used to reconstruct total mass at ingestion, by using regression equations (Lu and Ickeringill, 2002). Values for stage of digestion were allocated to each prey item and ranged from 1 (little or no digestion) to 4 (advanced state of digestion) (Bolaño Martínez, 2009).

Diet was quantified by using percentage of prey, by number (%N), weight (%W), and frequency of occurrence (%O) (Hyslop, 1980). The index of relative importance (IRI) was calculated as $IRI=\%O\ (\%N + \%W)$. It was then divided by the total IRI for all items to express the

[1] Castañeda, J. 2001. Biología y pesquería del "tiburón martillo" (*Sphyrna zygaena*) en Lambayeque, 1991–2000. Inst. Mar Perú Inf. Prog. 139:17–32. [Available from website.]

[2] and at the Laboratorio de Biologia Marina of the Universidad Cientifica del Sur.

IRI as a percentage (%IRI; Cortés, 1997). Items rarely found in stomachs (e.g., rocks, snails) and parasites (e.g., isopoda) were not included in the analysis.

Statistical analysis

Cumulative prey curves were constructed to determine whether an adequate number of stomachs had been collected to accurately describe the diet of smooth hammerhead (Jimenez and Hortal, 2003). The order in which stomachs were analyzed was randomized 1000 times to eliminate bias. The number of stomachs analyzed is considered sufficient in describing the diet when a cumulative prey curve reaches an asymptote. Therefore, a slope value less than 0.1 indicates a good representation of diet (Soberón and Llorente, 1993).

We used 2 indices to evaluate trophic niche width of prey taxa: Levin index and Berger–Parker index. The Levin index was based on %N values. The index values range from 0 to 1: low values (<0.6) indicate a diet dominated by few prey items (specialist predator) and higher values (>0.6) indicate a generalist diet (Labropoulou and Eleftheriou, 1997). The Berger–Parker index uses the formula of Magurran (1988), $d=(n_i\ max)/N$, where N represents the number of all recorded food components (taxa) and n_i max represents the number of specimens from taxon i (the most numerous taxon in the diet). This index ranges between 1/N and 1: values closer to 1 represents a specialist feeder and a value closer to 1/N indicates a generalist feeder.

We calculated trophic position on the basis of %IRI values of the prey species presented in the stomach content. We used the following equation:

$$TL=1+(\Sigma\ DC_{ij})\times(TL_j) \quad \text{(Christensen and Pauly, 1992),} \quad (1)$$

where DC_{ij} = the composition of the diet in which j is the proportion of preys in the diet of the predator I; and
TL_j = the trophic level of the preys.

The trophic level of the fishes were taken from Froese and Pauly[3] and Espinoza (2014) and the trophic level of the cephalopods were taken from Cortés (1999) and Espinoza (2014).

We analyzed differences in diet according to 6 factors: body size and sex of sharks, location of capture, season, year, and environmental conditions (El Niño–Southern Oscillation event: November 2014 to December 2015). For body size we divided the sharks into size classes. This division was based on analyses of similarities (ANOSIM) where we chose the size classes that showed the highest R-statistic and the lowest P-value (Clarke, 1993). The division of the locations (north: Zorritos, Acapulco, Cancas, Mancora, and Yacila; south: San Jose; and Salaverry) was justified because of biogeographic characteristics of the Tropical East Pacific and Warm Temperate Southeastern Pacific marine provinces where the collection sites were located (Spalding et al., 2007) (Fig. 1). The division of the seasons was based upon the seasonality of chlorophyll-a concentration and primary production; for which the highest levels occurred during the austral summer and fall (Pennington et al., 2006). Therefore, we divided the data into 2 seasons: season 1 (austral summer and fall) and season 2 (austral winter and spring).

Nonmetric dimensional scaling (nMDS) ordinations generated from a Bray–Curtis similarity matrix on numeric abundance of prey (%N) was used to determine whether sex, body size, capture location, season, year, or environmental conditions exerted the greatest overall influence on the dietary composition of smooth hammerhead. ANOSIM was used to test whether dietary compositions differed significantly, by generating a R-statistic, stress value, and a P-value. R-statistic values describe the extent of similarity (Clarke, 1993), with values near 1 indicating that the 2 groups are entirely separate and values close to 0 indicating that there are no differences between the 2 groups. Stress value measures the goodness-of- fit of the nMDS model to the data, where values closer to zero indicate excellent representation (without risk of misinterpretation) and values larger than 0.2 indicate that the interpretation is unreliable (Clarke, 1993). Similarity percentages (SIMPER) were employed to determine the dietary categories that typified particular groups or contributed most (or typified a combination of both categories) to the similarities between groups (Clarke, 1993). If significant differences existed in the diets by factors (e.g., sex), then trophic niche width, degree of overlap (based on the Bray–Curtis index) and trophic position were calculated for each factor.

Statistical analyses were performed by using RStudio, vers. 0.96.122 (RStudio, 2012) with R, vers. 3.2.2 (R Core Team, 2016).

Results

A total of 485 samples of gut contents were collected. Individual smooth hammerheads measured between 53 and 294 cm TL. The slope value of 0.002 (less than 0.1) for the cumulative prey curve showed that sufficient stomach contents were examined to adequately and reliably describe the diet of smooth hammerhead. With the cumulative prey curve, we calculated that the contents from 39 stomachs would be needed to accurately analyze the diet of smooth hammerhead.

Food items were found in 78% of the stomachs. Of these, 92% were in an advanced state of digestion (stages 3 and 4). Prey composition comprised 25 prey items: 14 teleosts and 11 cephalopods (Table 1). According to %IRI values, the most important prey species were Patagonian squid (*Doryteuthis* (*Amerigo*) *gahi*) (37%) and jumbo squid (27%). These 2 species comprised more than 60% of the diet. The trophic position was high

[3] Froese R., and D. Pauly. 2012. FishBase, vers. 02/2012. [World Wide Web electronic publication; available from http://www.fishbase.org.]

Table 1

Composition of prey identified in stomachs of smooth hammerhead (*Sphyrna zygaena*) collected from December 2012 through June 2015 in northern Peru: %N=percentage by number; %W=percentage by weight; %O=percentage by frequency of occurrence, %IRI=index of relative importance, and SD=standard deviation.

Prey category	%W	%N	%O	%IRI (SD)
Chordata				
Teleostei				
Fish remains	2.7		12.9	
Scomber japonicus	0.3	0.2	0.4	0.3 (3.72)
Odontesthes regia	0.0	0.0	0.2	0.0 (0.13)
Peprilus sp.	3.2	3.3	4.0	3.3 (16.24)
Opisthonema libertate	0.4	0.5	0.9	0.5 (6.16)
Sardinops sagax	0.3	0.1	0.2	0.2 (3.87)
Selene brevoortii	0.1	0.2	0.2	0.0 (0.86)
Scomberesox saurus scombroides	0.1	0.1	0.2	0.1 (2.55)
Trachurus murphyi	0.1	0.1	0.2	0.1 (1.64)
Hemanthias peruanus	0.2	0.1	0.2	0.1 (2.74)
Merluccius gayi peruanus	1.7	1.4	2.2	1.9 (11.80)
Engraulidae	0.6	0.4	0.9	0.5 (6.10)
Engraulis ringens	0.0	0.4	0.7	0.2 (2.34)
Anchoa nasus	0.3	0.3	0.2	0.3 (5.42)
Fistulariidae	0.1	0.1	0.2	0.1 (2.15)
Mollusca				
Cephalopoda				
Teuthoidea				
Octopoteuthis sicula	1.2	1.3	5.1	1.3 (7.33)
Gonatus antarcticus	7.5	6.6	17.3	7.1 (18.44)
Stigmatoteuthis hoylei	2.2	1.3	4.7	1.8 (9.05)
Mastigoteuthis dentata	9.1	12.2	20.9	10.9 (25.18)
Dosidicus gigas	30.5	23.8	30.9	26.6 (36.28)
Ommastrephes bartramii	1.0	1.2	2.4	1.1 (9.08)
Doryteuthis (Amerigo) gahi	34.5	38.4	44.0	37.5 (41.56)
Ancistrocheirus lesueurii	1.6	3.5	12.0	2.3 (7.96)
Architeuthis dux	0.1	0.6	2.2	0.4 (5.55)
Octopodea [1]	2.1	4.1	9.8	3.4 (14.28)

[1] *Argonauta* spp., *Tremoctopus violaceus*

(4.3), indicating that the smooth hammerhead is a top predator.

The trophic niche width was narrow with a low Levin index value (<0.6) for the 2 groups of prey taxa: cephalopods and fishes. Also the value of d for the Berger–Parker index was closer to 1 than 1/N for both groups. This value means that the diet of smooth hammerhead is dominated by few prey species (Table 2). Moreover, the average frequency of occurrence of cephalopods (89%) in gut contents was higher than the average frequency of occurrence of fishes (11%). The most common number of prey species per stomach was 1, followed by 2 prey species (41% of stomachs contained 1 prey species, and 26% of the stomachs had 2 prey species) (Fig. 2). For stomachs that contained 1 prey species, the single prey species was the Patagonian squid in 60% of stomachs and the jumbo squid in 20% of the cases.

The average number of prey items per stomach was 5.3 with a mode of 1 and a maximum value of 74. The greatest number of prey items was found in a shark that measured 230 cm TL which contained 74 pairs of squid beaks (equivalent to 74 cephalopods).

Comparisons of dietary composition

There were statistically significant differences in diet based upon body size. For this analysis, we divided the sharks into 4 size classes: I (53–70 cm TL, n=40), II (71–100 cm TL, n=175), III (101–190 cm TL, n=111) and IV (191–294 cm TL, n=10). The stress value (0.11) of the nMDS plot indicated that this plot provides an accurate representation of the data, and an overall ANOSIM showed significant differences among the size classes (R-statistic=0.4, P<0.001). The nMDS plot and the overall R-statistic indicate that the diet of the size classes overlap but are clearly distinct.

By analyzing each of the pairwise comparisons, we found that all size classes had significant differences (P<0.05), except size classes III and IV. Among the size

Table 2

Trophic niche width of 2 groups of taxa in the diet of smooth hammerhead (*Sphyrna zygaena*) collected from December 2012 through June 2015 in northern Peru, according to Levin and Berge–Parker indices. The Berger-Parker index uses this formula: $d=(n_i\ max)/N$, where N=the number of all recorded food components and n_i max=the number of specimens with the most numerous taxon in the diet.

		Berger–Parker index	
	Levin index	d	$1/N$
Cephalopods	0.24	0.31	0.0102
Fish species	0.30	0.39	0.0005
Total	0.27	0.38	0.0005

classes that presented a significant difference, size classes I–III had the highest R-statistic and the lowest overlap, and therefore their diets are well separated. Size classes II and III had the lowest R-statistic and the highest overlap; therefore their diets were minimally separated (Table 3).

According to analysis with SIMPER, the prey species that most contributed to the diet in size class I are *M. dentata,* teleosts and the Patagonian squid; in size class II they were the Patagonian squid, the jumbo flying squid, and *M. dentata*; in size class III they were the jumbo flying squid and Patagonian squid; and in size class IV they were the jumbo flying squid, sharpear enope squid, *Gonatus antarcticus*, and giant squid (*Architeuthis dux*) in order of importance. The IRI showed a similar trend. Sharks in size class I fed chiefly on Patagonian squid (31% of IIR), teleosts (26%) and whip-lash squid (25%); whereas sharks in size class II fed chiefly on Patagonian squid (49%), whip-lash squid (13%) and jumbo squid (13%); sharks in size class III fed chiefly on jumbo flying squid (54%) and Patagonian squid (24%); and sharks in size class IV fed chiefly on jumbo flying squid (62%), giant squid (15%) and sharpear enope squid (9%) (Fig. 2).

We were also able to identify some general trends in the diet as sharks increased in size, such as, a reduction in the consumption of teleosts and whip-lash squid and an increase in the consumption of jumbo flying squid and sharpear enope squid. The giant squid was present only in the diets of sharks in size class IV (Fig. 3). Sharks in size classes II and III were the most specialized feeders, whereas sharks in size class I were the least specialized. Sharks in size class II (mean trophic position: 4.34 cm TL) had the lowest trophic position, and sharks in size class IV had the highest trophic position (mean trophic position: 4.63 cm TL). As an overall trend, sharks increased their trophic position as they increased in size.

Of all the other factors assessed (sex, location, season, year, and environmental conditions), ANOSIM showed that the dietary composition of smooth hammerhead differed significantly only between location and year. However, these differences were small (R-statistic<0.25, P<0.05) and an overlap exists between the dietary composition of these factors (Clarke, 1993). We therefore concluded that the diet of smooth hammerhead did not show variability according to the sex, location, season, year, or environmental conditions.

Discussion

Our analyses indicate that the smooth hammerhead has a narrow trophic niche width and a high trophic position and can therefore be considered a specialized top predator. These results complement the findings from other diet studies of smooth hammerhead in the eastern Pacific Ocean (Ecuador and Baja California) and southeastern Africa—studies in which this shark species was found to feed mainly on cephalopods (e.g., jumbo squid, Patagonian squid, whip-lash squid, and sharpear enope squid) (Smale, 1991; Smale and Cliff, 1998; Castañeda and Sandoval, 2004; Estupiñan-Montaño and Cedeño-Figueroa, 2005; Galvan-Magaña et al., 2013). Studies from Ecuador and Baja California showed that the smooth hammerhead is a specialist predator with a trophic level between 4 and 4.5,

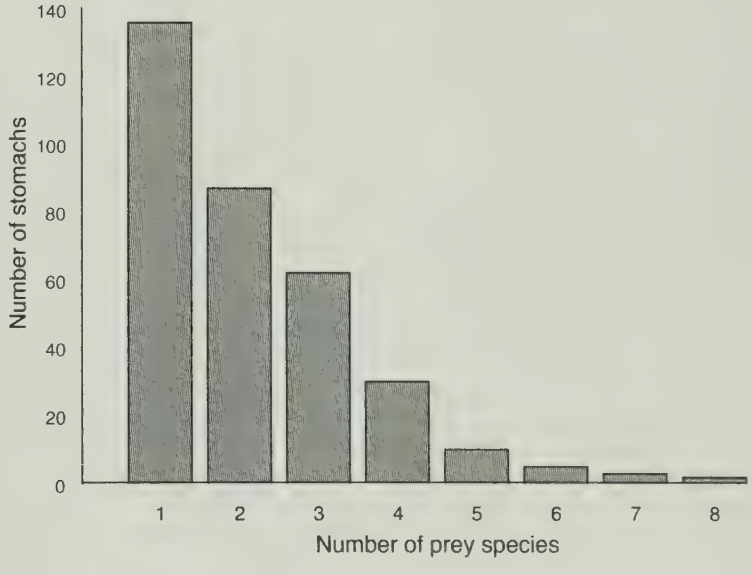

Figure 2

Number of prey species in stomachs of smooth hammerhead (*Sphyrna zygaena*). Smooth hammerheads were collected off northern Peru from December 2012 through June 2015.

Table 3

Comparison of prey items in the diet of smooth hammerhead (*Sphyrna zygaena*) collected from December 2012 through June 2015 in northern Peru, generated from a Bray–Curtis index that is based on the percentage by number of prey (%N) and from *R*-statistics and *P*-values generated from analysis of similarities. Size classes of sharks: I (53–70-cm-TL), II (71–100 cm TL), III (101–190 cm TL) and IV (191–294 cm TL). An asterisk (*) indicates comparisons for which differences were significant ($P<0.001$). "Overlapping" indicates that the diet of smooth hammerhead overlaps for the 2 size classes in each paired comparison (of horizontal and vertical values).

	Size class I		Size class II		Size class III	
	Overlapping	*R*	Overlapping	*R*	Overlapping	*R*
Size class II	33	0.47*	—	—	—	—
Size class III	25	0.71*	66	0.27*	—	—
Size class IV	36	0.29*	26	0.6*	32	0.2

similar to the result of 4.3 that we found in this study (Castaneda, 2004; Estupiñan-Montaño and Cedeño-Figueroa, 2005; Bolaño Martínez, 2009; Galvan-Magaña et al., 2013). Additionally, the fact that 92% of stomach contents examined were in an advanced state of digestion indicates that smooth hammerhead is an intermittent feeder. Stomach contents of a continuous feeder would have food items at different stages of digestion (Medved et al., 1985).

Although we were able to analyze the contribution of cephalopods in the diet, we were limited in our ability to quantify the contribution of fish in the diet. According to the percentage of prey by frequency of occurrence, 12.9% of the diet was composed of fish that could not be identified at a species level owing to their advance state of digestion. Otoliths are often used to identify species because they resist the digestive process. However, in our study, smooth hammerhead preyed upon pelagic fishes with small and expellable otoliths, often preventing species identification (Lombarte et al., 2010). Conversely, the hard structures of squid beaks were easier to detect owing to their larger sizes and resistance to digestion (Braccini et al., 2005). Despite these challenges, although fish as prey may be underestimated, we were still able to identify otoliths and it is clear that fish comprise an important component of the diet of the smooth hammerhead. Future studies could better refine these estimates with the use of complementary methods, such as molecular analysis, that are helpful in identifying taxonomic groups with precision (King et al., 2008). Moreover, future studies should emphasize the collection of samples from sharks greater than 200 cm TL. We were able to collect only 10 samples for size class IV (191–294 cm TL). Therefore our results more accurately represent the diet of neonates and juveniles.

Life stages

Shark species change their diet over the course of their life (Lowe et al., 1996; Wetherbee and Cortés, 2004). In Ecuador, as smooth hammerhead grew, Patagonian squid decreased proportionally in the overall diet composition; whereas jumbo flying squid increased (Bolaño Martínez, 2009). Similarly, in South Africa, juveniles fed on loliginids and adults fed on *Ancistrocheirus* sp. and red flying squid (*Ommastrephes bartramii*) (Smale and Cliff, 1998). Our results are consistent with those reported for Ecuador and South Africa. We found that all size classes had statistically significant differences, except for size classes III and IV, which could be explained by the low sample size of size class IV. Moreover, our samples were composed mainly of neonates and juveniles and included only a small sample size of adults. Therefore, further studies, should include a wider range of sizes to assess fully the trophic ecology of smooth hammerhead over its entire size range.

We found that neonates and small juveniles consumed coastal species (i.e., Patagonian squid, *Peprilus* sp.; Jereb and Roper, 2010), and larger juveniles and adults consumed oceanic species (i.e., jumbo squid, *Ancistrocheirus lesueurii*; Nigmatullin et al., 2001; Jereb and Roper, 2010). These diet habits suggest a change of habitat and distribution. Sharks of size class IV were the only individuals that consumed giant squid, which is a deep-sea species with a vertical distribution range of 200–1000 m (Landman et al., 2004; Jereb and Roper, 2010). In New Zealand, an electronically tagged smooth hammerhead measuring 160 cm TL gave evidence of vertical migrations and a maximum depth recorded at 144 m (Francis, 2016). This finding suggests that larger sharks may be migrating vertically to capture prey. Furthermore, the change in diet from coastal to oceanic prey species can be explained partly by the need to consume prey species of greater biomass and energy content (Navia et al., 2007). The Patagonian squid, for example, provides 3.1 kJ/g, whereas jumbo flying squid provides 6.6 kJ/g (Croxall and Prince, 1982; Abitia-Cardenas et al., 1997). Trophic position of this species rises to a higher level in the food chain as the sharks increased in size, and this has also been ob-

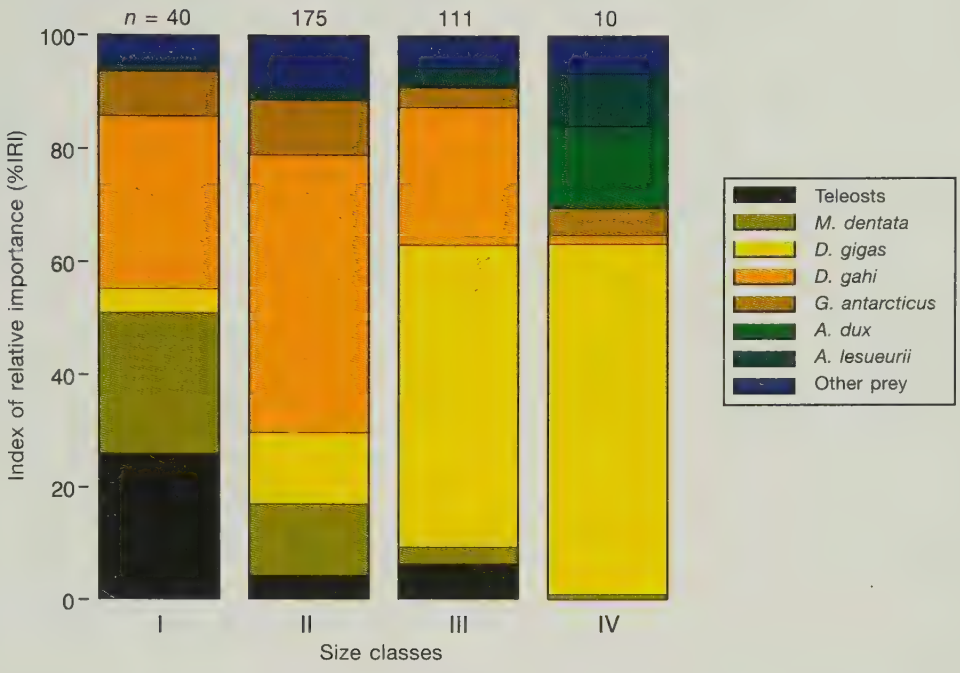

Figure 3

Index of relative importance expressed as a percentage (%IRI) for the 4 size classes (I: 53–70 cm TL, II: 71–100 cm TL, III: 101–190 cm TL, IV: 191–294 cm TL) of smooth hammerhead (*Sphyrna zygaena*) collected off northern Peru from December 2012 through June 2015. The numbers above the bars indicate the sample size (number of stomachs collected) for each size class.

served in other studies of smooth hammerhead (Bolaño Martínez, 2009; Ochoa-Díaz, 2009).

Foraging grounds and predator–prey relations

Populations of jumbo flying squid can impact the dynamics of marine ecosystems, owing in part to the rapid growth characteristics of the species (e.g., rapid growth rate, short life span) (Gilly et al., 2006). For example, an increase in the jumbo flying squid population resulted in population declines of Chilean hake (*Merluccius gayi*) and Pacific hake (*Merluccius productus*), and affected the catches of commercial fisheries for these species along Chile and California (Arancibia and Neira[4]; Jereb and Roper, 2010). In the eastern Pacific Ocean, this study, and previous studies, have identified smooth hammerhead as an important predator of jumbo flying squid and one of the main predators of cephalopods in the eastern Pacific Ocean (Galvan-Magaña et al., 1989; Castañeda and Sandoval, 2004; Estupiñan-Montaño and Cedeño-Figueroa, 2005; Bolaño Martínez, 2009; Ochoa-Díaz, 2009; Galvan-Magaña et al., 2013). It is likely, therefore, that the smooth hammerhead plays an important role as a biological control of cephalopods, and, as a result, has important direct and indirect effects on the viability of multiple fisheries. Furthermore, the high abundance of jumbo flying squid (Nesis, 1983; Nigmatullin et al., 2001; Argüelles et al., 2008) and massive smooth hammerhead fishery landings in northern Peru (Bonfil, 1994; Fischer et al., 2012; Gonzalez-Pestana et al., 2016) make clear that this ocean region represents an important feeding area for smooth hammerhead in the eastern Pacific Ocean. This study contributes to the basic understanding of the trophic ecology of smooth hammerhead and provides information that can also contribute to the design and implementation of national or regional conservation plans for the smooth hammerhead.

[4] Arancibia, H., and S. Neira. 2006. Assessing the potential role of predation by jumbo squid (*Dosidicus gigas*) and fishing on small pelagics (common sardine *Strangomera bentincki* and anchovy *Engraulis ringens*) and common hake (*Merluccius gayi*) in central Chile, 33–39°S. *In* The role of squid in open oceans ecosystems. Report of a GLOBEC-CLIOTOP/PFRP workshop, 16–17 November 2006, Honolulu, HI, USA (R. J. Olson and J. W. Young, eds.), p. 68–70. GLOBEC Rep. 24. [Available from website.]

Acknowledgments

The authors thank the following institutions who funded this study: Fondo para la Innovación, la Ciencia y la Tecnología (PIBA-369-2014), Rufford Foundation, PADI Foundation, Whitney Fund for Nature, and Darwin Initiative. They thank A. Jiménez, S. Pingo, J. Xavier, S.

Kohatsu, A. Sánchez, and A. Arévalo for assistance in collecting, analyzing, and identifying samples, and B. Ramsby for assistance in designing the figures.

Literature cited

Abitia-Cardenas, L. A., F. Galvan-Magaña, and J. Rodriguez-Romero.
1997. Food and energy values of prey of striped marlin, *Tetrapturus audax*, off the coast of Mexico. Fish. Bull. 95:360–368.

Alfaro-Shigueto, J., J. C. Mangel, M. Pajuelo, P. H. Dutton, J. A. Seminoff, and B. J. Godley.
2010. Where small can have a large impact: structure and characterization of small-scale fisheries in Peru. Fish Res. 106:8–17.

Argüelles, J., R. Tafur, A. Taipe, P. Villegas, F. Keyl, N. Dominguez, and M. Salazar.
2008. Size increment of jumbo flying squid *Dosidicus gigas* mature females in Peruvian waters, 1989–2004. Prog. Oceanogr. 79:308–312.

Bolaño Martínez, N.
2009. Ecología trófica del tiburon martillo *Sphyrna zygaena* (Linnaeus, 1758) en aguas Ecuatorianas. M.S. thesis, 140 p. Instituto Politécnico Nacional, Centro Interdisciplinario de Ciencias Marinas, La Paz, Mexico.

Bonfil, R.
1994. Overview of world elasmobranch fisheries. FAO Fish. Tech. Pap. 341, 119 p. Rome, Italy.

Braccini, J. M., B. M. Gillanders, and T. I. Walker
2005. Sources of variation in the feeding ecology of the piked spurdog (*Squalus megalops*): implications for inferring predator–prey interactions from overall dietary composition. ICES J. Mar. Sci. 62:1076–1094.

Casper, B. M., A. Domingo, N. Gaibor, M. R. Heupel, E. Kotas, A. F. Lamónaca, J. C. Pérez-Jimenez, C. Simpfendorfer, W. D. Smith, J. D. Stevens, A. Soldo, and C. M. Vooren.
2005. *Sphyrna zygaena*. The IUCN Red List of Threatened Species 2005: e.T39388A10193797. [Available from website, accessed June 2016.]

Castañeda, J., and L. Sandoval.
2004. Habitos alimentarios de los tiburones martillo *Sphyrna lewini* y *Sphyrna zygaena* en el Pacífico Ecuatoriano. Bachelor's thesis, 138 p. Univ. Jorge Tadeo Lozano, Bogota, Colombia.

Cheung, G. C. K., and C. Y. Chang.
2011. Cultural identities of Chinese business: networks of the shark-fin business in Hong Kong. Asia Pac. Bus. Rev. 17:343–359.

Chirichigno, N., and M. R. Cornejo.
2001. Catalogo comentado de los peces marinos del Perú, 314 p. Publ. Espec. Inst. Mar Perú, Callao, Peru.

Christensen, V., and D. Pauly.
1992. ECOPATH II—software for balancing steady-state ecosystem models and calculating network characteristics. Ecol. Model. 61:169–185.

Clarke, M. R. (ed.).
1986. Handbook for the identification of cephalopod beaks, 273 p. Clarendon Press, Oxford, UK.

Clarke, K. R.
1993. Non-parametric multivariate analysis of changes in community structure. Aust. J. Ecol. 18:117–143.

Cortés, E.
1997. A critical review of methods of studying fish feeding based on analysis of stomach contents: application to elasmobranch fishes. Can. J. Fish. Aquat. Sci. 54:726–738.
1999. Standardized diet compositions and trophic levels of sharks. ICES J. Mar. Sci. 56:707–717.

Cortés E., F. Arocha, L. Beerkircher, F. Carvalho, A. Domingo, M. Heupel, H. Holtzhausen, M. N. Santos, M. Ribera, and C. Simpfendorfer.
2010. Ecological risk assessment of pelagic sharks caught in Atlantic pelagic longline fisheries. Aquat. Living Resour. 23:25–34.

Croxall, J. P., and P. A. Prince.
1982. Caloric content of squid (Mollusca: Cephalopoda). Br. Antarct. Surv. Bull. 55:27–31.

Diemer, K. M., B. Q. Mann, and N. E. Hussey.
2011. Distribution and movement of scalloped hammerhead *Sphryna lewini* and smooth hammerhead *Sphyrna zygaena* sharks along the east coast of southern Africa. Afr. J. Mar. Sci. 33:229–238.

Espinoza, P.
2014. Trophic dynamics in the northern Humboldt Current system: insights from stable isotopes and stomach content analyses. Ph.D. diss., 131 p. Univ. Bretagne Occidentale, Brest, France.

Estupiñan-Montaño, C., and L. Cedeño-Figueroa.
2005. Estudio de los hábitos alimenticios mediante el análisis del contenido estomacal del tollo mico *Carcharhinus falciformis* (Bibron, 1839) y los tiburones martillo *Sphyrna lewini* (Griffith & Smith, 1834) y *Sphyrna zygaena* (Linnaeus, 17758) en el área de Manta—Ecuador. Bachelor's thesis, 133 p. Univ. Laica Eloy Alfaro, Manabí, Ecuador.

Fischer, J., K. Erikstein, B. D'Offay, S. Guggisberg, and M. Barone.
2012. Review of the implementation of the International Plan of Action for the conservation and management of sharks. FAO Fish. Aquat. Circ.1076, 120 p. FAO, Rome.

Fowler, S. L., R. D. Cavanagh, M. Camhi, G. H. Burgess, G. M. Cailliet, S. V. Fordham, C. A. Simpfendorfer, and J. A. Musick (eds.).
2005. Sharks, rays and chimaeras: the status of the chondrichthyan fishes, 481 p. Status survey. IUCN/ SSC Shark Specialist Group. IUCN, Gland, Switzerland and Cambridge, UK.

Francis, M. P.
2016. Distribution, habitat and movement of juvenile smooth hammerhead sharks (*Sphyrna zygaena*) in northern New Zealand. N. Z. J. Mar. Freshw. Res. 50:506–525.

Galvan-Magaña, F., H. J. Nienhuis, and A. P. Klimley.
1989. Seasonal abundance and feeding habits of sharks of the lower Gulf of California, Mexico. Calif. Fish Game 75:74–84.

Galvan-Magaña, F., C. Polo-Silva, S. B. Heranández-Aguilar, A. Sandoval-Londoño, M. R. Ochoa-Díaz, N. Aguilar-Castro, D. Castañeda-Suárez, A. Cabrera Chavez-Costa, Á. Baigorrí-Santacruz, Y. E. Torres-Rojas, et al.
2013. Shark predation on cephalopods by sharks in the Mexican and Ecuadorian Pacific Ocean. Deep-Sea Res. II 95:52–62.

García-Godos Naveda, I.
2001. Patrones Morfológicos del otolito sagitta de algunos peces óseos del mar Peruano. Bol. Inst. Mar Perú 20(1–2):1–61.

Gilly, W. F., U. Markaida, C. H. Baxter, B. A. Block, A. Boustany, L. Zeidberg, K. Reisenbichler, B. Robison, G. Bazzino, and C. Salinas.
2006. Vertical and horizontal migrations by the jumbo squid *Dosidicus gigas* revealed by electronic tagging. Mar. Ecol. Progr. Ser. 324:1–17.

Gonzalez-Pestana, A., J. C. Kouri, and X. Velez-Zuazo.
2016. Shark fisheries in the Southeast Pacific: a 61-year analysis from Peru. F1000Research 3:164.

Hyslop, E. J.
1980. Stomach content analysis—a review of methods and their application. J. Fish Biol. 17:411–429.

Jereb, P., and C. F. E. Roper (eds.).
2010. Cephalopods of the world. An annotated and illustrated catalogue of cephalopod species known to date, vol. 2: myopsid and oegopsid squids. FAO Species Catalogue for Fisheries Purposes 4, vol. 2, 605 p. FAO, Rome.

Jimenez-Valderde, A., and J. Hortal.
2003. Las curvas de acumulación de especies y la necesidad de evaluar la calidad de los inventarios biolgicos. Rev. Ibérica Aracnologia 8:151–161.

King, R. A., D. S. Read, M. Traugott, and W. O. C. Symondson.
2008. Molecular analysis of predation: a review of best practice for DNA-based approaches. Mol. Ecol. 17:947–963.

Iverson, L. K., and L. Pinkas.
1971. A pictorial guide to beaks of certain eastern Pacific cephalopods. *In* Food habits of albacore, bluefin tuna, and bonito in California waters, p. 83–105. Calif. Dep. Fish Game, Fish Bull. 152.

Labropoulou, M., and A. Eleftheriou.
1997. The foraging ecology of two pairs of congeneric demersal fish species: importance of morphological characteristics in prey selection. J. Fish. Biol. 50:324–340.

Landman, N. H., J. K. Cochran, R. Cerrato, J. Mak, C. F. E. Roper, and C. C. Lu.
2004. Habitat and age of the giant squid (*Architeuthis sanctipauli*) inferred from isotopic analyses. Mar. Biol. 144:685–691.

Lombarte, A., M. Palmer, J. Matallanas, J. Gómez-Zurita, and B. Morales-Nin.
2010. Ecomorphological trends and phylogenetic inertia of otolith sagittae in Nototheniidae. Environ. Biol. Fish. 89:607–618.

Lowe, C. G., B. M. Wetherbee, G. L. Crow, and A. L. Tester.
1996. Ontogenetic dietary shifts and feeding behavior of the tiger shark, *Galeocerdo cuvier*, in Hawaiian waters. Environ. Biol. Fish. 47:203–211.

Lu, C. C., and R. Ickeringill.
2002. Cephalopod beak identification and biomass estimation techniques: tools for dietary studies of southern Australian finfishes. Mus. Vic. Sci. Rep. 6, 65 p. Mus. Vic., Fish. Res. Dev. Corp., Melbourne, Australia.

Magurran, A. E.
1988. Ecological diversity and its measurement, 179 p. Princeton Univ. Press, Princeton, NJ.

Medved, R. J., C. E. Stillwell, and J. J. Casey.
1985. Stomach contents of young sandbar sharks, *Carcharhinus plumbeus*, in Chincoteague Bay, Virginia. Fish. Bull. 83:395–402.

Navia, A. F., P. A. Mejía-Falla, and A. Giraldo.
2007. Feeding ecology of elasmobranch fishes in coastal waters of the Colombian Eastern Tropical Pacific. BMC Ecol. 7:8.

Nigmatullin, C. M., K. N. Nesis, and A. I. Arkhipkin.
2001. A review on the biology of the jumbo squid *Dosidicus gigas* (Cephalopoda: Ommastrephidae). Fish. Res. 54:9–19.

Nesis, K. N.
1983. *Dosidiscus gigas*. *In* Cephalopod life cycles, vol. 1: species accounts (P. R. Boyle, ed.), p. 215–231. Academic Press, London, UK.

Ochoa-Díaz, M. R.
2009. Espectro trófico del tiburón martillo *Sphyrna zygaena* (Linnaeus, 1758) en Baja California Sur: aplicación de $\delta^{13}C$ y $\delta^{15}N$. M.S. thesis, 90 p. Cent. Interdiscip. Cienc. Mar., Inst. Politéc. Nac., La Paz, Mexico.

Pennington, J. T., K. L. Mahoney, V. S. Kuwahara, D. D. Kolber, R. Calienes and F. P. Chavez.
2006. Primary production in the eastern tropical pacific: a review. Prog. Oceanogr. 69:285–317.

R Core Team.
2016. R: a language and environment for statistical computing. R Foundation for Statistical Computing, Vienna, Austria. [Available from website, accessed October 2016.]

RStudio.
2012. RStudio: integrated development environment for R. RStudio Inc., Boston, MA. [Available from website, accessed May 2012.]

Smale, M. J.
1991. Occurrence and feeding of three shark species, *Carcharhinus brachyurus, C. obscurus* and *Sphyrna zygaena*, on the Eastern Cape coast of South Africa. S. Afr. J. Mar. Sci. 11:31–42.

Smale, M. J., and G. Cliff.
1998. Cephalopods in the diets of four shark species (*Galeocerdo cuvier*, *Sphyrna lewini, S. zygaena* and *S. mokarran*) from KwaZulu-Natal, South Africa. S. Afr. J. Mar. Sci. 20:241–253.

Soberón, J., and J. Llorente.
1993. The use of species accumulation functions for the prediction of species richness. Conserv. Biol. 7:480–488.

Spalding, M. D., H. E. Fox, G. R. Allen, N. Davidson, Z. A. Ferdaña, M. Finlayson, B. S. Halpern, M. A. Jorge, A. Lombana, S. A. Lourie, et al.
2007. Marine ecoregions of the world: a bioregionalization of coastal and shelf areas. BioScience 57:573–583.

Xavier, J. C., and Y. Cherel.
2009. Cephalopod beak guide for the southern ocean, 129 p. Br. Antarct. Surv., Cambridge, UK.

Wetherbee, B. M., and E. Cortés.
2004. Food consumption and feeding habits. *In* Biology of sharks and their relatives. (J. A. Carrier, J. C. Musick, and M. R. Heithaus, eds.), p. 225–246. CRC Press, Boca Raton, FL.

Wolff, G. A.
1982. A beak key for eight eastern tropical Pacific cephalopod species with relationships between their beak dimensions and size. Fish. Bull. 80:357–370.
1984 Identification and estimation of size from the beaks of 18 species of cephalopods from the Pacific Ocean. NOAA Tech. Rep. NMFS 17, 50 p.

National Marine Fisheries Service
NOAA

Fishery Bulletin
established in 1881

Spencer F. Baird
First U.S. Commissioner of Fisheries and founder of *Fishery Bulletin*

Growth, mortality, and movement of cobia (*Rachycentron canadum*)

David A. Dippold (contact author)[1]
Robert T. Leaf[1]
James S. Franks[2]
J. Read Hendon[2]

EEmail address for contact author: dippold.14@buckeyemail.osu.edu

[1] Division of Coastal Sciences
The University of Southern Mississippi
703 East Beach Drive
Ocean Springs, Mississippi 39564
Present address for contact author: Department of Evolution, Ecology, and Organismal Biology
The Ohio State University
1314 Kinnear Road
Columbus, Ohio 43212

[2] Center for Fisheries Research and Development
Gulf Coast Research Laboratory
The University of Southern Mississippi
703 East Beach Drive
Ocean Springs, Mississippi 39564

Abstract—We describe the length-at-age relationship of cobia (*Rachycentron canadum*) with the use of 3 nonlinear models, and examine both the movement patterns of cobia in the Gulf of Mexico and South Atlantic Ocean and the instantaneous total mortality rate (Z, per year) from tag-recovery models with data from the Sport Fish Tag and Release Program of the University of Southern Mississippi Gulf Coast Research Laboratory. The estimated mean asymptotic length (L_∞) in this study (1172 mm in fork length [95% confidence interval (CI): 1151–1192]) was in the range of values reported for this species in the Gulf of Mexico and Atlantic Ocean, and the annual growth coefficient (k: 0.57 [95% CI: 0.52–0.61]) was greater than that reported for cobia elsewhere. Movements were reported between the Gulf of Mexico and the South Atlantic Ocean and a statistically significant seasonal trend in recaptures was observed, both of which suggest that cobia inhabit the Florida Keys during the winter and the northcentral Gulf of Mexico during the summer. The most supported tag-recovery model included time-invariant survivorship and time-dependent recovery probability and the estimated Z was 0.59/year (95% CI: 0.55–0.63). This study provides a summary of a long-term cobia tagging program and information for future management of this species.

Manuscript submitted 12 August 2016.
Manuscript accepted 6 July 2017.
Fish. Bull. 115:460–472 (2017).
Online publication date: 1 August 2017.
doi: 10.7755/FB.115.4.3

The views and opinions expressed or implied in this article are those of the author (or authors) and do not necessarily reflect the position of the National Marine Fisheries Service, NOAA.

The cobia (*Rachycentron canadum*) is a globally distributed, coastal pelagic species that supports both recreational and commercial fisheries in the Gulf of Mexico and U.S. Atlantic Ocean. Although cobia landings are primarily recreational (>80% of total annual landings 1990 to 2011; SEDAR[1]), cobia are also harvested commercially and caught incidentally as bycatch in shrimp fisheries. Cobia is currently managed and assessed as separate Gulf of Mexico and South Atlantic Ocean stocks, and harvest is regulated by an 84 cm (33 in) minimum fork length (FL) limit and a daily bag limit of 2 fish per angler. Since 2012, quotas have also been used to set annual harvest limits. Despite the historic and continued recreational and commercial harvest of cobia, very few assessments have been conducted to determine the status of the Gulf of Mexico and South Atlantic Ocean stocks. The Gulf of Mexico stock was previously assessed in 1996 (Thompson[2]) by using virtual population analysis and in 2001 by using a surplus production model (Williams, 2001). The South Atlantic Ocean stock was previously assessed in 1994 and 1995 by using virtual population analysis (Thompson[3,4]).

[1] SEDAR (Southeast Data Assessment and Review). 2013. SEDAR 28—Gulf of Mexico cobia stock assessment report, 616 p. SEDAR, North Charleston, SC. [Available from website.]

[2] Thompson, N. B. 1996. An assessment of cobia in southeast U.S. waters. Natl. Mar. Fish. Serv., Southeast Fish. Sci. Cent., Miami Lab. Contrib. No. MIA-95/96-28, 16 p. [Available from website.]

[3] Thompson, N. B. 1994. An assessment of cobia in southeast U.S. waters. Natl. Mar. Fish. Serv., Southeast Fish. Sci. Cent., Miami Lab. Contrib. No. MIA-93/94-38, 17 p. [Available from website.]

[4] Thompson, N. B. 1995. An assessment of cobia in southeast U.S. waters. Natl. Mar. Fish. Serv., Southeast Fish. Sci. Cent., Miami Lab. Contrib. No. MIA-94/95-31, 25 p. [Available from website.]

The species has only recently been assessed under the Southeast Data, Assessment, and Review (SEDAR) process (SEDAR[1]) and the most recent SEDAR assessment involved a separate assessment of the Gulf of Mexico and South Atlantic Ocean stocks.

In the most recent SEDAR assessments, several information gaps were identified which limited the determination of the status of both the Gulf of Mexico and South Atlantic Ocean cobia stocks. Specifically, there was an insufficient amount of information available to accurately determine stock boundaries, and further descriptions of life-history characteristics and population dynamics were needed. Towards this end, we used information from the Sport Fish Tag and Release Program of the University of Southern Mississippi Gulf Coast Research Laboratory (Hendon and Franks[5]) to investigate the growth, movement, and mortality of cobia in the Gulf of Mexico and South Atlantic Ocean in order to fill critical information gaps regarding life-history and population dynamics for this species, as well as to corroborate existing life-history descriptions by using an alternative source of information. We focus on the stocks of the Gulf of Mexico and South Atlantic Ocean, given that stocks of these areas were the focus of a cooperative tagging program.

Cooperative tagging programs can provide valuable information at the individual and population levels and on the fishery dynamics of recreationally and commercially harvested species (Wood and Cadrin, 2013). Cooperative tagging programs have been implemented for several groups of marine fishes, such as dolphinfish, sailfish, marlin, and sharks, and information from these programs has provided invaluable and previously unreported information on the movement and biology of these taxa (Jones and Prince, 1998; Kohler et al., 1998; Ortiz et al., 2003). For example, cooperative tagging programs have been used to estimate mortality (Pine et al., 2003; Wood and Cadrin, 2013), describe individual growth dynamics (Simpfendorfer, 2000; Dippold et al., 2016), and show movement patterns (Hendon et al., 2002; Queiroz et al., 2005; Hussey et al., 2009). In this study we used similar methods with a 27-year cooperative tagging data set (Hendon and Franks[5]). Although other cobia tagging programs exist in the Gulf of Mexico and South Atlantic Ocean (Shaffer and Nakamura, 1989; Burns and Neidig[6]; Wiggers[7]; Orbesen[8]), to our knowledge the Sport Fish Tag and Release Program is the most comprehensive.

Individual growth has previously been described in cobia by using otolith- and scale- derived age estimates, and annuli formation has been validated by using marginal increment analysis (Richards, 1967; Thompson et al.[9]; Smith, 1995; Franks et al., 1999). However, the use of marginal increment analysis as a method for age validation can be problematic because of the difficulty in interpreting the otolith margin and because of the need to validate annuli formation across the entire lifespan of a species (Campana, 2001). Age corroboration, or the estimation of growth parameters with alternative methods, is used to increase confidence in growth model parameter estimates (Campana, 2001). Specifically, tag-recapture information for estimating growth parameters has been used as an alternative method for describing the length-at-age relationship in several marine species (Natanson et al., 1999; Dippold et al., 2016). No age corroboration method has been evaluated for cobia, and because cobia are assessed by using a statistical catch-at-age model (SEDAR[1]), accurate descriptions of length-at-age are needed to estimate age-specific vital rates such as instantaneous fishing-induced [also termed "fishing mortality] and natural mortality. In this study, we use a suite of nonlinear length-at-age models to analyze tag-recapture data in order to corroborate existing estimates of the length-at-age relationship of cobia.

In addition to describing the length-at-age relationship, information from tagging programs can be used to describe general and seasonal movement and distribution patterns and to determine stock boundaries (Wood and Cadrin, 2013; Kneebone et al., 2014). The results of small-scale cooperative tagging of cobia have suggested that some individuals migrate long distances and indicate seasonal movement patterns (Shaffer and Nakamura, 1989; Burns and Neidig[6]; Wiggers[7]; Orbesen[8]). However, in these studies, either relatively few individuals were tagged, only a small portion of tagged individuals was recaptured, the study occurred over a small sampling period, or long-distance movement was reported for only a few individuals. The determination of cobia stock boundaries is critical given the reported movements of this species between ocean basins. Genetic analysis to determine cobia stock discrimination has been evaluated for the Atlantic Ocean but has not been evaluated for the Gulf of Mexico (Darden et al., 2014). Because of the lack of resolution regarding seasonal movement patterns and the degree of mixing between the Gulf of Mexico and Atlantic Ocean cobia populations from both tagging and genetic studies, the current stock boundary between the Gulf of Mexico and

[5] Hendon, J. R. and J. S. Franks. 2010. Sport fish tag and release in Mississippi coastal waters and the adjacent Gulf of Mexico. Gulf Coast Res. Lab. Tech. Rep. F-132, 34 p. [Available from Gulf Coast Research Laboratory, 703 East Beach Dr., Ocean Springs, MS 39564.]

[6] Burns, K. M., and C. L. Neidig. 1992. Cobia (*Rachycentron canadum*) amberjack (*Seriola drumerili*) and dolphin (*Corypheana hippurus*) migration and life history study off the southwest coast of Florida. Mote Mar. Lab. Tech. Rep. 267, 58 p. [Available from website.]

[7] Wiggers, R. K. 2010. South Carolina marine game fish tagging program 1978–2009. South Carolina Dep. Nat. Resour., Charleston, SC. [Available from website.]

[8] Orbesen, E. 2012. Constituent based tagging of cobia in the Atlantic and Gulf of Mexico waters. Southeast Data Assessment and Review SEDAR28-DW13, 10 p. [Available from website.]

[9] Thompson, B. A., C. A. Wilson, J. H. Render, and M. Beasley. 1992. Age, growth, and reproductive biology of greater amberjack and cobia from Louisiana waters, 55 p. Louisiana State University, Baton Rouge, LA.

Atlantic Ocean cobia stocks needs to be more accurately defined (SEDAR[1]) to aid future assessments.

Estimates of mortality from tagging programs can improve stock assessment efforts by providing an alternative estimate of natural, fishing, or total mortality independent of the stock assessment model (Wood and Cadrin, 2013; Kerns et al., 2015). Several types of tag-recapture methods exist (Pine et al., 2003), and for cooperative tagging programs, tag-recovery models are used to estimate survivorship and the probability of tag recovery (Brownie et al., 1985). Tag-recovery methods for estimating mortality have been used for yellowtail flounder (*Limanda ferruginea*) in New England (Wood and Cadrin, 2013), walleye (*Sander vitreus*) in Lake Erie (Vandergoot and Brenden, 2014) and paddlefish (*Polyodon spathula*) in a South Dakota lake (Pierce et al., 2015). Estimates of mortality derived from tag-recapture data can be used to corroborate estimates derived with age-structured models or life-history–based approaches (Then et al., 2015).

The goals for this study were to use data from a 27-year cooperative tagging program to describe the growth, mortality, and movement of cobia in the Gulf of Mexico and South Atlantic Ocean. Specifically, we 1) describe the length-at-age relationship of cobia using a suite of nonlinear length-at-age models fitted to the tag-recapture data, 2) report cobia movement between the Gulf of Mexico and South Atlantic Ocean, 3) describe the spatial and seasonal distribution of cobia in the Gulf of Mexico, and 4) estimate annual instantaneous total mortality (Z), using a suite of tag-recovery models. The results of this study will help fill existing information gaps and provide critical information to support the sustainable management of cobia in the Gulf of Mexico and South Atlantic Ocean.

Materials and methods

Tagging and recapture

The Sport Fish Tag and Release Program (Hendon and Franks[5]) began in 1988 as a cooperative tagging program during which volunteer recreational anglers tagged cobia with 10-cm plastic-tipped dart tags (Hallprint Pty. Ltd. [10], Hindmarsh Valley, Australia). Anglers participating in the program received tagging kits containing tags with unique numerical identifiers, data reporting cards, a tag applicator, and a booklet containing tagging instructions. Tagging guidelines provided with the tagging kit instructed anglers on the proper tag-release procedures to enhance tag retention and ensure safe handling of tagged fish before release. At the time of tagging, volunteer anglers recorded information on the approximate tagging location, date, the length of the fish (typically measured as FL in inches), and a qualitative description of fish condition at time of release. Anglers then mailed the tag-reporting card to the Gulf Coast Research Laboratory where the tagging data were recorded and entered into an electronic tag-recapture database. If a fish was recaptured, anglers were asked to report their catch by email, mail, or phone to the Gulf Coast Research Laboratory and provide information on the date of capture, location of catch, length-at-recapture, and whether the fish was retained or released, and if released, to provide a qualitative report on its condition.

The cooperative tagging program was advertised broadly and frequently. Posters describing the program were distributed to bait and tackle shops, boat launches, fishing tournaments, and sporting goods stores. The program was also occasionally reported in the media through newspaper articles, local television interviews, and regional fishing magazines. No financial incentives were offered during the program duration, but anglers who tagged numerous cobia in a given year were given informal recognition in the media and regional fishing magazines. Often, anglers who recaptured a tagged cobia became interested in obtaining a cobia tagging kit.

Growth

To describe the length-at-age relationship, 3 nonlinear length-at-age models were fitted to the cobia tag-recapture informatiion. Multimodel approaches for describing growth can help reduce model misspecification and can help identify the most appropriate length-at-age model to use for a particular species (Katsanevakis, 2006). Each of the 3 models used were reparameterized versions of commonly used length-at-age models, reformulated to fit the observed change in length information over the time that tagged fish were at large. Before model fittings, if a length-at-tagging or recapture was reported as total length (TL), it was converted to FL by using a TL-to-FL linear model conversion. The first model used was the Fabens (1965) von Bertalanffy growth function (VBGF). The Fabens model is

$$\Delta L = (L_\infty - L_t)(1 - e^{-k\Delta t}), \quad (1)$$

where L_∞ = the mean asymptotic length (millimeters in FL); and
k = the growth coefficient (per year).

The observed data used in the model are ΔL, the change in length (millimeters in FL), and Δt, the time between tagging and recapture events (in years).

The second model used to describe the length-at-age relationship of cobia was a reparameterized Gompertz model (Troynikov et al., 1998):

$$\Delta L = L_\infty \left(\frac{L_i}{L_\infty}\right)^{\exp(-k\Delta t)} - L_i, \quad (2)$$

where L_∞ = again the mean asymptotic FL (millimeters in FL); and
k = the decrease in growth increment (per year) as length increases.

The observed data used in the model are Δt (years), the

[10]Mention of trade names or commercial companies is for identification purposes only and does not imply endorsement by the National Marine Fisheries Service, NOAA.

time between tagging and recapture, and L_i the length at tagging (millimeters in FL).

The final model used to describe the length-at-age relationship of cobia was the VBGF formulation GROTAG, which is based on the methods discussed in Francis (1988). The Francis (1988) equation is

$$\Delta L = \left(\frac{\beta g_\alpha - \alpha g_\beta}{g_\alpha - g_\beta} - L_1\right)\left(1 - \left(1 + \frac{g_\alpha - g_\beta}{\alpha - \beta}\right)^{\Delta t}\right), \quad (3)$$

where ΔL = the expected change in length (millimeters in FL);
Δt= the time-at-large (years);
L_1 = the length of an individual at tagging (millimeters in FL); and
g_α and g_β = the mean annual growth rates (millimeters per year) of fish at user-selected lengths α and β (millimeters in FL).

The lengths α and β are chosen based on the range of lengths included in the tag-recapture records so that g_α and g_β are descriptive of the individual growth rates encompassed by the tagging data (Francis, 1988). In this study α was 500 mm FL and β was 1100 mm FL. After fitting the model, L_∞ (millimters in FL) can be estimated from g_α and g_β with the following equation:

$$L_\infty = \left(\beta g_\alpha - \alpha g_\beta\right)\left(g_\alpha - g_\beta\right). \quad (4)$$

Similarly, k (per year) can be calculated from the GROTAG VBGF model parameters by using the following equation:

$$k = -\ln(1 + (g_\alpha - g_\beta)/(\alpha - \beta)) \quad (5)$$

The 95% confidence intervals (CIs) of L_∞ and k were determined by using bootstrap methods similar to those described in Simpfendorfer (2000).

After each model was fitted, the performance of the 3 candidate models was compared by using Akaike's information criterion (AIC) (Burnham and Anderson, 2002) and model support was evaluated by using Akaike weights (w_i). The mean growth-parameter estimates of the best supported model(s) were compared with those reported in other studies of cobia growth published in the literature. All analyses were conducted in R, vers. 3.3.0 (R Core Team, 2016).

Movement and seasonal distribution

Broad-scale seasonal and general movements were described in this study by defining 7 spatial zones and quantifying the spatial and temporal patterns of fish tagged and recaptured among the zones. The criteria we used to define the 7 spatial zones were based on areas where recreational fishermen are known to target cobia and where boundaries exist that could be useful to managers when setting harvest regulations (e.g., state boundaries). Zones were also identified because exact locations of capture or recapture are generally not reported. In this study, the 7 geographic zones defined were Texas, Louisiana, northcentral Gulf of Mexico, Florida panhandle, Florida Gulf Coast, Florida Keys, and the U.S. South Atlantic Ocean (Fig. 1). We focused on the Gulf of Mexico and South Atlantic Ocean because those were the areas in which the cooperative tagging program occurred. Movement among zones was described by calculating the proportion of recaptured individuals in each zone that were tagged in a specific zone. We included only individuals whose time at liberty was greater than or equal to 30 days. Our analysis was used to investigate large-scale movement between geographic areas and to identify whether individual cobia traveled between the Gulf of Mexico and South Atlantic Ocean.

The relationship between recapture zone and month of recapture was evaluated by using a loglinear model to infer trends in seasonal distribution of recaptured cobia in the Gulf of Mexico. Recaptures from the South Atlantic Ocean were not included in the analysis to meet assumptions in the model regarding nonzero expected frequencies within each month–zone combination and because of the limited number of reported recaptures in the South Atlantic Ocean. We set a minimum time-at-liberty of 30 days to allow for tagged fish to return to normal mixing behavior. Loglinear models are an extension of the chi-square test and are used to determine associations between categorical variables (Knoke and Burke, 1980). A saturated loglinear model (with recapture zone and recapture month as the main effects) and a 2-way interaction term were constructed to evaluate the association between month of recapture and recapture zone. The saturated model is

$$\log(u_{ij}) = \lambda^{\text{zone}} + \lambda^{\text{month}} + \lambda^{\text{zone} \times \text{month}}, \quad (6)$$

where $\log(u_{ij})$ = the expected counts in each zone–month combination; and
λ = the main effect of each predictor variable.

If no significant interaction is observed in the saturated model (indicating a good model fit), the interaction term is dropped and a second model with only the main effects is constructed. If this model is significant, i.e., the model does not fit the data well after removing the interaction term, the association between the main effects is considered significant (i.e., the model fits better when there is an association between the main effects). Finally, a mosaic plot was constructed that was based on the loglinear model to identify specific recapture zone and recapture month combinations that were statistically significant. Mosaic plots are useful visual representations that allow determination of statistically significant month–zone groups. Typically, the shading of mosaic plots represents the residuals (deviations) from the loglinear model for each cell. In this study, the shading of the mosaic plot represents the values of the Pearson (standardized) residuals and a value greater than 2 or less than –2 is considered significant.

Mortality

Estimates of Z were determined by using a suite of tag-recovery models fitted to the cobia tagging data in

Figure 1

Map of the 7 geographic zones used to determine large-scale and seasonal movements of cobia (*Rachycentron canadum*) tagged and recaptured in the Gulf of Mexico and South Atlantic Ocean during 1988–2014. The 7 zones are Texas (TX), Louisiana (LA), northcentral Gulf of Mexico (NcGOM), Florida panhandle (FLPH), Florida Gulf Coast (FLGC), Florida Keys (FLK), and the South Atlantic Ocean (ATL).

Program MARK, vers 7.2 (Brownie et al., 1985; White and Burnam, 1999). The tag-recovery model is based on the probability that a tagged individual will experience one of the following 3 events: it will survive to the next year; be harvested by an angler and reported; or it will die of natural causes or be harvested and not reported (Fig. 2). In this analysis, maximum likelihood was used to estimate 2 parameters in the tag-recovery model: survivorship to the next year (S) and the probability of tag recovery (f). The f parameter is the joint probability that a tagged cobia will be recaptured, harvested, and reported. In all candidate models, an annual time-step was used (n=27 years). We assume that all tagged individuals had an equal probability of being recaptured, and that tagging occurs instantaneously during the designated time interval. The suite of models we evaluated included all combinations of time-dependent (t) and time-independent (.) survi-

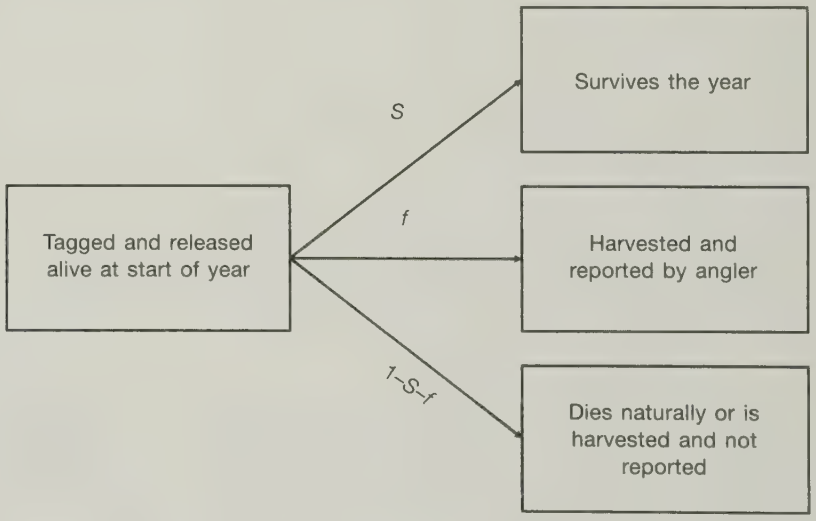

Figure 2

Conceptual diagram of the Brownie et al. (1985) tag-recovery model used to estimate instantaneous total mortality of cobia (*Rachycentron canadum*) in the Gulf of Mexico and South Atlantic Ocean, with 2 parameters, for survivorship (S) and probability of tag recovery (f).

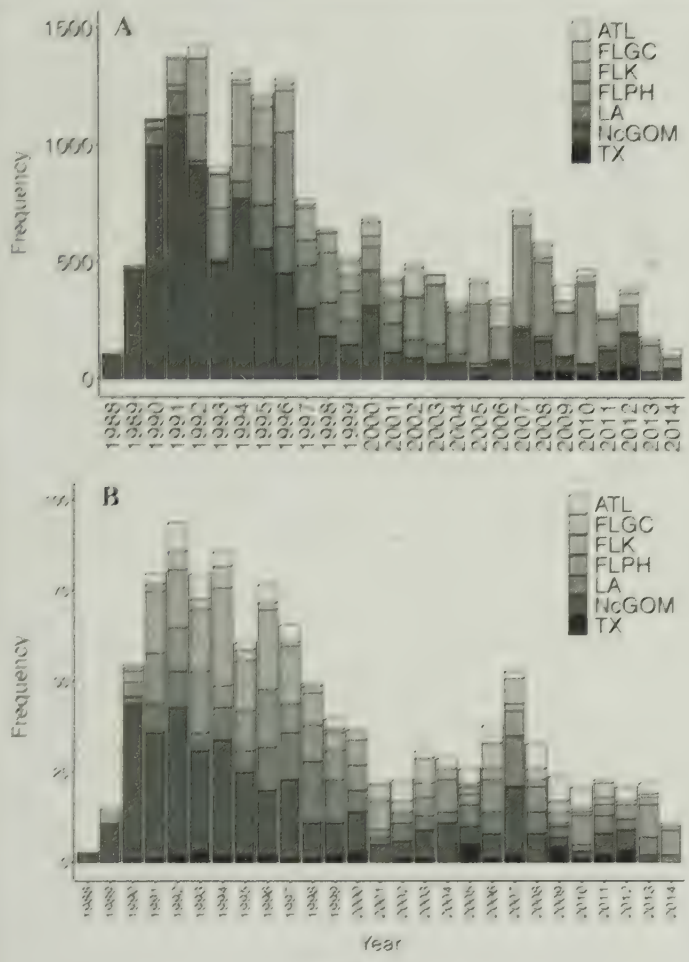

Figure 3

Total number of cobia (*Rachycentron canadum*) (**A**) tagged and (**B**) recaptured by year in each of 7 geographic zones in the Gulf of Mexico and South Atlantic Ocean during 1988–2014. The 7 defined zones are the South Atlantic Ocean (ATL),Florida Gulf Coast (FLGC), Florida Keys (FLK), Florida panhandle (FLPH), Louisiana (LA), northcentral Gulf of Mexico (NcGOM), and Texas (TX).

vorship and tag-recovery (4 candidate models). Time-dependent parameters were those that varied by year and time-independent parameters were those that were constant through the duration of the tagging program. The global model (fully parameterized) was defined as having time-dependent survivorship, $S(t)$, and time-dependent tag-recovery, $f(t)$. Global model fit was evaluated by using the constant noted as $\hat{c}$, which is an estimate of dispersion used in Program MARK. To estimate dispersion, a simulation procedure is used in which data are generated at varying levels of $\hat{c}$ and a logistic model is then fitted to estimate $\hat{c}$ for the global model. A $\hat{c}$ value of less than 3.0 indicates adequate model fit. After the suite of candidate models were fitted to the tag-recapture data and the global model was determined to adequately fit the data, model support was evaluated by using AIC (Burnham and Anderson, 2002). The model with the greatest support (lowest AIC value) was used to estimate mean annual Z. The estimates of Z derived in this study were then compared with the mortality values reported in both the Gulf of Mexico and South Atlantic Ocean cobia stock assessments (SEDAR[1]) by converting the value of S estimated in this study to an estimate of Z with the equation

$$S = e^{-Z}. \quad (7)$$

Results

Tagging program

A total of 17,875 cobia were tagged from 1988 to 2014. The number of individuals tagged annually ranged from 113 to 1423 individuals. A majority (57%) of tagging occurred between 1990 and 1998 (Fig. 3). The reported length of tagged individuals ranged from 178 mm to 1549 mm FL (Fig. 4A). A total of 1137 individuals were recaptured, and the number of recaptured individuals annually varied from 3 to 94 individuals. The annual number of individuals recaptured was greatest from 1990 to 1998 (Fig. 3). The reported length of recaptured individuals ranged from 305 to 1448 mm FL (Fig. 4B), and the time between tagging and recapture ranged from 1 to 2973 days at large (Fig. 4C). Of the 7 zones defined in this study, the northcentral Gulf of Mexico zone had the greatest number of tagged and recaptured individuals and the Texas zone had the fewest number of tagged and recaptured individuals (Table 1).

Growth

Only individuals for which lengths at tagging and recapture were recorded were used in the growth analysis (n=926). All reported lengths were converted to FL using the linear relationship between TLs and FLs (FL=0.91TL+0.23; coefficient of determination [r^2]=0.98) developed from lengths reported in this study. Sex of tagged and recaptured individuals was not reported in this cooperative tagging program and therefore we modeled sex-combined length-at-age. The 3 nonlinear length-at-models were fitted, and the relative model support was evaluated with AIC (Table 2). Of the 3 candidate models, the GROTAG VBGF was best supported on the basis of calculated values of w_i (~1.0). However, on the basis of the mean and 95% CIs of the L_∞ parameter, there was no difference in the mean estimates of L_∞ among the 3 candidate models. The mean value of k did vary (on the basis of 95% CIs) for each of the 3 candidate models. Specifically, the mean value of k estimated in the GROTAG VBGF

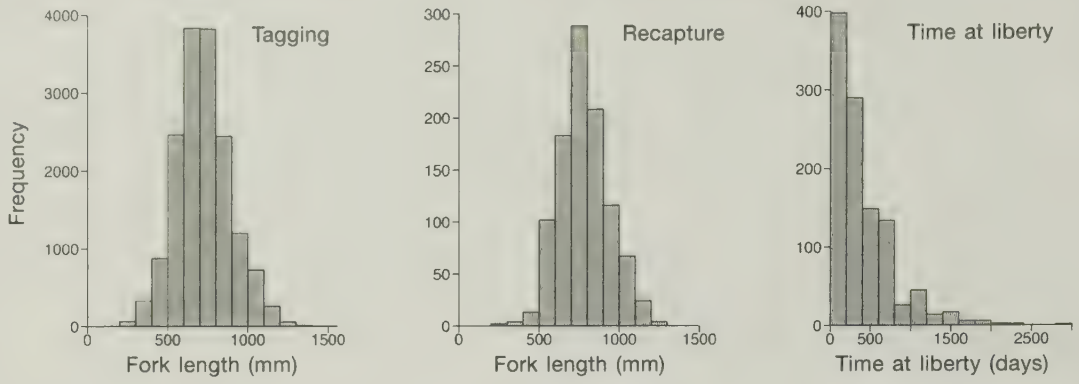

Figure 4

Histograms of length frequency for cobia (*Rachycentron canadum*) at tagging, and recapture , and time at liberty from time of tagging to time of recapture in the Gulf of Mexico and South Atlantic Ocean during 1988–2014.

Table 1

Total number of cobia (*Rachycentron canadum*) tagged and recaptured during 1988–2014 in each of 7 geographic zones in the Gulf of Mexico and South Atlantic Ocean. The 7 zones are South Atlantic Ocean (ATL), Florida Gulf Coast (FLGC), Florida Keys (FLK), Florida panhandle (FLPH), Louisiana (LA), northcentral Gulf of Mexico (NcGOM), and Texas (TX).

Zone	Tagged	Recaptured
ATL	557	90
FLGC	961	73
FLK	1518	189
FLPH	4620	190
LA	1703	166
NcGOM	8112	373
TX	227	40

(0.57/year [95% CI: 0.52–0.61]) was lower than the values from both the Fabens VBGF model (0.62/year [95% CI: 0.56–0.69]) and the Gompertz model (0.84/year [95% CI: 0.77–0.92]). The estimated value of L_∞ from the GROTAG VBGF model was in the range of values reported from Virginia, Louisiana, North Carolina and the Gulf of Mexico (Richards, 1967; Thompson et al.[9]; Smith, 1995; Franks et al., 1999; Table 3). However, the estimate of k was higher in our analysis than those values reported for Virginia, North Carolina and the Gulf of Mexico (Table 3). The closest values to those estimated in this study were the estimates of k reported from Louisiana (Thompson et al.[9]). In the most recent Gulf of Mexico and South Atlantic Ocean assessments, the models used to describe length-at-age relationships were also sex aggregated (SEDAR[1]), however the estimates of L_∞ in the SEDAR assessments were greater than the estimate in our study and the SEDAR estimates of k were lower than the value estimated in our study (Table 3).

Table 2

Parameter estimates, with 95% confidence intervals, from nonlinear models fitted to information on tagging and recapture of cobia (*Rachycentron canadum*) in the Gulf of Mexico and South Atlantic Ocean during 1988–2014. The mean asymptotic length (L_∞), provided as millimeters in fork length (CI=confidence interval), and the annual growth coefficient (k) were estimated for 2 parameterizations of the von Bertalanffy growth function (VBGF) and a Gompertz model. The 2 parameterizations were the VBGF used in the program GROTAG and the VBGF used by Fabens (1965). The relative model support was evaluated by using Akaike's information criterion (AIC), and Akaike weight (w_i) was calculated for each model.

Model	L_∞ (CI)	k	ΔAIC	w_i
GROTAG VBGF	1172 (1151–1192)	0.57 (0.52–0.61)	0.00	1.00
Fabens VBGF	1189 (1163–1219)	0.62 (0.56–0.69)	119.70	0.00
Gompertz	1157 (1135–1181)	0.84 (0.770.92)	153.80	0.00

Table 3

Estimates of von Bertalanffy growth function parameters for cobia (*Rachycentron canadum*) from previously published studies and this study. The 3 parameters are mean asymptotic length (L_∞), provided as millimeters in fork length (FL), annual growth coefficient (k), and hypothetical age at length of zero (t_0). For parameter values, standard errors of the mean are provided for some studies and the 95% confidence intervals (CIs) are provided for this study in parentheses. The locations were Virginia (VA), Louisiana (LA), North Carolina (NC), the northeastern Gulf of Mexico (nGOM), and the Gulf of Mexico (GOM).

Study	Location	Sex	n	L_∞ (mm FL)	k	t_0 (years)
Richards, 1967	VA	M	88	1210	0.28	−0.06
		F	135	1640	0.23	−0.08
Thompson et al.[9]	LA	M	464	1132	0.49	−0.49
		F	218	1294	0.56	0.11
Smith, 1995	NC	M	116	1050 (18.5)	0.37 (0.04)	−1.08 (0.29)
		F	92	1350 (38.2)	0.24 (0.03)	−1.53 (0.39)
Franks et al., 1999	nGOM	M	170	1171 (28.1)	0.43 (0.05)	−1.15 (0.17)
		F	395	1555 (35.1)	0.27 (0.02)	−1.25 (0.09)
SEDAR[1]	GOM	combined		1282	0.42	−0.53
SEDAR[1]	Atlantic Ocean	combined	2485	1324	0.27	−0.47
This study	GOM	combined	926	1172 (1151–1192)	0.57 (0.52–0.61)	NA

Movement and seasonal distribution

Movement among zones Seven geographic zones were defined in our study to determine the large-scale and seasonal movements of cobia (Fig. 1). Large-scale movement patterns of cobia in the Gulf of Mexico and South Atlantic Ocean were observed. Notably, a portion of the individuals tagged in the Florida Keys, Florida panhandle, Louisiana, and northcentral Gulf of Mexico zones were recaptured in the South Atlantic Ocean zone and therefore indicated that cobia migrate around Florida between the Gulf of Mexico and South Atlantic Ocean (Table 4). Individuals tagged in the Texas zone were recaptured only in the Louisiana and Texas zones and thus indicated that cobia in the western Gulf of Mexico may exhibit limited movement or could be a resident group (Table 4). However, it is important to note that a relatively low number of individuals were tagged and recaptured in the Texas zone over the entire duration of the tagging program (227 tagged, 40 recaptured, Table 1). A majority of individuals tagged in a given zone were recaptured in the same zone for all zones except the Florida panhandle zone where the majority of recaptures were distributed among the Florida panhandle, Louisiana, and northcentral Gulf of Mexico zones (Table 4). Unfortunately, because of the lack of resolution in the reported tagging and recapture locations, we could not evaluate how time-at-liberty affects individual movement between zones.

Table 4

A matrix of the number and proportion of cobia (*Rachycentron canadum*) (n=875, time-at-liberty ≥30 days) tagged and recaptured in the Gulf of Mexico and South Atlantic Ocean during 1988–2014 and the recapture percentage among the 7 geographic zones used in this study. The zones are the South Atlantic Ocean (ATL). Florida Gulf Coast (FLGC), Florida Keys (FLK), Florida panhandle (FLPH), Louisiana (LA), northcentral Gulf of Mexico (NcGOM), and Texas (TX).

	Zone of recapture								Recapture percentage						
Zone of tagging	ATL	FLGC	FLK	FLPH	LA	NcGOM	TX	Total	ATL	FLGC	FLK	FLPH	LA	NcGOM	TX
ATL	**30**	0	5	2	1	2	0	40	**0.75**	0	0.12	0.05	0.02	0.05	0
FLGC	0	**30**	7	6	2	1	0	46	0	**0.65**	0.15	0.13	0.04	0.02	0
FLK	6	9	**63**	18	4	7	1	108	0.06	0.08	**0.58**	0.17	0.04	0.06	0.01
FLPH	30	9	24	**73**	61	63	16	276	0.11	0.03	0.09	**0.26**	0.22	0.23	0.06
LA	3	1	3	5	**41**	3	5	61	0.05	0.02	0.05	0.08	**0.67**	0.05	0.08
NcGOM	15	10	33	55	35	**184**	7	339	0.04	0.03	0.1	0.16	0.1	**0.54**	0.02
TX	0	0	0	0	1	0	**4**	5	0	0	0	0	0.2	0	**0.8**
Total	84	59	135	159	145	260	33	875							

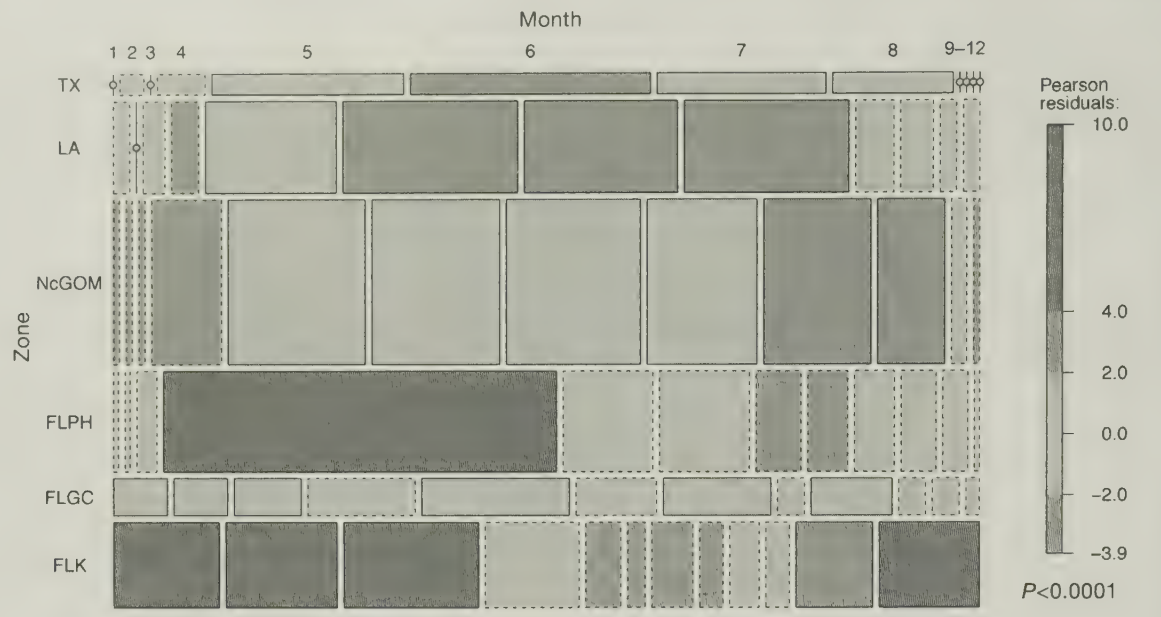

Figure 5

Mosaic plot of results from the loglinear model used to evaluate the relationship between geographic zone and month of recapture of cobia (*Rachycentron canadum*) in the Gulf of Mexico during 1988–2014. The shading indicates the magnitude of the Pearson residuals for the frequency of recapture in a specific month, with the 2 darkest shades indicating a statistically different frequency of recapture in a specific month compared with other months in a specific zone (P<0.0001). The dashed lines represent negative Pearson residuals, and the solid lines represent positive Pearson residuals. The length and width dimensions of each rectangle indicates the number of recaptures in a specific zone (width) in a specific month (length) in relation to the total number of recaptures. The 6 zones in the Gulf of Mexico are Texas (TX), Louisiana (LA), northcentral Gulf of Mexico (NcGOM), Florida panhandle (FLPH), Florida Gulf Coast (FLGC), and the Florida Keys (FLK).

Seasonal distribution A strong seasonal trend in cobia recaptures was observed with a large portion of winter recaptures occurring in the Florida Keys zone and summer recaptures occurring in the northcentral Gulf of Mexico and Louisiana zones. The largest number of recaptures in the Louisiana and northcentral Gulf of Mexico zones occurred from May through August. The saturated loglinear model was not significant (χ^2: 0.0, P=1) and upon removal of the interaction term, the model became significant (χ^2: 465.6, P<0.001), indicating there was a significant association between recapture zone and month of recapture. Specifically, based on the Pearson residuals and resulting mosaic plot, the frequency of cobia recaptures in the Florida Keys zone was significantly lower from May to August and significantly greater from November to March than for other months (Fig. 5). Additionally, the frequency of cobia recaptures in the northcentral Gulf of Mexico zone was significantly lower from December to April and significantly greater in September and October than for other months (Fig. 5). In the Louisiana zone, the frequency of cobia recaptures was significantly greater from June to August than in other months, in the Texas zone, the frequency of cobia recaptures was significantly greater in June, and in the Florida panhandle zone the frequency of recaptures was significantly greater in April than in other months and lower in July and August (Fig. 5).

Mortality

An annual recovery matrix containing 27 years of tag-recovery data was used to determine estimates of S and f parameters in the software program MARK. Only individuals that were not rereleased (i.e., were harvested) and whose dates of tagging and recapture were reported were used in the analysis (n=903). Four candidate models were evaluated, each having a unique combination of time-dependent and time-independent survivorship and tag-recovery (Table 5). Global model fit, for the $S(t)$ and $f(t)$ parameters, was evaluated by using $\hat{c}$. The estimated value of $\hat{c}$ determined from the goodness-of-fit simulation was 2.02 and indicated some overdispersion. The best supported candidate model included $S(.)$ and $f(t)$ parameters (Table 5). The estimate of annual survival from the most supported model was 0.56 (95% CI: 0.53–0.58). This value is equivalent to an annual Z of 0.59/year (95% CI: 0.55–0.63). The an-

Table 5

Candidate models evaluated for estimation of survivorship (S) and probability of tag recovery (f) with data from tagging and recapture of cobia (*Rachycentron canadum*) in the Gulf of Mexico and South Atlantic Ocean during 1988–2014. Time-invariant parameters are represented by (.) and time-variant parameters are represented by (t). The models were evaluated by using Akaike's information criterion (AIC), and Akaike weight (w_i) was calculated for each model.

Model	AICc	ΔAICc	AICc weight	Model likelihood
$S(.)f(t)$	10081.5	0.00	0.79	1.00
$S(.)f(.)$	10084.2	2.72	0.20	0.26
$S(t)f(t)$	10091.3	9.82	0.01	0.01
$S(t)f(.)$	10109.7	28.19	0.00	0.00

nual tag-recovery rate ranged from 0.013 to 0.041 and averaged 0.023 (Fig. 6). Peaks in tag-recovery rates occurred in 1993 and from 2006 to 2007; however, the f parameter remained relatively constant throughout the duration of the tagging program (Fig. 6).

Discussion

In the most recent Gulf of Mexico cobia stock assessment (SEDAR[1]), several research needs were identified that, if resolved, would help enable reviewers to evaluate the appropriateness of an assessment model and allow the determination of stock status to be made. The information provided in this study fills information gaps that exist for cobia in the Gulf of Mexico and South Atlantic Ocean that will aid in future assessment efforts and allow for an accurate determination of stock status. The information includes an alternative approach to modeling the length-at-age relationship, a description of the annual Z and elucidation of the annual movement, and the distribution patterns of individuals.

A primary objective of our research was to provide alternative length-at-age parameter estimates and compare them with estimates available in the published literature. Of the models we evaluated, the GROTAG VBGF model resulted in the best option for fitting growth increment information from tag-recapture studies because it explicitly addresses variability in individual growth, effectively handles the presence of outliers, and is able to accurately evaluate mean values of L_∞—a failing of other algorithms with tag and recapture information (e.g., Fabens, 1965). Our mean estimate of L_∞ derived from the length-at-age analysis with the GROTAG VBGF model is lower than estimates reported in other studies of individual growth dynamics with the use of otoliths. This result could be due to the sex-aggregated nature of the tagging data that were available (our estimate was often higher than male-specific estimates and lower than female-specific estimates, Table 3). The lack of sex-specific information is a confounding feature of cooperative tagging programs (Dippold et al., 2016) and likely has an effect on the estimated length-at-age parameters. Another possible explanation for the lower L_∞ reported here is that anglers typically keep cobia of legal length (≥84 cm or 33 in) and tagged individuals were generally smaller or close to the minimum length limit, both of which may bias our length-at-age parameter estimates. We also found that the mean k in this study was greater than that of many other published estimates (Table 3). Because the VBGF parameters are strongly and negatively correlated, the higher k estimate may be in part caused by the lower estimate of L_∞. Despite the sexual dimorphism in length-at-age between males and females, both the SEDAR assessments of cobia in the Gulf of Mexico and Atlantic Ocean used a sex-combined 3-parameter VBGF to describe the length-at-age relationship. Therefore, although in the tagging program data that we evaluated, sex was not recorded, and the lack of sex determination is a disadvantage of coop-

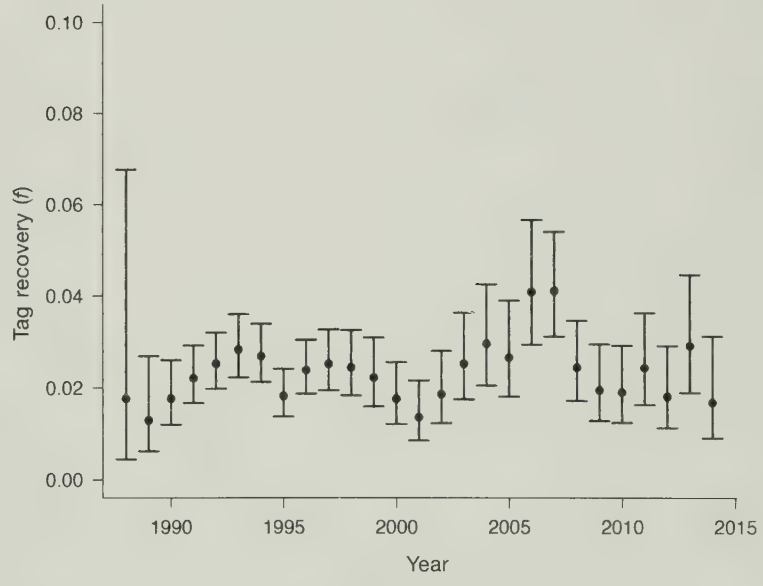

Figure 6

The estimated probability of tag recovery (f) from the best supported tag-recovery mortality model fit to data from tagging and recapture of cobia (*Rachycentron canadum*) in the Gulf of Mexico and South Atlantic during 1988–2014. Error bars indicate 95% confidence intervals.

erative tagging programs, our estimates are still a relevant method of corroboration given that sex-combined length-at-age models are used in current assessment models. However, in the future, we recommend that sex of recaptured individuals be reported if available. This information could be collected at fishing tournaments where scientists are often on site gathering biological information, or incentives could be offered to bring carcasses to scientists for sex identification.

As with the description of individual growth dynamics, we provide an independent estimate of Z that can be used to corroborate mortality values estimated by using an age-structured stock assessment model. In most stock assessment frameworks, natural and fishing mortality rates are difficult to estimate and are often obtained by theoretical estimates (Then et al., 2015). Tag-recovery models do not require the use of a specific natural mortality function to estimate Z, and thus avoid some potential biases in describing the natural mortality component of Z. In this study, we estimated annual Z by using tag-recovery models (0.59/year [95% CI: 0.55–0.63]). In the 2013 stock assessment of cobia in the Gulf of Mexico, the current estimated annual total mortality (the sum of the geometric mean fishing mortality and natural mortality) was 0.62/year. During the period included in the assessment, fishing mortality varied annually but has remained relatively stable, especially in the most recent years of the assessment. Our estimate of Z is similar to those values estimated in the stock assessment model. We included recaptures from both the Gulf of Mexico and a limited number from the South Atlantic Ocean in our analysis (to account for individuals tagged in Gulf of Mexico and harvest in South Atlantic Ocean) and recognize that our estimate is by necessity stock-aggregated.

Clarification of the stock boundary along the Atlantic coast of Florida was considered a research need of high importance by assessment scientists (SEDAR[1]), and cooperative research efforts can contribute to this effort (Lucy and Davy, 2000). This study confirms the presence of large scale movements of individual cobia within the Gulf of Mexico and into the South Atlantic Ocean. The scale of our work, in terms of both the number of individuals tagged and the spatial coverage, is greater than that of previous studies and strengthens the descriptions of cobia movement. Previously, Burns and Neidig[6] tagged 171 cobia from 1990 to 1992, recaptured 10 individuals and suggested both seasonal northern and southern movements and seasonal onshore-offshore movements. Orbesen[8] synthesized cooperative tagging information collected from the NOAA Southeast Fisheries Science Center, information that included 1510 tagged cobia and 148 recaptures over 58 years. Using that synthesized recapture information and the 6 defined geographic zones (as opposed to the 7 zones defined in our study), Orbesen[8] observed mixing among all 6 zones, and that more mixing occurred between the Keys and the Gulf zones than between any other 2 zones. For the South Carolina Marine Game Fish Tagging Program, 1066 cobia were tagged between 1986 and 2009 and 201 individuals were recaptured (Wiggers[7]). On the basis of the reported tagging and recapture locations, most fish showed site fidelity, although some mixing between the Gulf of Mexico and South Atlantic Ocean was observed. Other studies have also reported mixing between the Gulf of Mexico and South Atlantic Ocean on the basis of a few recaptured individuals (Shaffer and Nakamura, 1989). Most of these tagging studies had a small number of recaptured individuals or were conducted for a relatively short time period (or were a combination of both). Because of the observed long-distance movements and the current problems with identification of the stock boundary between the Gulf of Mexico and South Atlantic Ocean stocks, the relatively greater number of tagged and recaptured individuals used in this study and the duration of the tagging program allow stronger inferences of seasonal and long-distance movement patterns of cobia in the Gulf of Mexico and South Atlantic Ocean.

The results of our work indicate that there is an evident seasonal distribution pattern: individuals are more frequently recaptured in the Florida Keys during the winter and in the northern Gulf of Mexico during the summer. Currently, the South Atlantic Ocean and Gulf of Mexico stocks are divided at the Florida–Georgia state line (SEDAR[1]). The boundary is determined on the basis of ease of management; however, there is little evidence from genetic or tagging work to confirm the validity of this designation (SEDAR[1]). Some genetic evidence indicates homogeny among offshore cobia along the Atlantic coast and some genetic distinction among inshore aggregations; however, no similar genetic information on population structure and partitioning exists for cobia in the Gulf of Mexico (Darden et al., 2014). We find that of the individuals tagged in the Gulf of Mexico zones, no more than 11% of recaptures of individuals tagged in a given Gulf of Mexico zone occurred in the South Atlantic Ocean. Additionally, of the individuals tagged in the Atlantic Ocean and subsequently recaptured, only 14% were recaptured in the Florida Keys, and recapture rates in the other Gulf of Mexico zones ranged from 0 to 5%. These results suggest that the Florida Keys may be a mixing zone and that the current stock boundary at the Florida Georgia state line may be inappropriate. However, we did not incorporate differences in fishing and sampling effort into our modeling approaches and we note that seasonal differences in fishing effort between zones may bias our descriptions of movement and seasonal recapture patterns. Additionally, because of the scope of the cooperative tagging program, we were limited to providing descriptions of movement and distribution to the Gulf of Mexico and South Atlantic Ocean.

The results of our research suggest a seasonal pattern of distribution of cobia in the Gulf of Mexico. Specifically, the results of the loglinear analysis presented here indicate that the Florida Keys may be a wintering ground for cobia and that individuals may exhibit northward movement toward the Florida panhandle

in the spring, followed by summer residence in the northern Gulf of Mexico and Louisiana. These patterns are similar to patterns reported in other cooperative tagging studies (Shaffer and Nakamura, 1989; Burns and Neidig[6]). However, to our knowledge, this is the first study to quantify and statistically test potential trends in seasonal distribution of cobia recaptures. The observed seasonal movement patterns may have implications for cobia management in the Gulf of Mexico. Inappropriate designation of the stock boundary could affect the spatial extent of the indices of abundance used in the assessment, as well as on the spatial allocation of harvest patterns on the Atlantic coast of Florida. However, we do note that differences in seasonal fishing effort may be in part responsible for observed differences in recapture distribution.

Acknowledgments

We thank the numerous anglers whose tremendous tagging efforts made this study possible. We also thank D. Gibson for management of the database. Funding for the Sport Fish Tag and Release Program was provided by the U.S. Fish and Wildlife Service's Sport Fish Restoration Program and the Mississippi Department of Marine Resources. Funding for this study was provided by the Mississippi Department of Marine Resources Tidelands Trust Fund Program "Mississippi Stock Assessment Panel" grant awarded to J. Hendon and R Leaf.

Literature cited

Brownie, C., D. R. Anderson, K. P. Burnham, and D. S. Robson.
1985. Statistical inference from band recovery data: a handbook, 2nd ed. U.S. Fish Wildl. Serv. Resour. Publ. 156, 305 p.

Burnham, K. P., and D. R. Anderson.
2002. Model selection and multimodel inference: a practical information-theoretic approach, 2nd ed., 266 p. Springer-Verlag, New York.

Campana, S. E.
2001. Accuracy, precision and quality control in age determination, including a review of the use and abuse of age validation methods. J. Fish Biol. 59:197–242.

Darden, T. L., M. J. Walker, K. Brenkert, J. R. Yost, and M. R. Denson.
2014. Population genetics of Cobia (*Rachycentron canadum*): implications for fishery management along the coast of the southeastern United States. Fish. Bull. 112:24–35.

Dippold, D. A., R. T. Leaf, J. R. Hendon, and J. S. Franks.
2016. Estimation of the length-at-age relationship of Mississippi's Spotted Seatrout. Trans. Am. Fish. Soc. 142:295–304.

Fabens, A. J.
1965. Properties and fitting of the von Bertalanffy growth curve. Growth 29:265–289.

Francis, R. I. C. C.
1988. Maximum likelihood estimation of growth and growth variability from tagging data. N. Z. J. Mar. Freshw. Res. 22:43–51.

Franks, J. S., J. R. Warren, and M. V. Buchanan.
1999. Age and growth of cobia, *Rachycentron canadum*, from the northeastern Gulf of Mexico. Fish. Bull. 97:459–471.

Hendon, J. R., J. R. Warren, J. S. Franks, and M. V. Buchanan.
2002. Movements of spotted seatrout (*Cynoscion nebulosus*) in Mississippi coastal waters based on tag-recapture. Gulf Mex. Sci. 20:91–97.

Hussey, N. E., I. D. McCarthy, S. F. J. Dudley, and B. Q. Mann.
2009. Nursery grounds, movement patterns and growth rates of dusky sharks, *Carcharhinus obscurus*: a long-term tag and release study in South African waters. Mar. Freshw. Res. 60:571–583.

Jones, C. D., and E. D. Prince.
1998. The cooperative tagging center mark-recapture database for Istiophoridae (1954–1995), with an analysis of the west Atlantic ICCAT billfish tagging program. Collect. Vol. Sci. Pap. ICCAT 47:311–322.

Katsanevakis, S.
2006. Modelling fish growth: model selection, multi-model inference and model selection uncertainty. Fish. Res. 81:229–235.

Kerns, J. A., M. S. Allen, J. R. Dotson, and J. E. Hightower.
2015. Estimating regional fishing mortality for freshwater systems: a Florida largemouth bass example. North Am. J. Fish. Manage. 35:681–689.

Kneebone, J., J. Chisholm, and G. Skomal.
2014. Movement patterns of juvenile sand tigers (*Carcharias taurus*) along the east coast of the USA. Mar. Biol. 161(5):1149–1163.

Knoke, D., and P. J Burke.
1980. Log-linear models, vol. 20, 80 p. Sage Publications Inc. Thousand Oaks, CA.

Kohler, N. E., J. G. Casey, and P. A. Turner.
1998. NMFS cooperative shark tagging program, 1962–93: an atlas of shark tag and recapture data. Mar. Fish. Rev. 60(2):1–87.

Lucy, J., and K. Davy.
2000. Benefits of angler-assisted tag and release programs. Fisheries 25(4):18–23.

Natanson, L. J., J. G. Casey, N. E. Kohler, and T. Colket IV.
1999. Growth of the tiger shark, *Galeocerdo cuvier*, in the western North Atlantic based on tag returns and length frequencies; and a note on the effects of tagging. Fish. Bull. 97:944–953.

Ortiz, M., E. D. Prince, J. E. Serafy, D. B. Holts, K. B. Davy, J. G. Pepperell, M. B. Lowry, and J. C. Holdsworth.
2003. Global overview of the major constituent-based billfish tagging programs and their results since 1954. Mar. Freshw. Res. 54:489–507.

Pierce, L. L., B. D. S. Graeb, D. W. Willis, and J. S. Sorensen.
2015. Evaluating effects of exploitation on annual apparent mortality rates of paddlefish using mark–recapture data. Trans. Am. Fish. Soc. 144:337–344.

Pine, W. E., K. H. Pollock, J. E. Hightower, T. J. Kwak, and J. A. Rice.
2003. A review of tagging methods for estimating fish population size and components of mortality. Fisheries 28(10):10–23.

Queiroz, N., F. P. Lima, A. Maia, P. A. Ribeiro, J. P. Correia, and A. M. Santos.
2005. Movement of blue shark, *Prionace glauca*, in the north-east Atlantic based on mark–recapture data. J. Mar. Biol. Assoc. U. K. 85:1107–1112.

R Core Team.
2016. R: a language and environment for statistical computing. R Foundation for Statistical Computing, Vienna, Austria. [Available from Article, accessed May 2016.]

Richards, C. E.
1967. Age, growth and fecundity of the cobia, *Rachycentron canadum*, from Chesapeake Bay and adjacent mid-Atlantic waters. Trans. Am. Fish. Soc. 96:343–350.

Shaffer, R. V., and E. L. Nakamura.
1989. Synopsis of biological data on the cobia *Rachycentron canadum* (Pisces: Rachycentridae). NOAA Tech. Rep. NMFS 82, 21 p.

Simpfendorfer, C. A.
2000. Growth rates of juvenile dusky sharks, *Carcharhinus obscurus* (Lesueur, 1818), from southwestern Australia estimated from tag-recapture data. Fish. Bull. 98:811–822.

Smith, J.
1995. Life history of cobia, *Rachycentron canadum* (Osteichthyes: Rachycentridae), in North Carolina waters. Brimleyana 23:1–23.

Then, A. Y., J. M. Hoenig, N. G. Hall, and D. A. Hewitt.
2015. Evaluating the predictive performance of empirical estimators of natural mortality rate using information on over 200 fish species. ICES J. Mar. Sci. 72:82–92.

Troynikov, V. S., R. W. Day, and A. M. Leorke.
1998. Estimation of seasonal growth parameters using a stochastic Gompertz model for tagging data. J. Shellfish Res. 17:833–838.

Vandergoot, C. S., and T. O. Brenden.
2014. Spatially varying population demographics and fishery characteristics of Lake Erie walleyes inferred from a long-term tag recovery study. Trans. Am. Fish. Soc. 143:188–204.

White, G. C., and K. P. Burnham.
1999. Program MARK: survival estimation from populations of marked animals. Bird Study 46:S120–S138.

Williams, E. H.
2001. Assessment of cobia, *Rachycentron canadum*, in the waters of the U.S. Gulf of Mexico. NOAA Tech. Memo. NMFS-SEFSC-469, 55 p.

Wood, A. D., and S. X. Cadrin.
2013. Mortality and movement of yellowtail flounder (*Limanda ferruginea*) tagged off New England. Fish. Bull. 111:279–287.

National Marine
Fisheries Service
NOAA

Fishery Bulletin
established in 1881

Spencer F. Baird
First U.S. Commissioner
of Fisheries and founder
of *Fishery Bulletin*

Gestation period and pupping seasonality of female spiny dogfish (*Squalus acanthias*) off southern New England

Lisa J. Natanson (contact author)[1]
Camilla T. McCandless[1]
Kelsey James[2]
John Hoey[1]

Email address for contact author: lisa.natanson@noaa.gov

[1] Northeast Fisheries Science Center
National Marine Fisheries Service, NOAA
28 Tarzwell Drive
Narragansett, Rhode Island 02882

[2] Department of Biological Sciences
University of Rhode Island
120 Flagg Road
Kingston, Rhode Island 02881

Abstract—Recently, it has been suggested that spiny dogfish (*Squalus acanthias*) in the western North Atlantic Ocean have a shorter gestation period than the widely cited 2 years, have an asynchronous reproductive cycle, and carry pups in various stages of development. Mature female spiny dogfish were collected monthly from July 2013 through June 2015 to confirm gestation period and pupping seasonality off southern New England, and data on 2545 embryos from 622 females were obtained. Recent postpartum females and females with candled embryos appeared from January through April indicating parturition that was followed closely by mating. Vitellogenesis is concurrent with embryo growth, and therefore ova are ready for fertilization immediately after pupping. Visible embryos were observed in June, and growth continued until the external and internal yolks were absorbed and the umbilical scar was partially healed. Gestation period was approximately 23 months. No individual was observed with first and second year embryos. Average fecundity per female was estimated on the basis of the largest group of oocytes (5.3), free-living embryos (4.3), and total embryos (candled and free-living) (4.5). These values are similar to those of previous studies, but average fecundity by maternal size class has decreased from that of previous studies and is negatively correlated with spawning stock biomass, which provides supporting evidence for density dependent fecundity.

Manuscript submitted 30 September 2016.
Manuscript accepted 24 July 2017.
Fish. Bull. 115:473–483 (2017).
Online publication date: 8 August 2017.
doi: 10.7755/FB.115.4.4

The views and opinions expressed or implied in this article are those of the author (or authors) and do not necessarily reflect the position of the National Marine Fisheries Service, NOAA.

Spiny dogfish (*Squalus acanthias*) occur in the western North Atlantic (WNA) Ocean from Labrador, Canada, to Florida, United States, but are most abundant from Nova Scotia, Canada, to Cape Hatteras, North Carolina (Collette and Klein-MacPhee, 2002). Seasonal migrations occur northward in the spring and summer and southward in the fall and winter (Hisaw and Albert, 1947; Jensen, 1965; McMillan and Morse, 1999). Conventional and satellite tagging studies also suggest some localized movement occurs within these large-scale seasonal migrations, for instance, a southern and a northern group overlap in the Gulf of Maine (Campana et al.[1]; and references within) and off southern New England (SNE) (Carlson et al., 2014).

The fishery on mature female spiny dogfish in the 1990s led to a significant reduction in female spawning stock biomass in the WNA (Rago and Sosebee, 2009), because the resulting size-selective mortality exceeded the growth and reproductive rates of this *K*-selected species. Additionally, the size at first maturity for female spiny dogfish declined by 10 cm in length between the late 1980s and the late 1990s and may have been a result of this reduction in female spawning stock biomass (Sosebee, 2005). However, the size-selective nature of the fishery left the abundance of the generally smaller male spiny dogfish relatively unaffected (Rago and Sosebee, 2009). Recent updates on the status of spiny dogfish show that the female spawning stock biomass has been rebuilt, the population is no longer overfished, and overfishing is not oc-

[1] Campana, S. E., A. J. F. Gibson, L. Marks, W. Joyce, R. Rulifson, and M. Dadswell. 2007. Stock structure, life history, fishery and abundance indices for spiny dogfish (*Squalus acanthias*) in Atlantic Canada. Canadian Science Advisory Secretariat, Res. Doc. 2007/089, 133 p. [Available from website.]

curring (Rago and Sosebee[2,3]). Sustainability of this fishery is directly linked to the reproduction of adult females and an overabundance of males may, in fact, be detrimental to recruitment (Rago[4]). Despite success in rebuilding the female spawning stock biomass and the increased efficiency in use of the resource (a decrease in the ratio of discards to landings), spiny dogfish management still faces many challenges.

Numerous studies have been conducted on the reproduction of the spiny dogfish worldwide (Kaganovskaia, 1937; Yamamoto and Kibezaki, 1950; Jensen, 1965; Ketchen, 1972; Hanchet, 1988; Avsar, 2001; Chatzispyrou and Megalofonou, 2005; Di Giacomo et al., 2009; Capapé and Reynaud, 2011; Gračan et al., 2013). Studies specific to the WNA have suggested that there is an 18–25 month gestation period, which may depend on water temperature (Templeman, 1944; Hisaw and Albert, 1947; Bigelow and Schroeder, 1953; Nammack et al., 1985; Campana et al., 2009; Bubley, 2010, Bubley et al., 2013). Although these reports all suggest a similar gestation period, in most cases the time periods over which the research was conducted were not adequate to fully support these conclusions. Many of these studies were dependent either on samples that were collected over only a few months or on sporadic partial-year sampling (Templeman, 1944; Hisaw and Albert, 1947; Nammack et al., 1985; Campana et al., 2009). Nammack et al. (1985); for example, data were collected between Cape Fear, North Carolina, and the Gulf of Maine between November and May to characterize the reproduction of the spiny dogfish off the northeastern United States. Furthermore, these studies suggested a similar pattern for the gestation period that had been described by Jones and Geen (1977) for spiny dogfish in the Pacific Ocean, a species that has now been identified as a separate species with different life history parameters: the Pacific spiny dogfish (*Squalus suckleyi*) (Campana et al., 2006; Ebert, 2010). More recently, Campana et al. (2009) described a 2-year gestation period for spiny dogfish in the WNA off of the Eastern Coast of Canada, however, as in other studies, this conclusion was based on limited sampling between June and October. Nevertheless, a 2-year gestation period is currently used in the stock assessment process for WNA spiny dogfish. Studies of shark reproduction, in general, have shown substantial latitudinal variation, as well as mixed gestational periodicity in a species in the same area (Driggers and Hoffmayer, 2009; Hoffmayer et al., 2013; Taylor et al., 2016). In particular, it has been suggested that there are regional differences in the reproductive cycles in the WNA spiny dogfish population (Sulikowski et al.[5]). Specifically these authors suggest that regional asynchronies in reproductive biology exist and that there is the need for regional sampling and detailed examination of the reproductive state of spiny dogfish for comparative purposes.

Because of the significance of female reproduction for the sustainability of the WNA spiny dogfish fishery and because of new data on the plasticity and latitudinal variations in other elasmobranchs (Driggers and Hoffmayer, 2009; Taylor et al., 2016), more information specific to this stock in each region is required to determine whether latitudinal plasticity exists and to ensure accurate assessments and reliable projections that lead to more sustainable management practices. An intensive sampling regimen was initiated to obtain detailed life history data as part of the Cooperative Research Program of the National Marine Fisheries Service's (NMFS). We report on one portion of this study, specifically, the gestation period and pupping seasonality of mature female spiny dogfish off SNE between Massachusetts and Rhode Island and in the mid-Atlantic off the coast of New Jersey. We address a lack of adequate data on reproductive characteristics in this region and revisit fecundity at maternal length to evaluate any density-dependent effects that may have occurred as the female spawning stock biomass was rebuilding.

Materials and methods

An attempt was made to collect a minimum of 30 mature female spiny dogfish greater than or equal to 50% maturity (which was estimated at 75 cm in stretched total length, STL] [66.1 cm fork length, FL] [Bubley, 2010]), per month for 2 years from July 2013 through July 2015. Female spiny dogfish were requisitioned from commercial fishing vessels fishing primarily off SNE between Massachusetts and Rhode Island but some sampling occurred off the coast of New Jersey through the NMFS Cooperative Research Program. Sampling location and date were noted and the samples were frozen. If sample length was <75 cm STL and the sample was mature it was included in the study.

Fork, total, and stretched total lengths were measured over the body (FL: from the tip of the snout to the fork in the tail; TL: from the tip of the snout to a point on the horizontal axis intersecting a perpendicular line extending downward from the tip of the upper caudal lobe to form a right angle; and STL: from

[2] Rago, P., and K. Sosebee. 2014. Update of landings and discards of spiny dogfish in 2014, 19 p. [Available from the Mid-Atlantic Fishery Management Council, 800 North State St., Ste. 201, Dover, DE 19901.]

[3] Rago, P., and K. Sosebee. 2015. Update on the status of spiny dogfish in 2015 and projected harvest at the Fmsy proxy and Pstar of 40%, 65 p. Mid-Atlantic Fishery Management Council, Dover, DE. [Available from website.]

[4] Rago, P. 2015. Spiny dogfish: New England's favorite species. Presentation for the Cape Cod Commercial Fisherman's Alliance in Chatham, MA, on 2 March 2015. [Available from website, accessed October 2015.]

[5] Sulikowski, J., B. Galuardi, W. Bubley, W. Driggers III, E. Hoffmayer, A. Cicia, A. Carlson, and P. Tsang. 2010. Dismissing dogma? What do we really know about the spiny dogfish, *Squalus acanthias*, population in the U.S. western north Atlantic Ocean. ICES CM 2010/E:16, 8 p. [Available from website.]

the tip of the snout to the upper lobe of the caudal fin pulled downward to align with the body) to the nearest millimeter on each specimen. A girth measurement was taken behind the pectoral fins of each specimen. Each fish was weighed to the nearest tenth of a kilogram.

After external measurements were taken, an incision was made from the cloaca through the pectoral girdle along the ventral surface to retract the belly flap and expose the abdominal cavity. Organ terms follow those of Hamlett and Koob (1999). Both sides of the female spiny dogfish reproductive tract are functional; therefore, both sides of each specimen were dissected and measured. Measurements were taken to the nearest millimeter and weights to the nearest tenth of a gram in the following order: ovary weight, diameter of each of the largest group of oocytes and at least 1 of the next size group. In pregnant females, all embryos were measured (FL and STL, in centimeters along a straight line), weighed (in grams) (without external yolk which was weighed separately [in grams]) and visually examined for developmental stage of the litter (i.e., according to the condition of the umbilical scar). If there was no external yolk, the embryo was weighed and the internal yolk was removed and weighed (in grams). Litter sizes and sex of an embryo were also recorded. In many cases it was clear that pups had been aborted before dissection and these instances were noted. Developmental stages were the following: mature ovarian oocyte, candled embryo (embryo and yolk covered by a membranous envelope (stage 1 in Hisaw and Albert, 1947), free-living embryo (no longer candled), embryo with external yolk, and embryo with no eternal yolk and with healing umbilical scars.

Fecundity

Three estimates of fecundity were calculated: 1) by counting the number of oocytes in the largest group of oocytes in the ovaries, which were presumed to be the next litter; 2) by using total embryo count (candled and free-living embryos), and 3) by using counts of only free-living embryos. Mean number of all 3 indices per female were plotted against maternal size. Additionally, the data were presented by 5-cm maternal size increments for comparison with data from previous studies. Fecundity measures for each 5-cm maternal size class and female spawning stock biomass, estimated by using a 3-point moving average (Rago and Sosebee[3]), were plotted over time to determine potential signs of density dependence. Fecundity data from 1998 through 2002 were obtained from Sosebee (2005) and data from 2006 to 2009 were obtained from Bubley (2010). Data summaries that included only averages across years were plotted at the midpoint of the time series. Additionally, correlation analyses were conducted to determine correlations between the mean fecundity of each 5-cm maternal size class and spawning stock biomass (SSB), estimated by using a 3-point moving average (Rago and Sosebee[3]), and with relative abundance estimates based on mean number of mature females caught per tow during the NOAA Northeast Fisheries Science Center spring bottom-trawl survey (Silva, 1993).

Reproductive seasonality

Gestation period was determined by plotting the size of the embryos over time, assuming samples were from the same stock. The concurrent increase in follicle size with embryo size (see the *Results* section) also allows one to infer the mating period on the basis of the increase of follicle size in the ovaries followed by a sudden decrease and presence of fertilized eggs in the uterus. Each shark was also examined for evidence of mating scars.

Size of full-term embryos

The determination of the size that the embryos were considered full term was based on observation of umbilical scars, size of internal yolks, and maximum sizes of embryos in relation to minimum sizes of free-living swimming individuals. These data were confounded by the differences in size of term embryos in relation to maternal size (see the *Results* section).

Results

Between July 2013 and June 2015, 622 mature female dogfish ranging in size from 75.3 to 104.2 cm STL (mean 88.5 cm STL; 66.8–94.5 cm FL [mean 79.2 cm FL]) were sampled. Between July 2013 and June 2014, spiny dogfish were obtained from SNE between Massachusetts and Rhode Island in all months, except October, when a federal government furlough precluded sampling (Table 1, Fig. 1). Between July 2014 and June 2015, samples were obtained in in this region in 6 out of 12 months (Table 1). In October and December 2014 samples were obtained from off shore of New Jersey in an attempt to maintain the monthly sampling time series. No samples were available during September 2014 and March and May 2015 as a result of the establishment of a gear-restricted area as an accountability measure for windowpane (*Scophthalmus aquosus*) in 2014 and 2015 (GARFO[6,7]). This measure restricted fishing in the areas where spiny dogfish are

[6] GARFO (Greater Atlantic Regional Fisheries Office). 2014. Greater Atlantic Region Bulletin. Northeast multispecies common pool fishery fishing year 2014 regulations, 7 p. Greater Atlantic Regional Fisheries Office, NOAA, Gloucester, MA. [Available from website.]

[7] GARFO (Greater Atlantic Regional Fisheries Office). 2015. Greater Atlantic Region Bulletin. Groundfish fishermen: NOAA Fisheries approves Framework 52 to the Groundfish Plan—southern windowpane flounder restricted gear area reduced in size, 3 p. Greater Atlantic Regional Fisheries Office, Greater Atlantic Regional Fisheries Office, NOAA, Gloucester, MA. [Available from website.]

Table 1

Locations, numbers, and dates of sampling of female spiny dogfish (*Squalus acanthias*) off southern New England, between Massachusetts and Rhode Island, and off New Jersey from July 2013 to July 2015.

Month/Year	General location	Date	Latitude (N°)	Longitude (W°)	No. of samples
July 2013	Southern New England	7/9/2013	4104.47	7137.01	30
August 2013	Southern New England	8/21/2013	4108.18	7119.16	19
	Southern New England	8/29/2013	4103.44	7129.24	11
September 2013	Southern New England	9/11/2013	4102.58	7123.01	28
October 2013	No samples				
November 2013	Southern New England	11/5/2013	4100.44	7133.70	30
December 2013	Southern New England	12/8/2013	4054.55	7130.94	30
January 2014	Southern New England	1/29/2014	4057.56	7116.28	30
February 2014	Southern New England	2/9/2014	4019.61	7117.72	23
	Southern New England	2/26/2014	4106.54	7120.69	7
March 2014	Southern New England	3/25/2014	4049.07	7131.32	6
	Southern New England	3/24/2014	4035.88	7123.47	8
April 2014	Southern New England	4/21/2014	4054.08	7132.74	30
	Southern New England	4/22/2014	4100.00	7135.00	31
May 2014	Southern New England	5/27/2014	4113.66	7129.06	31
June 2014	Southern New England	6/17/2014	4116.11	7127.14	42
	Southern New England		4116.00	7143.00	
July 2014	Southern New England	7/8/2014	4113.48	7128.45	12
	Southern New England	7/25/2014	4100.40	7133.97	17
August 2014	Southern New England	8/26/2014	4100.12	7137.83	14
		8/25/2014	4100.12	7137.00	16
September 2014	No samples				
October 2014	New Jersey	10/29/2014	3947.43	7358.87	30
November 2014	Southern New England	11/4/2014	4116.68	7124.79	29
December 2014	New Jersey	12/11/2014	3950.00	7401.00	30
January 2015	Southern New England	1/14/2015	4059.24	7113.29	31
February 2015	Southern New England	2/4/2015	4051.59	7132.05	28
March 2015	No samples				
April 2015	Southern New England	4/7/2015	4036.22	7149.37	32
May 2015	No samples				
June 2015	Southern New England	6/5/2015	4113.45	7141.31	14
	Southern New England	6/4/2015	4114.30	7139.00	13

traditionally caught (Fig. 1). Quantity, date, and location of sampling varied owing to fishing activity.

Fecundity and litter characteristics

Most spiny dogfish (n=551) contained embryos in the uteri. Of the samples without embryos (n=71), 64 were caught between January and April and all but 2 of these fish had mature ovarian follicles that were ready for ovulation. Those 2 females appeared to be maturing for the following mating season. Of the 7 remaining individuals: 4 appeared to have pupped owing to stress, 2 appeared to be maturing, and it could not be determined why the last individual did not have pups. A bimodal distribution of embryo sizes was observed in most months of sampling and indicated that some females were in the first year of gestation, while some were in the second year. In no case were candled (first year) and free-living (second year) embryos found in the same individual; therefore only 1 set of developing embryos was observed per female.

A total of 2545 embryos, ranging in size from non-visible candled to term (30.8 cm STL), were examined. Of these, 1447 embryos were developed sufficiently for sex determination. Although individual litters were commonly seen to be predominantly of one sex, the overall sex ratio was 1:1 (733 female, and 714 male). Candled embryos were visible to the naked eye in June and had an average size of 0.21 cm STL and by November they averaged 6 cm STL. Embryos averaged 19 cm STL by the following June.

Fecundity was estimated by the number of developing embryos in the uteri and the number of developing oocytes in the ovaries. Many of the dogfish, regardless of the stage of gestation, appeared to lose embryos before dissection. Evidence for this consisted in observations of pups being partially extruded through the clo-

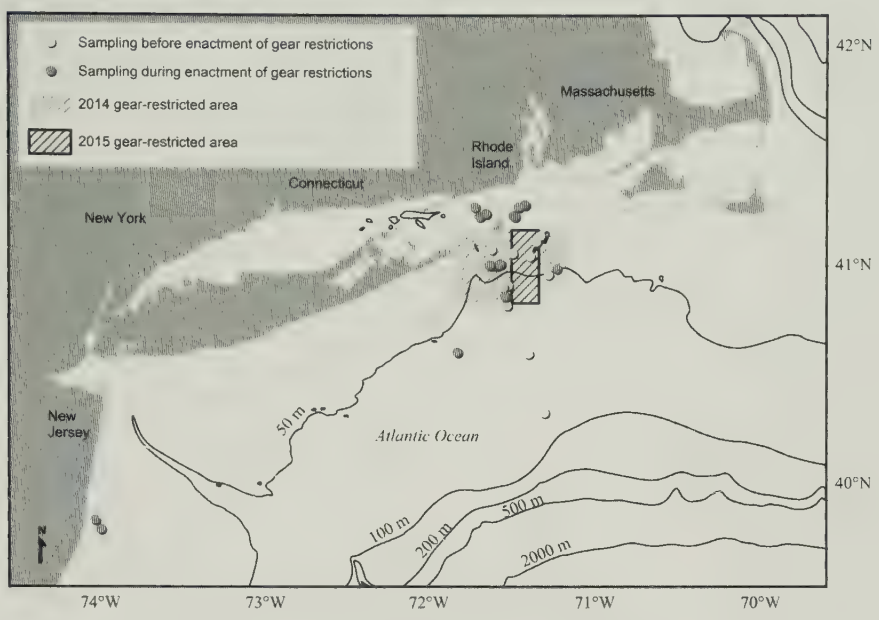

Figure 1

Map of locations where spiny dogfish (*Squalus acanthias*) were sampled off southern New England; between Massachusetts and Rhode Island, and off New Jersey from July 2013 to July 2015. A gear-restricted area was established as an accountability measure for windowpane (*Scophthalmus aquosus*) in 2014 and 2015.

aca, of extra pups in the bottoms of the bags containing the samples, and of partly flaccid uteri, with or without 1 or more embryos. For these reasons the number of free-living embryos per female is a biased (and probably low) estimate of fecundity, whereas the number of developing oocytes of the largest group of developing oocytes in the ovaries may be an upper estimate, some may ultimately not have been fertilized. The number of embryos per female was calculated both with total embryos (free-living and candled litters: mean=4.5 embryos, range=1–11 embryos, n=542) and with free-living embryos only (mean=4.3 embryos, range=1–9 embryos; n=338) for comparison with results of other publications (Table 2). Because of the similarity in these estimates, total embryos were used in relation to female size classes. The number of maturing oocytes for the next litter was difficult to discern in newly mated females; therefore the fecundity estimates based on number of developing oocytes were taken only from females with visible embryos (mean=5.3 embryos, range=1–10 embryos; n=443).

The mean values from all 3 types of fecundity estimates (developing oocytes, total embryos, and free-living (only) embryos) indicate a significant (P<0.0001) positive relationship between litter size and maternal size (Fig. 2, A–C). This increase in litter size with maternal size is also evident when the total and free-living embryo data are broken down into 5-cm STL size

Table 2

Mean number of free-living and total embryos per female spiny dogfish (*Squalus acanthias*) and sample size for each size class of females, defined by 5-cm intervals of stretched total length in centimeters. Values for total embryos (candled and free-living embryos combined) are given in parentheses.

Size class (cm)	Mean	Standard deviation	Sample size
75–79	2.25 (3.25)	1.50 (1.58)	4 (8)
80–84	3.26 (3.45)	1.29 (1.31)	57 (95)
85–89	4.08 (4.23)	1.32 (1.31)	136 (203)
90–94	4.89 (5.11)	1.33 (1.31)	114 (184)
95–99	4.70 (5.20)	2.20 (2.19)	20 (40)
100–104	6.00 (6.33)	2.38 (2.84)	7 (12)
All size classes	4.27 (4.50)	1.55 (1.59)	338 (542)

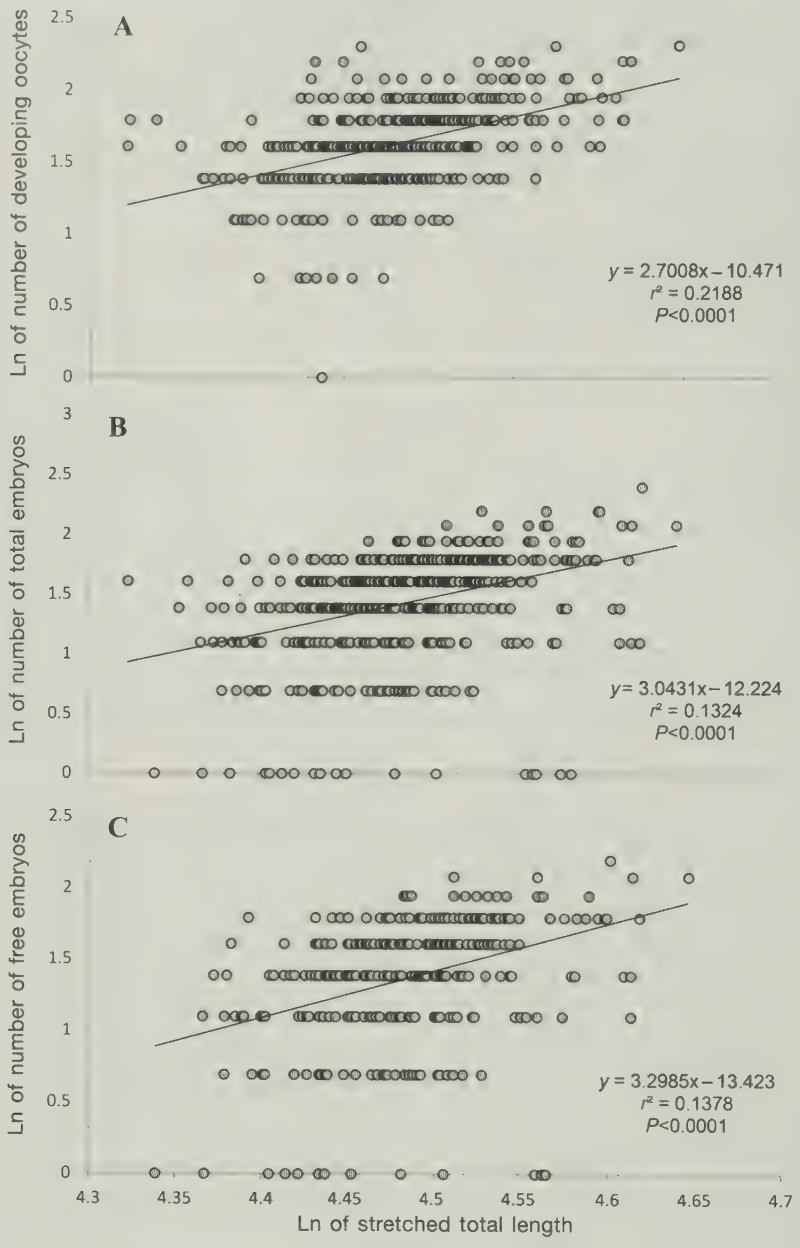

Figure 2

Comparison of fecundity estimates with stretched total length of female spiny dogfish (*Squalus acanthis*) collected off southern New England and New Jersey in 2013 to 2015, by using the natural log (ln) of numbers for (**A**) developing oocytes, (**B**) total embryos (candled embryo litters and free-living embryo litters), and (**C**) free-living embryos only. Each oocyte or embryo is represented by an open circle, and the regression line is included. r^2=coefficient of determination.

classes (Table 2). The only exception is the 95–99 cm STL size class for free-living embryos, which shows a decrease from the previous size class; however, the mean number nearly triples for free-living embryos and nearly doubles for total embryos from the smallest to the largest size class (Table 2). A plot showing fecundity by size class and female spawning stock biomass over time reveals a divergent pattern between fecundity and biomass during the 2000s (Fig. 3). Correlation analyses indicate negative correlations between female spawning stock biomass and fecundity for each size class, although significant correlations were found only within the smallest (80–84 cm STL) and largest (95–99 cm STL) size classes analyzed (Fig. 4). Analy-

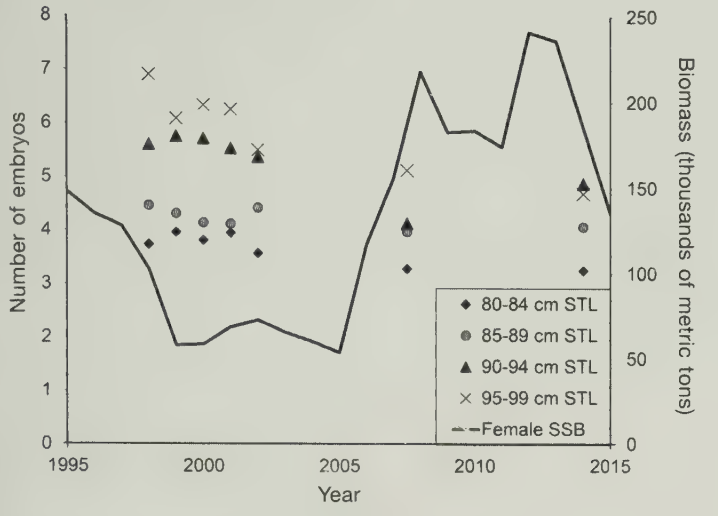

Figure 3

Mean fecundity of females by maternal size class, defined in 5-cm increments of stretched total length (STL), and female spawning stock biomass (SSB), estimated by using a 3-point moving average (Rago and Sosebee[3]), for catch of spiny dogfish (*Squalus acanthias*) from the NOAA Northeast Fisheries Science Center spring bottom trawl survey, plotted over time. Fecundity data from 1998 to 2002 were obtained from Sosebee (2005), an average from 2006 to 2009 was obtained from Bubley (2010), and an average from 2013 to 2015 was obtained from this study.

ses with the use of relative abundance estimates also showed negative correlations between abundance and fecundity for each size class. Significant correlations with the use of relative abundance were found only for the 90–95 cm STL size class during the 2000s (Fig. 4).

Reproductive seasonality

The shift from a predominance of large full-term embryos, to empty uteri, and then candled embryos in the uteri took place between January and April. The first females with flaccid, empty uteri were caught in January of both 2014 and 2015, and the first females with candled embryos were caught in February of 2014 and January of 2015. The occurrence of both these stages and the observation of full-term pups proceeded through at least April of both years, after which all females were either in the first or second year of gestation. These data suggest that protracted pupping and subsequent mating take place between January and April, possibly extending from late December to early May, although embryo development among individuals is synchronous during the rest of the year. No mating scars were observed at any time of the year to corroborate or refute mating periodicity. On the basis of these data, we plotted growth of the embryos starting in January (month 1) as the first month of possible fertilization. We used data gathered for newly mated females from February through June of 2014 (months 2–6) plotted in front of the data collected in July 2013 (month 7) with candled embryos, to illustrate the entire 2-year growth cycle during gestation, with the result showing growth from fertilization (month 1) through birth (month 23; Fig. 5A). Moreover, the decrease in external yolk size is plotted to show the use of the yolk during growth. Assuming that those oocytes that are fertilized first are pupped first, one can calculate the gestation period as 23 months: mating first occurs in January and parturition possibly as early as December, 23 months later.

Data plotted by using the mean weight of the ovaries during the growth period of these same fish show a concurrent increase in ovary size during gestation (Fig. 5B). The data from January 2014 were limited (n=4) but indicated a drastic decrease in ovary size followed by an increase that is most likely an artifact of the small sample size. Together, these data suggest a 2-year synchronous growth cycle such that once the embryos are pupped, the female is ready to mate again. This is further supported by the observation of a short period where females had flaccid empty uteri followed immediately by females with candled embryos. The lack of any significant number of mature nongravid females at any other time of the year also supports this conclusion.

Size of full-term embryos

The lack of an external yolk sac was not a decisive indicator of the terminal stage of embryonic development because litters were observed with no external yolks. Additionally, embryos were found with no internal yolk and they had healing or healed umbilical scars, indicating that term embryos would have no internal or external yolks. Full-term embryos (no internal yolk) ranged in size from 22.0 to 30.8 cm STL. The smallest mean litter size with no external yolks and healed umbilical scars was 20.2 cm STL (from a 77.6-cm-FL female); the average weight of the internal yolks was 1.3 g and this litter was caught at the end of October. The largest mean size of pups in a litter was 30.5 cm STL (78.4 cm FL). These embryos were observed at the beginning of April, had no external or internal yolks, and they had healing umbilical scars. The data indicate that a full-term embryo has a mostly healed umbilical scar and no internal or external yolk.

Discussion

With this study, we confirm that spiny dogfish have a 2-year reproductive period in the region off SNE between Massachusetts and Rhode Island. Our data indicate that these spiny dogfish have at least a 23-month gestation period, which we determined by following the development of a group of embryos from candled em-

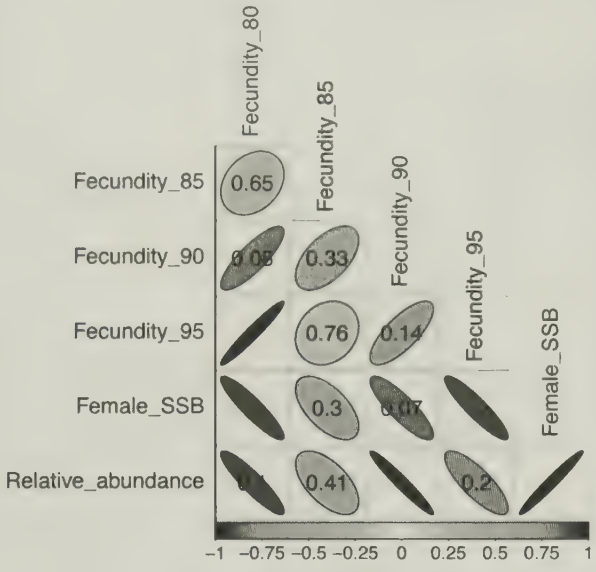

Figure 4

Correlation matrix of fecundity and abundance trends of spiny dogfish (*Squalus acanthias*) during 2000–2015. Mean fecundity of females by maternal size class, defined in 5-cm increments of stretched total length, is correlated with spawning stock biomass (SSB), estimated by using a 3-point moving average (Rago and Sosebee[3]), and with relative abundance estimates based on mean number of mature females caught per tow during the NOAA Northeast Fisheries Science Center spring bottom-trawl survey (Silva, 1993). Fecundity for the 4 maternal size classes, 80–84, 85–89, 90–94, and 95–99 cm in stretched total length, are labeled as Fecundity_80, Fecundity_85, Fecundity_90, and Fecundity_95, respectively. Numerical values denote *P*-values for nonsignificant correlations at an alpha level of 0.05. Fecundity data from 2000 to 2002 were obtained from Sosebee (2005), data from 2006 to 2009 were obtained from Bubley (2010), and data from 2013 to 2015 came from this study.

bryos to parturition. This gestation period is slightly longer than that found by Hisaw and Albert (1947; 20–22 months), slightly shorter than that reported by Templeman (1944; 24 months), and similar to that described by Bubley (2010; 22–23 months).

We found a large range in the sizes of ova ready for fertilization and a corresponding large size range of full-term pups. This was also observed in other studies and it has been suggested that larger ovarian eggs have a larger supply of yolk and would grow into larger embryos and would remain in the uterus longer than smaller eggs (Ford, 1921; Templeman, 1944; Hisaw and Albert, 1947). The embryonic growth rate that we observed was similar to that proposed by Campana et al. (2009) and Henderson et al. (2002), that is slow growth during the first few months followed by faster growth in July through October. Campana et al. (2009) found approximately 3-cm-TL embryos by October in year 1, and although we are missing October data, our November average was 6 cm STL. By the following June, their samples were approximately 16 cm FL and those from the current study averaged 19 cm STL (17.0 cm FL). Our results were similar to those of Henderson et al. (2002) who observed candled embryos in December through July. The size of full-term embryos in our investigation ranged from 19.7 to 30.8 cm STL, which is again similar to results of full-term and near-term size estimates from other studies in the WNA (Templeman, 1944; Hisaw and Albert, 1947; Nammack et al., 1985). Although many similar size embryos were found with internal yolk sacs, they did not appear ready for natural parturition. The observation of litters with full-term–size individuals and no internal yolks suggests that the internal yolk is consumed before parturition. This suggestion is in contrast to the suggestion by Jones and Geen (1977) that the internal yolk is maintained for 2 months past parturition.

Our data show that parturition is followed closely by ovulation and mating and all of these events occur between January and April, although most commonly from February through March. This time frame is longer than previously proposed for this geographic area (Hisaw and Albert, 1947) and is also different from that found in the Gulf of Maine by Bubley (2010), who reported parturition before January (October–December) followed closely by fertilization. Additionally, Campana et al. (2009) found similar results off eastern Canada with a 22–24 month gestation period, pupping from January through March, and fertilization immediately after pupping. The timing of parturition observed in our study is further corroborated by the finding of large numbers of neonate spiny dogfish in February off Block Island, Rhode Island, close to our sampling area (Sulikowski et al., 2013).

Studies have shown that there is a greater plasticity in elasmobranch reproduction than previously thought (Driggers and Hoffmayer, 2009), although the results from studies of dogfish throughout the WNA are reasonably consistent. There may be latitudinal differences. Bubley (2010), for example, reported results from the Gulf of Maine that are approximately 1 month earlier than those that we found for SNE between Massachusetts and Rhode Island. Essentially all the regional studies of spiny dogfish in the WNA have a similar gestation period and have only slightly offset mating and parturition times. The variation in all these studies could be due to latitude or plasticity of the reproductive cycle of this species, and could be potentially related to environmental conditions. More regional studies on spiny dogfish and elasmobranchs in general are required to determine whether differences observed are truly specific to a region or are due to plasticity or size (or both), or age of the female (Lombardi-Carlson et al., 2003; Driggers and Hoffmayer, 2009; Hoffmayer et al., 2013; Rochowski et al., 2015; Taylor et al., 2016).

The average number of pups from this study, based on follicle number, total litter size, and number of

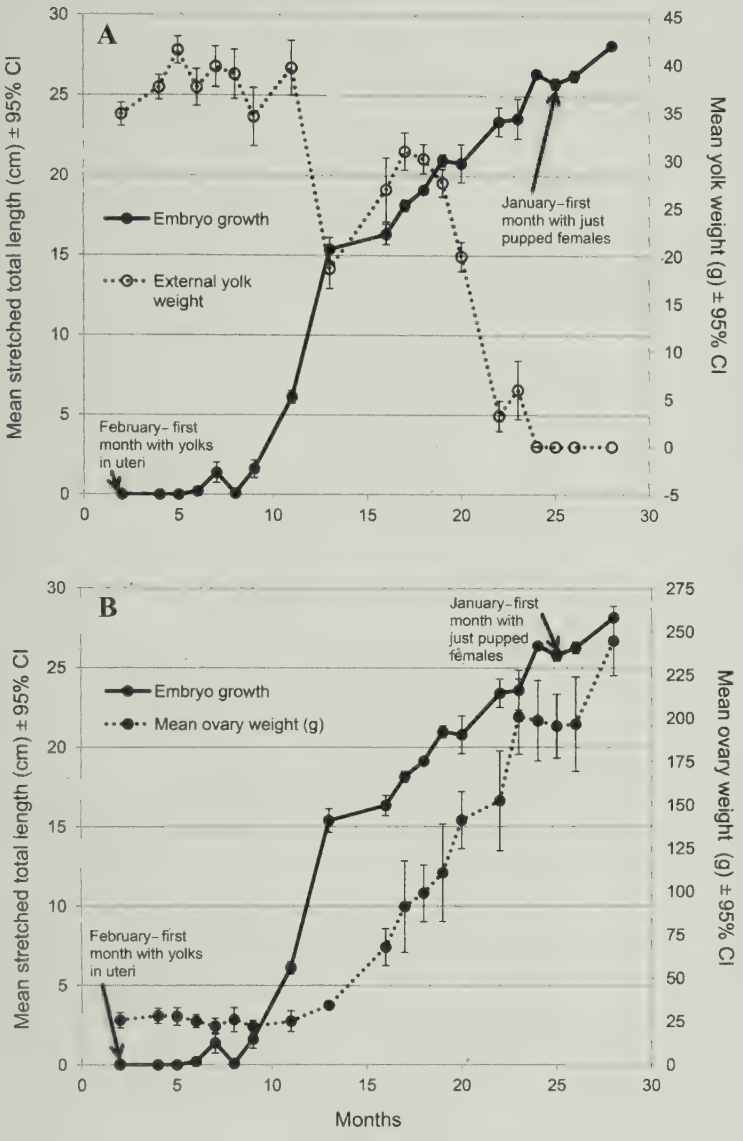
A
Mean stretched total length (cm) ± 95% CI
Mean yolk weight (g) ± 95% CI
Embryo growth
External yolk weight
January–first month with just pupped females
February–first month with yolks in uteri
B
Mean stretched total length (cm) ± 95% CI
Mean ovary weight (g) ± 95% CI
Embryo growth
Mean ovary weight (g)
January–first month with just pupped females
February–first month with yolks in uteri
Months

Figure 5

Growth of embryos and (**A**) external yolk and (**B**) ovary weight through the 2-year gestation period of spiny dogfish (*Squalus acanthias*) sampled off southern New England and New Jersey in 2013–2015. Month 1 corresponds to January of the first year of the cycle. For months 2–6, data are from just fertilized embryos from February to June 2014 and are included to exemplify the typical first 6 months of growth. Months 7–23 correspond to monthly samples collected from July 2013 to April 2015. Error bars indicate 95% confidence intervals (CIs).

only free-living embryos, was similar although the estimates based on oocytes were higher than those based on embryo counts. Jensen (1965) noted premature delivery of near-term pups directly after collection aboard fishing vessels and speculated that this phenomenon is widespread, but is not often reported. He stated that the premature pupping was never excessive and therefore reported estimates of fecundity are still appropriate (Jensen, 1965). The fecundity estimate based on oocytes (5.3) is the highest of the 3 estimates and suggests that not all oocytes are successfully fertilized. Nammack et al. (1985) also found higher numbers of oocytes than embryos and found evidence of ovulation failure. The estimate of fecundity per female from the number of free-living embryos only (4.3) is slightly lower than the estimate from the number of total embryos (4.5) suggesting the potential influence of premature pupping on the estimate of free-living embryos. Because the total estimate eliminates some of the decrease caused by premature pupping, this is the more accurate estimate of fecundity of spiny dogfish. The estimate of free-living embryos from this study falls within the range of other studies in the WNA (Templeman, 1944 [mean: 3.7]; Nammack et al., 1985 [mean: 6.6]; Sosebee, 2005 [mean: 4.4]; Campana et al., 2009 [mean: 4.7]).

Nammack et al. (1985) suggested a possible compensatory increase in the number of pups (overall and by size class) was due to a reduction in stock biomass but noted that the increase could simply be due to differences in sampling locations. Silva (1993) found a negative correlation between spiny dogfish fecundity by size class and abundance estimates from the WNA through 1991 (including data from Templeman [1944] and Nammack et al. [1985]). Additionally, significant correlations for the 80–84, 85–89, and 90–94 cm STL size classes suggest that spiny dogfish fecundity is density dependent (Silva, 1993). Sosebee (2005) reported that the reduction in overall mean fecundity in her study in comparison with results from the Nammack et al. (1985) study is likely due to a truncation of the population size structure resulting from the size selective nature of the fishery. There was also no evidence of density-dependent changes in mean fecundity by maternal size class in the study by Sosebee (2005). At that time, reproductive spiny dogfish were no longer declining in abundance, which may have negated any changes that would result from density dependence (Sosebee, 2005). Our overall mean fecundity based on free-living embryos is similar to that of Sosebee (2005), but data by size class in all length groups showed a decrease in mean fecundity from Sosebee (2005) and more notable drops in the larger size classes. Because status updates (Rago and Sosebee[2,3]) indicate that female spawning stock biomass has been rebuilding since the time of the study

by Sosebee (2005) was completed, it is possible that the reductions in fecundity reflect environmentally controlled, density-dependent reproduction.

This study was a regionally based study designed to determine whether spiny dogfish in the waters off SNE between Massachusetts and Rhode Island follow the pattern of those from the Gulf of Maine and other northwest Atlantic regions. Our sampling regime allowed for a more detailed examination of gestation than that which has previously been accomplished. Although this study was designed to be regional, we cannot ignore the fact that these fish migrate between the Gulf of Maine, SNE, and the mid-Atlantic (Rulifson et al.[8]; Sulikowski et al., 2010). In fact, some recent satellite tagging data indicate significant regional movements (Carlson et al., 2014). Spiny dogfish located off SNE throughout the year may include components of both resident and migrating populations. This is in line with Campana et al. (2009), who also found resident and migratory populations in their study area off the coast of eastern Canada.

Acknowledgments

We thank all the commercial fishermen who collected the samples for this project. We also could not have completed this project without help from NMFS Cooperative Research Program, particularly: K. Burchard, C. Alexander, B. Gervelis, E. Marchetti, and C. Sarro. We also appreciate the help of C. Flight and S. Chen in recording data. R. Guilmette and J. Tully were essential for sample removal. We would also like to thank R. McBride and K. Sosebee for their thoughtful comments on our draft.

Literature cited

Avsar, D.
2001. Age, growth, reproduction and feeding of the spurdog (*Squalus acanthias* Linnaeus, 1758) in the southeastern Black Sea. Est. Coast. Shelf Sci. 52:269–278.

Bigelow, H. B., and W. C. Schroeder.
1953. Fishes of the Gulf of Maine. Fish. Bull. 53:1–577.

Bubley, W.
2010. Updated life history and population structure assessment of spiny dogfish, *Squalus acanthias*, in the Gulf of Maine. Ph.D. diss, 144 p. Univ. New Hampshire, Durham, NH.

Bubley, W. J., J. A. Sulikowski, D. M. Koester, and P. C. W. Tsang.
2013. Using a multi-parameter approach to reassess maturity of spiny dogfish, *Squalus acanthias*, following increased fishing pressure in the Western North Atlantic. Fish. Res. 147: 202–212.

Campana, S. E., C. Jones, G. A. McFarlane, and S. Myklevoll.
2006. Bomb dating and age validation using the spines of spiny dogfish (*Squalus acanthias*). Environ. Biol. Fish. 77:327–336.

Campana, S. E., W. Joyce, and D. W. Kulka.
2009. Growth and reproduction of spiny dogfish off the eastern coast of Canada, including inferences on stock structure. *In* Biology and management of dogfish sharks (V. F. Gallucci, G. A. McFarlane, and G. G. Bargmann, eds.), p. 195–207. Am. Fish. Soc., Bethesda, MD.

Capapé, C., and C. Reynaud.
2011. Maturity, reproductive cycle and fecundity of the spiny dogfish *Squalus acanthias* (Chondrichthyes: Squalidae) off the Languedocian coast (southern France, northern Mediterranean). J. Mar. Biol. Assoc. U.K. 91:1627–1635.

Carlson, A. E., E. R. Hoffmayer, C. A. Tribuzio, and J. A. Sulikowski.
2014. The use of satellite tags to redefine movement patterns of spiny dogfish (*Squalus acanthias*) along the U.S. East Coast: implications for fisheries management. PLoS ONE 9(7):e103384.

Chatzispyrou, A., and P. Megalofonou.
2005. Sexual maturity, fecundity and embryonic development of the spiny dogfish, *Squalus acanthias*, in the eastern Mediterranean Sea. J. Mar. Biol. Assoc. U.K. 85:1155–1161.

Collette, B. B., and G. Klein-MacPhee (eds.).
2002. Bigelow and Schroeder's fishes of the Gulf of Maine, 3rd ed., 748 p. Smithsonian Institution Press, Washington, DC.

Di Giacomo, E. E., M. R. Perier, and M. Coller.
2009. Reproduction of spiny dogfish in San Matías Gulf, Patagonia (Argentina). *In* Biology and management of dogfish sharks (V. F. Gallucci, G. A. McFarlane, and G. G. Bargmann, eds.), p. 209–215. Am. Fish. Soc., Bethesda, MD.

Driggers, W. B., III, and E. R. Hoffmayer.
2009. Variability in the reproductive cycle of finetooth sharks, *Carcarhinus isodon*, in the northern Gulf of Mexico. Copeia 2009:390–393.

Ebert, D. A., W. T. White, K. J. Goldman, L. J. V. Compagno, T. S. Daly-Engel, and R. D. Ward.
2010. Resurrection and redescription of *Squalus suckleyi* (Girard, 1854) from the North Pacific, with comments on the *Squalus acanthias* subgroup (Squaliformes: Squalidae). Zootaxa 2612:22–40.

Ford, E.
1921. A contribution to our knowledge of the life-histories of the dogfishes landed at Plymouth. J. Mar. Biol. Assoc. U.K. 12:468–505.

Gračan, R., B. Lazar, I. Posavec, G. Gregorović, and G. Lacković.
2013. Maturation, fecundity and reproductive cycle of spiny dogfish, *Squalus acanthias*, in the Adriatic Sea. Mar. Biol. Res. 9:198–207.

Hamlett, W. C. and T. J. Koob.
1999. Female reproductive system. *In* Sharks, skates, and rays: the biology of elasmobranch fishes (W. C. Hamlett, ed.), p. 398–444. Johns Hopkins Univ. Press, Baltimore, MD.

Hanchet, S.
1988. Reproductive biology of *Squalus acanthias* from the

[8] Rulifson, R. A., T. M. Moore, and C. S. Hickman. 2002. Biological characterization of the North Carolina spiny dogfish (*Squalus acanthias)* fishery. Report for Project No. 97FEG-28. [Available from Fisheries Resource Grant Program, North Carolina Sea Grant, P.O. Box 8605, NCSU, Raleigh, NC 27695-8605.]

east coast, South Island, New Zealand. N. Z. J. Mar. Freshw. Res. 22:537–549.

Henderson, A. C., K. Flannery, and J. Dunne.
2002. Growth and reproduction in spiny dogfish *Squalus acanthias L.* (Elasmobranchii: Squalidae), from the west coast of Ireland. Sarsia 87:350–361.

Hisaw, F. L., and A. Albert.
1947. Observations on the reproduction of the spiny dogfish, *Squalus acanthias*. Biol. Bull. 92:187–199.

Hoffmayer, E. R., W. B. Driggers III, L. M. Jones, J. M. Hendon, and J. A. Sulikowski.
2013. Variability in the reproductive biology of the Atlantic sharpnose shark in the Gulf of Mexico. Mar. Coast. Fish. 5:139–151.

Jensen, A. C.
1965. Life history of the spiny dogfish. Fish. Bull. 65:527–554.

Jones, B. C., and G. H. Geen.
1977. Reproduction and embryonic development of spiny dogfish (*Squalus acanthias*) in the Strait of Georgia, British Columbia. J. Fish. Res. Board Can. 34:1286–1292.

Kaganovskaia, S. M.
1937. On the commercial biology of *Squalus acanthias*. Izv. Tikhookean. Nauch.-Issled. Inst. Ryb. Khoz. Okeanogr. 10:105–115.

Ketchen, K. S.
1972. Size at maturity, fecundity, and embryonic growth of the spiny dogfish (*Squalus acanthias*) in British Columbia waters. J. Fish. Res. Board Can. 29:1717–1723.

Lombardi-Carlson, L. A., E. Cortés, G. R. Parsons, and C. A. Manire.
2003. Latitudinal variation in life-history traits of bonnethead sharks, *Sphyrna tiburo,* (Carcharhiniformes: Sphyrnidae) from the eastern Gulf of Mexico. Mar. Freshw. Res. 54:875–883.

McMillan, D. G., and W. W. Morse.
1999. Essential fish habitat source document: spiny dogfish, *Squalus acanthias*, life history and habitat characteristics. NOAA Tech Memo NMFS-NE-150, 19 p.

Nammack, M. F., J. A. Musick, and J. A. Colvocoresses.
1985. Life history of spiny dogfish off the northeastern United States. Trans. Am. Fish. Soc. 114:367–376.

Rago, P. J., and K. A. Sosebee.
2009. The agony of recovery: scientific challenges of spiny dogfish recovery programs. *In* Biology and management of dogfish sharks (V. F. Gallucci, G. A. McFarlane, and G. G. Bargmann, eds.), p. 343–372. Am. Fish. Soc., Bethesda, MD.

Rochowski, B. E. A., T. I. Walker, and R. W. Day.
2015. Geographical variability in life-history traits of a midslope dogfish: the brier shark *Deania calcea*. J. Fish Biol. 87:728–747.

Silva, H. G. M.
1993. Population dynamics of spiny dogfish, *Squalus acanthias*, in the NW Atlantic. Ph.D. diss., 239 p. Univ. Mass. Amherst, Amherst, MA.

Sosebee, K. A.
2005. Are density-dependent effects on elasmobranch maturity possible? J. Northwest Atl. Fish. Sci. 35:115–124.

Sulikowski, J. A., B. Galuardi, W. Bubley, N. B. Furey, W. B. Driggers III, G. W. Ingram Jr., and P. C. W. Tsang.
2010. Use of satellite tags to reveal the movements of spiny dogfish *Squalus acanthias* in the western North Atlantic Ocean. Mar. Ecol. Prog. Ser. 418:249–254.

Sulikowski, J. A., B. K. Prohaska, A. E. Carlson, A. M. Cicia, C. T. Brown, and A. C. Morgan.
2013. Observation of neonate spiny dogfish, *Squalus acanthias*, in southern New England: a first account of a potential pupping ground in the northwestern Atlantic. Fish. Res. 137:59–62.

Taylor, S. M., A. V. Harry, and M. B. Bennett.
2016. Living on the edge: latitudinal variations in the reproductive biology of two coastal species of sharks. J. Fish Biol. 89:2399–2418.

Templeman, W.
1944. The life-history of the spiny dogfish (*Squalus acanthias*) and the vitamin A values of dogfish liver oil. Dep. Nat. Resour. the Newfoundland, Res. Bull.15, 102 p.

Yamamoto, T., and O. Kibezaki.
1950. Studies on the spiny dogfish *Squalus acanthias* (L.) on the development and maturity of genital glands and growth. Hokkaido Reg. Fish. Resour. Res. Rep. 3:531–538.

National Marine
Fisheries Service
NOAA

Fishery Bulletin
established in 1881

Spencer F. Baird
First U.S. Commissioner
of Fisheries and founder
of *Fishery Bulletin*

A new underwater shark capture method used by divers to catch and release nurse sharks (*Ginglymostoma cirratum*)

Serge Aucoin (contact author)
Steve Weege
Max Toebe
Jeff Guertin
Jonathan Gorham
Michael Bresette

Email address for contact author: saucoin@gmail.com

Inwater Research Group
4160 NE Hyline Drive
Jensen Beach, Florida 34957

Abstract—We developed an alternative capture-and-release method for sharks using a simple poker-and-hook tool for divers to quickly capture nurse sharks (*Ginglymostoma cirratum*) entering the intake canal of a nuclear power plant in Florida. The capture technique consists of using a short metal rod (poker) with a barbless J-hook (size 10/0) to snag the base of a shark's tail (caudal peduncle), then safely hauling the individual into a boat by the buoy line that has been hooked to its tail. We captured 20 nurse sharks ranging from 11.8 to 80.3 kg, and 9 individuals were monitored over time. Six sharks were released into the canal and 3 sharks were put in an open tank for 23–24 days for daily observations. All hook wounds resulting from this technique were assessed between 9 and 42 days, and no ill effects were observed throughout the study period. The capture method caused a small superficial wound to the caudal peduncle that averaged 11.3 mm^2 (standard deviation 8.7; n=23). Wound closure was observed after 9 days and re-epithelialization was almost complete (or the wound had completely healed) between 22 and 42 days. Landing nurse sharks this way is less traumatic than traditional methods (e.g., angling, netting). This study provides preliminary information on, and validates, the use of this tool as an efficient and less invasive capture method than traditional methods and as a method that could be applied to broader areas of shark research.

Manuscript submitted 26 November 2016.
Manuscript accepted 28 July 2017.
Fish. Bull. 115: 484–495 (2017).
Online publication date: 15 August 2017.
doi: 10.7755/FB.115.4.5

The views and opinions expressed or implied in this article are those of the author (or authors) and do not necessarily reflect the position of the National Marine Fisheries Service, NOAA.

Capturing animals is often a necessary part of wildlife management activities and ecological research. Studies involving the capture of animals have enabled researchers to understand certain species behavior that otherwise would not have been possible (e.g., intraspecific competition; Hoelzer, 1990; Webster and Hixon, 2000) or to uncover some of the social factors influencing physiological processes (e.g., sex-reversal; Shapiro and Boulon, 1982; Goodwin, 2009). Capture–recapture methods with various types of tags for surveying animals have also allowed researchers to track the movement of species (Kohler et al., 1998; Wiley and Simpfendorfer, 2007), determine species range (Kramer and Chapman, 1999), estimate population size (Pine et al., 2003; Gwinn et al., 2011), and assess other demographic parameters (e.g., Zeller and Russ, 1998; Jones et al., 1999) that have contributed to our understanding of the natural world and facilitated resource management (Davis and Dodrill, 1989; Clark and Kaimmer, 2006).

Trapping, chemical immobilization, and many other methods have been used to capture animals for research, relocation, and other management purposes (Williams et al., 2002; Silvy, 2012). Ethically, capture methods should aim to minimize animal suffering (Cuthill, 1991; Jenkins et al., 2014), as well as reduce stress responses, which can bias many types of data collected (Sheriff et al., 2011; Gallagher et al., 2014). Ideally, capture methods should be developed and refined by experienced wildlife biologists and technicians who have studied, planned, and tested methods before starting any wildlife research or management program (Schemnitz et al., 2012).

Knowledge of the behavior and activity patterns of the targeted species is necessary to maximize capture efficiency when developing capture methods. The nurse shark (*Ginglymostoma cirratum*) was the target species in this study. It is a bottom-dwelling opportunistic predator that feeds primarily on small fish and some invertebrates (Castro, 2000). Juveniles are typically found on the bottom of shallow coral reefs, seagrass flats, and around mangrove islands. Older individuals typically

reside in and around deeper reefs and rocky areas, where they tend to seek shelter in crevices and under ledges during the day and leave their shelter at night to feed on the seabed in shallower areas (Castro, 2000).

Nurse sharks have a wide but patchy geographical distribution along tropical and subtropical coastal waters of the eastern Atlantic Ocean, western Atlantic Ocean, and eastern Pacific Ocean (Campagno, 2002; Karl et al., 2012). They have long residency times and show strong site fidelity (typical of reef sharks), and they are one of the few shark species known to exhibit mating-site fidelity (Carrier et al., 2004). Nurse sharks are also exceptionally sedentary, unlike most other shark species (Heithaus et al., 2007; Karl et al., 2012; Whitney et al., 2016). They are targeted directly in some fisheries and are considered as bycatch in others. The conservation status of the nurse shark is globally assessed as being data deficient in the IUCN List of Threatened Species owing to the lack of information across its range in the eastern Pacific Ocean and eastern Atlantic Ocean (Rosa et al., 2006). They are considered to be a species of least concern in the United States and in The Bahamas, but considered to be near threatened in the western Atlantic Ocean because of their vulnerable status in South America and reported threats throughout many areas of Central America and the Caribbean (Rosa et al., 2006).

Nurse sharks are known to be robust and able to tolerate capture, handling, and tagging extremely well (Carrier, 1985; Dooley and Flajnik, 2005) and are an important species for shark research (predominantly in physiology). Over 30% of current studies from all published research on 29 reef shark species have focused on nurse sharks (Osgood and Baum, 2015). Studies that involved capturing nurse sharks have successfully used fishing nets or baited hook-and-line gear, but these methods are not without limitations or problems (Garla et al., 2006; Skomal, 2007; Gallagher et al., 2014). These traditional capture methods can prolong treatment and handling times on account of gear entanglement and recovery delays (Smith, 1992; Mandelman and Farrington, 2007; Morgan and Carlson, 2010) or cause severe hooking injuries that increase morbidity and mortality (Bansemer and Bennett, 2010; Danylchuk et al., 2014).

Shark survival and recovery after capture varies widely and depends on a variety of factors (reviewed in Skomal and Bernal, 2010). Assessing 25 species of chondrichthyans (i.e., evaluating >11,000 sharks, rays, and chimaeras) in a commercial shark fishery, Braccini et al. (2012) indicated postcapture survival to be generally high. Tracking studies on the postrelease mortality of lemon sharks (*Negaprion brevirostris*) and Atlantic sharpnose sharks (*Rhizoprionodon terraenovae*) captured by baited hook-and-line gear indicated a 10–12.5% postrelease mortality rate for these species (Gurshin and Szedlmayer, 2004; Danylchuk et al., 2014), but this may be an underestimate owing to either low sample sizes or to short monitoring times, or both (i.e., delayed mortality due to infection and disease).

Hooking injuries are considered the primary cause of angling-related mortality and are the result of many factors, including hook type and hook configuration, as well as fishing technique and experience (see Brownscombe et al., 2017). Moreover, evidence indicates that cartilaginous skeletons of sharks do not heal properly after damage (Ashhurst, 2004), thus hooking trauma to cartilaginous structures in the jaw or skull may have long lasting impacts.

In this study, we present technical information on a more efficient and less invasive capture method that we used to catch and release nurse sharks. The technique involves hooking the area of the caudal peduncle (between the caudal fin and 2nd dorsal fin) where shark skin is thick and posterior musculature has been reported as being the most damage-tolerant area (Towner et al., 2012). The tail base is also away from the more vascularized tissues and sensory organs concentrated anteriorly (e.g., gills, eyes, nostrils, ampullae of Lorenzini, mandibular neuromasts; Hueter et al., 2004). The resulting damage to these areas from typical baited fishing, as well as gut injuries from swallowed hooks, can render sharks more susceptible to late onset morbidity and mortality (Bansemer and Bennet, 2010). Although the remarkable ability of sharks to heal quickly from various types of body wall and other types of injuries has long been documented (Olsen, 1953; Bird, 1978; Reif, 1978; Towner et al., 2012; Kessel et al., 2017), we examined wound recovery from this new poker-and-hook method for up to a 42-day period to validate its use as a minimally invasive capture technique for sharks.

Materials and methods

Study area

Nurse sharks will occasionally inhabit the seawater intake canal at the Florida Power and Light St. Lucie Nuclear Power Plant located on Hutchinson Island, Florida (Fig. 1). The offshore intake pipes that draw cooling water (365 m offshore, 7 m off the seafloor) use velocity caps that effectively deter and reduce fish from entering (see review by Fedorenko, 1991), but some nurse sharks and other marine wildlife still enter from time to time (Bresette et al., 1998).

Marine wildlife entering the canal need to be removed by biologists in order to return them to their natural habitat. In the past, nurse sharks that entered the canal were captured by traditional baited hook-and-line gear (e.g., rod and reel, hand lines), but the use of these methods in the canal can take hours to land a few individuals, if any. The inefficiency of these methods in this case is due to the tendency of nurse sharks to aggregate at discharge ends of the canal intake pipes where strong currents and obstructions (e.g., pier columns) occur and can pre-

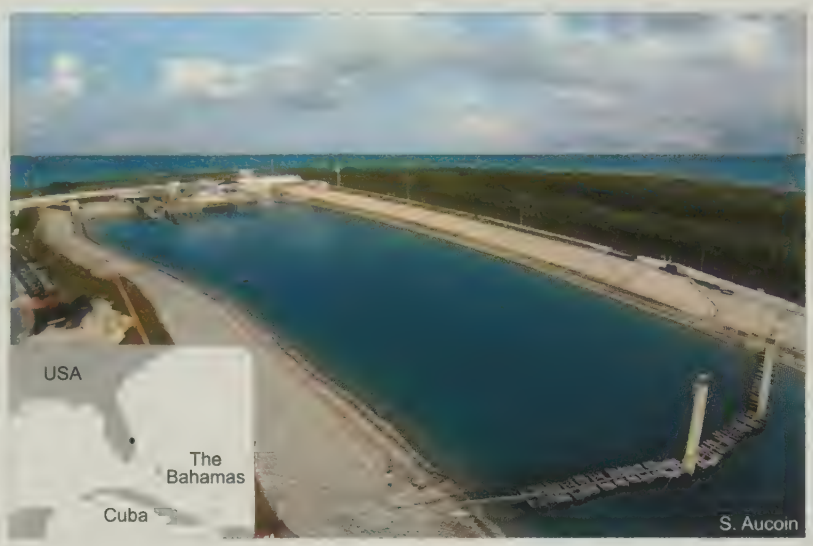

Figure 1

Photograph and location of the intake canal of the Florida Power and Light St. Lucie Nuclear Power Plant on Hutchinson Island, where nurse sharks (*Ginglymostoma cirratum*) were captured with the poker-and-hook tool and monitored to evaluate this new underwater method for catching sharks.

vent the deployment of gill nets and can easily sever fishing lines.

Equipment and capture technique

The poker-and-hook tool consisted of a long shanked stainless-steel J-hook (size 10/0 with its barb removed) attached to an 80-cm twine leader (90-kg test), a 20-m rope and retrieval buoy, and a 90-cm metal rod (the poker) (Fig. 2A). We wrapped the twine leader 2–3 times around the poker to avoid entanglement underwater (Fig. 2B). The steel hook was fastened to the poker with 2-mm cable ties: 2 cable ties were threaded through a hole at the end of the poker and through the eye of the hook, and a third cable tie cinched the hook towards the tip (Fig. 2C). We also flattened the back of the hook and the tip of the poker for added stability, and lightly scored the cable ties to facilitate their breaking under pressure.

To capture a nurse shark, a diver descended to the targeted individual with the poker-and-hook tool in hand, keeping the twine leader taut (Fig. 2B) and hooked the side of the caudal peduncle (region between the anal and tail fins); hereafter, referred to as the tail base (Fig. 3). The diver aimed to hook the upper- or lower-lateral part of the nurse shark's tail base because the species is primarily a nocturnal feeder and therefore frequently dependent on its lateral line for feeding. Moreover, the skin of the upper and lower parts of the tail base in sharks is often thicker and adjoining muscle below the skin is also less vascularized than that of the middle-lateral part (Shadwick and Goldbogen, 2012). Once the tail base was hooked, the cable ties broke or slid off as a result of the shark swimming away with the hook (with the poker remaining in hand) and the line, now attached to the shark, was released. A short video demonstrating this underwater capture technique is available (video).

We then used a 4-m boat with low sides (i.e., modified gunnels) and pulled in the line by hand until the shark's tail could be used to haul the individual onboard. For large sharks (≥70 kg), we lassoed the shark's tail at the water surface to facilitate hauling these heavier individuals into the boat. None of the nurse sharks we hauled into the boat exhibited any stress-induced vertebral 'popping' (dislocation of vertebrae) that can occur when lifting large fish by their tail (e.g., Pacific halibut [*Hippoglossus stenolepis*], senior author, personal observ.). Once onboard, the shark was restrained by hand and our total handling and processing time was under 5 min. This period included the time to dock the boat and to move the individual with a wet push cart to a weigh station, to a holding tank, or to the beach for release (see next section).

Postcapture monitoring and wound assessment

A total of 20 nurse sharks were captured and released between 8 August and 23 October 2014. At first, 4 sharks were removed from the canal by using this new technique. These nurse sharks ranged from 48.9 to 79.6 kg and experienced hook wounds that were relatively superficial (i.e., shallow punctures with no bleeding). After each individual was examined, we recorded weight, maximum total length, and took photos of hook wounds to scale. All the sharks were released back into the ocean without issue.

We then proceeded to capture 16 more sharks ranging from 11.8 to 80.3 kg, but this time we assessed hook wounds in a more systematic way. When sharks were hauled into the boat, we first measured hook penetration if the hook did not fall out, which was often the case. Hook penetration or depth was reported as the straight distance between the tip of the hook to the first visible part of the hook shank at the surface of the shark's skin. Of these 16 sharks captured, we released 6 nurse sharks ranging from 11.8 to 43.8 kg back into the canal and 3 sharks ranging from 14.9 to 21.2 kg were put into a nearby 3-m diameter open flow-through tank (~0.5 L/s) in the shade. All sharks >48.9 kg were returned to the ocean to reduce handling large individuals a second time, and these returned sharks included 2 individu-

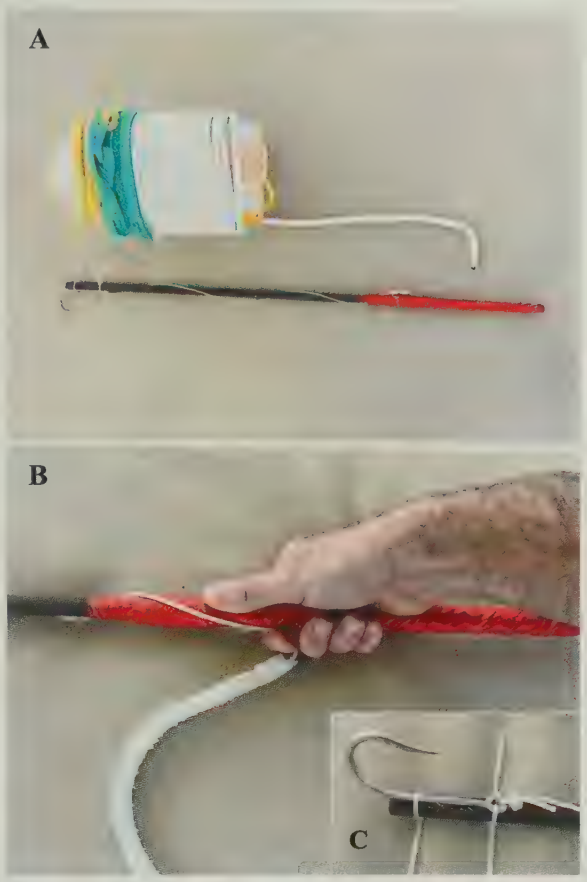

Figure 2

Images of (**A**) the poker-and-hook gear used to capture nurse sharks (*Ginglymostoma cirratum*) in this study, (**B**) how the lead line or ganion is kept taut around the poker (line and rope awareness is critical to avoid diver entanglement), and (**C**) how the cable ties are threaded through the eye of the hook and the hole at the end of the poker and used to cinch the hook bend at the poker tip.

als that we suspected were pregnant (64.8 kg, 66.0 kg; see Castro, 2000). Two more sharks were released into the ocean (14.2 kg, 32.0 kg) because we already had a number of similar-size individuals. We monitored the 6 sharks in the canal by snorkeling when water clarity permitted, whereas the 3 sharks in the tank were observed daily (and with video footage) and fed every 3–4 days. The 3 sharks released in the holding tank were then re-assessed after 23–24 days and the sharks in the canal were randomly recaptured and re-assessed between 9 and 42 days. All individuals were tagged with numbered plastic Rototags[1] (Dalton ID Systems Ltd., Henley-on-Thames, UK) on their dorsal fins (see Latour, 2005), their weight and total length were recorded, and their hook wounds were photographed to scale.

To standardize our evaluation of each hook wound, we first put a measuring tape next to the wound and photographed both the wound and tape together with the camera lens directly above the plane of the skin surface. We then quantified hook wounds by processing digital images in Adobe Photoshop CC, vers. 2015 (Adobe Systems, Inc., San Jose, CA) to calculate the geometrical parameters of wound severity: wound area; circumference; and circularity by using the Photoshop ruler tool to measure pixel length to scale, and then manually outlining the wound margin with the polygonal lasso tool (Sedgewick, 2008). Recording the 4 parameters of hook depth, wound area, circumference, and circularity provided baseline data on initial wound status. Because medical studies show that wound area and circumference correlate with wound volume (Melhuish et al., 1994; Flanagan, 2003), we used SPSS Statistics, vers. 20.0.0 (IBM Corp., Armonk, NY) to examine wound area in relation to hook depth (as a proxy for wound volume) by applying an analysis of covariance (ANCOVA), with shark body size as the covariate. To further examine hook injury, specifically,

[1] Mention of trade names or commercial companies is for identification purposes only and does not imply endorsement by the National Marine Fisheries Service, NOAA.

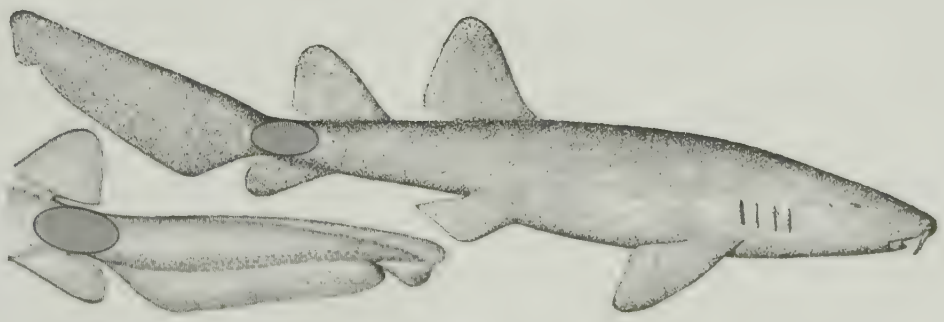

Figure 3

Illustration of the caudal peduncle (i.e., tail base) indicated by the gray ellipse, that was targeted with the poker-and-hook capture method for nurse sharks (*Ginglymostoma cirratum*). It is a modification of a public domain image from Evermann et al. (1900). Courtesy of the Freshwater and Marine Image Bank, Univ. Washington, Seattle, WA.

Table 1

Description of nurse sharks (*Ginglymostoma cirratum*) captured with the poker-and-hook method in a nuclear power plant intake canal in Florida during 2014, and resulting hook wound characteristics. Minimum bleeding indicates either a few drops of blood (Fig. 4A) or residual blood (Fig. 4E) observed once individuals were hauled into the boat. Circularity is defined as 4π(area/circumference^2), where a value of 1 indicates a perfect circle and a value approaching 0 indicates an increasingly elongated shape (i.e., skin tear). Hook depth is a relative measure that was recorded as the straight distance between the tip of the hook to the first visible part of the hook shank at the surface of the shark's skin. A superscript *R* signifies recapture and identifies individuals captured twice by the poker-and-hook method. Principal component analysis (PCA) with weight and length together was used to indicate a score for shark body size. f/o=fell out (hook fell out by itself when the shark was landed). n/a=not available (hook depth not measured). A mean and standard deviation (SD) are given for wound area, circumference, and circularity.

Weight (kg)	Total length (cm)	PCA score	Sex	Hook depth (mm)	Hematuria (bleeding)	Area (mm^2)	Circumference (mm)	Circularity (0–1)
11.8^R	135	−1.445	M	f/o	minimal	2.2	11.2	0.21
				37	none	10.0	21.3	0.50
12.7	137	−1.397	F	24	minimal	21.9	38.2	0.39
14.2	143	−1.282	M	29	none	8.5	15.1	0.47
14.2	145	−1.255	F	f/o	none	3.6	26.6	0.06
14.9	151	−1.158	F	23	none	10.5	30.1	0.15
19.8	163	−0.886	M	19	minimal	10.1	14.1	0.64
21.2	167	−0.800	M	16	minimal	6.9	26.6	0.12
32.0	186	−0.302	F	33	minimal	18.9	28.4	0.30
41.2^R	204	0.148	M	35	none	10.1	12.3	0.85
				f/o	minimal	4.8	9.0	0.75
43.7	205	0.217	M	23	minimal	13.0	49.8	0.07
43.8	209	0.274	M	21	none	7.8	15.0	0.43
48.9	210	0.401	F	f/o	none	13.9	19.4	0.43
52.9	211	0.504	M	18	minimal	5.2	17.3	0.22
52.9	218	0.599	F	24	minimal	2.3	7.0	0.58
56.5	238	0.951	M	f/o	minimal	5.2	9.8	0.68
60.0	214	0.703	F	n/a	minimal	37.8	30.6	0.51
64.8	233	1.068	F	n/a	none	10.0	15.1	0.54
66.0^R	231	1.067	F	25	minimal	16.7	27.0	0.29
				37	minimal	6.8	11.5	0.65
79.6	222	1.248	F	15	none	5.6	17.6	0.44
80.3	245	1.576	F	38	minimal	29.4	24.9	0.60
					Mean	11.3	20.8	0.43
					SD	(8.7)	(10.4)	(0.22)

circularity (defined as 4π(area/circumference^2)) as an index of skin tearing in relation to shark size, we used a binomial logistic regression, which included calculating the Nagelkerke pseudo-coefficient of determination (Nagelkerke pseudo-r^2) and the Homer-Lemeshow test of the goodness of fit to help explain the overall model. In this case, we used categories more severe (circularity ≤0.5) and less severe (circularity >0.5), where a value approaching 0 indicates an increasingly elongated shape and therefore a more pronounced skin tear. The Omnibus test of model coefficients (i.e., likelihood ratio chi-square test) was used for the overall model, whereas the Wald chi-square test was used for the odds ratio (see McCormick and Salcedo, 2017).

Before-and-after photos of hook wounds were used to re-assess 3 nurse sharks recaptured after 9–10 days, 4 nurse sharks after 22–24 days, and 2 nurse sharks after 37–42 days. We included all hook wounds (n=23) to calculate descriptive statistics, which included 2 individuals captured twice because they escaped from our boat the first time, and 1 individual recaptured over time. Anglers targeting large groupers recaptured the remaining 5 nurse sharks in the canal. We compared before-and-after weights of 4 nurse sharks after 22–24 days (1 nurse shark in the canal and 3 sharks in the tank). To minimize handling time, the 5 other sharks released in the canal were weighed only before being released in the ocean.

Results

Table 1 shows shark description and wound information, including mean values for wound area, circularity,

Table 2

The logistical binary regression applied to data from nurse sharks (*Ginglymostoma cirratum*) captured with the poker-and-hook method in Florida during 2014 to ascertain the effects of body size on the likelihood of more pronounced skin tears (i.e., circularity ≤0.5) produced a significant model ($\chi^2(1)=6.124$, $P=0.01$). The model explained 31.7% (Nagelkerke pseudocoefficient of determination [pseudo-r^2]) of the variance in the outcome and correctly classified 73.9% of cases. The output for variables in the equation indicated that increasing body size was associated with a 72% reduction in the likelihood of exhibiting more pronounced skin tears (odds ratio: 0.279) when the 10/0 barbless J-hook was used in our study. The asterisk (*) indicates statistical significance ($\alpha<0.05$); β=beta weight coefficient (i.e., intercept); SE=standard error; Wald=Wald chi-square value; df=degrees of freedom; Exp(β)=exponentiation of the coefficients (i.e., odds ratios for the predictors).

	β	SE	Wald	df	*P* value	Exp(β)
Body size	−1.277	0.608	4.411	1	0.036*	0.279
Constant	14.9	0.524	1.449	1	0.229	1.878

Table 3

Difference in weight at capture and 22–24 days after recapture for 4 nurse sharks (*Ginglymostoma cirratum*) captured by the poker-and-hook method and released in Florida during 2014. The remaining sharks sampled for this study were weighed only upon their release back into the ocean to minimize handling time.

Total length (cm)	Initial weight (kg)	Final weight (kg)	Weight gain (kg)	Time (d)	Gain rate (g/d)
135	11.8	12.1	0.3	22	14
151	14.9	15.5	0.6	23	27
163	19.8	20.3	0.5	24	20
167	21.2	22.0	0.8	23	35

and circumference. Hook depth (as a proxy for wound volume) in relation to wound area, circularity, and circumference was initially examined. Because the variables are correlated (different types of measurements of the same wound) we first tested for multicollinearity, which indicated dropping the variable circumference in subsequent analysis. We then tested whether wound area predicted hook depth by using ANCOVA. Because measurements of shark weight and total length were strongly positively correlated, we used a principle component analysis to reduce these variables into component scores as a better indicator of shark body size (i.e., as a covariate) and to increase the degrees of freedom available to estimate variability. Nonetheless, the model did not reveal any significant relationship between wound area and hook depth or body size.

The logistical binary regression applied to ascertain the effects of body size on the likelihood of more pronounced skin tears (i.e., circularity ≤0.5) produced a significant model, indicated by the Omnibus test of model coefficients ($\chi^2(1)=6.124$, $P=0.01$), with the Hosmer-Lemeshow test strongly suggesting the model was a good fit to the data ($P=0.42$). The model explained 31.7% (Nagelkerke pseudo-r^2) of the variance in the outcome, correctly classified 73.9% of cases, and the odds ratio indicated that increasing body size was associated with a 72% reduction in the likelihood of exhibiting more pronounced skin tears when using the 10/0 barbless J-hook in our study (Table 2).

Photos were taken to measure wound and healing progression over time; all wounds were nearly or completely healed after 22 days. Typical healing stages for small wounds in nurse sharks begin with mucus secretion, followed by wound contraction, epidermal expansion, and scale neogenesis (Reif, 1978). Figure 4 shows typical before-and-after photos of hook wounds from sampled nurse sharks. At 9–10 days, wounds showed that the dermis had begun regenerating (seen beneath its mucus covering; Fig. 4, A and B) or were already transitioning to the epidermal expansion stage. At 22–24 days, repair scales within a fully regenerated epidermis were obvious (Fig. 4, C and D) and easily identified by their white color (in comparison with fully mineralized scales that are brown). At 37–42 days, only a small scar remained, and although no histological assessment was performed the formed scales appeared to be normal (Fig. 4, E and F), identified by their brown color which was due to pigment deposited together with inner layers of dentine in the skin (Reif, 1978).

Table 3 shows before-and-after weights of 4 nurse sharks re-assessed after 22–24 days. All individuals had gained weight upon recapture (mean: 0.6 kg [standard deviation 0.2]). The smallest of these 4 sharks, which was released into the canal, gained less weight than the 3 larger individuals released into the holding tank that were fed regularly.

Discussion

Studies on the survival of fish after their capture and release are technically challenging and the long-term effects of physical and physiological trauma associated with varying capture techniques remain mostly unknown (Davis, 2002; Skomal and Bernal, 2010; Gallagher, 2015). Recent studies are beginning to document postcapture sharks for extended periods and indicate that capture-related morbidity and mortality in sharks varies widely among species (Brill et al., 2008; Frick et al., 2010; Heberer et al., 2010; Gallager et al., 2014). Although postcapture mortality rates for sharks are still generally considered to be low (Gurshin and

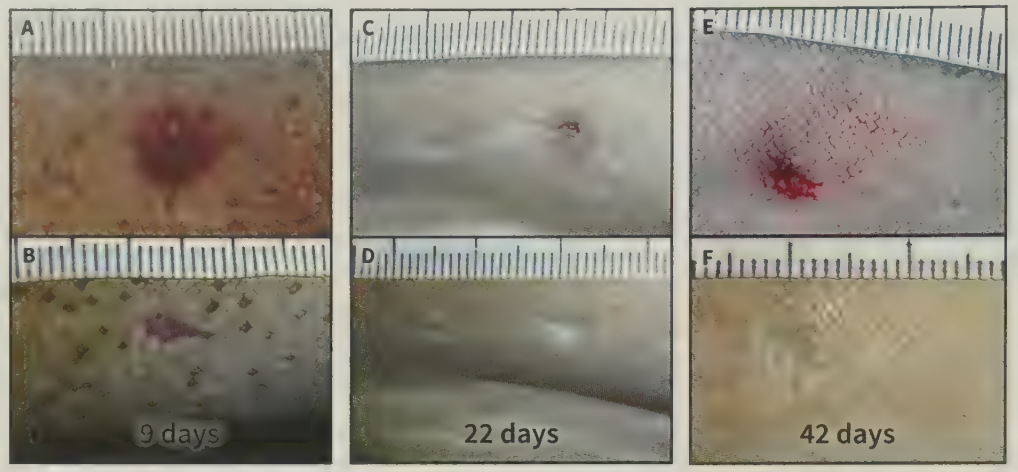

Figure 4

Before-and-after images of hook wounds, with scale (in millimeters), that resulted from use of the poker-and-hook tool to capture nurse sharks (*Ginglymostoma cirratum*) in Florida during 2014. (**A**) Wound shows minimal blood (a few drops), then (**B**) healthy mucus secretion after 9 days; (**C**) a wound with no blood, then (**D**) epidermal regeneration and repair scales present after 22 days; and (**E**) a wound with residual blood, then (**F**) fully formed mineralized scales present in the scar after 42 days.

Szedlmayer, 2004; Braccini et al., 2012; Danylchuk et al., 2014), low levels are still arguably of concern for important apex predators such as sharks. Local populations of sharks are likely highly susceptible to even low levels of postcapture mortality because of life history characteristics such as low reproductive output (e.g., litter size) and late age-at-maturity (Stevens et al., 2000; Dulvy and Forrest, 2012).

The intake canal at the Florida Power and Light St. Lucie Nuclear Power Plant provided an ideal environment to monitor nurse sharks over time after their capture by the poker-and-hook method. All 20 nurse sharks captured by this method showed no immediate ill effects and the 9 individuals monitored between 9 and 42 days survived with no observed abnormal behavior (although behavior was not evaluated in a systematic way). All wounds from the poker-and-hook capture method were either healing well or fully healed during this period and no signs of inflammation of tissue deterioration occurred.

The 4 nurse sharks whose weights were recorded before and after 22–24 days all increased in weight. This further corroborates evidence of a quick recovery and minimal postcapture stress. When the 3 nurse sharks were put into the tank, they fed immediately, as well as voraciously, and continued to do so at each feeding every 3–4 days. The sharks were fed to satiation and any uneaten food (freshly chopped fish) or small live fish that we stunned and that settled on the tank bottom would be eaten overnight, thereby suggesting that no injury occurred to the lateral line system (which is used in prey detection and contributes to the localization of food by the olfactory organs; see Kleerekoper and Gruber, 1975; Gardiner and Atema, 2007; Gardiner, 2012) or that any resulting injury to the lateral line could be deemed negligible.

An important stage in wound healing in sharks is the continual replacement of their dermal denticles (scales) (Reif, 1978). The extraordinarily tough skin of nurse sharks further makes them well suited for the poker-and-hook capture method. Both male and female nurse sharks are characterized by their thick, dense integument known to withstand multiple bites during mating (Klimley, 1980; Pratt and Carrier, 2001) and to resist damage while living in typical habitats of rock and coral (i.e., sustaining collisions with reef substrate during pursuit of prey; Campagno, 2002; senior author, personal observ.). The sides of the tail base are also without lateral keels or precaudal pits that could affect hooking efficacy or injury (or both). More importantly, the main circulatory vessels taper at the tail base (Rosenzweig, 1988), which is dense in muscle and is reported as damage tolerant (Naresh et al., 1997; Towner et al., 2012). The caudal area further appears to be well suited for this capture method because evidence suggests that drawing blood from this area is also less physiologically taxing (Cooper and Morris, 1998; Mandelman and Skomal, 2009) and the upper-and-lower targeted part of the tail base (away from the lateral line) has very little vascularization (Shadwick and Goldbogen, 2012).

Of the 23 hook wounds resulting by this capture method, 9 hook wounds did not bleed and 14 hook wounds showed only minimal bleeding (a couple drops

of blood at most) that quickly coagulated. Although the elasticity in shark skin is connected to internal propulsion muscles (Wainwright et al., 1978; Naresh et al., 1997), swimming and other movements never appeared compromised during regular observations of sharks in the holding tank, nor during our intermittent observations of individuals in the canal.

Values of hook wound parameters that were examined, such as wound area, were small and remained small regardless of shark size (up to 80 kg). Medical studies have shown wound area and circumference to correlate with wound volume (Melhuish et al., 1994; Flanagan, 2003), which was not the case with regard to recorded hook depth in our study. Although we recognize our measurements of hook depth were a crude estimate and not necessarily indicative of potential wound sinus formation, the fact that hook penetration was mostly superficial, with the hook often falling out by itself when the shark was hauled onboard, suggests internal injury was minimal. When the hook did penetrate deeper, hook penetration remained parallel to the skin on account of the bend in the J-hook, thus limiting perpendicular penetration. Reducing the hook gap (the space between the hook point and the hook shank) should further reduce perpendicular penetration, but could be more prone to tearing the skin (measured by circularity). Our results indicated that the type and size of hook we used was less prone to tearing the skin of larger individuals than the skin of smaller ones; therefore, it would be useful to experiment with a range of smaller hooks for smaller individuals in future studies.

The poker-and-hook capture method is also well suited for nurse sharks because of their feeding behavior. Nurse sharks are obligate suction feeders capable of generating suction forces that are among the highest recorded for any aquatic vertebrate to date (Tanaka, 1973; Motta et al., 2008). The poker-and-hook capture method prevents many sublethal effects or the delayed mortality that can be caused by traditional baited hook-and-line gear (or prevents both). This is especially the case for more internally hooked fish as has been reported for blue sharks (*Prionace glauca*; Borucinska et al., 2001; Borucinska et al., 2002) and lemon sharks (Danylchuk et al., 2014). Nurse sharks further exhibit a suck-and-spit behavior or shake their head violently (or exhibit a combination of both) to reduce the size of food items (Motta et al., 2002; Motta, 2004), which could further increase the risk of hooking to sensory and vital organs concentrated anteriorly.

The behavioral response of nurse sharks is also appropriate for the poker-and-hook capture method because nurse sharks in our study always retreated upon being hooked underwater. Nonetheless, as inoffensive as nurse sharks may appear, they are still ranked fourth in documented shark bites on humans (Ricci et al., 2016). Nurse sharks are known to attack when approached too closely, especially in a confined space or if their retreat is prevented (Limbaugh, 1963; Nelson et al., 1986). Our divers using this method were highly experienced in handling underwater wildlife. It is possible that the poker-and-hook method could trigger more erratic or aggressive responses in other shark species, and therefore shark safety and cautious planning are advised with this technique for other species.

Nurse sharks also exhibit relatively subdued fighting during capture compared with that of other sharks (Gallagher, 2015). Fighting intensity and hooking severity could be more pronounced with larger, more aggressive species. The tiger shark (*Galeocerdo cuvier*) has been captured on the water surface by a similar technique in order to attach satellite transmitters to their dorsal fin (Fitzpatrick et al., 2012). In the latter tiger shark study, a detachable clamp and buoy system was closed around the base of the shark's tail as it swam at the water surface near their boat. Remarkably, video footage of this technique indicates tiger sharks also become quickly subdued after momentarily dragging the attached buoy through the water. Whereas nurse sharks and tiger sharks are known to display more subdued behavior when hooked anteriorly or captured by their tails, blacktip sharks (*Carcharhinus limbatus*) have shown bouts of intense fighting at the onset of being hooked anteriorly (Gallagher et al., 2017). We speculate that blacktip sharks, as well as other shark species that exhibit intense fighting behavior when hooked anteriorly, would also fight intensely if captured by the tail.

Shark breathing is another important consideration when using the poker-and-hook method to capture different shark species. Although most sharks are facultative ram ventilators some are obligate ram ventilators that need to swim continuously to breathe (Milsom and Taylor, 2015). The common thresher shark (*Alopias vulpinus*) is an example of an obligate ram ventilator, and therefore pulling this species backwards or adding drag would affect their breathing and survival (Heberer et al., 2010; Sepulveda et al., 2015). Interestingly, common thresher sharks are usually pulled in backwards when fished because their caudal fin gets hooked when trying to immobilize bait perceived as prey (Aalbers et al., 2010). Large common thresher sharks do not survive capture times >85 min, unlike smaller common thresher sharks or individuals landed with much shorter capture times (Cartamil et al., 2010; Heberer et al., 2010).

Capture time has been identified as a critical factor in postrelease survival (Cooke and Suski, 2005). Nurse sharks in the canal were landed within a few minutes with the poker-and-hook capture method and with less effort than when similar-size individuals were landed by baited hook-and-line gear. It is likely that sharks were simply less agitated and traumatized when hooked posteriorly than when hooked anteriorly. However, pulling the shark backwards (with the buoy line attached to the shark tail) may have affected the functional mobility of the caudal fin or general swimming behavior, thus impairing thrust or swimming speed (see Wilga and Lauder, 2002). It is also possible that the backward motion or inverted position of the

shark being hauled in may have induced an immobility reflex or slight tonic immobility state as documented for a number of shark species (Henningsen, 1994; Holland et al., 1999).

Little scientific attention has been given to the process of wound healing in sharks (Towner et al., 2012) and little is known about related shark behavior. Our study area provides favorable conditions for pursuing this line of research on nurse sharks and our continued use of the poker-and-hook method could provide valuable insight on the process of wound healing in sharks in general. In the future, the effects on blood biochemistry (as an indicator of stress response, morbidity, etc.) could also be examined in relation to post-capture behavior and survivorship in comparison with other capture methods (e.g., Hyatt et al., 2012; Hyatt et al., 2016). Currently, strong evidence supports the continued use and development of the poker-and-hook method and its application in research. Compared with traditional methods such as angling or gillnetting, the poker-and-hook method is less invasive and more efficient. Targeted individuals are captured quickly and efficiently, thereby reducing capture time and associated stress, and bycatch can be entirely eliminated with this method.

As of March 2016, 5 individuals captured with the poker-and-hook method, tagged and then released, have returned to the canal and have provided information on residency and movement of nurse sharks in the area. Given the increasing importance of tagging for understanding the connectivity between individual mobility (e.g., range, residency), the internal dynamics of populations (e.g., mating aggregations, philopatry), and the effective management of nurse shark populations at large (Chapman et al., 2015), we recommend using the poker-and-hook capture method to facilitate tagging and subsequent tracking of nurse sharks elsewhere, as well as other feasible shark species.

Acknowledgments

We would like to thank Florida Power and Light and the St. Lucie Nuclear Power Plant for their support. We would also like to thank N. Álvarez-Berríos, C. Bajzak, and 3 anonymous reviewers who provided constructive input to this manuscript. All fish removal activities in the canal were in accordance with the latest special activities license issued by the Florida Fish and Wildlife Conservation Commission (permit no. SAL-15-0018-SR).

Literature cited

Aalbers, S. A., D. Bernal, and C. A. Sepulveda.
2010. The functional role of the caudal fin in the feeding ecology of the common thresher shark *Alopias vulpinus*. J. Fish Biol. 76:1863–1868.

Ashhurst, D. E.
2004. The cartilaginous skeleton of an elasmobranch fish does not heal. Matrix Biol. 23:15–22.

Bansemer, C. S., and M. B. Bennett.
2010. Retained fishing gear and associated injuries in the east Australian grey nurse sharks (*Charcharias taurus*): implications for population recovery. Mar. Freshw. Res. 61:97–103.

Bird, P. M.
1978. Tissue regeneration in three carcharhinid sharks encircled by embedded straps. Copeia 1978:345–349.

Borucinska, J., J. Martin, and G. Skomal.
2001. Peritonitis and pericarditis associated with gastric perforation by a retained fishing hook in a blue shark. J. Aquat. Anim. Health 13:347–354.

Borucinska, J., N. Kohler, L. Natanson, and G. Skomal.
2002. Pathology associated with retained fishing hooks in blue sharks, *Prionace glauca* (L.), with implications for their conservation. J. Fish. Dis. 25:515–521.

Braccini, M., J. van Rijn, and L. Frick.
2012. High post-capture survival for sharks, rays and chimaeras discarded in the main shark fishery of Australia? PLoS ONE. 7:e32547.

Bresette M., J. Gorham, and B. Peery.
1998. Site fidelity and size frequencies of juvenile green turtles (*Chelonia mydas*) utilizing near shore reefs in St. Lucie County, Florida. Mar. Turtle Newsl. 82:5–7.

Brill, R., P. Bushnell, S. Schroff, R. Seifert, and M. Galvin.
2008. Effects of anaerobic exercise accompanying catch-and-release fishing on blood-oxygen affinity of the sandbar shark (*Carcharhinus plumbeus*, Nardo). J. Exp. Mar. Biol. Ecol. 354:132–143.

Brownscombe, J. W., A. J. Danylchuk, J. M. Chapman, L. F. G. Gutowsky, and S. J. Cooke.
2017. Best practices for catch-and-release recreational fisheries—angling tools and tactics. Fish. Res. 186:693–705.

Campagno, L. J. V.
2002. Family Ginglymostomatidae. *In* Sharks of the World. An annotated and illustrated catalogue of shark species known to date. Volume 2. Bullhead, mackerel and carpet sharks (Heterodontiformes, Lamniformes and Orectolobiformes). FAO Species Catalogue for Fishery Purposes, no. 1, vol. 2, p. 188–201. FAO, Rome.

Carrier, J. C.
1985. Nurse sharks (*Ginglymostoma cirratum*) of Big Pine Key, Florida (U.S.A.): an investigation of growth and movement and a comparison of the success of several types of external tags. *In* Proceedings of the Fifth International Coral Reef Congress, vol. 6; Tahiti, 27 May–1 June (C. Gabrie and M. Harmelin, assoc. eds.), p. 655–660. Antenne Museum-EPHE, Moorea, French Polynesia.

Carrier, J. C., H. L. Pratt, and J. I. Castro.
2004. Reproductive biology of elasmobranchs. *In* Biology of sharks and their relatives (J. C. Carrier, J. A. Musick, and M. R. Heithaus, eds.), p. 269–286. CRC Press, Boca Raton, FL.

Cartamil, D., N. C. Wegner, S. Aalbers, C. A Sepulveda, A. Baquero, and J. B. Graham.
2010. Diel movement patterns and habitat preferences of the common thresher shark (*Alopias vulpinus*) in the Southern Bight. Mar. Freshw. Res. 61:596–604.

Castro, J. I.
2000. The biology of the nurse shark, *Ginglymostoma cirratum*, off the Florida east coast and the Bahama Islands. Environ. Biol. Fish. 58:1–22.

Chapman, D. D., K. A. Feldheim, Y. P. Papastamatiou, and R. E. Hueter.
2015. There and back again: a review of residency and return migrations in sharks, with implications for population structure and management. Annu. Rev. Mar. Sci. 7:547–570.

Clark, W. G., and S. M. Kaimmer.
2006. Estimates of commercial longline selectivity for Pacific Halibut (*Hippoglossus stenolepis*) from multiple marking experiments. Fish. Bull. 104:465–467.

Cooke, S. J., and C. D. Suski.
2005. Do we need species-specific guidelines for catch-and-release recreational angling to effectively conserve diverse fisheries resources? Biodiversity Conserv. 14:1195–1209.

Cooper, A. R., and S. Morris.
1998. The blood respiratory, haematological, acid-base and ionic status of the Port Jackson shark, *Heterodontus portusjacksoni*, during recovery from anaesthesia and surgery: a comparison with sampling by direct caudal puncture. Comp. Biochem. Physiol., A. 119:895–903.

Cuthill, I.
1991. Field experiments in animal behaviour: methods and ethics. Anim. Behav. 42:1007–1014.

Danylchuk, A. J., C. D. Suski, J. W. Mandelman, K. J. Murchie, C. R. Haak, A. M. L. Brooks, and S. J. Cooke.
2014. Hooking injury, physiological status and short-term mortality of juvenile lemon sharks (*Negaprion brevirostris*) following catch-and-release recreational angling. Conserv. Physiol. 2(1):cot036.

Davis, M. W.
2002. Key principles for understanding fish bycatch discard mortality. Can. J. Fish. Aquat. Sci. 59:1834–1843.

Davis, G. E., and J. W. Dodrill.
1989. Recreational fishery and population dynamics of spiny lobsters, *Panulirus argus*, in Florida Bay, Everglades National Park, 1977–1980. Bull. Mar. Sci. 44:78–88.

Dooley, H., and M. F. Flajnik.
2005. Shark immunity bites back: affinity maturation and memory response in the nurse shark, *Ginglymostoma cirratum*. Eur. J. Immunol. 35:936–945.

Dulvy, N. K., and R. E. Forrest.
2012. Life histories, population dynamics, and extinction risks in Chondrichthyans. *In* Biology of sharks and their relatives (J. C. Carrier, J. A. Musick, and M. R. Heithaus, eds.), p. 639–679. CRC Press, New York.

Evermann, B. W., and M. C. Marsh.
1900. The fishes of Porto Rico. Fish. Bull. 20:49–350.

Fedorenko, A. Y.
1991. Guidelines for minimizing entrainment and impingement of aquatic organisms at marine intakes in British Columbia. Can. Manuscr. Rep. Fish. Aquat. Sci. 2098 E, 86 p. [Available from website.]

Fitzpatrick, R., M. Thums, I. Bell, M. G. Meekan, J. D. Stevens, and A. Barnett.
2012. A comparison of the seasonal movements of tiger sharks and green turtles provides insight into their predator-prey relationship. PLoS ONE 7(12):e51927

Flanagan, M.
2003. Wound measurement: can it help us to monitor progression to healing? J. Wound Care 12:189–194.

Frick, L. H., R. D. Reina, and T. I. Walker.
2010. Stress related physiological changes and post-release survival of Port Jackson sharks (*Heterodontus portusjacksoni*) and gummy sharks (*Mustelus antarcticus*) following gill-net and longline capture in captivity. J. Exp. Mar. Biol. Ecol. 385:29–37.

Gallagher, A. J.
2015. Shark vulnerability to fishery interactions: assessing ecological, physiological, and social agents of risk. Ph.D. diss., 180 p. Univ. Miami, Coral Gables, FL.

Gallagher, A. J., J. E. Serafy, S. J. Cooke, and N. Hammerschlag.
2014. Physiological stress response, reflex impairment, and survival of five sympatric shark species following experimental capture and release. Mar. Ecol. Prog. Ser. 496:207–218.

Gallagher, A. J., E. R. Staaterman, S. J. Cooke, and N. Hammerschlag.
2017. Behavioural responses to fisheries capture among sharks caught using experimental fishery gear. Can. J. Fish. Aquat. Sci. 74:1–7.

Gardiner, J. M.
2012. Multisensory integration in shark feeding behavior. Ph.D. diss., 267 p. Univ. S. Florida, Tampa, FL.

Gardiner, J. M., and J. Atema.
2007. Sharks need the lateral line to locate odor sources: rheotaxis and eddy chemotaxis. J. Exp. Biol. 210:1925–1934.

Garla, R. C., D. D. Chapman, M. S. Shivji, B. M. Wetherbee, and A. F. Amorim.
2006. Habitat of juvenile Caribbean reef sharks, *Charcharhinus perezi*, at two oceanic insular marine protected areas in the southwestern Atlantic Ocean: Fernando de Noronha Archipelago and Atol das Rocas, Brazil. Fish. Res. 81:236–241.

Goodwin, J.
2009. Social determination of sex in reef fishes. Sem. Cell. Dev. Biol. 20:264–270.

Gurshin, C. W. D., and S. T. Szedlmayer.
2004. Short-term survival and movements of Atlantic sharpnose sharks captured by hook-and-line in the north-east Gulf of Mexico. J. Fish Biol. 65:973–986.

Gwinn, D. C., P. Brown, J. C. Tetzlaff, and M. S. Allen.
2011. Evaluating mark–recapture sampling designs for fish in an open riverine system. Mar. Freshw. Res. 62:835–840.

Heberer, C., S. A. Aalbers, D. Bernal, S. Kohin, B. DiFiore, and C. A. Sepulveda.
2010. Insights into catch-and-release survivorship and stress-induced blood biochemistry of common thresher sharks (*Alopias vulpinus*) captured in the southern California recreational fishery. Fish. Res. 106:495–500.

Heithaus, M. R., D. Burkholder, R. E. Hueter, L. I. Heithaus, H. L. Pratt Jr., and J. C. Carrier.
2007. Spatial and temporal variation in shark communities of the lower Florida Keys and evidence for historical population declines. Can. J. Fish. Aquat. Sci. 64:1302–1313.

Henningsen, A. D.
1994. Tonic immobility in 12 elasmobranchs: use as an aid in captive husbandry. Zoo Biol. 13:325–332.

Hoelzer, G. A.
1990. Male-male competition and female choice in the Cortez damselfish, *Stegastes rectifraenum*. Anim. Behav. 40:339–349.

Holland, K. N., B. M. Wetherbee, C. G. Lowe, and C. G. Meyer.
1999. Movements of tiger sharks (*Galeocerdo cuvier*) in coastal Hawaiian waters. Mar. Biol. 134:665–673.

Hueter, R. E., D. A. Mann, K. P. Maruska, J. A. Sisneros, and L. S. Demski.
2004. Sensory biology of elasmobranchs. *In* Biology of sharks and their relatives (J. C. Carrier, J. A. Musick, and M. R. Heithaus, eds), p. 326–368. CRC Press, Boca Raton, FL.

Hyatt, M. W., P. A. Anderson, P. M. O'Donnell, and I. K. Berzins.
2012. Assessment of acid–base derangements among bonnethead (*Sphyrna tiburo*), bull (*Carcharhinus leucas*), and lemon (*Negaprion brevirostris*) sharks from gillnet and longline capture and handling methods. Comp. Biochem. Physiol., A 162:113–120.

Hyatt, M. W., P. A. Anderson, and P. M. O'Donnell.
2016. Behavioral release condition score of bull and bonnethead sharks as a coarse indicator of stress. J. Coast. Res. 32:1464–1472.

Jenkins, J. A., H. L. Bart Jr., P. R. Bowser, J. R. MacMillan, J. G. Nickum, J. D. Rose, P. W. Sorensen, G. W. Whitledge, J. W. Rachlin, and B. E. Warkentine.
2014. Guidelines for the use of fishes in research, 90 p. Am. Fish. Soc., Betheseda, MD.

Jones, G. P., M. J. Milicich, M. J. Emslie, and C. Lunow.
1999. Self-recruitment in a coral reef fish population. Nature 402:802–804.

Karl, S. A., A. L. F. Castro, and R. C. Garla.
2012. Population genetics of the nurse shark (*Ginglymostoma cirratum*) in the western Atlantic. Mar. Biol. 159:489–498.

Kessel, S. T., J. Fraser, W. G. Van Bonn, J. L. Brooks, T. L. Guttridge, N. E. Hussey, and S. H. Gruber.
2017. Transcoelomic expulsion of an ingested foreign object by a carcharhinid shark. Mar. Freshw. Res. [Online early only.]

Kleerekoper, H., D. Gruber, and J. Matis.
1975. Accuracy of localization of a chemical stimulus in flowing and stagnant water by the nurse shark *Ginglysmostoma cirratum*. J. Comp. Physiol. 98:257–275.

Klimley, A. P.
1980. Observations of courtship and copulation in the nurse shark, *Ginglymostoma cirratum*. Copeia 1980:878–882.

Kohler, N. E., J. G. Casey, and P. A. Turner.
1998. NMFS Cooperative Shark Tagging Program, 1962–93: an atlas of shark tag and recapture data. Mar. Fish. Rev. 60(2):1–87.

Kramer, D. L., and M. R. Chapman.
1999. Implications of fish home range size and relocation for marine reserve function. Environ. Biol. Fish. 55:65–79.

Latour, R. J.
2005. Tagging methods and associated data analysis. *In* Management techniques for elasmobranch fisheries (J. A. Musick and R. Bonfil, eds.), p. 45–61. FAO Fish. Tech. Pap. 474. FAO, Rome.

Limbaugh, C.
1963. Field notes on sharks. *In* Sharks and survival (P. W. Gilbert, ed.), p. 63–94. Heath & Co., Boston, MA.

McCormick, K., and J. Salcedo.
2017. SPSS statistics for data analysis and visualization, 528 p. John Wiley & Sons, Indianapolis, IN.

Mandelman, J. W., and M. A. Farrington.
2007. The estimated short-term discard mortality of a trawled elasmobranch, the spiny dogfish (*Squalus acanthias*). Fish. Res. 83:238–245.

Mandelman, J. W., and G. B. Skomal.
2009. Differential sensitivity to capture stress assessed by blood acid-base status in five carcharihinid sharks. J. Comp. Physiol., B. 179:267–277.

Melhuish, J. M., P. Plassman, and K. G. Harding.
1994. Circumference, area and volume of the healing wounds. J. Wound Care 3:380–384.

Milsom, W. K., and E. W. Taylor.
2015. Control of breathing in elasamobranchs. *In* Physiology of elasmobranch fishes: internal processes, vol. 34B (R. E. Shadwick, A. P. Farrell, and C. J. Brauner, eds.), p. 83–126. Academic Press, Oxford, UK.

Morgan, A., and J. K. Carlson.
2010. Capture time, size and hooking mortality of bottom longline-caught sharks. Fish. Res. 101:32–37.

Motta, P. J.
2004. Prey capture behavior and feeding mechanics of elasmobranchs. *In* Biology of sharks and their relatives (J. C. Carrier, J.A. Musick, and M.R. Heithaus, eds.), p. 165–202. CRC Press, Boca Raton, FL.

Motta, P. J., R. E. Hueter, T. C. Tricas, and A. P. Summers.
2002. Kinematic analysis of suction feeding in the nurse shark, *Ginglymostoma cirratum* (Orectolobiformes, Ginglymostomidae). Copeia 2002:24–38.

Motta, P. J., R. E. Hueter, T. C. Tricas, A. P. Summers, D. R. Huber, D. Lowry, K. R. Mara, M. P. Matott, L. B. Whitenack, and A. P. Wintzer.
2008. Functional morphology of the feeding apparatus, feeding constraints, and suction performance in the nurse shark *Ginglymostoma cirratum*. J. Morphol. 269:1041–1055.

Naresh, M. D., V. Arumgam, and R. Sanjeevi.
1997. Mechanical behaviour of shark skin. J. Biosci. 22:431–437.

Nelson, D. R., R. R. Johnson, J. N. McKibben, and G. G. Pittenger.
1986. Agonistic attacks on divers and submersibles by gray reef sharks, *Carcharinus amblyrhynchos*: antipredatory or competitive? Bull. Mar. Sci. 38:68–88. [Available from website]

Olsen, A. M.
1953. Tagging of school shark, *Galeorhinus australis* (Macleay) (Carcharanidae) in south-eastern Australian waters. Aust. J. Mar. Freshw. Res. 4:95–107.

Osgood, G. J., and J. K. Baum.
2015. Reef sharks: recent advances in ecological understanding to inform conservation. J. Fish Biol. 87:1489–1523.

Pine, W. E., K. H. Pollock, J. E. Hightower, T. J. Kwak, and J. A. Rice.
2003. A review of tagging methods for estimating fish population size and components of mortality. Fisheries 28:10–23. https://doi.org/10.1577/1548-8446(2003)28[10:AROTMF]2.0.CO;2

Pratt, H. L., Jr., and J.C. Carrier.
2001. A review of elasmobranch reproductive behavior with a case study on the nurse shark, *Ginglymostoma cirratum*. Environ. Biol. Fish. 60:157–188.

Reif, W.-E.
1978. Wound healing in sharks: form and arrangement of repair scales. Zoomorphologie 90:101–111.

Ricci, J. A., C. R. Vargas, D. Singhal, and B. T. Lee.
2016. Shark attack-related injuries: epidemiology and implications for plastic surgeons. J. Plast. Reconstr. Aesthet. Surg. 69:108–114.
Rosa, R. S., A. L. F. Castro, M. Furtado, J. Monzini, and R. D. Grubbs.
2006. *Ginglymostoma cirratum*. The IUCN List of Threatened Species 2006: e.T60223A12325895. [Available from website]
Rosenzweig, L. J.
1988. Anatomy of the shark: text and dissection guide, 120 p. W.C. Brown Publs., Dubuque, IA.
Schemnitz, S. D., G. R. Batcheller, M. J. Lovallo, H. B. White, and M. W. Fall.
2012. Capturing and handling wild animals. *In* The wildlife techniques manual, vol. 1 (N. J. Silvy, ed.), p. 64–117. Johns Hopkins Univ. Press, Baltimore, MD.
Sedgewick, J.
2008. Scientific imaging with Photoshop: methods, measurement, and output, 312 p. New Riders Press, Berkeley, CA.
Sepulveda, C. A., C. Heberer, S. A. Aalbers, N. Spear, M. Kinney, D. Bernal, and S. Kohin.
2015. Post-release survivorship studies on common thresher sharks (*Alopias vulpinus*) captured in the southern California recreational fishery. Fish. Res. 161:102–108.
Shadwick, R. E., and J. A. Goldbogen.
2012. Muscle function and swimming in sharks. J. Fish Biol. 80:1904–1939.
Shapiro, D. Y. and R. H. Boulon Jr.
1982. The influence of females on the initiation of female-to-male sex change in a coral reef fish. Horm. Behav. 16:66–75.
Sheriff, M. J., B. Dantzer, B. Delehanty, R. Palme, and R. Boonstra.
2011. Measuring stress in wildlife: techniques for quantifying glucocorticoids. Oecolgia 166:869–887.
Silvy, N. J.
2012. The wildlife techniques manual, vol. 1–2, 7th ed., 1136 p. John Hopkins Univ. Press, Baltimore, MD.
Skomal, G. B.
2007. Evaluating the physiological and physical consequences of capture on post-release survivorship in large pelagic fishes. Fish. Manag. Ecol. 14:81–89.
Skomal, G. B., and D. Bernal.
2010. Physiological responses to stress in sharks. *In* Sharks and their relatives II: biodiversity, adaptive physiology, and conservation (J. C. Carrier, J. A. Musick, and M. R. Heithaus, eds.), p. 460–484. CRC Press, Boca Raton, FL.
Smith, M. F. L.
1992. Capture and transportation of elasmobranchs, with emphasis on the grey nurse shark (*Carcharias taurus*). Aust. J. Mar. Freshw. Res. 43:325–343.
Stevens, J. D., R. Bonfil, N. K Dulvy, and P. A. Walker.
2000. The effects of fishing on sharks, rays, and chimaeras (chondrichthyans), and the implications for marine ecosystems. ICES J. Mar. Sci. 57:476–494.
Tanaka, S. K.
1973. Suction feeding by the nurse shark. Copeia 1973: 606–608.
Towner, A., M. J. Smale, and O. Jewel.
2012. Boat-strike wound healing in *Carcharodon carcharias*. *In* Global perspectives on the biology and life history of the white shark (M. L. Domeier, ed.), p. 77–83. CRC Press, Boca Raton, FL.
Wainwright, S. A., F. Vosburgh, and J. H. Hebrank.
1978. Shark skin: function in locomotion. Science 202:747–749.
Webster, M. S., and M. A. Hixon.
2000. Mechanisms and individual consequences of intraspecific competition in a coral-reef fish. Mar. Ecol. Prog. Ser. 196:187–194.
Whitney, N. M., K. O. Lear, L. C. Gaskins, and A. C. Gleiss.
2016. The effects of temperature and swimming speed on the metabolic rate of the nurse shark (*Ginglymostoma cirratum*, Bonaterre). J. Exp. Mar. Biol. Ecol. 477:40–46.
Wiley, T. R., and C. A. Simpfendorfer.
2007. The ecology of elasmobranchs occurring in the Everglades National Park, Florida: Implications for conservation and management. Bull. Mar. Sci. 80:171–189.
Wilga, C. D., and G. V. Lauder.
2002. Function of the heterocercal tail in sharks: quantitative wake dynamics during steady horizontal swimming and vertical maneuvering. J. Exp. Biol. 205:2365–2374.
Williams, B. K., J. D. Nichols, and M. J. Conroy.
2002. Analysis and management of animal populations, 817 p. Academic Press, San Diego, CA.
Zeller, D. C. and G. R. Russ.
1998. Marine reserves: patterns of adult movement of the coral trout (*Plectropomus leopardus* (Serranidae)). Can. J. Fish Aquat. Sci. 55:917–924.

National Marine
Fisheries Service
NOAA

Fishery Bulletin
established in 1881

Spencer F. Baird
First U.S. Commissioner
of Fisheries and founder
of *Fishery Bulletin*

A method for predicting trawlability in the Gulf of Alaska with the use of calibrated, split-beam, echosounder backscatter

Paul G. von Szalay (contact author)
David A. Somerton

Email address for contact author: paul.von.szalay@noaa.gov

Resource Assessment and Conservation Engineering Division
Alaska Fisheries Science Center
National Marine Fisheries Service, NOAA
7600 Sand Point Way NE
Seattle, Washington 98115

Abstract—We examined the feasibility of distinguishing trawlable from untrawlable bottom using acoustic backscatter data from a calibrated single-beam echosounder to better define and map continental shelf areas of the Gulf of Alaska (GOA) that are too rough and rocky to be sampled by the National Marine Fisheries Service's biennial bottom trawl groundfish survey. Bottom classification algorithms were applied to backscatter data collected from areas of known trawlability to provide 9 metrics of bottom type from small sections of bottom (~50 records within a 15-min trawl tow). Prediction models, based on both generalized additive models (GAMs) and generalized linear models (GLMs), were developed to relate the bottom type metrics to the known state of trawlability. The models were then tested to judge their performance on new data by using 33% cross validation. Although the best GAM had a higher correct prediction rate (82.4%) than the best GLM (76.9%), under cross validation both models had nearly the same correct prediction rate (75.0%). This result is a sufficiently high prediction rate to allow the development of better trawlability maps by applying the model to data collected along acoustic track lines during the GOA bottom trawl surveys.

Manuscript submitted 16 December 2016.
Manuscript accepted 8 August 2017.
Fish. Bull. 115:496–503 (2017).
Online publication date: 16 August 2017.
doi: 10.7755/FB.115.4.6

The views and opinions expressed or implied in this article are those of the author (or authors) and do not necessarily reflect the position of the National Marine Fisheries Service, NOAA.

The Alaska Fisheries Science Center of the National Marine Fisheries Service has conducted a bottom trawl survey in the Gulf of Alaska (GOA) biennially since 1999 to assess the distribution and abundance of groundfish for fisheries management (von Szalay and Raring, 2016). The survey area, which consists of 59 strata based on depth, benthic habitat, and management areas, spans the continental shelf and upper continental slope from the Islands of Four Mountains eastward to Dixon Entrance, and from nearshore waters to a depth of 1000 m (Fig. 1). Although the purpose for the survey is to randomly sample this area under the assumption that the entire area is trawlable (can be sampled with the Poly-Nor'eastern 4-seam survey trawl), in practice, this concept is an approximation because the GOA is a mosaic of habitat types. Some habitats are untrawlable; that is, they are too rocky, rugged, or steep to allow a fully random choice of sampling locations when using the standard survey trawl. Furthermore, the GOA has never been mapped with sufficient spatial resolution to permit identification of bottom types that would preclude successful trawling. Consequently, the locations of untrawlable bottom (in the varying opinions of experienced GOA survey vessel captains) and even the proportion of the area comprising such habitat is not known. The relative abundance of each species is therefore currently estimated by extrapolating the mean abundance in trawlable areas to the entire survey area. A potential problem with this approach is that it may result in biased estimates of abundance because fish density is a function of habitat type, which is correlated with trawlability (Yoklavich et al., 2000; Pirtle et al., 2015). The bias is likely positive for flatfish and other fish species, which prefer relatively smooth and sandy bottoms in trawlable habitats (McConnaughey and Smith, 2000; Busby et al., 2005), and negative for rockfish (*Sebastes* spp.) and other fish species, which prefer rough, rocky bottoms in untrawlable habitats (Richards, 1986; Stein et al., 1992; Clausen and Heifetz, 2002; Jagielo et al., 2003; Zimmermann, 2003; Jones et al., 2012).

An alternative survey design now being considered by the Alaska Fisheries Science Center for the GOA is one in which the abundance estimates derived from survey trawl catches, based on catch weight per unit of swept area, would be extrapo-

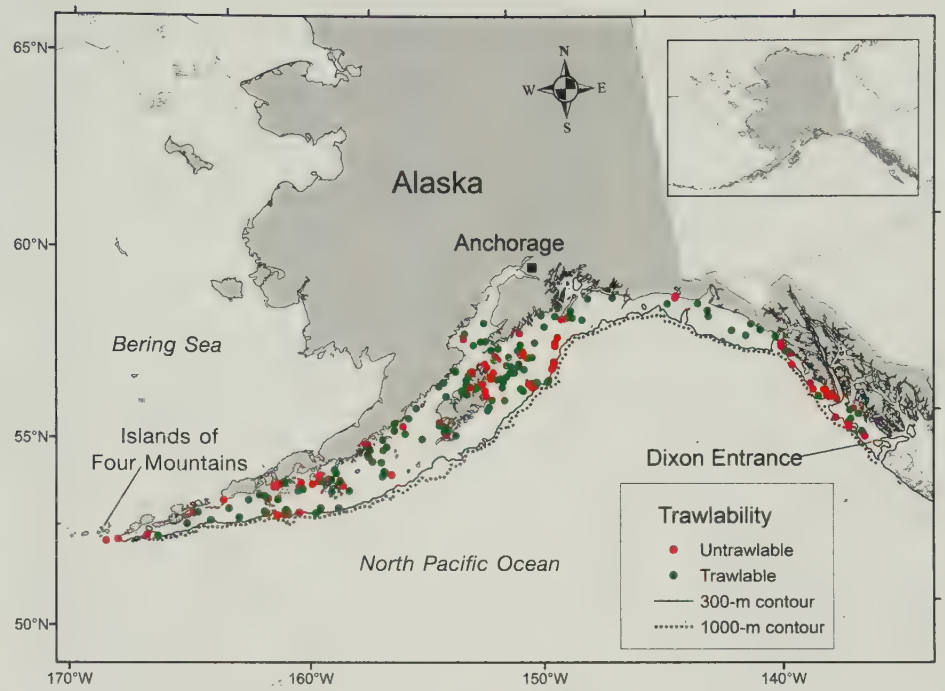

Figure 1

Map of the survey area for the bottom trawl survey conducted biennially in the Gulf of Alaska by the National Marine Fisheries Service since 1999, confined by the 1000-m isobath (dotted line). The area confined by the 300-m isobath (solid line) represents the area where acoustic data within a grid of cells were used to predict trawlability. Green circles represent acoustic data segments from trawlable areas, and red circles represent acoustic segments from untrawlable areas.

lated only to areas that are trawlable, and some new sampling methods (e.g., the use of acoustic, longline, or camera gear) would be applied to the untrawlable areas (Rooper et al., 2010; Williams et al., 2010; Jones et. al., 2012; Thorson et al., 2013). To implement this sampling design, the relative proportions of trawlable and untrawlable areas must be known, proportions that require a technique for identifying and quantifying trawlable and untrawlable habitats (Cordue, 2007).

Previously, the approach to identify the trawlability status of an area was based on the historical performance of the survey within individual cells of a grid of 5×5 km cells superimposed on the survey area. These cells, which number ~14,000, are the potential sampling units of the survey. To be considered trawlable, a sampling cell must have been successfully trawled (with a Poly-Nor'eastern 4-seam survey trawl in standard fishing configuration and without sustaining any damage throughout the tow) by a survey vessel during a prior GOA bottom trawl survey. To be considered untrawlable, a sampling cell must be judged so on the basis of the vessel captain's assessment of the echogram, which is a real-time image of the backscatter data collected from a hull-mounted single-beam echosounder on a survey vessel. Any seabed feature that a vessel captain deems likely to result in moderate to severe damage to fishing gear or prevents the fishing gear from maintaining proper configuration and bottom contact throughout a tow provides a valid reason for declaring a sampling cell untrawlable. Nine categories of untrawlable seabed features have been identified: 1) hard+rocky substrate, 2) steep slopes, 3) rolling seabed, 4) pinnacles, 5) unnavigable areas, 6) snags, 7) ledges, 8) presence of underwater cable, and 9) presence of fixed fishing gear.

Captains of survey vessels have learned to recognize bottom features visible on echosounder traces and that could damage a survey trawl (Poly-Nor'eastern 4-seam bottom trawl with roller gear; Stauffer, 2004). Therefore, a sampling cell is classified as untrawlable if the captain fails to find a suitable bottom, at least 1 km in length, after systematically searching a sampling cell for 2 h, a duration that is considered sufficient to cover a sampling cell. Although consistent with the operational survey procedures of the bottom-trawl survey, this approach provides a qualitative and relatively slow assessment of seafloor character (only 42% of the survey area classified by this method to date).

We are exploring the use of acoustics to detect bottom features associated with trawlability to increase

the rate and precision at which the bottom-trawl survey sampling cells are classified to improve our ability to efficiently sample areas that are trawlable and avoid untrawlable ground. One approach described by Weber et al. (2013) and Pirtle et al. (2015), involves modeling trawlability as a function of seafloor metrics derived from bathymetry and backscatter data collected from multibeam acoustic surveys conducted by the National Marine Fisheries Service. Because no multibeam acoustic data are collected during the GOA trawl survey, we considered another method for this study, one that is based on the analysis of calibrated, single-beam acoustic backscatter data. The Alaska Fisheries Science Center has routinely collected these data since 2005 on all chartered fishing vessels used to conduct the bottom trawl survey. Although single-beam acoustic backscatter from the seabed has been analyzed in a number of studies to distinguish a variety of habitat types (Kloser et al., 2001; Anderson et al., 2002; Freitas et al., 2003; Riegl et al., 2005; Bartholomä, 2006), we consider the response variable as binary, as simply distinguishing between trawlable and untrawlable bottoms. The objectives for this study were 1) to examine the feasibility of developing a trawlability prediction model based on backscatter data from areas of known trawlability and 2) to evaluate the use of applying the model to predict trawlability in unknown areas on the basis of measured backscatter properties of acoustic data collected along track lines of future surveys conducted by the same vessel and with the same echosounder that was used to collect data for this study.

Materials and methods

The acoustic data were collected aboard the 38.4-m stern trawler FV *Sea Storm* during the 2013 GOA bottom trawl survey by using a Simrad[1] ES60 echosounder (Kongsberg Maritime AS, Horten, Norway) equipped with a 7.1° beam width, 38-kHz, split-beam transducer, which operated at a ping rate of 1 Hz and pulse duration of 1.024 ms. The echosounder was calibrated on-axis with a copper sphere according to standard procedures described by Foote et al. (1983). A total of 238 individual acoustic data segments were used in the analysis, half from trawlable and half from untrawlable areas. The trawlable and untrawlable segments were randomly selected from a pool of segments spanning the entire range of the survey area that satisfied the basic criteria identified in the next paragraph for the sampling cells containing the segments (Fig. 1). An acoustic data segment is an echosounder-insonified section of a vessel track line, and all segments from both trawlable and untrawlable areas consisted of data collected over 15-min time intervals, corresponding to the duration of a standard trawl haul. Although the depth range of the biennial bottom trawl groundfish survey extends to water depths as deep as 1000 m, the depths associated with the segments of this specific study were all less than 300 m because unacceptably slow ping rates (producing poor echogram resolution of the seabed) are required for deeper depths. Depths less than 300 m comprised 90% of the survey area (Fig. 1).

As with the selection process for trawlable and untrawlable segments, the sampling cells containing the selected segments were chosen randomly from a pool of cells satisfying certain criteria. Among the trawlable cells, only sampling cells that represented areas that had been successfully towed without any documented incidents such as tears in nets or trawl door entanglements with the bottom on at least 2 separate surveys were included in the analysis. Among the untrawlable cells, only sampling cells classified as untrawlable owing to 1 of the 5 hard or rough categories, or combination categories (i.e., hard+rocky, rolling seabed, pinnacles, snags, ledges) were used in the analysis. Cells classified as unnavigable were not used because acoustic data cannot be collected from areas that the survey vessel cannot navigate. Furthermore, the fixed fishing gear and underwater cable categories are for cells with man-made obstructions; these cells do not necessarily have acoustic signatures that identify them as untrawlable, yet it would be ill advised to trawl in these areas. Another major reason for considering an area untrawlable is that it is considered too steep. However, for the purposes of this analysis, such cells were not considered because acoustic features associated with steep slopes have been shown to be distinct from those of more level areas, regardless of substrate type (von Szalay and McConnaughey, 2002). Furthermore, steep slope areas are primarily confined to relatively deep waters (>200), and the models developed in this study are intended only for use in the continental shelf portion of a survey area.

The raw acoustic data files were processed before analysis to remove noise in the form of triangle wave dither that degrades the ES60-generated raw files, by using the known period and amplitude of the dither (Ryan and Kloser[2]). The triangle wave-corrected raw files were subsequently analyzed by using the seabed classification module in Echoview, vers. 6.1.72 (Echoview Software, Pty. Ltd., Hobart, Australia). Seven settings, which are used by an algorithm within the software to detect the bottom by using the data collected (bottom line pick), were specified before we derived classification data. The values of the settings used in this study (Table 1) were the defaults recommended by Echoview under most circumstances, except for the value for the minimum volume backscatter strength (min S_v for good pick), which was modified for this study after consulting with an Echoview Software represen-

[1] Mention of trade names or commercial companies is for identification purposes only and does not imply endorsement by the National Marine Fisheries Service, NOAA.

[2] Ryan, T., and R. Kloser. 2004. Quantification and correction of a systematic error in Simrad ES60 echosounders, 9 p. ICES FAST, Gdansk. [Available from Marine and Atmospheric Research, Commonwealth Scientific Industrial Research Organisation, GPO Box 1538, Hobart, TAS 7001, Australia.]

Table 1

Settings of the bottom-line-picking algorithm in Echoview software used before classification of seabed habitats. These values "told" the software how to detect the bottom (pick the bottom line) in the acoustic data collected during the National Marine Fisheries Service biennial bottom trawl survey of the Gulf of Alaska.

Setting	Value
Start depth (m)	10
Stop depth (m)	500
Min S_v for good pick (dB)	−80.00
Discrimination level	−40.00
Back step range	0.00
Peak threshold (dB)	−40.00
Minimum threshold (dB)	−70.00

tative. Next, the Echoview algorithm for background noise removal was applied to the data by using a signal-to-noise ratio setting of 10 and a maximum noise level subject to a removal setting of 0 dB. Echoview algorithms for bottom classification were then used to derive the 9 standard feature parameters from the first and second echo returns of the signal from the bottom. Echoview Software has determined that these feature parameters distinguish general seabed features. No attempt was made to narrow the 9 features down to those believed to be most relevant in distinguishing trawlability. The bottom echo threshold at 1 m, which is used to determine the end of the first and second echoes, was set to −125 dB and the reference normalization depth was set to 300 m.

The names of the feature parameters derived from the first echo are: roughness, first bottom length, bottom rise time, depth, maximum S_v (max S_v), kurtosis, and skewness; the names of the parameters derived from the second echo are: hardness and second bottom length (Table 2). Information on how Echoview processes backscatter data, including definitions of the terms used to derive the 9 feature parameters, and equations defining the parameters can be found in the help file for the software (available from website). Each of the 238 acoustic data segments consisted of ~50 records, where a record is made up of the 9 acoustic feature parameter values derived from groups of 10 consecutive pings. In this study, a record is the basic classification unit of an acoustic segment. The parameter values of the individual records were modeled directly without using the classification feature in the Echoview bottom classification module, which uses principal component and cluster analyses to categorize individual records into a user-specified number of bottom types.

Trawlability was modeled as a function of the 9 acoustic feature parameters by using both generalized linear modeling and generalized additive modeling functions in *R*, vers. 3.2.0 (R Core Team, 2015). A binomial error distribution was assumed for both types of models.

Three different classes of generalized linear models (GLMs) were evaluated by using the minimum value of the Akaike's information criterion (AIC) to choose the best-fitting model within each class (Table 3). The 3 classes consisted of models with all linear terms, mixtures of linear and polynomial terms, and mixtures of

Table 2

Definitions of the 9 standard parameters used in the Echoview algorithms for classification of seabed habitats. These feature parameters were covariates in all models used in this study to predict whether sampling areas in the Gulf of Alaska were trawlable. X=affirmative.

Parameter	Definition	Depth normalized
First echo		
Roughness	Tail energy. Integration of the tail of the first echo. Exclusively due to incoherent backscattering from facets inclined towards the transducer	X
First bottom length	Total duration of the first bottom echo (bottom line depth to bottom echo threshold at 1 m).	X
Bottom rise time	Attack duration (bottom line sample to the peak sample of the first echo).	X
Depth	Water depth	
Max Sv	Maximum energy. Maximum volume backscatter strength	
Kurtosis	Tailedness. Sharpness of the first echo peak	
Skewness	Asymmetry around the first echo peak	
Second echo		
Hardness	Total energy of the second echo (integration of the complete second acoustic bottom return).	X
Second bottom length	Total duration of the second echo (bottom line depth to bottom echo threshold at 1 m).	X

Table 3

Classes of generalized linear models (GLMs) and generalized additive models (GAMs) evaluated for goodness of fit in this study for the use of acoustic data to predict whether sampling areas in the Gulf of Alaska are trawlable. The best model in each category is shown in boldface. An asterisk (*) indicates an interaction term. The parameters include roughness, hardness, first bottom length (length 1), second bottom length (length 2), bottom rise time, depth, maximum volume backscatter strength (Sv), kurtosis, and skewness. NS=not significant; poly=polynomial ; S=smooth; d=degree of polynomial; k=number of knots.

	Roughness	Hardness	Length 1	Length 2	Rise time	Depth	Max Sv	Kurtosis	Skewness
GLM									
Model 1	linear	linear	linear	linear	linear	linear	NS	linear	linear
Model 2	poly (d=3)	linear	poly (d=2)	linear	linear	linear	NS	linear	poly (d=2)
Model 3	linear	linear	*skewness	linear	linear	linear	linear	linear	*length 1
GAM									
Model 1	S()	S()	S()	S()	S()	S()	S()	S()	S()
Model 2	S(k=4)	S(k=4)	S(k=4)	S(k=4)	S(k=4)	S(k=4)	NS	NS	S(k=4)
Model 3	S()	S()	*skewness	S()	S()	S()	S()	S()	*length 1

linear and interaction terms. When interaction terms were introduced, the choice of which terms to include in each interaction was based on their correlation. Specifically, the correlation between skewness and first bottom length, skewness and kurtosis, and between hardness and max S_v were high at 0.92, 0.97, and 0.82, respectively, and were therefore examined for potential interaction effects. The step function in *R*, which calculates the AIC value of models starting with the full model that used all 9 parameters and then in a stepwise fashion eliminates 1 parameter at a time, was applied to each candidate model to determine whether a simpler, reduced model would result in a better fit. The best GLM among the 3 classes was then chosen as the one with the lowest AIC value.

Three classes of generalized additive models (GAMs) were also evaluated, again with the minimum AIC value to choose the best-fitting model within each class (Table 3). The 3 classes consisted of models with all unconstrained smoothing terms, models with constrained smoothing terms, and models with mixtures of unconstrained and bivariate smoothing terms (interaction terms). Constraining the smoothing functions consisted of setting the maximum number of knots allowed (in all cases, 4 knots). Choice of the variables used in the interaction terms was again based on the magnitude of the correlation between variables. Model selection for the GAMs proceeded with a process similar to that used for the GLMs, but was done manually because a step function is unavailable for GAMs. Instead, we used the *P*-values from the analysis of variance of the model to sequentially eliminate nonsignificant terms. In the event of more than 1 nonsignificant term, the term with the least significance was first eliminated, then the reduced model was refitted and further nonsignificant terms were sequentially removed. The best overall GAM was again chosen among the best models within each class on the basis of minimum AIC.

After selecting the best candidate GLM and GAM, we compared them in terms of their ability to correctly classify data not used in the model building process. The best model (i.e., the one with the highest predictive accuracy) when applied to the training data is not necessarily the best choice when applied to new data. To assess the relative robustness of the models when subjected to new data, we used 33% holdout cross validation (Arlot and Celisse, 2010; Maunder and Harley, 2011), which proceeded as follows. Random samples of 160 segments, split equally between trawlable and untrawlable data, were selected without replacement from the pool of 238 acoustic segments. These data were then used as a training sample to construct prediction functions by fitting the best GLMs and GAMs. The remainder of the sample was used as a proxy for new data. Each of the fitted models was then applied to the new data to estimate the probability that each of the ~50 records within each segment was trawlable by using the "predict" function in *R*. Probabilities >0.5 was used as a criterion to classify individual records as trawlable. Likewise, the criterion used to classify entire segments as trawlable was that the proportion of records classified as trawlable was also >0.5. After the trawlability of all segments was estimated, the values were compared with the trawlability classification of the sampling cells. The proportion of correctly classified segments was then calculated. This process was repeated 100 times and the average proportion of correct classification was used as a measure of how well each model predicted trawlability.

Results and discussion

On the basis of the minimum value of AIC, the best GAM, with 7 unconstrained smoothing terms and 1 interaction term, produced an overall (trawlable and

Table 4

Goodness of fit, based on Akaike's information criterion (AIC), prediction accuracy of untrawlable and trawlable sampling cells (sampling units) in the survey area, overall prediction accuracy, and prediction accuracy after cross-validation of the 3 generalized linear models (GLMs) and 3 generalized additive models (GAMs) evaluated in this study for the use of acoustic data to predict whether sampling areas in the Gulf of Alaska are trawlable. The best model in each category is shown in boldface.

	AIC	Untrawlable prediction rate (%)	Trawlable prediction rate (%)	Overall prediction rate (%)	Cross validation prediction (%)
GLM					
Model 1	12,353	82.0	70.6	76.3	
Model 2	12,230	84.0	69.7	76.9	75.0
Model 3	12,351	84.0	71.4	77.7	
GAM					
Model 1	10,435	81.5	82.4	82.0	
Model 2	11,496	81.9	75.2	78.6	
Model 3	10,343	81.5	83.2	82.4	75.0

untrawlable segments combined) classification accuracy of 82.4% (Table 4). In contrast, the best GLM with 5 linear terms and 3 polynomial terms, but no interaction terms, produced an overall classification accuracy of only 76.9%, suggesting that the GAM was superior to the GLM. However, after subjecting these 2 models to cross validation to estimate their expected classification accuracy with new data, a different picture emerged with respect to their relative performance. Although the prediction accuracy of the GAM declined substantially (from 82.4% to 75.0%; Table 4) in the cross validation, the prediction accuracy of the GLM remained relatively stable (76.9 to 75.0%). This difference indicates that the GAM, because of its greater number of estimated parameters, over-fitted the original data. Because the cross-validated prediction accuracy did not differ between models, the more stable and simpler GLM was chosen as the best model. A map showing the classification results of this model is provided in Figure 2.

One potential shortcoming with our method for predicting bottom trawlability is that it cannot be applied to the deeper parts of the survey area because of the requirement for a second echo in the acoustic data. The second echo is needed by the Echoview software to estimate 2 of the 9 parameters (hardness and second bottom length) and therefore contributes to prediction accuracy. However, resolution of the second echo in the acoustic data depends on water depth and ping rate, and the ping rate is limited to at least 1 Hz for vessel captains to recognize bottom features that are likely to result in net damage. This limitation on ping frequency, in turn, limits the maximum depth to ~375 m at which our method could be applied. However, much of the deep areas of the continental slope tend to be relatively steep, which adversely affects the classification accuracy of single-beam systems (von Szalay and McConnaughey, 2002), and would therefore have been excluded anyway. Despite these limitations, only a relatively small portion of the survey area (~10%) needs to be excluded (Fig. 1).

Unlike earlier acoustic software for determining bottom types, such as the programs that were part of the QTC VIEW (Ellingsen et al., 2002) and Rox-Ann (Greenstreet et al., 1997) seabed classification systems, the Echoview bottom typing module requires calibration of the echosounder so that the strength of the bottom echo can be interpreted directly . Because GOA survey vessels routinely perform an echosounder calibration with copper spheres at the beginning and ending of each survey, this additional requirement did not add an additional burden for the collection of acoustic data and presumably provided additional information that improved our ability to determine bottom trawlability.

Although the primary motivation for this study was to develop a method that can be used to estimate the relative proportions of trawlable and untrawlable areas in the GOA bottom trawl survey area so that abundance estimates derived from survey trawl catches are extrapolated only to trawlable areas, another application of this method is to improve survey efficiency. The current survey design process involves randomly selecting stations within the survey grid that have been either declared trawlable, on the basis of criteria specified in the introduction, or whose trawlability status is unknown. Stations that have been declared untrawlable are not part of the sampling pool. The selection of stations that are unclassified with respect to trawlability contributes to an inefficient survey method because these stations are sampled with equal probability and yet may result in much fruitless search

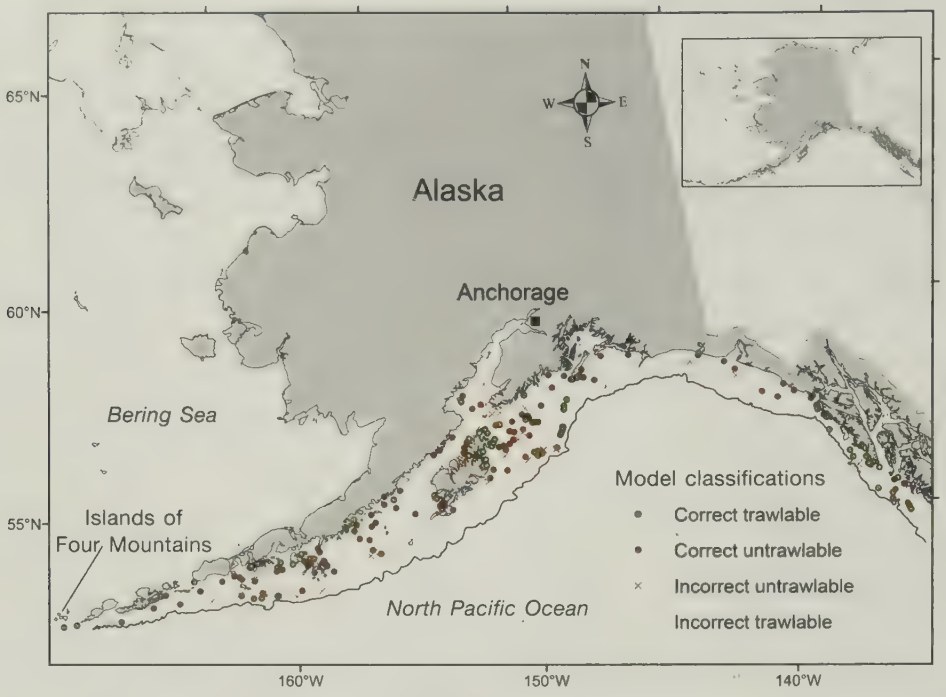

Figure 2

Bottom classification results of the best generalized linear model for 238 acoustic data segments that were collected in the Gulf of Alaska and used in the building and validation of this model. The segments, each represented by a symbol on the map at its collection area, are divided into 4 categories: area correctly classified as trawlable (green circles), area correctly classified as untrawlable (red circles), untrawlable area incorrectly predicted as trawlable (green x's), and trawlable area incorrectly predicted as untrawlable (red x's).

effort for trawlable ground in sampling cells that ultimately turn out to be untrawlable. Much of this inefficiency can be eliminated by minimizing the number of untrawlable sampling cells that make up the unclassified category of the sample of survey stations. This can be achieved by applying our model to the unclassified sampling cells so that a tentative trawlability status can be assigned to them. However, because of the lower confidence in the trawlability status of these sampling cells, it would not be appropriate to assign them binary sampling probabilities (0 or 1) as is done with sampling cells whose trawlability status is determined by traditional means. On the other hand, it is not necessary to assign equal sampling probabilities to these model-classified cells as is currently the case with the unclassified sampling cells. Instead, higher sampling probabilities would be assigned to sampling cells that our model predicts to be trawlable than to those that our model predicts to be untrawlable. The ratio of these sampling probabilities is a function of the prediction accuracy of the model.

Acknowledgments

S. Kotwicki, S. Stienessen, W. Palsson, J. Napp, J. Thorson, and 2 anonymous reviewers provided valuable comments which resulted in substantial improvements to the initial manuscript. J. Benson provided technical assistance with ArcMap in generating the figures. Funding was provided by the Office of Science and Technology, National Marine Fisheries Service, via the Improvement of Stock Assessment initiative. We thank all individuals involved in collecting the acoustic data on the FV *Sea Storm* during the 2013 GOA bottom trawl survey.

Literature cited

Anderson, J. T., R. S. Gregory, and W. T. Collins.
2002. Acoustic classification of marine habitats in coastal Newfoundland. ICES J. Mar. Sci. 59:156–167.

Arlot, S., and A. Celisse.
2010. A survey of cross-validation procedures for model selection. Stat. Surv. 4:40–79.

Bartholomä, A.
2006. Acoustic bottom detection and seabed classification in the German Bight, southern North Sea. Geo-Mar. Lett. 26:177–184.

Busby, M. S., K. L. Mier, and R. D. Brodeur.
2005. Habitat associations of demersal fishes and crabs in the Pribilof Islands region of the Bering Sea. Fish. Res. 75:15–28.

Clausen, D. M., and J. Heifetz.
2002. The northern rockfish, *Sebastes polyspinis*, in Alaska: commercial fishery, distribution, and biology. Mar. Fish. Rev. 64(4):1–28.
Cordue, P. L.
2007. A note on non-random error structure in trawl survey abundance indices. ICES J. Mar. Sci. 64:1333–1337.
Ellingsen, K. E., J. S. Gray, and E. Bjørnbom.
2002. Acoustic classification of seabed habitats using the QTC View system. ICES J. Mar. Sci. 59:825–835.
Foote, K. G., H. P. Knudsen, and G. Vestnes.
1983. Standard calibration of echo sounders and integrators with optimal copper spheres. Fisk.dir. Skr., Ser. Havunders. 17:335–346.
Freitas, R., S. Silva, V. Quintino, A. M. Rodrigues, K. Rhynas, and W. T. Collins.
2003. Acoustic seabed classification of marine habitats: studies in the western coastal-shelf area of Portugal. ICES J. Mar. Sci. 60:599–608.
Greenstreet, S. P. R, I. D. Tuck, G. N. Grewar, E. Armstrong, D. G. Reid, and P. J. Wright.
1997. An assessment of the acoustic survey technique, RoxAnn, as a means of mapping seabed habitat. ICES J. Mar. Sci. 54:939–959.
Jagielo, T., A. Hoffman, J. Tagart, and M. Zimmermann.
2003. Demersal groundfish densities in trawlable and untrawlable habitats off Washington: implications for the estimation of habitat bias in trawl surveys. Fish. Bull. 101:545–565.
Jones, D. T., C. D. Wilson, A. De Robertis, C. N. Rooper, T. C. Weber, and J. L. Butler.
2012. Evaluation of rockfish abundance in untrawlable habitat: combining acoustic and complementary sampling tools. Fish. Bull. 110:332–343.
Kloser, R. J., N. J. Bax, T. Ryan, A. Williams, and B. A. Barker.
2001. Remote sensing of seabed types in the Australian South East fishery; development and application of normal incidence acoustic techniques and associate 'ground truthing.' Mar. Freshw. Res. 52:475–489.
Maunder, M. N., and S. J. Harley.
2011. Using cross validation model selection to determine the shape of nonparametric selectivity curves in fisheries stock assessment models. Fish. Res. 110:283–288.
McConnaughey, R. A., and K. R. Smith.
2000. Associations between flatfish abundance and surficial sediments in the eastern Bering Sea. Can. J. Fish. Aquat. Sci. 57:2410–2419.
Pirtle, J. L., T. C. Weber, C. D. Wilson, and C. N. Rooper.
2015. Assessment of trawlable and untrawlable seafloor using multibeam-derived metrics. Methods Oceanogr. 12:18–35.
R Core Team.
2015. R: a language and environment for statistical computing. R Foundation for Statistical Computing, Vienna, Austria. [Available from website, accessed June 2015.]
Richards, L. J.
1986. Depth and habitat distributions of three species of rockfish (*Sebastes*) in British Columbia: observations from the submersible PISCES IV. Environ. Biol. Fish. 17:13–21.
Riegl, B. M., R. P. Moyer, L. J. Morris, R. W. Virnstein, and S. J. Purkis.
2005. Distribution and seasonal biomass drift macroalgae in the Indian River Lagoon (Florida, USA) estimated with acoustic seafloor classification (QTCView, Echo*plus*). J. Exp. Mar. Biol. Ecol. 326:89–104.
Rooper, C. N., G. R. Hoff, and A. De Robertis.
2010. Assessing habitat utilization and rockfish (*Sebastes* spp.) biomass on an isolated rocky ridge using acoustics and stereo image analysis. Can. J. Fish. Aquat. Sci. 67:1658–1670.
Stauffer, G. (compiler).
2004. NOAA protocols for groundfish bottom trawl surveys of the nation's fishery resources. NOAA Tech. Memo. NMFS-F/SPO-65, 205 p.
Stein, D. L., B. N. Tissot, M. A. Hixon, and W. Barss.
1992. Fish-habitat associations on a deep reef at the edge of the Oregon continental shelf. Fish. Bull. 90:540–551.
Thorson, J. T., M. E. Clarke, I. J. Stewart, and A. E. Punt.
2013. The implications of spatially varying catchability on bottom trawl surveys of fish abundance: a proposed solution involving underwater vehicles. Can. J. Fish. Aquat. Sci. 70:294–306.
von Szalay, P. G., and R. A. McConnaughey.
2002. The effect of slope and vessel speed on the performance of a single beam acoustic seabed classification system. Fish. Res. 54:181–194.
von Szalay, P. G., and N. W. Raring.
2016. Data report: 2015 Gulf of Alaska bottom trawl survey. NOAA Tech. Memo. NMFS-AFSC-325, 249 p.
Weber, T. C., C. Rooper, J. Butler, D. Jones, and C. Wilson.
2013. Seabed classification for trawlability determined with a multibeam echo sounder on Snakehead Bank in the Gulf of Alaska. Fish. Bull. 111:68–77.
Williams, K., C. N. Rooper, and R. Towler.
2010. Use of stereo camera systems for assessment of rockfish abundance in untrawlable areas and for recording pollock behavior during midwater trawls. Fish. Bull. 108:352–362.
Yoklavich, M. M., H. G. Greene, G. M. Cailliet, D. E. Sullivan, R. N. Lea, and M. S. Love.
2000. Habitat associations of deep-water rockfishes in a submarine canyon: an example of a natural refuge. Fish. Bull. 98:625–641.
Zimmermann, M.
2003. Calculation of untrawlable areas within the boundaries of a bottom trawl survey. Can. J. Fish. Aquat. Sci. 60: 657–669.

National Marine
Fisheries Service
NOAA

Fishery Bulletin
established in 1881

Spencer F. Baird
First U.S. Commissioner
of Fisheries and founder
of *Fishery Bulletin*

Spatial and temporal patterns of abundance of juvenile black sea bass (*Centropristis striata*) in Maryland coastal bays

Rebecca Peters
Paulinus Chigbu (contact author)

Email address for contact author: pchigbu@umes.edu

Department of Natural Science
University of Maryland Eastern Shore
#1 Backbone Road
Princess Anne, Maryland 21853

Abstract—Black sea bass (*Centropristis striata*) is a warm temperate species that is associated with structured habitats along the U.S. Atlantic coast and Gulf of Mexico. The northern stock is considered data poor, and the lack of information on the life history, especially at the juvenile stage, is a concern. We analyzed trawl survey data collected during 1989–2013 from the Maryland coastal bays (MCBs) by the Maryland Department of Natural Resources, and used catch-per-unit-of-effort (CPUE) to determine spatial and temporal patterns in abundance of black sea bass. The highest CPUE occurred at sites close to the MCBs inlets, suggesting the presence of suitable habitats for this species in these areas. Spatial patterns of abundance of black sea bass showed no consistent relationship with temperature, salinity, dissolved oxygen, and Secchi disk depth, a measure of water transparency (P>0.05), but CPUE was positively correlated with water depth (P=0.025). Average growth rate of the fish was 0.58 mm total length (TL)/day, ranging from 0.46 to 0.72 mm TL/day. Results of a generalized linear model with a Poisson distribution indicated that salinity and the North Atlantic Oscillation index best predicted interannual variation in CPUE of age-0 fish, but not CPUE of age-1 black sea bass. Information from this study can be used to form a basis for future studies in the coastal bays of Maryland and other coastal lagoon systems.

Manuscript submitted 14 December 2016.
Manuscript accepted 14 August 2017.
Fish. Bull. 115:504–516 (2017).
Online publication date: 29 August 2017.
doi: 10.7755/FB.115.4.7

The views and opinions expressed or implied in this article are those of the author (or authors) and do not necessarily reflect the position of the National Marine Fisheries Service, NOAA.

Estuaries on the Atlantic and Gulf coasts of the United States serve as nursery areas for many commercially and recreationally harvested fish species. However, some smaller estuaries throughout this region are relatively understudied, resulting in a limited understanding of how important they are as habitats for some marine fish species. This lack of information causes difficulties for the protection of nursery areas of a particular species (Beck et al., 2001). One such species is the black sea bass (*Centropristis striata*), which is currently considered data poor owing in part to its protogynous hermaphroditic nature (Able et al., 1995; Shepherd[1]).

The black sea bass is a temperate fish species that occupies an extensive range from the Gulf of Maine to the Gulf of Mexico (Steimle et al., 1999). It is commercially and recreationally harvested throughout its range, requiring management by state and federal fishery management agencies. Because of the large extent of its range, the black sea bass is managed as 3 stocks: the northern, southern, and Gulf of Mexico stocks, which have differences in migratory behavior and genetic makeup (Steimle et al., 1999). The northern stock, from the Gulf of Maine to north of Cape Hatteras, North Carolina, is seasonally migratory, occupying coastal habitats in warmer months and moving offshore to areas along the continental shelf for the winter (Musick and Mercer, 1977; Drohan et al., 2007; Moser and Shepherd, 2009). While in their coastal habitats, adults spawn from April to November, and peak spawning occurs between June and September (Able et al., 1995). Spawning begins earlier in southern areas of the stock, with the earliest larvae found during March off North Carolina, but later in July off New Jersey (Able et al., 1995). Young-of-the-year (YOY) black sea bass may enter estuaries from July until September at total lengths (TLs) of roughly 13–24 mm (Musick and Mercer, 1977), but they can enter as early as March in southern areas near Virginia (Kimmel, 1973). The differences in habitat use of YOY and adult black sea bass, along with differences in timing of spawning and migration into estuarine habitats (Drohan et al., 2007), make it necessary for age-specific and

[1] Shepherd, G. R. 2009. Black sea bass. *In* The Northeast Data Poor Stocks Working Group report, December 8–12, 2008 Meeting. Part A. Skate species complex, deep sea red crab, Atlantic wolffish, scup, and black sea bass. Northeast Fish. Sci. Cent. Ref. Doc. 09-02A&B, p. 423–463. [Available from website.]

estuary-specific studies to be conducted to provide effective information for management of this species.

Young-of-the-year and age-1+ black sea bass are captured in estuarine habitats during the warmer months of the year when the northern stock occupies inshore areas of the continental shelf. Studies of juvenile black sea bass have been conducted in a few estuaries in their northern range, especially with regard to their distribution, abundance, growth, habitat fidelity, and feeding habits (Richards, 1963; Kimmel, 1973; Allen et al., 1978; Festa[2]; Heck and Orth, 1980; Werme, 1981). The species has been reported (see Steimle et al., 1999) in various estuaries in the Mid-Atlantic Bight, such as southern Chincoteague Bay, Virginia (Schwartz, 1961), Magothy Bay, Virginia (Kimmel, 1973), central Long Island Sound (Richards, 1963), Raritan and Sandy Hook Bays (Wilk et al.[3]) and Barnegat Bay, New Jersey (Tatham et al., 1984). The preferred estuarine nursery habitats are shallow areas with structure that can serve as a refuge from predators (Steimle et al., 1999). While in estuaries they exhibit site fidelity (Able and Hales, 1997) and can be found around bridge pilings, rock jetties, artificial reefs, and oyster reefs along with seagrass beds (Steimle et al., 1999). During this time, black sea bass grow rapidly at a rate of 0.74 mm TL/day during the summer (Able and Hales, 1997). Little growth occurs during their overwintering time offshore, and 95% of black sea bass are mature at around 28 cm TL (length at 50% maturity occurring at 20.4 cm [Shepherd and Nieland[4]]). Because of the possibility of size selective overwinter mortality, the time black sea bass spend in estuaries is vital to their growth, survival, and subsequent recruitment to the adult population.

Information on the ecology of black sea bass in Maryland coastal bays (MCBs), the series of 5 bays located on the eastern shore of Maryland, is scarce. Such information is needed to assess the extent to which the MCBs serve as nursery habitats for black sea bass and contribute to the adult population in the coastal ocean. In 2013 Maryland accounted for 11% of the 984.30 metric tons (2.17 million lb) commercial catch quota and 19.14 of the 598.74 metric tons (or 42,200 lb of the 1.32 million lb) of total allowable landings for recreational harvest (Butowski et al.[5]), hence estuaries in the Maryland area including the MCBs may be important nursery grounds for black sea bass.

The Maryland Department of Natural Resources conducts the Coastal Bays Fisheries Investigations Trawl and Beach Seine Survey in the MCBs to assess trends in juvenile fish abundance (Butowski et al.[4]). This survey takes place monthly from April to October each year at 20 fixed sites, and was standardized in 1989 (Pincin et al., 2014). The data from these surveys have been used to examine trends in abundance and distribution of juveniles for some finfish and crab species (Murphy and Secor, 2006; Love et al., 2009; O'Brien, 2013; Pincin et al., 2014; Malagon, 2015) but not for the black sea bass. A recent study showed that the indices of abundance of juvenile black sea bass determined from the NOAA Northeast Fisheries Science Center trawl surveys in the mid-Atlantic were highly correlated with indices of abundance from independent surveys conducted by a number of state agencies (Miller et al., 2016). This finding suggests that data from trawl surveys may be useful for describing seasonal, as well as interannual, variations in the abundance of black sea bass in estuaries such as those in the MCBs.

The objectives for this study were 1) to describe spatial and seasonal changes in the abundance and size composition of black sea bass, and assess the role of environmental factors in the spatial distribution pattern, and 2) to evaluate the influence of environmental (temperature and salinity) factors and major climatic phenomena, such as the North Atlantic Oscillation (NAO) and El Niño Southern Oscillation (ENSO) events, and the influence of spawning stock biomass of black sea bass on the recruitment dynamics of juvenile black sea bass. Previous studies have shown that the NAO affects other species in the northwest Atlantic. For example, abundance of the northern shortfin squid (*Illex illecebrosus*) was found to be higher in years with a negative NAO index, which provides weak winter northwesterly winds (Dawe et al., 2000). Other similar studies, found that NAO affected the recruitment of Atlantic cod (*Gadus morhua*) in European waters, especially when spawning stock biomass was low (Brander, 2005), and contributed to the decline of the northern stock of Atlantic cod off of Canada (Mann and Drinkwater, 1994; Parsons and Lear, 2001). Understanding the role that climatic factors have in recruitment into nursery areas for economically valuable species is important for the future management of the stocks, particularly as management moves toward ecosystem-based management.

Materials and methods

Study location

The MCBs located on the eastern shore of Maryland and separated from the Atlantic Ocean by 2 barrier Islands (Pincin et al., 2014) are composed of 5 bays: Assawoman, Isle of Wight, Sinepuxent, Newport, and Chincoteague

[2] Festa, P. J. 1979. Analysis of the fish forage base in the Little Egg Harbor Estuary. New Jersey Department of Environmental Protection, Division of Fish Game and Shellfish, Bureau of Fisheries, Nacote Creek Station, Tech. Rep. 24M, 134 p. [Available from website.]

[3] Wilk, S. J., E. M. MacHaffie, D. G. McMillan, A. J. Pacheco, R. A. Pikanowski, and L. L. Stehlik. 1996. Fish, megainvertebrates, and associated hydrographic observations collected in the Hudson-Raritan Estuary, January 1992–December 1993. Northeast Fish. Sci. Cent. Ref. Doc. 96-14, 95 p. [Available from website.]

[4] Shepherd, G. R., and J. Nieland. 2010. Black sea bass 2010 stock assessment update. Northeast Fish. Sci. Cent. Ref. Doc. 10–13, 25 p. [Available from website.]

[5] Butowski, N., R. Morin, and M. Topolski. 2013. 2012 Fishery management plan: report to the legislative committees, 185 p. Maryland Dep. Nat. Resour., Fish. Serv., Annapolis, MD. [Available from website.]

Figure 1

Map showing the 20 sites sampled for the Maryland Department of Natural Resources' Coastal Bays Fisheries Investigations Trawl and Beach Seine Survey in Maryland coastal bays.

Bay (Fig. 1). The northern bays (area north of the Ocean City Inlet) are Assawoman and Isle of Wight Bay, and the southern bays (area south of the Ocean City Inlet) are Newport Bay, Sinepuxent, and Chincoteague Bay (Fig. 1). The MCBs are one of the most diverse estuaries on the east coast (U.S. EPA, 2006). The system covers about 453 km^2 and supports many species including finfish, mollusks, crustaceans, birds, and mammals (ANEP[6]). Groundwater is the primary source of freshwater flow into the bays (Wazniak et al., 2004a); salinities are high in the bays except in areas upstream in the tributary rivers and creeks (Wazniak et al., 2004b). Flushing is slow because of limited tidal exchange between the bays and the ocean through the Ocean City and Chincoteague Inlets, and circulation is limited by wind (Wazniak et al., 2004b). The Ocean City Inlet was opened as a corridor by a hurricane in 1933 and has been kept open as a navigation channel by 2 rock jetties along its north and south banks (Wazniak et al., 2004a).

The coastal bays are a tourist attraction, bringing more than 11 million visitors annually to the Eastern Shore of Maryland (MCBP[7]). This high level of use has caused the bays to degrade over time, lowering water quality and resulting in a current overall condition rating of "Moderate," a C+ rating on a multiagency report card which is used to track the health of the MCB ecosystem and is updated annually (IAN, 2015). There is evidence that the abundance of forage fish has declined in the lagoons over the past 20 years (Casey et al.[8]; Pincin et al., 2014), suggesting that fish populations in the MCBs are changing and require further investigations.

Sampling and data analysis

The Maryland Department of Natural Resources Coastal Bays Fisheries Investigations Trawl and Beach Seine Survey is conducted annually at 20 fixed locations that are sampled once a month in the MCBs (Fig. 1) from April until October. The gear used is a 4.9-m semiballoon trawl with 3.18 cm mesh in the outer net, 1.27 cm of mesh in the inner liner, and 2.86 cm of mesh in the codend; a tickler chain is used, and trawling duration at each of the 20 sites was 6 min (Bolinger et al.[9]). Along with numbers of black sea bass at each site, abiotic factors were recorded, including water temperature (degrees Celsius), dissolved oxygen (milligrams per liter), salinity, Secchi disk depth (centimeters), and water depth (meters). The time series of data collected from 1989 to 2013 was used to assess the spatial and temporal changes in abundance of black sea bass.

Catch-per-unit-of-effort (CPUE) was used as an indicator of abundance for black sea bass (Bolinger et al.[8]),

[6] NEP (Association of National Estuary Programs). 2001. Maryland Coastal Bays. Fact Card. [Available from Maryland Coastal Bays Program, 8219 Stephen Decatur Hwy. Berlin, MD 21811.]

[7] MCBP (Maryland Coastal Bays Program). 2017. Mission and history. Maryland Dep. Nat. Resour., Annapolis, MD. [Available from website, accessed July 2017.]

[8] Casey, J. F., S. B. Doctor, and A. E. Wesche. 2001. Investigation of Maryland's Atlantic Ocean and Coastal Bay Finfish Stocks, 28 p. Federal Aid Project No. F-50-R. [Available from Maryland Dep. Nat. Resour., Fish. Serv., Tawes State Office, Bldg. 2, 580 Taylor Ave., Annapolis, MD.]

[9] Bolinger, A., S. Doctor, A. Luettel, M. Luisi, and G. Tyler. 2007. Investigation of Maryland's coastal bays and Atlantic Ocean finfish stock: 2007 report, 153 p. Federal Aid Project No. F-50-R-16. Maryland Dep. Nat. Resour., Fish. Serv., Annapolis, MD.. [Available from website.]

and was calculated as the number of black sea bass caught divided by the number of tows. CPUE was calculated for each year, month, and site, and was used to evaluate patterns in temporal and spatial abundance. To determine whether any of the abiotic factors recorded in the survey influence spatial distribution of black sea bass in the MCBs, generalized linear models (GLMs) with a quasi-Poisson distribution due to over dispersion, were run for each month. The abiotic factors used in the GLMs were water temperature, dissolved oxygen, salinity, and Secchi disk depth because analyses of variance determined that these factors varied between sites and months. Water depth was not used in each monthly GLM because it did not vary at sites between months. For the monthly models, number of fish at each of the 20 sampling sites was used as the dependent variable, and abiotic variables were used as the predictor variables. A separate regression analysis was run with total CPUE at each site (from 1990 to 2012) as the dependent variable and average depth (in meters) at each site (from 1990 to 2012) as the predictor variable. All statistical analyses were run in R statistical software (vers. 3.2.0; R Core Team, 2015).

Because previous studies found that YOY black sea bass enter estuaries from July to September (Able et al., 1995), 1 January was determined to be the birth date and fish caught during April and May the following year were assumed to be age 1 (juveniles) (Able et al., 1995). Fish length frequencies were examined each month and the 2 standard deviations greater and less than the mode were used to distinguish between year classes (Gulland and Rosenberg, 1992). Black sea bass less than 2 standard deviations of the mode were designated as age 0, and those greater than 2 standard deviations were considered age 1+. The CPUE of YOY fish, used as a recruitment index, was examined in relation to abiotic factors (temperature and salinity), climatic events (annual NAO index, NAO winter, spring, and summer indices, ENSO index, ENSO winter and spring indices, which were calculated and downloaded from the NOAA Climate Prediction Center; website, accessed April 2015), and spawning stock biomass of black sea bass, the latter of which was provided by the Northeast Fisheries Science Center. For this analysis, only data from 1990 to 2012 were used because those were the years with full records of environmental factors measured at each site for each month. A GLM with a Poisson distribution (R Core Team, 2015) was used in a stepwise approach to determine which model and variables best predict recruitment of YOY black sea bass. The model with the lowest Akaike information criterion (AIC) value was chosen as the best indicator for predicting recruitment.

Growth rate of juvenile (age 1) black sea bass was also assessed for years when, at least, 5 black sea bass individuals were captured in May, and in September. Length of black sea bass (TL in millimeters) in May was averaged and subtracted from the average length in September, and the value was then divided by the total number of days over that time period (May–September) (n=152) to estimate growth rates (mm per day) for each year (Tucker, 2000). These values were then averaged together to estimate absolute growth rate of juvenile black sea bass in the MCBs. Regression analysis was then performed to determine whether growth rates were related to abundance or temperature.

Results

Size composition and growth of black sea bass in Maryland coastal bays

The length-frequency distributions of fish collected each month (April–October) from 1989 to 2013 are presented in Figure 2. Trawl catches consisted mostly of age-1 fish; however a few age-0 black sea bass were caught. Black sea bass began to enter MCBs in April in low numbers at sizes ranging from 45 to 95 mm TL. In June they began to enter in higher numbers at sizes of 27 to 205 mm. By October, they had attained sizes of about 58–240 mm TL. Samples collected in April showed the presence of fish that were approximately 1 year old that had entered the MCBs from the coastal ocean. The size range of these fish was similar to the size range of YOY fish captured in October of the previous year, suggesting there was minimal growth during the winter.

Growth rate of age-1 black sea bass from May to September was fastest in 1992 (0.72 mm TL/day) and slowest in 1990 and 2002 (0.46 mm TL/day) and averaged 0.58 mm TL/day. Growth rate had no correlation (P>0.05) with average temperature and abundance data for each year.

Interannual variation in abundance of black sea bass

CPUE of age-1 black sea bass showed no significant increasing or decreasing trend over time (Fig. 3A) but was characterized by low values in 1989, 1993, 1996, 1998, 2004 and 2005 and by the highest CPUE in 2008. In contrast, CPUE of age-0 fish showed a significant annual increasing trend (P<0.05) during 1989–2013, although it also exhibited fluctuations in relative abundance between years. The largest CPUE occurred in 2002, 2008, and 2013, whereas the lowest CPUE was observed in 1989, 1990, 1993 and 1996 (Fig. 3B). The patterns in CPUE of age-1 and age-0 black sea bass over time were somewhat similar, with peak abundances occurring in similar years.

Spatial distribution of black sea bass in Maryland coastal bays

On average from 1989 to 2013, mean CPUE was relatively low at a site (site 5) in the St. Martin River, and at 4 sites (sites 13, 14, 15, 18) in the central part of Chincoteague Bay (Fig. 4). In May, black sea bass were most abundant in the southernmost site located by the Maryland/Virginia border in Chincoteague Bay (Fig.

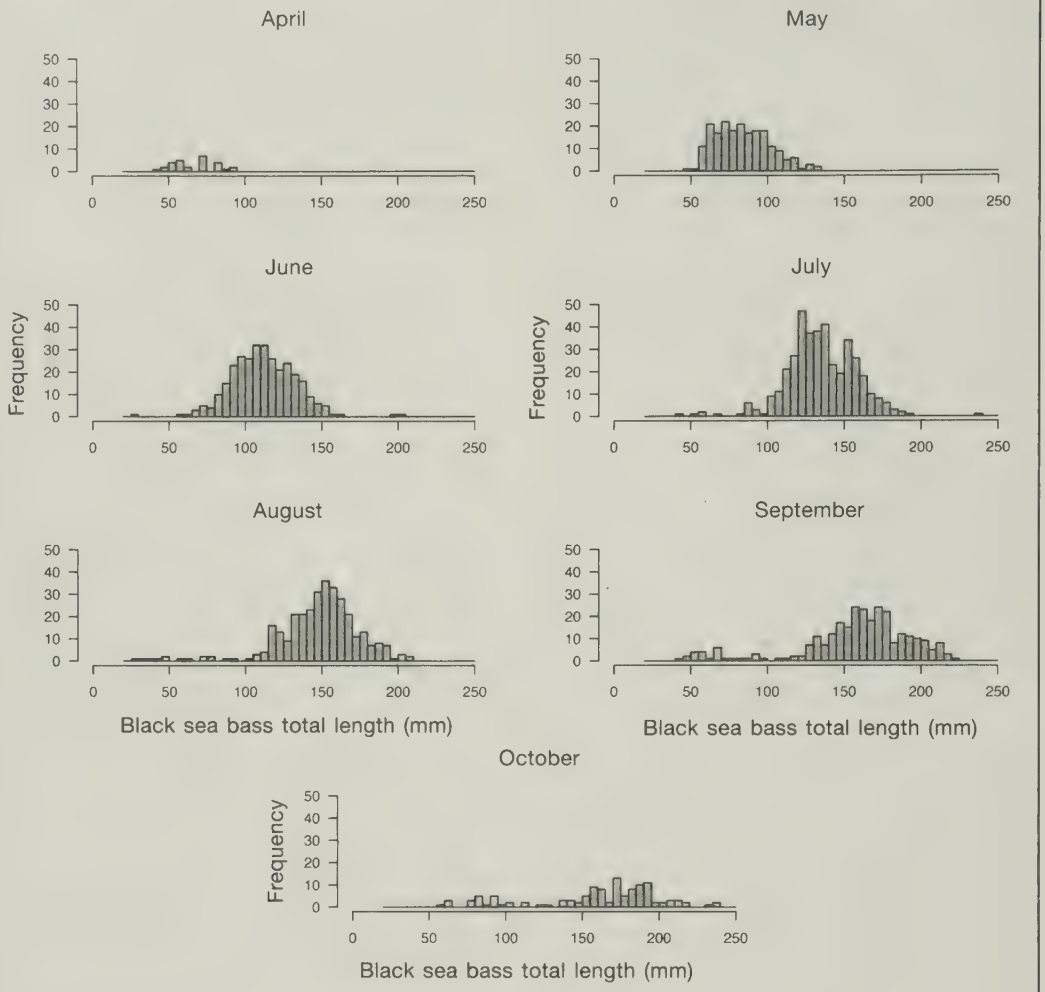

Figure 2

Total-length-frequency distributions of black sea bass (*Centropristis striata*) caught in trawl surveys conducted in Maryland coastal bays by the Maryland Department of Natural Resources during 1989–2013.

5). As temperatures began to warm, black sea bass became more abundant in July in the MCBs, especially in the northern bays. Toward September and October when water temperature began to decrease, black sea bass began to concentrate at sites relatively close to Ocean City and Chincoteague Inlets (Fig. 5).

Results from the GLMs for April, June, August, September and October, showed that temperature, salinity, dissolved oxygen, and Secchi disk depth were not significant predictor variables for catch of black sea bass at the 20 sampling sites (P>0.05). In May, salinity was an important predictor variable (P=0.01), whereas in July, Secchi disk depth was a significant predictor variable (P=0.03) for catch of black sea bass. Catch per unit of effort of black sea bass was related to average water depth (coefficient of determination [r^2]=0.21, P=0.025) and higher CPUE occurred at deeper (>2 m) sites (Fig. 6).

Seasonal patterns of abundance of black sea bass and temperature

Black sea bass (age 1) began to enter the MCBs from the ocean at an average temperature of 14.21°C in April and 19.34°C in May (Fig. 7, A and B) at sizes ranging from about 45 to 135 mm TL (Fig. 2). Throughout the annual sampling period, size of black sea bass increased and sizes of fish caught ranged from 45 to 224 mm TL in September. Starting in June, smaller size fish (age 0) were captured in the bays (Figs. 2 and 7). The abundance of age-0 fish peaked in September, whereas the abundance for the age-1 year class peaked in July (Fig. 7A) when temperature also peaked at 27.5°C (Fig. 7B). The CPUE of age-1 black sea bass declined from July to October (Fig. 7A) when temperature also began to decrease (Fig. 7B).

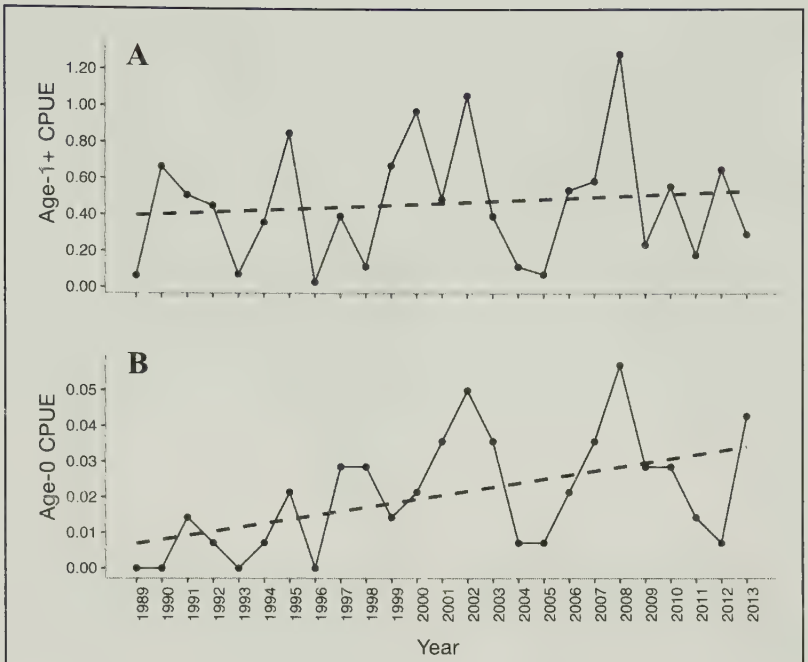

Figure 3

Catch per unit of effort (CPUE) of (**A**) age-1 and (**B**) age-0 black sea bass (*Centropristis striata*) in Maryland coastal bays from trawl surveys conducted during 1989–2013. The dashed line in panel B indicates a significant positive increase ($P<0.05$).

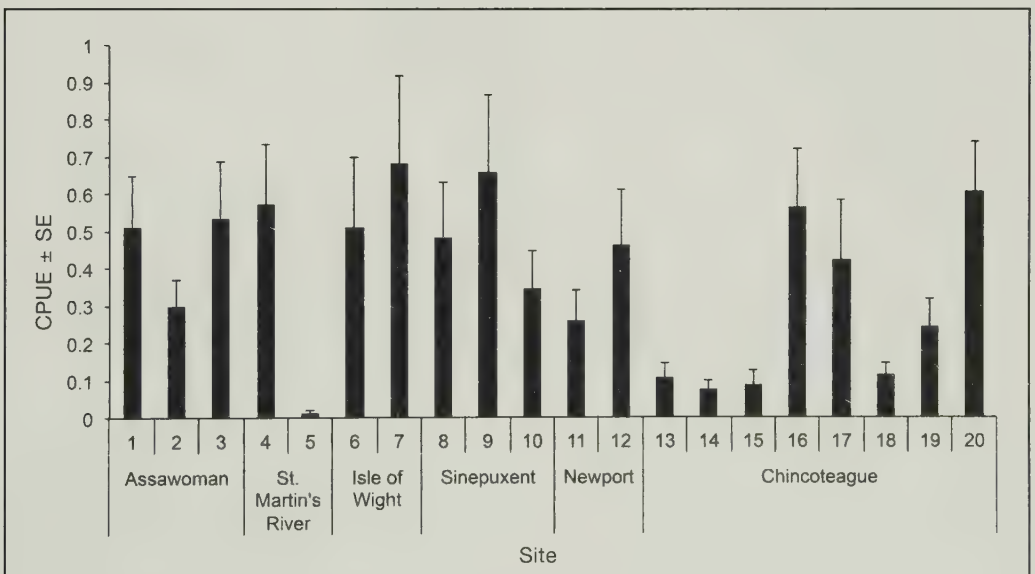

Figure 4

Mean catch per unit of effort (CPUE) for black sea bass (*Centropristis striata*) at various sites in Maryland coastal bays sampled during trawl surveys during 1989–2013. Data were averaged across years. Error bars indicate standard error of the mean.

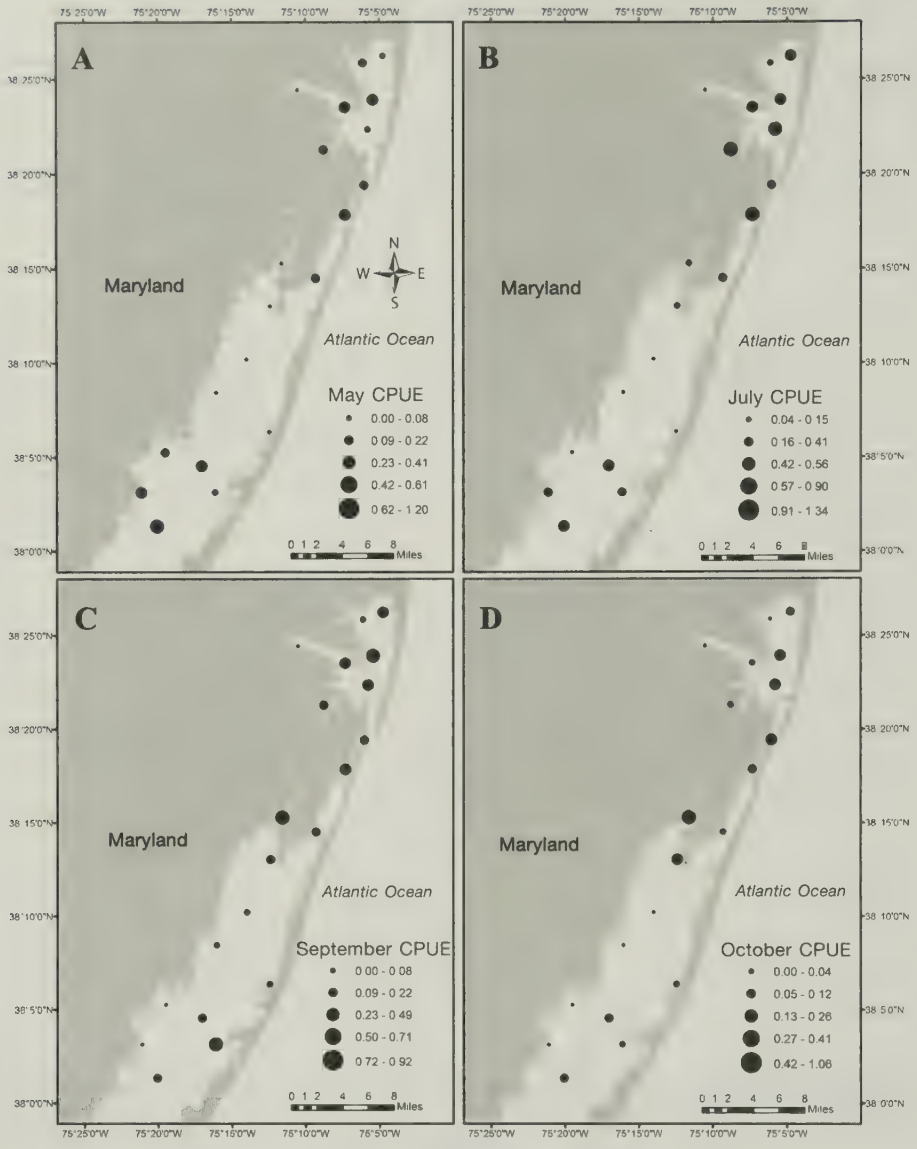

Figure 5

Spatial distribution of black sea bass (*Centropristis striata*) in Maryland coastal bays in (**A**) May, (**B**) July, (**C**) September, and (**D**) October, derived from a time series of catch per unit of effort (CPUE) determined from trawl surveys conducted monthly during 1989–2013.

Results from the GLMs show that average salinity at the sampling sites and the annual NAO index (AIC=90.07) are the most informative predictors of YOY abundance in the MCBs each year, and that salinity is the only significant predictor variable (Tables 1 and 2); the annual NAO index alone was not an informative predictor of age-0 catch (AIC=109.7). Catch of age-0 black sea bass was affected positively by salinity (P=0.0015) and negatively by the annual NAO index (P=0.0468).

Model results showed no trend in the residuals (Fig. 8) and a chi-square goodness-of-fit test showed no significant difference (P=0.166) between the observed and predicted values (Fig. 9). Owing to possible overdispersion, a negative binomial and zero-inflated model were run to compare AIC values from the Poisson model and the negative binomial and zero-inflated model. Comparisons of AIC values indicated that the GLM with a Poisson distribution (AIC=90.07) had the lowest AIC value and fitted the data best when compared with the 2 other models (negative binomial AIC=92.07, zero-inflated AIC=92.26).

Discussion

There was no significant increasing or decreasing trend in abundance of juvenile black sea bass from 1989 to

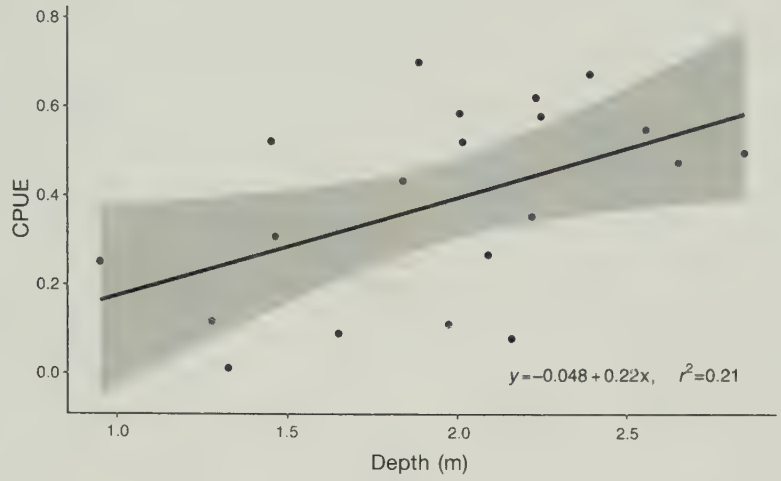

Figure 6

Relationship between catch per unit of effort (CPUE) for juvenile black sea bass (*Centropristis striata*) and average water depth (in meters) (P=0.025) from trawl surveys conducted by the Maryland Department of Natural Resources during 1989–2013. r^2=coefficient of determination.

Table 1

Generalized linear model results used to examine the relationship between catch of age-0 black sea bass (*Centropristis striata*) and environmental factors. Average salinity and annual North Atlantic Oscillation (NAO) index (Akaike information criterion [AIC]=90.07) are the best predictors of abundance of young-of-the-year black sea bass. Other factors in the models include temperature, NAO winter, spring, and summer indices, El Niño Southern Oscillation (ENSO), ENSO index, spring (ENSO.MAM) and winter (ENSO.DJF) indices, and spawning stock biomass (SSB). Catch data used were from a time series collected during 1989–2013 in Maryland coastal bays.

Model no.	Model	AIC
1	Age-0 catch ~ Salinity + Temperature + NAO + ENSO + ENSO.MAM + ENSO.DJF + NAO.summer + NAO.winter + NAO.spring+ SSB	100.14
2	Age-0 catch ~ Salinity + Temperature + NAO + ENSO + ENSO.MAM + ENSO.DJF + NAO.winter + NAO.spring + NAO.summer	99.14
3	Age-0 catch ~ Salinity + Temperature + NAO + ENSO + ENSO.MAM + ENSO.DJF + NAO.winter + NAO.spring	97.68
4	Age-0 catch ~ Salinity + Temperature + NAO + ENSO + ENSO.MAM + ENSO.DJF + NAO.winter	95.73
5	Age-0 catch ~ Salinity + Temperature + NAO + ENSO + ENSO.MAM + ENSO.DJF	93.76
6	Age-0 catch ~ Salinity + Temperature + NAO + ENSO + ENSO.MAM	92.75
7	Age-0 catch ~ Salinity + Temperature + NAO + ENSO	93.37
8	Age-0 catch ~ Salinity + Temperature + NAO	91.76
9	Age-0 catch ~ Salinity + Temperature	93.73
10	Age-0 catch ~ Salinity + NAO	90.07
11	Age-0 catch ~ Salinity	91.74

2013; however, some years did show strong year classes. Miller et al. (2016) found that spring during years of 2000, 2002, 2008, and 2012 were strong recruitment years for age-1 black sea bass, which is similar to our results. The catch of age-0 black sea bass did not correlate with abundance of age-1 black sea bass for the following year (t+1), indicating that the catch of age-0 black sea bass cannot predict abundance of age-1 fish of the following year. A similar observation was made by Miller et al. (2016) and was attributed to overwinter mortality that determined the strength of the year class.

Table 2

Results from the generalized linear model with the lowest Akaike information criterion (model 10 in Table 1), indicating that catch of age-0 black sea bass (*Centropristis striata*) in the Maryland coastal bays during 1989–2013 was affected positively by salinity (P=0.00153) and negatively by the annual North Atlantic Oscillation (NAO) index (P=0.04685). Standard errors (SEs) and 95% confidence intervals (CIs) are given for estimates. *z-value*=estimated regression coefficient divided by the standard error of the regression coefficient; the test statistic for the Wald test.

	Estimate	SE	*z*-value	*P*-value	95% CI
Intercept	−5.53401	2.09018	−2.648	0.00811	−9.79–(−1.57)
Salinity	0.23363	0.07374	3.168	0.00153	0.09–0.38
NAO	−0.54019	0.27177	−1.988	0.04685	−1.05–0.01

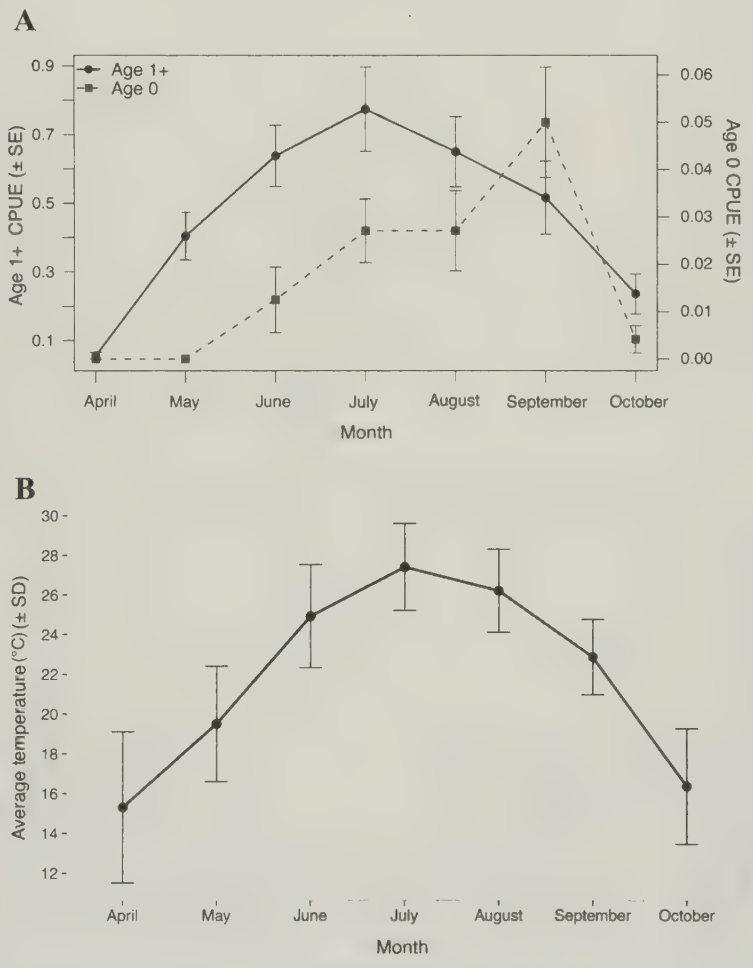

Figure 7

Monthly average (**A**) catch per unit of effort (CPUE) for age-1 and age-0 black sea bass (*Centropristis striata*) and (**B**) temperature from trawl surveys conducted during 1989–2013 in Maryland coastal bays. Data are averages across years. Error bars indicate standard error and standard deviation, respectively.

There was an increasing trend in YOY black sea bass caught in the MCBs from 1989 to 2013, suggesting increasing recruitment of black sea bass to estuarine habitats over time. Juvenile black sea bass were first captured in the bays in April and May and peaked in abundance in July; YOY were caught in the trawls in June and their abundance peaked in September. Adult black sea bass in the Mid-Atlantic Bight spawn from April until November and spawning occurs earlier in southern areas by Virginia (Shepherd and Nieland[3]). Depending on the year, YOY individuals can begin to enter the MCBs as early as June, but their abundance does not peak until September in the MCBs, which is consistent with Musick and Mercer's (1977) results showing that YOY enter estuaries after settling in coastal waters from July to September. In previous studies conducted in New Jersey, YOY were found in estuaries from July through October (Able et al., 1995).

Numbers of black sea bass began to increase in May, suggesting this is the time when they begin to enter the bays in larger numbers. In May they were most abundant in the southernmost part (site 20) of the Chincoteague Bay close to the Chincoteague Inlet. This finding suggests that black sea bass may enter initially through that inlet in May. When waters cool in the fall, black sea bass migrate offshore in a southerly direction to areas across the continental shelf (Musick and Mercer, 1977; Steimle et al., 1999). Once waters begin to warm in April they move inshore, generally along the same route (Kolek, 1990; Moser and Shepherd, 2009), which may be

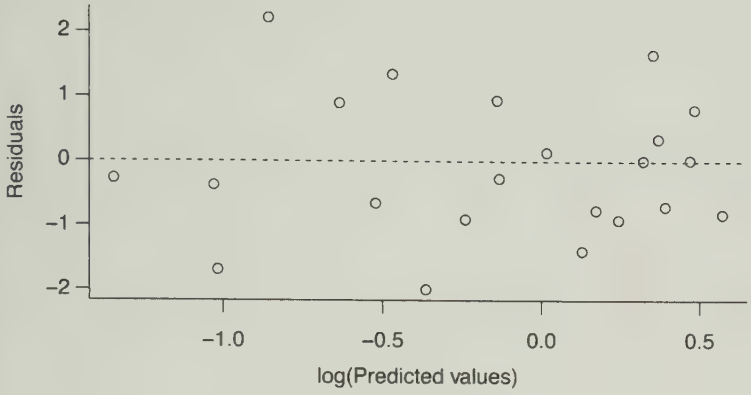

Figure 8

Diagnostic plot for the generalized linear model with the lowest Akaike information criterion (residuals versus log-transformed predicted values). This model was chosen as the best indicator for predicting recruitment of black sea bass (*Centropristis striata*) in the Maryland coastal bays.

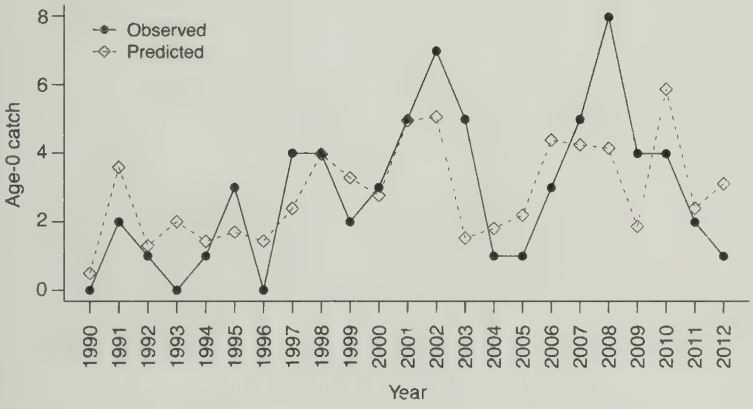

Figure 9

Observed and predicted values of catch of black sea bass (*Centropristis striata*) recorded during Maryland Department of Natural Resources surveys from the generalized linear model with a Poisson distribution and the lowest Akaike information criterion (age-0 catch ~ salinity + annual North Atlantic Oscillation index). A chi-square goodness of fit test (P=0.166) revealed no significant difference between the observed and predicted values.

why the highest abundance of black sea bass occurred in the southernmost site in May in this study.

Catch per unit of effort of black sea bass correlated with water depth, but not with temperature or dissolved oxygen. In the MCBs, there were not much within-season spatial differences in temperature and dissolved oxygen, which perhaps explains why the spatial distribution of juvenile black sea bass was not correlated with the environmental factors. In New Jersey estuaries, black sea bass were found in the deeper area of estuaries (>2 m), not the shallower parts (<1 m) (Able and Hales, 1997). The depth at each site in the MCBs ranged from 0.90 to 2.88 m. Low CPUE occurred at depths of 0.50–1.00 m and high CPUE at sites with depths greater than 2 m. Results from this study and past studies suggest juvenile black sea bass prefer deeper areas of estuaries.

Black sea bass were more abundant in Assawoman, Isle of Wight, and Sinepuxent Bays than in Newport Bay and the central part of Chincoteague Bay. Because abiotic factors measured did not show much correlation with the abundance of black sea bass, other factors, such as proximity to the inlets through which the black sea bass enter and leave the bays and availability of physical structure in the bays, are likely the reasons for differences in abundance between sites sampled in the survey. Able et al. (1995) found that black sea bass were more abundant in habitats with sand and shell bottoms, and in areas where amphipod tubes were abundant. A study that examined the effects of oyster shell planting on fish abundance in the Chincoteague Bay found that catch rates of black sea bass increased when shells were added (Arve, 1960). Because black sea bass are a structure-oriented species, their distribution may be affected by the presence and amount of available structured habitat; however, there is currently little information on the distribution of structured benthic habitats in the MCBs. The only known information on benthic cover is that seagrasses are more abundant on the eastern than the western half of the bays, macroalgae are more abundant in the northern than southern bays (Morales-Núñez and Chigbu, 2016), and oyster shells and beds are scarce. In other estuaries, juvenile black sea bass are rarely seen over nonvegetated sandy areas (Allen et al., 1978), but are commonly seen in areas of high shell density and structured habitats, such as wharves, oyster reefs, and rock reefs (Drohan et al., 2007).

The growth rate of black sea bass from May until September was determined to be 0.58 mm TL/day. There was no significant correlation between growth rate each year and the average temperature and abundance of black sea bass for those years; however, the numbers of fish caught in the trawls were low and this might have been responsible for the lack of significant correlations. Previous studies using a mark–recapture

method in a New Jersey estuary found that black sea bass grow rapidly during the summer, with a growth rate of 0.74 mm TL/day from July to September, and with an average of 0.45 mm TL/day from spring through fall (Able and Hales, 1997). A laboratory study found that growth of black sea bass was higher when habitat structure was provided (Gwak, 2003). Because black sea bass are found in areas of hard bottom, the availability of structure may affect the growth rate of the juveniles found in the MCBs. Future studies will have to be conducted to test this hypothesis, but in studies of juvenile North African catfish (*Clarias gariepinus*), an increase in resting time was observed when structure in the habitat was present—increased resting time would lead to an increase in growth rate (Hecht and Appelbaum, 1988).

Understanding climatic effects on recruitment of black sea bass is crucial for the management of the species because the abundance of the fish that contribute to the fishery depends on the number of recruits. In this study, we found that average salinity and the NAO index best predict recruitment of black sea bass. Catch of YOY black sea bass showed a significant positive relationship with salinity, which suggests that their abundance is relatively higher in the MCBs in years of lower-than-average freshwater discharge. In fact, the relatively high CPUE of YOY black sea bass in 1991, 1997 to 2002, and 2006–2008 corresponded with years of higher salinity, whereas the lower CPUE in 1990 and 2004–2005 corresponded with years of lower salinity in the MCBs (P. Chigbu, unpubl. data). Cotton et al. (2003) found that 20 and 30 were optimal salinity levels for YOY black sea bass. YOY black sea bass can tolerate salinities as low as 9 (Berlinsky et al., 2000), but they are primarily found in higher salinity areas of estuaries (Drohan et al., 2007). Because YOY black sea bass prefer areas of higher salinity and structured habitats, largely polyhaline coastal lagoons such as the MCBs may be very important habitats in contrast to river-dominated estuaries that experience larger salinity fluctuations. A recent study found that salinity may be important in the habitat selection of juvenile black sea bass in offshore areas of the continental shelf in the Mid-Atlantic Bight (Miller et al., 2016). During the overwintering period, juvenile black sea bass were found in areas with salinity levels of 33–35; years with strong recruitment in the spring were also years with warmer temperatures, higher salinity levels, and higher shelf water volume (Miller et al., 2016).

In the MCBs, CPUE of age-0 black sea bass was also higher when the NAO index was negative, which is associated with decreased westerly winds and lower temperatures in the region. The colder air during years with negative NAO indices brings less precipitation to the eastern United States and results in less freshwater discharge and higher salinity in estuaries and the coastal ocean (Cullen et al., 2002) that, perhaps, favor recruitment of black sea bass.

This study provides the first information on the spatial and temporal fluctuations in abundance of juvenile black sea bass in the MCBs. The results of our study provide insight into how a changing environment may impact recruitment of black sea bass into estuaries and show that future studies assessing the effects of climate change on recruitment of YOY black sea bass are important for the future conservation of the estuarine habitats that black sea bass inhabit and for the fishery that targets this species. Information from this study can form a basis for more studies of black sea bass in mid-Atlantic coastal lagoons in order to increase our understanding of the importance of these features as nursery habitats for the species.

Acknowledgments

We would like to thank A. Willey and S. Doctor from the Maryland Department of Natural Resources for providing the data. We would also like to thank the Coastal Bays Fisheries Investigation Trawl and Beach Seine Survey team for collection of the data over the years. R. Peters was supported in part by the NSF CREST Center for the Integrated Study of Coastal Ecosystem Processes and Dynamics in the mid-Atlantic region and by the NOAA Living Marine Resources Cooperative Science Center.

Literature cited

Able, K. W., and L. S. Hales Jr.
1997. Movements of juvenile black sea bass *Centropristis striata* (Linnaeus) in a southern New Jersey estuary. J. Exp. Mar. Biol. Ecol. 213:153–167.

Able, K. W., M. P. Fahay, and G. R. Shepherd.
1995. Early life history of black sea bass, *Centropristis striata*, in the Mid-Atlantic Bight and a New Jersey estuary. Fish. Bull. 93:429–445.

Allen, D. M., J. P. Clymer III, and S. S. Herman.
1978. Fishes of Hereford Inlet Estuary, southern New Jersey, 138 p. Department of Biology, Center for Marine Environmental Studies, Lehigh University, Bethlehem, PA, and the Wetland Institute, Stone Harbor, NJ.

Arve, J.
1960. Preliminary report on attracting fish by oyster-shell plantings in Chincoteague Bay, Maryland. Chesapeake Sci. 1:58–65.

Beck, M. W., K. L. Heck Jr., K. W. Able, D. L. Childers, D. B. Eggleston, B. M. Gillanders, B. Halpern, C. G. Hays, K. Hoshino, T. J. Minello, et al.
2001. The identification, conservation, and management of estuarine and marine nurseries for fish and invertebrates: a better understanding of the habitats that serve as nurseries for marine species and the factors that create site-specific variability in nursery quality will improve conservation and management of these areas. Bioscience 51:633–641.

Berlinsky, D., M. Watson, G. Nardi, and T. M. Bradley.
2000. nvestigations of selected parameters for growth of larval and juvenile black sea bass *Centropristis striata* L. J. World Aquac. Soc. 31:426–435.

Brander, K. M.
2005. Cod recruitment is strongly affected by climate when stock biomass is low. ICES J. Mar. Sci. 62:339–343.
Cotton, C. F., R. L. Walker, and T. C. Recicar.
2003. Effects of temperature and salinity on growth of juvenile black sea bass, with implications for aquaculture. North Am. J. Aquac. 65:330–338.
Cullen, H. M., A. Kaplan, P. A. Arkin, and P. B. deMenocal.
2002. Impact of the North Atlantic Oscillation on Middle Eastern climate and streamflow. Climate Change 55:315–338.
Dawe, E. G., E. B. Colbourne, and K. F. Drinkwater.
2000. Environmental effects on recruitment of short-finned squid (*Illex illecebrosus*). ICES J. Mar. Sci. 57:1002–1013.
Drohan, A. F., J. P. Manderson, and D. B. Packer.
2007. Essential fish habitat source document: black sea bass, *Centropristis striata*, life history and habitat Characteristics,. 2nd ed. NOAA Tech. Memo. NMFS-NE-200, 68 p.
Gulland, J. A., and A. A. Rosenberg.
1992. A review of length-based approaches to assessing fish stocks. FAO Fish. Tech. Pap. 323, 100 p. FAO, Rome.
Gwak, W.-S.
2003. Effects of shelter on growth and survival in age-0 black sea bass, *Centropristis striata* (L.). Aquac. Res. 34:1387–1390.
Hecht, T., and S. Appelbaum.
1988. Observations of intraspecific aggression and coeval sibling cannibalism by larval and juvenile *Clarias gariepinus* (Claridae: Pisces) under controlled conditions. J. Zool. 214:21–44.
Heck, K. L., Jr., and R. J. Orth.
1980. Seagrass habitats: the roles of habitat complexity, competition and predation in structuring associated fish and motile macroinvertebrate assemblages. *In* Estuarine perspectives (V. S. Kennedy, ed.), p. 449–464. Academic Press, New York.
IAN (Integration and Application Network).
2015. Coastal Bays report card 2014, 5 p. Integration and Application Network, University of Maryland Center for Environmental Science, Cambridge, MD. [Available at website.]
Kimmel, J. J.
1973. Food and feeding of fishes from Magothy Bay, Virginia. M.S. thesis, 190 p. Old Dominion Univ., Norfolk, VA.
Kolek, D.
1990. Homing of black sea bass, *Centropristis striata*, in Nantucket Sound with comments on seasonal distribution, growth rate, and fisheries of the species, 12 p. Massachusetts Div. Mar. Fish., Pocassett, MA.
Love, J. W., P. Chigbu, and E. B. May.
2009. Environmental variability affects distributions of coastal fish species (Maryland). Northeast. Nat. 16:255–268.
Malagon, H.
2015. Population dynamics of young of the year summer flounder (*Paralichthys dentatus*) in Maryland Coastal Bays. M.S. thesis, 100 p. Univ. Maryland Eastern Shore, Princess Anne, MD.
Mann, K. H., and K. F. Drinkwater.
1994. Environmental influences on fish and shellfish production in the northwest Atlantic. Environ. Rev. 2:16–32.
Miller, A. S., G. R. Shepherd, and P. S. Frantantoni.
2016. Offshore habitat preference of overwintering juvenile and adult black sea bass, *Centropristis striata*, and the relationship to year-class success. PLoS ONE 11(1):e0147627.
Morales-Núñez, A. G., and P. Chigbu.
2016. Life history of *Dulichiella appendiculata* (Amphipoda, Senticaudata, Melitidae) in the Maryland Coastal Bays, USA. Aquat. Biol. 25:75–82.
Moser, J., and G. R. Shepherd.
2009. Seasonal distribution and movement of black sea bass (*Centropristis striata*) in the northwest Atlantic as determined from a mark-recapture experiment. J. Northwest Atl. Fish. Sci. 40:17–28.
Murphy, R. F., and D. H. Secor.
2006. Fish and blue crab assemblage structure in a U.S. mid Atlantic coastal lagoon complex. Est. Coast. 29:1121–1131.
Musick, J. A., and L. P. Mercer.
1977. Seasonal distribution of black sea bass, *Centropristis striata*, in the Mid-Atlantic Bight with comments on the ecology and fisheries of the species. Trans. Am. Fish. Soc. 106:12–25.
O'Brien, M. H. P.
2013. Marine influence on juvenile fish trophic ecology and community dynamics in Maryland's northern coastal lagoons. M.S. thesis, 107 p. Univ. Maryland, College Park, MD.
Parsons, L. S., and W. H. Lear.
2001. Climate variability and marine ecosystems impacts: a North Atlantic perspective. Prog. Oceanogr. 49:167–188.
Pincin, J., M. J. Wilberg, L. Harris, and A. Willey.
2014. Trends in abundance indices of fishes in Maryland's Coastal Bays during 1972–2009. Est. Coast. 37:791–800.
R Core Team.
2015. R: a language and environment for statistical computing. R Foundation for Statistical Computing, Vienna, Austria. [Available from website, accessed April 2015.]
Richards, S. W.
1963. The demersal fish population of Long Island Sound. II. Food of the juveniles from a sand-shell locality (Station 1). Bull. Bingham Oceanogr. Collect. 18:32–72.
Schwartz, F. J.
1961. Fishes of Chincoteague and Sinepuxent Bays. Am. Midl. Nat. 65:384–408.
Steimle, F. W., C. A. Zetlin, P. L. Berrien, and S. Chang.
1999. Essential fish habitat source document: black sea bass, *Centropristis striata*, life history and habitat characteristics. NOAA Tech. Memo. NMFS-NE-143, 42 p.
Tatham, T. R., D. L. Thomas, and D. J. Danila.
1984. Fishes of Barnegat Bay. *In* Ecology of Barnegat Bay, New Jersey (M. J. Kennish and R.A. Lutzs, eds.), p. 241–280. Springer, New York.
U.S. EPA (Environmental Protection Agency).
2006. Maryland Coastal Bays Program. *In* National Estuary Program coastal condition report. EPA/842-B-06/001, p. 179–192. Office of Water, U.S. EPA, Washington, DC. [Available from website.]

Wazniak, C., M. Hall, C. Cain, D. Wilson, R. Jesien, J. Thomas, T. Carruthers, and W. Dennison.
2004a. State of the Maryland coastal bays, 44 p. Maryland Dep. Nat. Resour., Annapolis, MD. [Available from website.]
Wazniak, C. D., D. Wells, and M. Hall.
2004b. The Maryland Coastal Bays ecosystem. *In* Maryland's Coastal Bays: ecosystem health assessment 2004. DNR-12-1202-0009, p. 1.9–1.20. Maryland Dep. Nat. Resour., Annapolis, MD. [Available from website.]
Werme, C. E.
1981. Resource partitioning in a salt marsh fish community. Ph.D. diss., 264 p. Boston Univ., Boston, MA.

National Marine Fisheries Service
NOAA

Fishery Bulletin
established in 1881

Spencer F. Baird
First U.S. Commissioner of Fisheries and founder of *Fishery Bulletin*

Seasonal and regional variation in egg size of the Argentine anchoita (*Engraulis anchoita*) in the southeastern Brazilian Bight

Jana M. del Favero (contact author)[1,3]
Mario Katsuragawa[1]
Fabricio S. C. Oliveira[2]
Nayara C. Tannure[1]
M. L. Zani-Teixeira[1]
Jefferson T. Turner[3]

Email address for contact author: delfaverojana@gmail.com

[1] Instituto Oceanográfico
Universidade de São Paulo
Praça do Oceanográfico, 191
05508-120, São Paulo, SP, Brazil

[2] Instituto de Oceanografia
Universidade Federal do Rio Grande
Avenida Itália km 8
96203-900, Rio Grande, RS, Brazil

[3] School for Marine Science and Technology
University of Massachusetts Dartmouth
706 S. Rodney French Boulevard
New Bedford, Massachusetts 02744-1221

Abstract—Eggs of the Argentine anchoita (*Engraulis anchoita*) are very abundant and frequently collected in research ichthyoplankton tows along the southern–southeastern Brazilian coast. The commercial exploitation of Argentine anchoita has also recently begun in southern Brazil. Therefore, there is a need for a better understanding of the population structure and dynamics of this species in order to manage the fishery for this species. Our objective was to determine seasonal and regional variability in the size of eggs of Argentine anchoita in the southeastern Brazilian Bight (SBB). Because there are no physical barriers in the ocean, defining stock limits for fish populations is difficult, particularly for a semimigratory species such as the Argentine anchoita. Eggs from the south of the SBB were larger than those from the north, indicating that eggs from the northern Santa Marta Cape region probably belong to the *bonaerense* stock. Also, eggs collected during the winter were larger than those collected during the summer. This difference in egg size may be due to either 1) larger adults coming from the south and spawning in or closer to the area sampled during winter, or 2) an adaptive response of spawning females to the changes in the abiotic conditions or 3) a combination of these 2 features.

Manuscript submitted 27 October 2016.
Manuscript accepted 15 August 2017.
Fish. Bull. 115:517–531 (2017).
Online publication date: 1 September 2017.
doi: 10.7755/FB.115.4.8

The views and opinions expressed or implied in this article are those of the author (or authors) and do not necessarily reflect the position of the National Marine Fisheries Service, NOAA.

Most marine fish eggs are identified by their size, shape and pigment characters, but many newly fertilized eggs are unpigmented and therefore egg diameter is the most distinguishing feature (Bagenal, 1971). Automated identification of fish eggs, based on their size and shape (Favero et al., 2015) is possible; however, egg size varies among species, among populations, and within populations of the same species owing to temporal, spatial, biological, and environmental factors (e.g., Phonlor, 1984; Wootton, 1990; Chambers and Waiwood, 1996; Llanos-Rivera and Castro, 2004). In addition to identification of fish eggs, it is important to understand variation in egg sizes because larger eggs typically hatch into larger larvae with the possibility of conferring a higher survival potential on the resulting offspring (e.g., Blaxter and Hempel, 1963; Blaxter and Hunter, 1982; Marteinsdottir and Able, 1992).

The Argentine anchoita (*Engraulis anchoita*) (Engraulidae: Clupeiformes) is a small pelagic fish, which is important as a secondary consumer near the bottom of the food chain, and is an essential prey for other fish species, marine mammals, and seabirds (Castello, 2007). It is economically important to the Argentine and Uruguayan fishery fleets (FAO, 2014), and exploitation of Argentine anchoita has recently begun in southern Brazil (Carvalho and Castello, 2013). This species is widely distributed over the continental shelf of the southwest Atlantic, from Vitoria, Brazil (20°S) to Gulf San Jorge, Argentina (48°S) (Castello, 2007). There are 3 distinct stocks: the *patagonic* (48–41°S), the *bonaerense*

(41–27°S) and a third, ranging from 27°S and 20°S, is known as the "Brazilian Southeastern Bight stock" (Carvalho and Castello, 2013). Different methods have been used to identify the 3 stocks: to distinguish the *patagonic* from the *bonaerense*, Hansen (1994) used growth rates, size–weight relationships and length at first maturation; Castello and Castello (2003) compared larval growth and length at first feeding from southeastern and southern Brazil; and Carvalho and Castello (2013) analyzed size and age composition and length-at-age data and concluded that anchovies from the Santa Marta Region (30–27°S) should be considered as a part of the *bonaerense* stock. Although the parameters used cannot reveal the genetic discreteness of these stocks, they are still powerful tools for stock identification purposes (Begg, 2005).

No study dedicated specifically to variation in egg size of the Argentine anchoita has been conducted in the southeastern Brazilian Bight (SBB; roughly between 22°S and 28°S). A few studies have focused off the southern coast of Brazil, and the coasts of Uruguay and Argentina (Ciechomski, 1973; Phonlor, 1984), but they cover only the *bonaerense* stock. Therefore, our objective was to evaluate seasonal and regional variability in the size of eggs of Argentine anchoita in the SBB, and to consider factors that may cause such variation.

Materials and methods

Study area

The Brazil Current flows southward along the continental slope of the SBB (Silveira et al., 2000) transporting warm and saline Tropical Water in the upper mixed layer and cold South Atlantic Central Water (SACW) at the pycnocline. An additional water mass exists in the neritic zone, the warm Coastal Water, with lower salinity than the Tropical Water (Castro Filho and Miranda, 1998). Except for some coastal areas that are under the influence of waters flowing from large embayments, such as Guanabara Bay in the state of Rio de Janeiro, oligotrophic conditions prevail in the study area owing to the dominance of Tropical Water in the upper layers, and oceanic nutrients trapped within the SACW (Lopes et al, 2006).

The intermittent coastal upwelling off Cape Frio is an important process that brings the nutrient-rich SACW into the euphotic zone (Valentin et al., 1987). These SACW intrusions vary seasonally, advancing toward the coast during spring and summer and retreating toward the shelf break in the autumn and winter (Cerda and Castro, 2014). Another physical process that fertilizes the euphotic zone occurs during the winter, when subantarctic and the Plata River Plume waters are driven northward by southerly winds from the continental shelf of Argentina and Uruguay into most of the inner shelf in the south of Brazil and even the SBB (Brandini 1990; Stevenson et al., 1998; Piola et al., 2000; Gaeta and Brandini, 2006; Piola et al., 2008a; Piola et al., 2008b).

To address the possible role of spatial (regional) and temporal (seasonal) variation in egg size of Argentine anchoita, we used data collected from 2 different sets of research cruises: for the regional variation, the study area comprised most of the SBB, between Cape Frio, in the state of Rio de Janeiro, and Cape Santa Marta Grande, in the state of Santa Catarina (roughly between 23°S and 28°S). For the seasonal variation, the study was carried in the northern part of the SBB, from off Cape São Tomé (22ºS) to São Sebastião Island (24ºS), in the state of São Paulo during the summer and winter of 2001 and 2002 (Fig. 1).

In situ data

To assess the seasonal variation in egg size of Argentine anchoita, we took advantage of biotic and abiotic data obtained from a set of 4 oceanographic cruises carried out during the summer and winter of 2001 and 2002. During both seasons of 2001, only one transect was performed in the Cape Frio region, but some sampling stations were sampled twice. Summer of 2002 covered 14 transects and winter of 2002 included 13 transects (Table 1, Fig. 1).

In order to address patterns in the spatial variation in egg size of Argentine anchoita, data were obtained from another set of cruises conducted during the summers over 5 years (1975, 1988, 1990, 1991, and 1993; Table 1) and the SBB was divided into 3 areas: area 1 from Cape São Tomé to São Sebastião Island; area 2 from São Sebastião Island to Paranaguá Bay; and area 3 from Paranaguá Bay to Cape Santa Marta Grande (Fig. 1). These areas were defined on the following bases: 1) Argentine anchoita stock identification as defined by Carvalho and Castello (2013) (area 3); 2) oceanographic conditions described by Miranda and Katsuragawa (1991) and Mahiques et al. (2004) (area 1 and area 2); 3) a spawning map obtained by Favero et al. (2017), so that the divisions would not separate any important spawning area.

Temperature and salinity data were obtained from Nansen bottles and reversing thermometers in 1975 and 1988. In the other 3 years, a conductivity, temperature, and depth (CTD) profiler, an SBE 917*plus*[1] (Sea-Bird Scientific, Bellevue, WA), was used to collect this information.

As described by Smith and Richardson (1977), a bongo net with a 0.61-m diameter mouth opening was used to sample ichthyoplankton. It was equipped with paired cylindrical-conical 0.333-mm and 0.505-mm mesh-size nets and with a flowmeter attached at the center of the mouth opening of each net in order to measure the volume of filtered water. The net was towed obliquely from the surface to the maxi-

[1] Mention of trade names or commercial companies is for identification purposes only and does not imply endorsement by the National Marine Fisheries Service, NOAA.

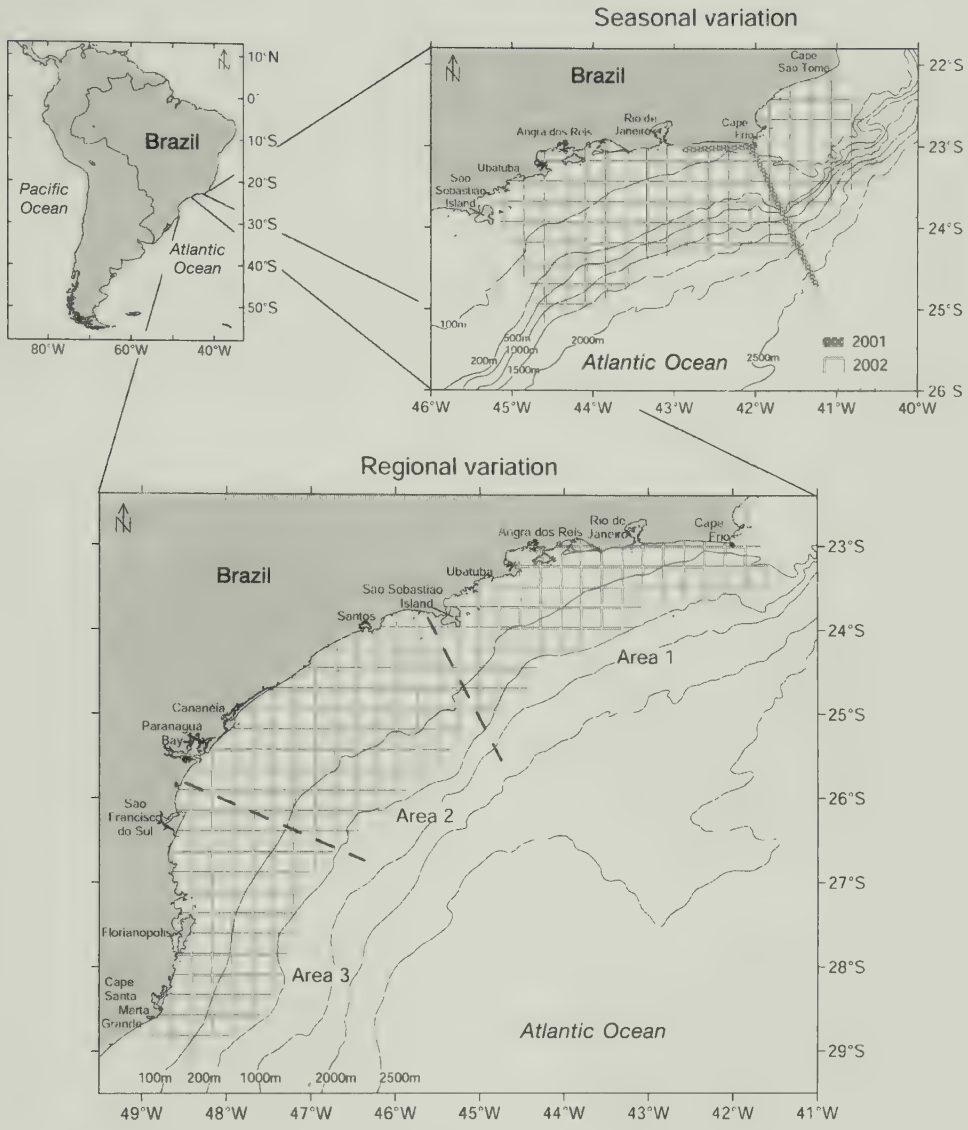

Figure 1

Maps of the study areas for our investigation of variation in egg size of Argentine anchoita (*Engraulis anchoita*): (upper right) area of the northern part of the southeastern Brazilian Bight sampled in 2001 and 2002 was used for the seasonal variation analyses, and (bottom) area of the nearly entire Southeastern Brazilian Bight sampled and divided into 3 areas, in 1975, 1988, 1990, 1991, and 1993, was used for the regional variation analyses. The 3 areas were those of Cape Frio to São Sebastião Island (area 1), São Sebastião Island to Paranaguá Bay (area 2), and Paranaguá Bay to Cape Santa Marta Grande (area 3).

mum depth possible, which did not exceed 200 m. If a sampling station was shallower than 60 m, the bongo net was lowered twice close to the bottom, increasing the volume of water filtered. Towing speed was about 2.8–3.7 km/h. We analyzed only the samples from the 0.333-mm mesh size net and that had been preserved at sea in 4% buffered formalin in seawater. All samples were archived in the Biological Collection "Prof. E. F. Nonato" (ColBIO) of the Oceanographic Institute, University of São Paulo, Brazil.

Eggs of Engraulidae were sorted on the basis of their ellipsoid shape, segmented yolk, and usually, absence of oil droplets (Ciechomski, 1965; Phonlor, 1984) and then imaged by using a digital camera attached to a stereomicroscope. Their major and minor axes were measured from the photographs by using the image-analysis program ImageJ2 (Schindelin et al., 2015) and egg volume was calculated by following the method of Vanzolini (1977). Finally, eggs of Argentine anchoita were identified by their morphometric characteristics

Table 1

Start and end dates for oceanographic cruises and number of sampling stations (N) used as data sources for analyses of seasonal and regional variation in egg sizes of Argentine anchoita (*Engraulis anchoita*) in the southeastern Brazilian Bight.

Oceanographic cruise	Date		N
	Start	End	
Seasonal			
Deproas I	2/7/01	2/13/01	19
Deproas II	7/12/01	7/19/01	17
Deproas III	1/5/02	1/24/02	72
Deproas IV	8/3/02	8/21/02	66
Regional			
FINEP I	11/29/75	12/18/75	140
EPM Sardinha	1/10/88	1/30/88	78
V. Hensen/JOPS	12/28/90	1/11/91	89
Sardinha I	12/8/91	12/18/91	110
Sardinha II	1/9/93	1/18/93	108

by using discriminant analysis, as described by Favero et al. (2015). Only a subsample of about 100 eggs per sampling station was measured.

Satellite data

Sea-surface temperature (SST) corresponds with level-3 gridded images obtained from the advanced very high resolution radiometer (AVHRR) on board NOAA satellites and processed by the Pathfinder Project. The Pathfinder data set is the result of a collaboration between the NOAA National Oceanographic Data Center and the University of Miami Rosenstiel School of Marine and Atmospheric Science, and is distributed at NASA's Physical Oceanography Distributed Active Archive Center (AVHRR Pathfinder Level 3 Daily SST, vers. 5: daytime, PODAAC-PATHF-DYD50, website, and nighttime, PODAAC-PATHF-DYN50, website, accessed December 2015) on a global scale, with a linear gridded projection, and within a spatiotemporal resolution of 4 km×4 km×1 month. Day and night-time data were used to compute SST monthly means. Surface chlorophyll-*a* concentration (CHL) was acquired by level-3 mapped images obtained from the Sea-viewing Wide Field-of-view Sensor on board the SeaStar satellite. These data were processed by the NASA Goddard Space Flight Center by using the Ocean Chlorophyll 4 algorithm, vers. 4 (O'Reilly et al., 2000), and distributed at NASA's Ocean Color Web (chlor_a, website, accessed December 2015) on a global scale, with cylindrical equidistant projection, and a spatiotemporal resolution of 9 km×9 km×1 month. Because the CHL is logarithmically distributed within the oceans, we chose to work with the log10-transformed CHL. We used monthly means of SST and surface CHL to characterize the typical summer and winter scenarios of 2001 and 2002, to correspond with the periods when the cruises were undertaken (Table 1). Monthly means were chosen to represent our study area for 2 reasons: 1) monthly means serve as a low-pass filter that removes high-frequency external processes that could be involved in the variability of SST and surface CHL (e.g., processes driven by the atmosphere), and 2) unlike the averages for the specific days of the cruises, monthly means include processes with a lag between their cause and effect (e.g., the time lag between the supply of nutrients to the upper ocean and the growth of primary production for a given area).

Data analyses

Egg abundance was calculated as

$$N=(x \times d)/V \text{ (Tanaka, 1973)},$$

where N = egg abundance (number of eggs per square meter at each sampling station);
x = the number of eggs sampled;
d = the maximum depth sampled in meters; and
V = the volume of water filtered in cubic meters.

The mean abundance was calculated for all the sampling stations, not just for those where eggs were collected. The calculation of the frequency of egg occurrence was based on Guille (1970).

One-way analysis of variance was used to test the differences in the egg major and minor axes, egg volumes, temperature, and salinity (at 10-m depth), when compared by season (winter and summer) and by area (areas 1, 2 and 3) within each year. A posteriori Tukey's honest significant difference test was performed in order to find means that were significantly different from each other. Temperature–salinity diagrams in relation to egg volume from ichthyoplankton tows were plotted to infer the distribution of egg sizes for Argentine anchoita with respect to water mass for each year, area, and season. We used the 10-m measurement for the abiotic data because the eggs of anchovies mainly occur close to the surface, in the upper 20 m (Tanaka, 1992; Sabatés et al., 2008). R software, vers. 3.2.1(R Core Team, 2015) was used for these analyses.

Results

Seasonal variation

Oceanographic conditions Mean seawater temperature measured at a depth of 10 m varied significantly within each period analyzed (F=8.732, df=3, P<0.01). Mean summer temperatures were higher than those of winter for both years, but the lowest individual temperature values were measured during summer (Table 2), owing to the SACW intrusion that occurred in both years surveyed, 2001 and 2002 (Goçalo et al., 2011; Araújo, 2013). The standard deviation (SD) in temperature pro-

Table 2

Mean, with standard deviation (SD), and the range of temperature (°C; Temp.) and salinity (Sal.) values measured at a 10-m depth during summer and winter of 2001 and 2002 in the northern area of the southeastern Brazilian Bight. Results are given from analysis of variance (ANOVA) and a posteriori Tukey's honestly significant difference (HSD) test that compared means between the summer and winter of 2001 and 2002. S01=summer 2001; W01=winter 2001; S02=summer 2002; W02=winter 2002.

		Period				ANOVA		Tukey's HSD (*P*)	
		Summer 2001	Winter 2001	Summer 2002	Winter 2002	*F*	*P*	S01 vs. W01	S02 vs. W02
Temp.	Mean (SD)	24.65 (3.18)	22.77 (0.62)	23.79 (2.86)	22.32 (1.21)	8.732	<0.01	0.009	0.001
	Range	14.70–27.65	22.17–24.72	14.88–27.08	16.50–24.44				
Sal.	Mean (SD)	36.83 (0.42)	36.04 (0.53)	36.08 (0.69)	35.58 (1.04)	15.13	<0.01	0.002	0.003
	Range	35.73–37.48	35.14–37.14	34.67–37.01	33.16–37.37				

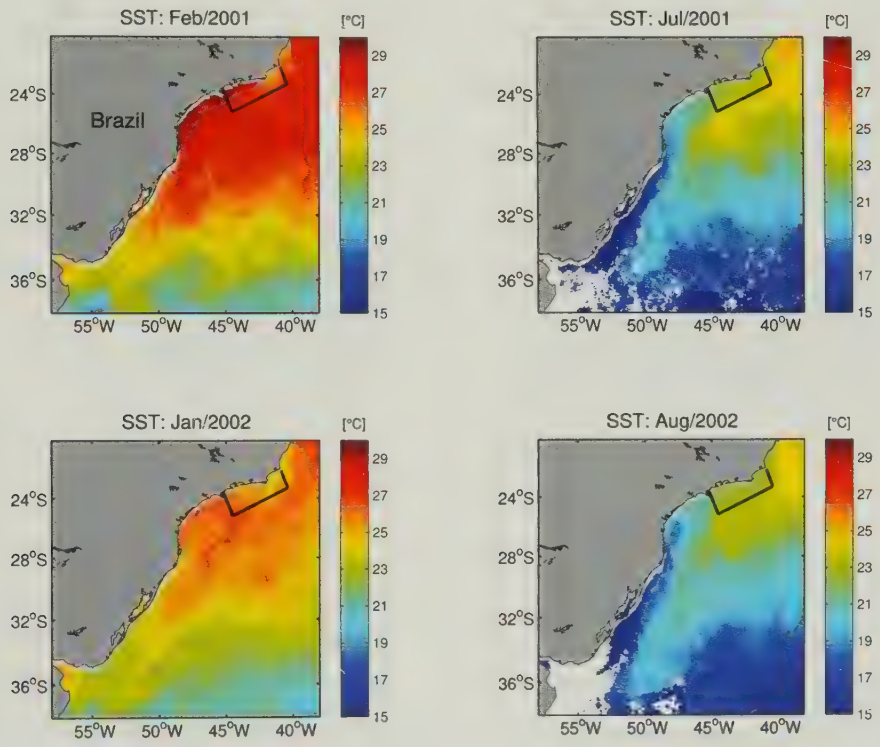

Figure 2

Horizontal distribution of sea-surface temperature (SST, °C), based on satellite data, during the winter (February or January) and summer (July or August) of 2001 and 2002 in the southwestern Atlantic Ocean off Brazil. The black line highlights the northern part of the southeastern Brazilian Bight that was the study area in 2002.

vided another indicator of SACW intrusion, which was greatest in summer for both years. Mean salinity at a depth of 10 m also varied significantly within the periods analyzed (F=15.13, df=3, P<0.01), with summer values higher than winter values in both years (Table 2).

The SST fields of the southwestern Atlantic showed strong thermal gradients in summer as a consequence of the mixing of relatively warmer waters from the Brazil Current and colder waters transported by the Malvinas Current from the south. Strong thermal gradients were also observed during winter but those were restricted to the Brazilian coast because of a northward advection of colder coastal waters coming from higher latitudes over the continental shelf and the weakening of the Brazil Current. No colder coastal waters coming from the south were observed in summer close to the study area (Fig. 2).

Table 3

Number of eggs of Argentine anchoita (*Engraulis anchoita*) sampled (*N*), frequency of occurrence (FO), and mean and standard deviation (SD) values of abundance, egg volume, egg major axis, and egg minor axis, obtained during summer and winter of 2001 and 2002 in the northern area of the Southeastern Brazilian Bight. Results are given from analysis of variance (ANOVA) and a posteriori Tukey's honestly significant difference (HSD) test which compared egg-size values from the summer and winter of 2001 and 2002. S01=summer 2001; W01=winter 2001; S02=summer 2002; W02=winter 2002.

	Period				ANOVA		Tukey's HSD (*P*)	
	Summer 2001	Winter 2001	Summer 2002	Winter 2002	*F*	*P*	S01 vs. W01	S02 vs. W02
N	99	56	9904	430				
FO (%)	4.27	26.96	27.78	18.18				
Abundance (eggs/m^2)	1.9 (9.3)	0.7 (1.5)	32.8 (148.8)	1.4 (5.5)				
Volume (mm^3)	0.142 (0.015)	0.206 (0.018)	0.177 (0.020)	0.206 (0.021)	415.4	<0.01	0.000	0.000
Major axis (mm)	1.031 (0.047)	1.138 (0.047)	1.106 (0.053)	1.140 (0.052)	133.2	<0.01	0.000	0.000
Minor axis (mm)	0.512 (0.026)	0.587 (0.022)	0.552 (0.023)	0.587 (0.025)	429.8	<0.01	0.000	0.000

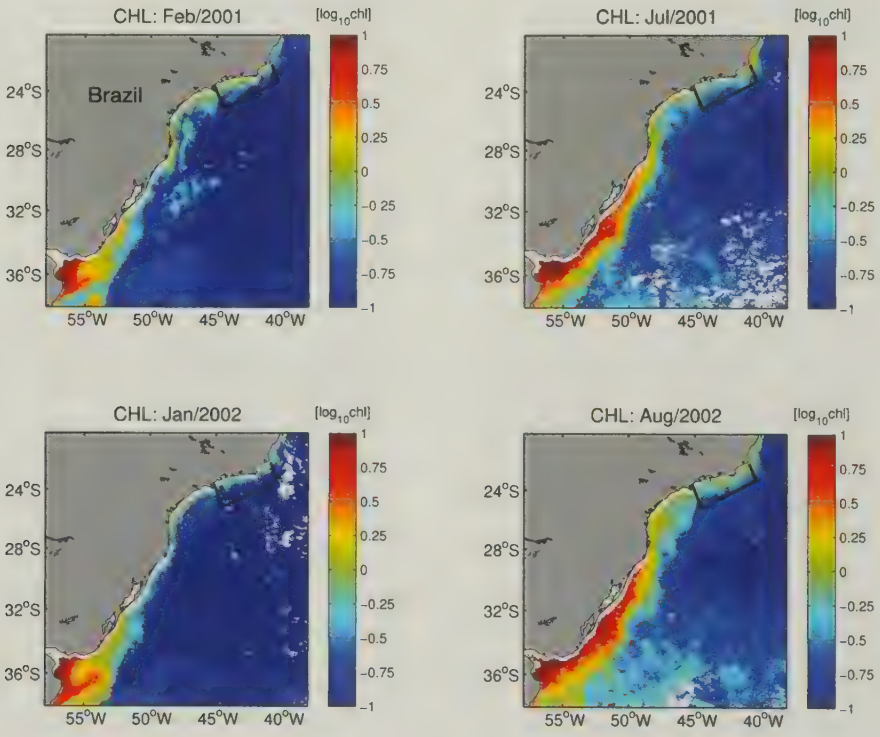

Figure 3

Horizontal distribution of the log10-transformed surface chlorophyll-*a* concentration (CHL, mg/m^3), determined from satellite data, during the winter (February or January) and summer (July or August) of 2001 and 2002 in the southwestern Atlantic Ocean off Brazil. The black line highlights the northern part of the southeastern Brazilian Bight that was the study area in 2002.

The highest values of the surface CHL were observed close to the estuary of the Plata River (around 36°S) in summer. During the winter of both years the high CHL spread from the Plata River to the southernmost region of the SBB, reaching latitudes of about 28°S (Fig. 3).

Further information about water column stratification, water mass intrusions, and horizontal distribution of the SST for the same area and period studied was described by Goçalo et al. (2011) and Namiki et al. (2017).

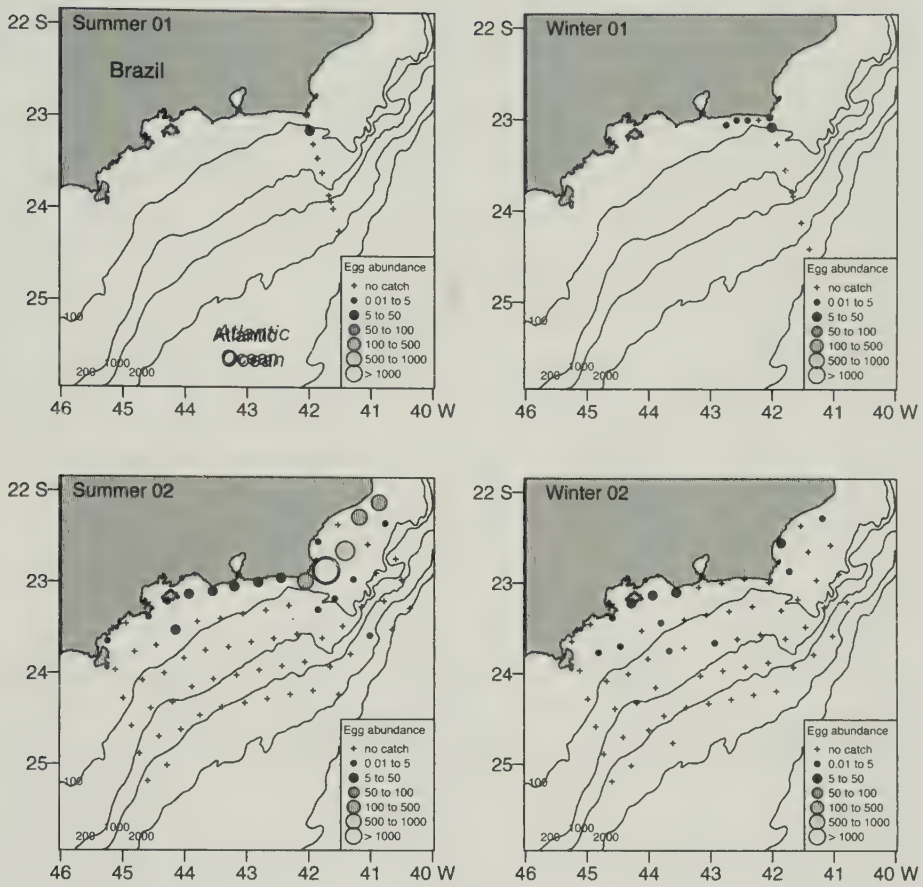

Figure 4

Spatial distribution of abundance of eggs (eggs/m^2) of Argentine anchoita (*Engraulis anchoita*) sampled in the northern part of the southeastern Brazilian Bight with ichthyoplankton tows during summer and winter of 2001 and 2002.

Seasonal variation in eggs A total of 10,710 eggs of Engraulidae were sampled. Eggs of Argentine anchoita represented 98.6% of all eggs sampled (n=10,489) and they were more abundant during the summers of both years (Table 3).

During the summer of 2001, on the only transect sampled, eggs occurred at only one sampling station close to the coast. During the winter of 2001 eggs were collected at 7 stations, all close to the coast (Fig. 4). During the summer of 2002, eggs of Argentine anchoita were more abundant at Cape Frio and Cape São Tomé, in the north of the area sampled. Conversely, during the winter, these eggs were much less abundant, and were frequently found in the southern part of the area sampled (Fig. 4).

Eggs of Argentine anchoita experienced large variations in temperature and salinity and were collected within the entire range of temperature and salinity values that characterized the 3 water masses occurring in the study areas. Low numbers of eggs were found in waters with a salinity higher than 36.5 (Fig. 5). Stations with higher mean egg volume occurred during the winter and when temperatures were lower (Fig. 5).

Of the total number of eggs of Argentine anchoita that were collected, 2794 were measured. Volume, major axis and minor axis mean values were significantly different in comparisons of eggs from summer and winter of 2001 and 2002 (Table 3). Eggs were larger in winter than in summer for both years. A posteriori Tukey's tests showed that when only comparing both winters, the egg-size mean values were not significantly different (volume: P=0.994; major axis: P=0.991; minor axis: P=0.999) (Table 3).

Regional variation

Oceanographic conditions Temperature and salinity varied among the 3 areas analyzed during each year, except in January 1988, when no significant difference in salinity was found (Table 4). During January of 1988 there was a weak SACW intrusion at Cape Frio (located in area 1) (Fig. 6), represented by the lowest SD in temperature calculated for this area. Area 1 was usually the coldest and saltiest area, owing to the stronger SACW intrusions in this area. Temperature and salinity values were not significantly different between areas 2 and 3 (Table 4).

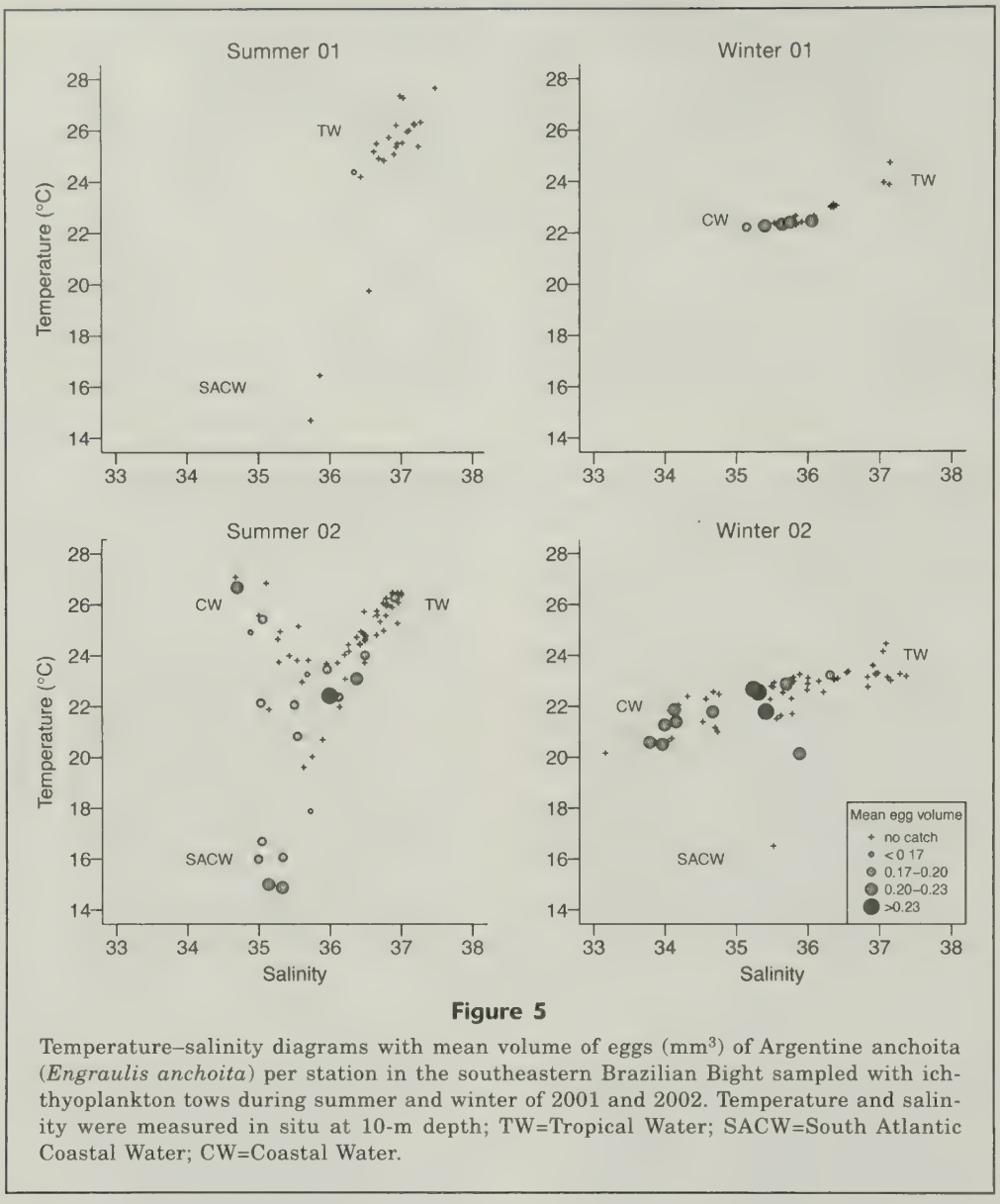

Figure 5

Temperature–salinity diagrams with mean volume of eggs (mm^3) of Argentine anchoita (*Engraulis anchoita*) per station in the southeastern Brazilian Bight sampled with ichthyoplankton tows during summer and winter of 2001 and 2002. Temperature and salinity were measured in situ at 10-m depth; TW=Tropical Water; SACW=South Atlantic Coastal Water; CW=Coastal Water.

Regional variation in eggs A total of 73,104 eggs of Engraulidae were collected. Argentine anchoita eggs represented 80.5% of all engraulid eggs sampled (n=58,826). They were sampled throughout the SBB, and their spatial horizontal distribution varied from one year to another (Fig. 7). Eggs of Argentine anchoita were collected over a wide range of temperatures and salinities in each area (Fig. 8).

A total of 8809 eggs of Argentine anchoita that were collected during the summer over 5 years and in all 3 areas were measured (Table 5). In a comparison of only areas 1 and 3, it was observed that, in general, eggs in area 3 were larger than eggs in area 1, with the exception of January 1988 when the opposite was found to be true. No size pattern was observed for eggs collected in area 2; egg sizes from this area were usually in between those of areas 1 and 3 and showed no significant differences in size when compared with eggs from other areas. During December of 1991 and January of 1993, eggs from area 2 were the largest sizes throughout the time period (Table 5, Fig. 8).

Discussion

Egg size varies among species and among populations because of temporal, biological, spatial, or environmental factors (or a combination of these factors). Within a species, planktonic egg size decreases as the spawning season progresses (Bagenal, 1971; Chambers and Waiwood, 1996). For species of Clupeiformes, this decrease in the egg size may be due to a reduction in maternal energy reserves over the spawning season, a switch in the stored energy from reproduction to

Table 4

Mean and standard deviation values of temperature (Temp. °C) and salinity (Sal.) and results from analysis of variance (ANOVA) and a posteriori paired Tukey's honestly significant difference (HSD) test that compared data from the 3 areas sampled (areas 1, 2, and 3) in the southeastern Brazilian Bight during the 5 years studied (December 1975, January 1988, December 1990, December 1991, and January 1993). *N* is the number of sampling stations considered. The 3 areas were from Cape Frio to São Sebastião Island (area 1), from São Sebastião Island to Paranaguá Bay (area 2), and from Paranaguá Bay to Cape Santa Marta Grande (area 3).

	Area			ANOVA		Tukey's HSD		
	1	2	3	*F*	*P*	2 vs. 1	3 vs. 1	3 vs. 2
Dec 75								
N	53	44	43					
Temp.	22.06 (2.17)	23.76 (0.97)	23.47 (0.87)	17.72	<0.01	0	0	0.65
Sal.	35.99 (0.67)	35.30 (0.76)	35.49 (0.94)	9.76	0	0	0	0.51
Jan 88								
N	24	35	19					
Temp.	24.16 (1.37)	26.40 (1.34)	25.40 (2.93)	10.41	0	0	0.08	0.15
Sal.	35.41 (0.33)	35.22 (0.60)	35.14 (0.73)	1.27	0.29			
Dec 90								
N	25	40	24					
Temp.	22.71 (1.92)	24.81 (0.56)	24.12 (2.78)	10.44	<0.01	0	0.02	0.31
Sal.	35.95 (0.63)	34.84 (0.63)	34.74 (0.86)	24.37	<0.01	0	0	0.86
Dec 91								
N	33	48	29					
Temp.	20.34 (2.94)	24.47 (1.91)	24.15 (1.86)	36.11	<0.01	0	0	0.81
Sal.	36.25 (0.70)	35.49 (0.68)	35.54 (0.52)	24.11	<0.01	0	0	0.06
Jan 93								
N	32	47	29					
Temp.	21.33 (3.33)	25.13 (1.79)	24.55 (2.82)	21.11	<0.01	0	0	0.62
Sal.	36.01 (0.55)	35.12 (0.59)	34.91 (0.47)	36	<0.01	0	0	0.25

growth, seasonal changes in the age structure of the spawning populations, changes during oogenesis that are correlated with some environmental conditions (e.g., temperature, photoperiod, and food supply) (Blaxter and Hunter, 1982; Chambers, 1997) or a co-occurrence of these factors, as suggested by Llanos-Rivera and Castro (2004) for eggs of anchoveta (*Engraulis ringens*) off the Chilean coast. Ciechomski (1973), who reported that the volume of eggs of Argentine anchoita off the Argentinian and Uruguayan coast decreased 23% throughout the spawning season, probably owing to multiple spawning or length composition of the spawners (or both) correlated with the differences in growth rate in relation to temperature.

Egg size increases with latitude, as shown by Llanos-Rivera and Castro (2004) who studied anchoveta from Chile and by Ciechomski (1973), who showed that egg size of Argentine anchoita increased from the north (35–36°S) to the south (40–41°S) and that this increase was not correlated with temperature or salinity because both parameters were similar throughout the area sampled. Egg size typically varies inversely with temperature and salinity, as has been shown for European anchovy (*Engraulis encrasicolus*) by Demir (1974) and for Argentine anchoita by Phonlor (1984). In our results, area 1, which usually exhibited the lowest temperature and highest salinity values, was the area that had the smallest eggs in 4 out of 5 years sampled. The exception occurred in January 1988, when the largest eggs were collected in that area. January 1988 was also a period of a weak SACW intrusion at Cape Frio (Fig. 6), which is reflected by greater temperature variability (SD, Table 4). Temperatures and salinities were similar throughout the 3 areas during this period in 1988. Conversely, in area 3 the highest temperature and lowest salinity values were found, and this area usually had the largest eggs. It is important to highlight that area 3 encompasses most of the *bonaerense* stock, whereas area 1 contains only the Brazilian Southeastern Bight stock. According to Carvalho and Castello (2013), who analyzed fewer samples than we did, the boundary between the Brazilian Southeastern Bight stock and the *bonaerense* stock (~27°S) is not well defined. Because the geographic limits of each stock are not clear, and the eggs from area 2 exhibited no consistent pattern, with the largest eggs in some samples, or with egg sizes exhibiting no significant differences between area 1 or area 3, area 2 was considered a transition zone, and will not be considered further in this discussion.

Individual Argentine anchoita from southeastern Brazil (22–27°S) were shorter at comparable ages than

Table 5

Mean and standard deviation values of the major axis (mm), minor axis (mm), and volume (mm^3) of eggs of Argentine anchoita (*Engraulis anchoita*) obtained in the southeastern Brazilian Bight in December 1975, January 1988, December 1990, December 1991 and January 1993 and results from analysis of variance (ANOVA) and a posteriori paired Tukey's honestly significant difference (HSD) test that compared data from the 3 areas sampled (areas 1, 2, and 3) during the 5 years studied. The 3 areas were from Cape Frio to São Sebastião Island (area 1), from São Sebastião Island to Paranaguá Bay (area 2), and from Paranaguá Bay to Cape Santa Marta Grande (area 3). *N* is the number of eggs measured.

	Area			ANOVA		Tukey's HSD		
	1	2	3	*F*	*P*	2 vs. 1	3 vs. 1	3 vs. 2
Dec 75								
N	437	139	322					
Major axis	1.022 (0.06)	1.021 (0.06	1.037 (0.05)	7.58	<0.01	0.99	0	0.01
Minor axis	0.523 (0.03)	0.515 (0.02)	0.533 (0.03)	26.36	<0.01	0.01	0	0
Volume	0.147 (0.02)	0.142 (0.02)	0.155 (0.02)	22.62	<0.01	0.06	0	0
Jan 88								
N	532	1123	398					
Major axis	1.111 (0.06)	1.066 (0.05)	1.077 (0.05)	124.1	<0.01	0	0	0
Minor axis	0.548 (0.03)	0.551 (0.03)	0.536 (0.03)	32.57	<0.01	0.19	0	0
Volume	0.176 (0.02)	0.171 (0.03)	0.163 (0.03)	33.41	<0.01	0	0	0
Dec 90								
N	249	400	651					
Major axis	1.096 (0.06)	1.114 (0.05)	1.121 (0.05)	18.33	<0.01	0	0	0.09
Minor axis	0.553 (0.03)	0.560 (0.03)	0.566 (0.03)	19.13	<0.01	0.01	0	0
Volume	0.177 (0.03)	0.184 (0.03)	0.189 (0.02)	22.97	<0.01	0	0	0
Dec 91								
N	132	544	557					
Major axis	1.052 (0.05)	1.044 (0.06)	1.043 (0.06)	1.33	**0.26**			
Minor axis	0.511 (0.03)	0.534 (0.03)	0.526 (0.03)	30.68	<0.01	0	0	0
Volume	0.145 (0.02)	0.157 (0.03)	0.152 (0.02)	16.77	<0.01	0	0	0
Jan 93								
N	391	1583	1351					
Major axis	1.066 (0.06)	1.077 (0.05)	1.053 (0.05)	74.40	<0.01	0	0	0
Minor axis	0.533 (0.03)	0.564 (0.04)	0.545 (0.03)	223.30	<0.01	0	0	0
Volume	0.160 (0.02)	0.184 (0.02)	0.164 (0.02)	219.30	<0.01	0	0	0

those from southern Brazil (30–35°S) (Carvalho and Castello, 2013). The southern region also exhibited a more diverse age composition, with older individuals ranging up to age 4, whereas the southeastern region had a predominance of 1-year-old anchovies (Carvalho and Castello, 2013). In relating sizes of females to eggs, 2 possibilities can occur: 1) larger females produce larger eggs (e.g., Ciechomski, 1966) or, 2) relative fecundity is higher in larger females (e.g., Pájaro et al., 1997). Knowing that the individuals from the *bonaerense* stock are larger than those making up the southeastern stock, it is possible to infer that eggs from area 3 would be larger than those from area 1 as a result of the differences in the composition of the respective maternal stocks.

In the SBB, the Argentine anchoita spawns yearround and peak spawning occurs during late spring and early summer (Matsuura et al., 1992). The Argentine anchoita is a semimigratory species that carries out trophic and reproductive migrations (Ciechomski, 1973) and no physical barriers exist that would prevent individual fish from moving between areas. During the austral winter, adults of Argentine anchoita migrate from Uruguayan and Argentinean waters off the Plata River (35–34°S) to Brazilian waters (34–29°S) where favorable spawning and feeding conditions prevail. They return southward in late spring (Lima and Castello, 1995). Even though our study area was north of the one described by Lima and Castello (1995), there is an equatorward flow of the colder and fresher Plata plume water in the inner shelf (Piola et al., 2008a; Piola et al., 2008b). This flow can transport biota of benthic and planktonic origin, such as species of Foraminifera, ostracods, and microbivalves, from cold and temperate waters to a tropical bay located at around 23°S (Stevenson et al., 1998). In addition, the Plata River estuarine front is well documented as an important area for feeding for Argentine anchoita because

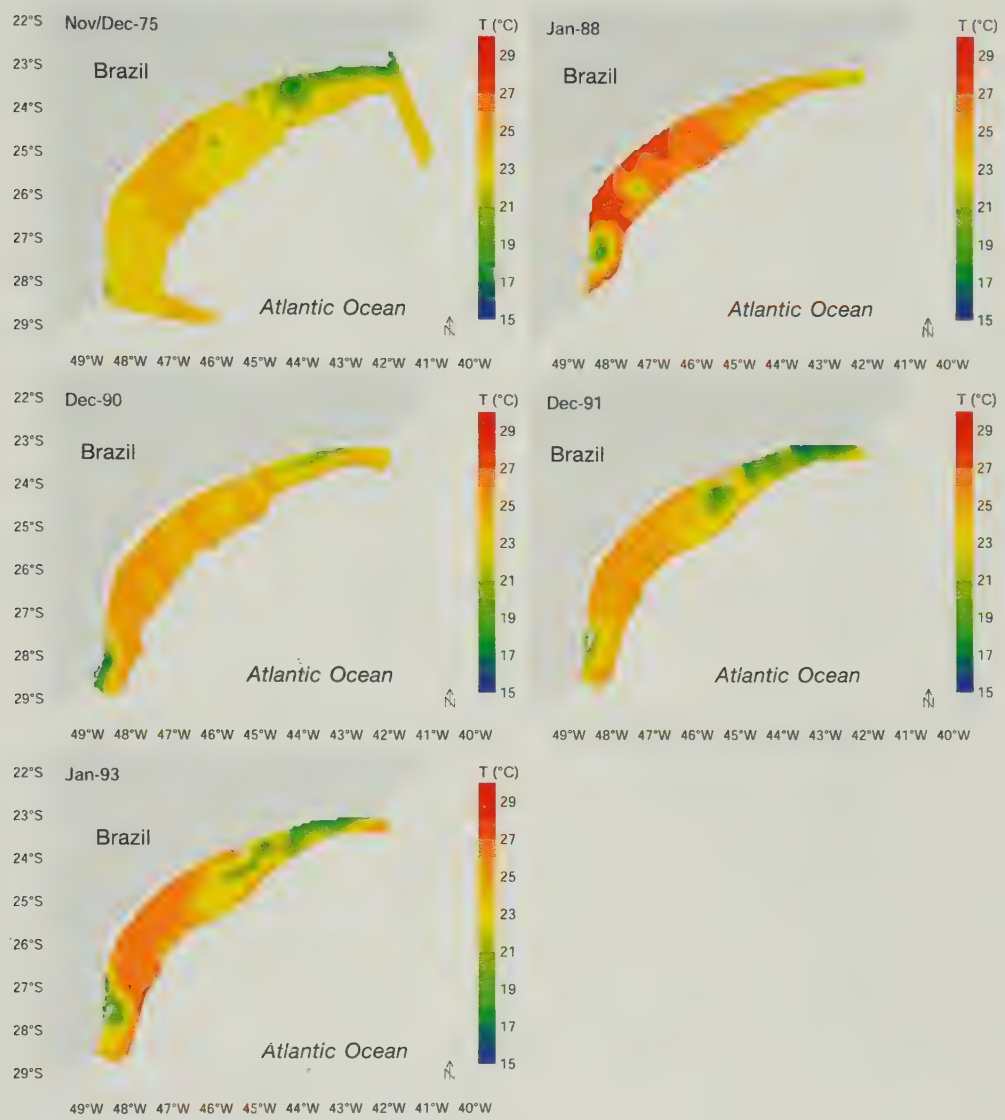

Figure 6

Horizontal distribution of temperature (°C) at a 10-m depth from in situ measurements taken during cruises conducted in the southeastern Brazilian Bight in 1975, 1988, 1990, 1991, and 1993.

the highest stomach fullness values were found at stations close to the surface salinity front (Padovani et al., 2011).

The satellite images in Figures 2 and 3 probably indicate the flow of Plata plume water carrying chlorophyll from the south to the north during the winter on the inner shelf. This flow could be guiding the migration of the Argentine anchoita northward, which also happens during the winter. Because the eggs collected during the winter are larger than those from the summer, one possibility for this difference is that larger adults coming from the south would be spawning in or closer to the study area in winter, but no conclusion can be made with the data from this study because there have been no studies in which the length and age structure of Argentine anchoita have been compared during different seasons in the SBB, nor have there been any genetic studies to differentiate the stocks of this species.

Seasonal variation in egg size may also be an adaptive response to the changes in the abiotic conditions that the eggs will encounter. An increase in temperature decreases the incubation period (time from fertilization to hatching), and a decrease in egg size decreases the incubation period (Wootton, 1990). In our results, temperature and salinity were higher during the summer than during winter for both years and, as expected, the eggs were smaller. Smallest eggs in populations spawning during the summer were also observed in the Atlantic herring (*Clupea*

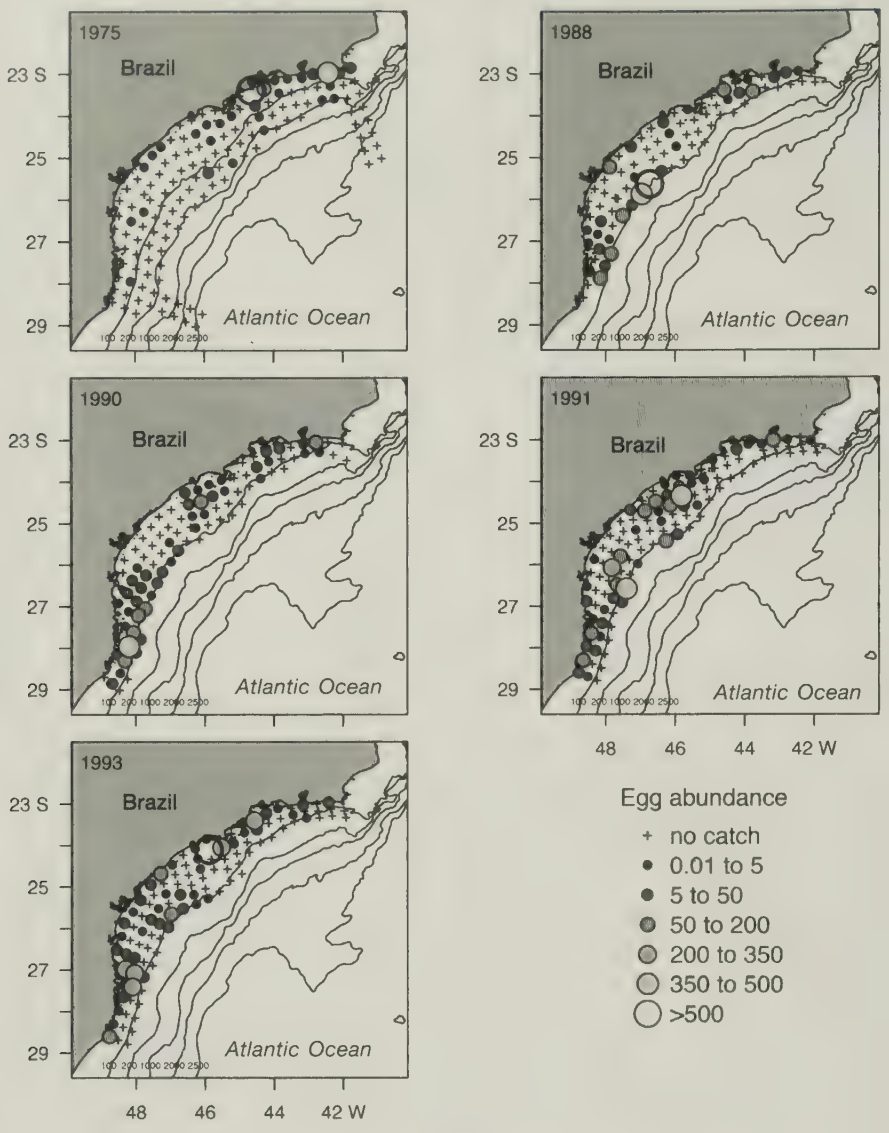

Figure 7

Spatial distribution of abundance of eggs (eggs/m²) of Argentine anchoita (*Engraulis anchoita*) sampled in the southeastern Brazilian Bight with ichthyoplankton tows during 1975, 1988, 1990, 1991, and 1993.

harengus) in the North Atlantic (Blaxter and Hempel, 1963).

The regional variations in the egg size of Argentine anchoita were probably a result of the differences in the stocks analyzed, whereas the reasons behind these seasonal variations remain unknown. At least 2 possibilities exist that would explain the observed seasonal variation in egg size of Argentine anchoita: differences in the maternal stock (e.g., migration northward of larger adults during the winter) and abiotic variability (e.g., temperature variability). As noted above, further studies are necessary to confirm our hypotheses, including comparisons between the size composition of the adults of the different seasons and the different areas, as well as genetic studies. The information that the regional variability in egg size may be caused due to different aspects of the stocks analyzed may be useful for management purposes.

Acknowledgments

The authors thank those responsible for the Biological Collection "Prof. E. F. Nonato" (Oceanographic Institute, University of São Paulo) for the egg samples. The senior author is thankful for the scholarships given by Fundação de Amparo à Pesquisa do Estado de São Paulo. Comments and suggestions from J. Dias, S. Cadrin, and J. Muelbert improved the quality of the manuscript, for which the authors are grateful.

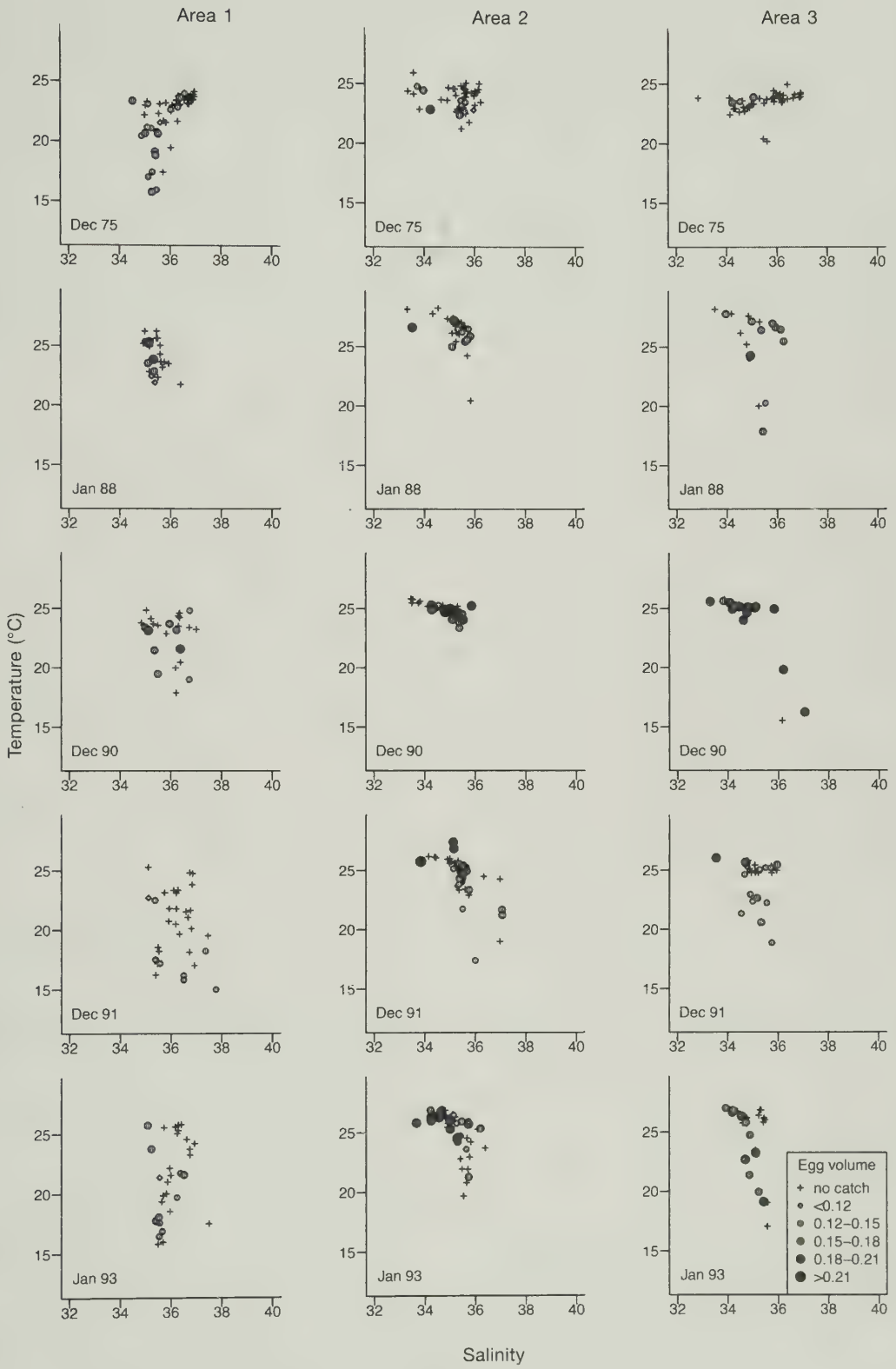

Figure 8

Temperature–salinity diagrams with mean volume of eggs (mm^3) of Argentine anchoita (*Engraulis anchoita*) per sampling station for the 3 areas sampled in the southeastern Brazilian Bight with ichthyoplankton tows in 1975, 1988, 1990, 1991, and 1993.

Literature cited

Araújo, C. C.
2013. Oceanografia pesqueira dos estágios iniciais de Loliginidae (Cephalopoda: Myopsida): paralarvas ao longo da plataforma continental entre o Cabo de São Tomé (RJ) e Cananéia (SP) (22–25°S). M.S. diss., 140 p. Univ. São Paulo, São Paulo, Brazil.

Bagenal, T. B.
1971. The interrelation of the size of fish eggs, the date of spawning and the production cycle. J. Fish Biol. 3:207–219.

Begg, G. A.
2005. Life history parameters. *In* Stock identification methods: applications in fishery science (S. X. Cadrin, K. D. Friedland, and J. R. Waldman, eds.), p. 119–150. Elsevier Academic Press, Burlington, MA.

Blaxter, J. H. S., and G. Hempel.
1963. The influence of egg size on herring larvae (*Clupea harengus* L.). ICES J. Mar. Sci. 28:211–240.

Blaxter, J. H. S., and J. R. Hunter.
1982. The biology of the clupeoid fishes. Adv. Mar. Biol. 20:1–223.

Brandini, F. P.
1990. Hydrography and characteristics of the phytoplankton in shelf and oceanic waters off southeastern Brazil during winter (July/August 1982) and summer (February/March 1984). Hydrobiologia 196:111–148.

Carvalho, F. M., and J. P. Castello.
2013. Argentine anchovy (*Engraulis anchoita*) stock identification and incipient exploitation in southern Brazil. Lat. Am. J. Aquat. Res. 41:820–827.

Castello, J. P.
2007. Síntese sobre a anchoíta (*Engraulis anchoita*) no sul do Brasil. *In* A prospecção pesqueira e abundância de estoques marinhos no Brasil nas décadas de 1960 a 1990: levantamento de dados e avaliação crítica (M. Haimovici, ed.), p. 197–218. Ministério do Meio Ambiente, Brasília, Brazil.

Castello, L., and J. P. Castello.
2003. Anchovy stocks (*Engraulis anchoita*) and larval growth in the SW Atlantic. Fish. Res. 59:409–421.

Castro Filho, B. M., and L. B. Miranda.
1998. Physical oceanography of the western Atlantic continental shelf located between 4°N and 34°S coastal segment (4°W). *In* The Sea, vol. 11 (A. R. Robinson and K. H. Brink, eds.), p. 209–251. John Wiley & Sons, Oxford.

Cerda, C., and B. M. Castro.
2014. Hydrographic climatology of South Brazil Bight shelf waters between Sao Sebastiao (24°S) and Cabo Sao Tome (22°S). Cont. Shelf Res. 89:5–14.

Chambers, R. C.
1997. Environmental influences on egg and propagule sizes in marine fishes. *In* Early life history and recruitment in fish populations (R. C. Chambers and E. Trippel, eds.), p. 63–102. Chapman & Hall, New York.

Chambers, R. C., and K. G. Waiwood.
1996. Maternal and seasonal differences in egg sizes and spawning characteristics of captive Atlantic cod, *Gadus morhua*. Can. J. Fish. Aquat. Sci. 53:1986–2003.

Ciechomski, J. D.
1965. Observaciones sobre la reproduccion desarollo embrionario y larval de la anchoita Argentina (*Engraulis anchoita*). Bol. Inst. Biol. Mar. 9:1–29.
1966. Development of the larvae and variations in the size of the eggs of Argentine anchovy, *Engraulis anchoita* Hubbs and Marini. ICES J. Mar. Sci. 30:281–190.
1973. The size of the eggs of the Argentine anchovy, *Engraulis anchoita* (Hubbs & Marini) in relation to the season of the year and to the area of spawning. J. Fish Biol. 5:393–398.

Demir, N.
1974. The pelagic eggs and larvae of teleostean fishes in Turkish waters. II. Engraulidae. Istanbul Univ. Fen Fak. Mecm., B. 39:49–66.

FAO.
2014. The state of world fisheries and aquaculture 2014, 223 p. FAO, Rome.

Favero, J. M., M. Katsuragawa, M. L. Zani-Teixeira, and J. T. Turner.
2015. Using new tools to identify eggs of *Engraulis anchoita* (Clupeiformes, Engraulidae). J. Fish Biol. 86:822–826.
2017. Spawning areas of *Engraulis anchoita* in the Southeastern Brazilian Bight during late-spring and early summer. Prog. Oceanogr. 153:37–49.

Gaeta, S. A., and F. P. Brandini.
2006. Produção primária do fitoplâncton na região entre o Cabo de São Tomé (RJ) e o Chuí (RS). *In* O ambiente oceanográfico da plataforma continental e do talude na região sudeste-sul do Brasil (C.L.D.B. Rossi-Wongtschowski and L.S.P Madureira, eds.), p. 219–264. Editora da Universidade de São Paulo, São Paulo.

Goçalo, C. G., M. Katsuragawa, and I. C. A. Silveira.
2011. Patterns of distribution and abundance of larval Phosichthyidae (Actinopterygii, Stomiiformes) in southeastern Brazilian waters. Braz. J. Oceanogr. 59:213–229.

Guille A.
1970. Benthic bionomy of the continental shelf of the French Catalan coast. II. Benthic communities of the macrofauna. Vie Milieu 21:149–280.

Hansen, J. E.
1994. Diferencias entre parâmetros vitales de las poblaciones bonaerense y patagonica de anchoita Argentina. Rev. Invest. Desarr. Pesq. 9:11–24.

Lima, I. D., and J. P. Castello.
1995. Distribution and abundance of South-west Atlantic anchovy spawners (*Engraulis anchoita*) in relation to oceanographic processes in the southern Brazilian shelf. Fish. Oceanogr. 4:1–16.

Llanos-Rivera, A., and L. R. Castro.
2004. Latitudinal and seasonal egg-size variation of the anchoveta (*Engraulis ringens*) off the Chilean coast. Fish. Bull. 102:207–212.

Lopes, R. M., M. Katsuragawa, J. F. Dias, M. A. Montú, J. H. Muelbert, C. Gorri, and F. P. Brandini.
2006. Zooplankton and ichthyoplankton distribution on the southern Brazilian shelf: an overview. Sci. Mar. 70:189–202.

Mahiques, M. M., M. G. Tesslera, A. M. Ciotti, I. C. A. Silveira, S. H. M. Sousa, R. C. L. Figueira, C. C. G. Tassinari, V. V. Furtado, and R. F. Passos.
2004. Hydrodynamically driven patterns of recent sedimentation in the shelf and upper slope off Southeast Brazil. Cont. Shelf Res. 24:1685–1697.

Marteinsdottir, G., and K. W. Able.
1992. Influence of egg size on embryos and larvae of *Fundulus heteroclitus* (L.). J. Fish Biol. 41:883–896.

Matsuura, Y., H. L. Spach, and M. Katsuragawa.
1992. Comparison of spawning patterns of the Brazilian sardine (*Sardinella brasiliensis*) and anchoita (*Engraulis anchoita*) in Ubatuba region, southern Brazil during 1985 through 1988. Bol. Inst. Oceanogr., Sao Paulo 40:101–115.

Miranda, L. B., and M. Katsuragawa.
1991. Estrutura térmica na região sudeste do Brasil (outubro/novembro de 1988). Publ. Espec. Inst. Oceanogr. Sao Paulo 8:1–14.

Namiki, C., M. Katsuragawa, D. C. Napolitano, M. L. Zani-Teixeira, R. A. Mattos, and I. C. A. Silveira.
2017. Hydrodynamically-driven distribution of lanternfish larvae in the Southeast Brazilian Bight. J. Mar. Syst. 170:115–133.

O'Reilly, J. E., S. Maritorena,, D. A. Siegel, M. C. O'Brien, D. Toole, B. G. Mitchell, M. Kahru, F. P. Chavez, P. Strutton, G. F. Cota, et al.
2000. Ocean color chlorophyll *a* algorithms for SeaWiFS, OC2, and OC4: version 4. *In* SeaWiFS postlaunch calibration and validation analyses, part 3. NASA Tech. Memo. 2000–206892 (S.B. Hooker and E.R. Firestone, eds.), p. 9–23. NASA Goddard Space Flight Center, Greenbelt, MD.

Padovani, L. N., M. D. Viñas, and M. Pájaro.
2011. Importance of the Río de la Plata estuarine front (southwestern Atlantic Ocean) in the feeding ecology of Argentine anchovy, *Engraulis anchoita* (Clupeiformes, Clupeidae). Lat. Am. J. Aquat. Res. 39:205–213.

Pájaro, M., G. J. Macchi, and R. P. Sánchez.
1997. Fecundidad y frecuencia reproductiva de las poblaciones bonaerense y patagónica de anchoita Argentina (*Engraulis anchoita*). Rev. Invest. Desarr. Pesq. 11:19–38.

Phonlor, G.
1984. Morfologia e biologia dos ovos de Engraulidae do sul do Brasil (Teleostei, Clupeiformes). Rev. Bras. Biol. 44:467 – 487.

Piola, A. R., E. J. D. Campos, O. O. Moller Jr., M. Charo, and C. Martinez.
2000. Subtropical shelf front off eastern South America. J. Geophys. Res. 105:6565–6578.

Piola, A. R., O. O. Moller Jr., R. A. Guerrero, and E. J. D. Campos.
2008a. Variability of the subtropical shelf front off eastern South America: winter 2003 and summer 2004. Cont. Shelf Res. 28:1639–1648.

Piola, A. R., S. I. Romero, and U. Zajaczkovski.
2008b. Space–time variability of the Plata plume inferred from ocean color. Cont. Shelf Res. 28:1556–1567.

R Core Team.
2015. R: a language and environment for statistical computing. R Foundation for Statistical Computing, Vienna, Austria. [Available from website, accessed July 2015.]

Sabatés, A., N. Zaragoza, C. Grau, and J. Salat.
2008. Vertical distribution of early developmental stages in two coexisting clupeoid species, *Sardinella aurita* and *Engraulis encrasicolus*. Mar. Ecol. Prog. Ser. 364:169–180.

Schindelin, J., C. T. Rueden, M. C. Hiner, and K. W. Eliceiri.
2015. The ImageJ ecosystem: an open platform for biomedical image analysis. Mol. Reprod. Dev. 82:518–529.

Silveira, I. C. A., A. C. K. Schmidt, E. J. D. Campos, S. S. Godoi, and Y. Ikeda.
2000. A corrente do Brasil ao largo da costa leste Brasileira. Rev. Bras. Oceanogr. 48:171–183.

Smith, P. E., and S. L. Richardson.
1977. Standard techniques for pelagic fish egg and larva surveys. FAO Fish. Tech. Pap. 175, 100 p.

Stevenson, M. R., D. Dias-Brito, J. L. Stech, and M. Kampel.
1998. How do cold water biota arrive in a tropical bay near Rio de Janeiro, Brazil? Cont. Shelf Res. 18:1595–1612.

Tanaka, S.
1973. Stock assessment by means of ichthyoplankton surveys. *In* Fish egg and larval surveys (contributions to a manual) (G. Hempel, ed.), p. 33–51. FAO Fish. Tech. Pap. 122.

Tanaka, Y.
1992. Japanese anchovy egg accumulation at the sea surface or pycnocline—observations and model. J. Oceanogr. 48:461 –472.

Valentin, J. L., D. L. Andre, and S. A. Jacob.
1987. Hydrobiology in the Cabo Frio (Brazil) upwelling: two-dimensional structure and variability during a wind cycle. Cont. Shelf Res. 7:77–88.

Vanzolini, P. E.
1977. A brief biometrical note on the reproductive biology of some South American Podocnemis (Testudines, Pelomedusidae). Pap. Avulsos Zool. 31:79–102.

Wootton, R. J.
1990. Ecology of teleost fishes, 404 p. Chapman and Hall, London.

National Marine Fisheries Service
NOAA

Fishery Bulletin
established in 1881

Spencer F. Baird
First U.S. Commissioner of Fisheries and founder of *Fishery Bulletin*

The physiological stress response, postrelease behavior, and mortality of blacktip sharks (*Carcharhinus limbatus*) caught on circle and J-hooks in the Florida recreational fishery

Nicholas M. Whitney (contact author)[1,2]
Connor F. White[1]
Paul A. Anderson[3,4]
Robert E. Hueter[5]
Gregory B. Skomal[6]

Email address for contact author: nwhitney@neaq.org

[1] Behavioral Ecology and Physiology Program
Mote Marine Laboratory
1600 Ken Thompson Parkway
Sarasota, Florida 34236

[2] Anderson Cabot Center for Ocean Life
New England Aquarium
1 Central Wharf
Boston, Massachusetts 02110

[3] The Florida Aquarium Center for Conservation
701 Channelside Drive
Tampa, Florida 33602

[4] Mystic Aquarium
Sea Research Foundation, Inc.
c/o University of Connecticut at Avery Point
1084 Shennecossett Road
Groton, CT 06340 USA

[5] Center for Shark Research
Mote Marine Laboratory
1600 Ken Thompson Parkway
Sarasota, Florida 34236

[6] Massachusetts Division of Marine Fisheries
1213 Purchase Street
New Bedford, Massachusetts 02740

Abstract—The blacktip shark (*Carcharhinus limbatus*) is the most commonly captured species in the Florida recreational shark fishery. We aimed to quantify the postrelease mortality of blacktip sharks and to determine whether hook type (circle or J) had any impact on survival. We measured capture variables (e.g., fight time, animal condition, etc.), blood gas analytes, and fine-scale behavior obtained by using acceleration data loggers for blacktip sharks (n=31) caught on rod and reel by recreational fishermen. Mortalities (n=3; 9.7%) all occurred within 2 h after release. Surviving sharks were monitored for 7 to 72 h (mean: 30 h [standard deviation (SD) 22]) and behaviorally recovered from capture within 11 h (SD 2.6), although larger individuals recovered faster. Hook type did not affect where a shark was hooked, animal condition, the likelihood of hook removal, or recovery time. We found relatively low levels of mortality for blacktip sharks caught in the recreational fishery that were kept in the water and had not sustained serious injuries.

Manuscript submitted 19 January 2017.
Manuscript accepted 15 August 2017.
Fish. Bull. 115:532–543 (2017).
Online publication date: 14 September 2017.
doi: 10.7755/FB.115.4.9

The views and opinions expressed or implied in this article are those of the author (or authors) and do not necessarily reflect the position of the National Marine Fisheries Service, NOAA.

The practice of catch-and-release has become more common in commercial and recreational fisheries in recent decades in order to ensure the sustainability of global fisheries (Bartholomew and Bohnsack, 2005). Although the catch-and-release method is advocated and broadly mandated to minimize impacts on fisheries stocks, postrelease mortality may still occur owing to stress, injuries, and an increased susceptibility to natural predation (Bartholomew and Bohnsack, 2005; Cooke and Schramm, 2007; Raby et al., 2014). In efforts to reduce mortality, management practices are enacted to reduce capture stress and physical trauma and thus, ultimately increase the sustainability of fisheries (Davis, 2002; Cooke and Schramm, 2007).

Most work on the impacts of catch-and-release fishing has focused on teleosts, even though global shark populations are declining and some are experiencing up to 90% reductions because of over-exploitation and bycatch in commercial fisheries (Ferretti et al., 2010). In addition to population declines from commercial fishing pressure, many elasmobranch stocks are experiencing increased recreational fishing pressure owing to the recent increases in the popularity of recreational shark fishing (Skomal, 2007; Danylchuk et al., 2014). Sharks are generally more susceptible to fishing pressure because of their K-selected life history traits (Hoenig and Gruber, 1990). There is somewhat limited information available on how elasmobranchs handle

capture stress and few studies have directly measured postrelease mortality because electronic tags can be cost prohibitive (Skomal and Bernal, 2010; Whitney et al., 2016). Studies that have assessed postrelease mortality in elasmobranch fisheries have found that postrelease mortality is variable between species and fisheries but can be quite high in certain circumstances (>60%, Sepulveda et al., 2015; for a review of elasmobranch postrelease mortality, see Ellis et al., 2017).

Efforts have been made to link perturbations in blood biochemistry to animal stress and mortality resulting from capture (Wells et al., 1986; Skomal, 2006; Hyatt et al., 2012). Exhaustive exercise such as fighting on a line, typically causes a marked decrease in blood pH (acidemia) resulting from metabolic (increasing H^+ as indicated by rising blood lactate and decreasing blood bicarbonate) and respiratory (increasing partial pressure of carbon dioxide [pCO_2]) acidoses (Wood, 1991; Milligan, 1996; Kieffer, 2000; Skomal, 2007; Skomal and Bernal, 2010; Skomal and Mandelman, 2012). These physiological indicators, if coupled with quantitative data on postrelease behavior or mortality, can provide insights into causative factors of physiological stress and mortality, as well as potential mitigation measures (Skomal, 2007).

One of the most commonly advocated fishing methods to minimize physical trauma (e.g., gut hooking) and reduce postrelease mortality is the use of circle-hooks (Cooke and Suski, 2004). Over the past decade, studies on the relative impact of circle-hooks vs. traditional J-hooks on pelagic teleosts have indicated that the former reduce the likelihood of injury to the fish by lodging in the mouth or jaw as opposed to the esophagus or stomach, thereby increasing postrelease survivorship with little impact on catch per unit of effort (Skomal et al., 2002; Kerstetter and Graves, 2006; Serafy et al., 2009; Serafy et al., 2012). Empirical data on these variables are lacking in recreational shark fisheries, but there is some evidence that sharks are less likely to be foul-hooked with the use of circle-hooks than with J-hooks (French et al., 2015; Sepulveda et al., 2015; Willey et al., 2016).

A main target species in the southeastern U.S. shark fisheries, both recreational and commercial, is the blacktip shark (*Carcharhinus limbatus*) (NMFS[1]). Although management measures beginning in 1993 have enabled blacktip sharks to rebound from a sharp decline (NMFS[1]), current fishing pressure on the blacktip shark may be increasing as an alternative to pressure on the sympatric sandbar shark (*C. plumbeus*), which is prohibited to be captured in federal waters (NMFS[2]). The NOAA Marine Recreational Information Program estimates that blacktip sharks are the most commonly captured shark species in the Florida recreational fishery, with 89% of individuals released alive after capture (National Marine Fisheries Service Marine Recreational Information Program, Recreational Fisheries Statistics, available from website).

The impact of capture on blacktip sharks is unknown, but the blood biochemistry of blacktip sharks caught on longlines and drum lines indicates that the magnitude of the stress response in this species is greater than that measured in other carcharhinid species, such as sandbar sharks (Mandelman and Skomal, 2009; Marshall et al., 2012; Gallagher et al., 2014). Furthermore, the observed at-vessel mortality rate for this species (88%) was much higher than that of the sandbar shark (43%) in one study of the North Atlantic Ocean longline fishery (Morgan and Burgess, 2007) and therefore raises further concerns about the response of blacktip sharks to capture. However, correlations between blood stress indicators and postrelease mortality have yet to be determined for this species.

In this study, we compared the effects of capture and hook type on blacktip sharks caught in the Florida recreational shark fishery. We compared sharks caught on circle and J-hooks to determine whether blood physiology, or visual at-vessel capture metrics, differed between hook types. We then used multidimensional acceleration data loggers (ADLs) to measure postrelease mortality to determine whether hook type or at-vessel metrics could accurately predict postrelease survival in blacktip sharks. ADLs record the frequency and force of swimming movements, as well as the animal's body orientation at subsecond intervals (e.g., Kawabe et al., 2003; Shepard et al., 2008; Whitney et al., 2012). These high-resolution data can be used to identify and quantify specific behaviors according to tailbeat frequency and amplitude, including active swimming, stalling, gliding, rolling, etc. Recently this technology has been shown to provide definitive measures of mortality and postrelease recovery period in coastal sharks (Whitney et al., 2016).

Materials and methods

Blacktip sharks were handled in this study in accordance with guidelines of the National Research Council (2011). Work was completed under Florida Fish and Wildlife Conservation Commission permit #SAL-11-0041-SRP and approved under Mote Marine Laboratory Institutional Animal Care and Use Committee (IACUC) #13-11-NW2, as well as the Florida Aquarium ACUC.

Field sites and sampling methods

We selected 2 study sites off the coast of Florida with a known seasonal prevalence of blacktip sharks:

[1] NMFS (National Marine Fisheries Service). 2006. Final consolidated Atlantic highly migratory species fishery management plan, 1600 p. Highly Migratory Species Manage. Div., Off. Sustainable Fish., Natl. Mar. Fish. Serv., Silver Spring, MD. [Available from website.]

[2] NMFS (National Marine Fisheries Service). 2008. Final ammendment 2 to the consolidated Atlantic highly migratory species fishery management plan, 705 p. Highly Migratory Species Manage. Div., Off. Sustainable Fish., Natl. Mar. Fish. Serv., Silver Spring, MD. [Available from website.]

Charlotte Harbor and surrounding waters in the Gulf of Mexico (26°47′18″N, 82°7′23″W), and off Cape Canaveral (28°19′8″N, 80°20′6″W) in the Atlantic Ocean. At both study sites, specific fishing locations and practices were directed by recreational charter captains to ensure methods were consistent with those commonly used in the recreational fishery. Sharks were caught between September 2011 and April 2013 by using rod and reel with 10/0 circle-hooks (circle offset-point octopus hook; Gamakatsu USA, Inc., Tacoma, WA) or 10/0 J-hooks (straight eye 4× strong offshore octopus hook; Gamakatsu USA, Inc.) baited with locally caught species, such as Spanish mackerel (*Scomberomorus maculatus*) and Atlantic bonito (*Sarda sarda*) and identical angling practices were used regardless of hook type. Once sharks were hooked, they were angled until they could be handled alongside the boat, at which point they were roped by the tail and secured to the side of the vessel with the shark facing toward the bow. The sharks remained in the water to ensure that their gills were oxygenated. The time from when the shark initially was hooked until it was secured alongside the vessel was recorded as fight time. Once secured, precaudal length, girth, and hooking location (jaw, mouth, gill, esophagus, gut, body) were recorded; and sharks were visually assessed for abrasions or bleeding. After initial assessments, an ADL was attached to the shark's dorsal fin and a sample of blood was drawn by a caudal venipuncture. Once sampling and tagging were completed, the hooks were removed or the leaders were cut at the captain's discretion. Blacktip sharks are obligate ram ventilators, but are able to endure short periods of restraint when their gills are flushed by ambient water movement alongside the vessel. If sharks were unresponsive after processing, they were revived by moving them forward and backward in the water to ventilate their gills—a standard practice among recreational fishermen and one recommended in fishery guidelines issued by NOAA and others (e.g., NMFS[3]). Sharks were assigned a behavioral release condition score (BRCS) between 1 and 5 upon release (1=good: no revival time, swiftly swimming away; 2=fair: no revival time, slowly swimming away; 3=poor: short revival time <30 s; 4=very poor: long revival time >30 s; and 5=dead: unable to revive), which has been shown to correspond with survival for this species on the basis of long-term recapture rates (see Hueter et al., 2006). The time from when the shark was initially secured to the side of the vessel until it swam away was recorded as handling time. Immediately after release, environmental parameters (temperature, dissolved oxygen) were measured by using a YSI Model 85 probe (YSI, Inc., Yellow Springs, OH).

[3] NMFS (National Marine Fisheries Service). 2013. Recreational shark fishing—healthy catch & release. [Available from website.]

Blood sampling and analysis

Once animals were restrained and measured, 1 cc of blood was drawn by caudal venipuncture with an 18–20 gauge 3.8-cm nonheparinized syringes (Mandelman and Farrington, 2007; Skomal, 2007). To avoid coagulation and not compromise blood gas accuracy after phlebotomy, sampled whole blood was immediately (within 30 s) analyzed for pH, pCO_2, and lactate concentration (La^-) in a portable blood gas analyzer (VetScan i-STAT; Abaxis North America, Union City, CA) thermostatted to 37°C. These values were then corrected to environmental temperature according to Mandelman and Skomal (2009).

Accelerometer deployment and recovery

To monitor postrelease mortality and behavior, sharks were tagged with ADLs (G6a; Cefas Technology, Ltd., Lowestoft, UK) set to record tri-axial acceleration at 25 Hz, depth at 1 Hz, and temperature at 0.033 Hz. Acceleration data loggers and a VHF transmitter were embedded in a custom-made float (7×11 cm, 125 g in air, 70 g positively buoyant in seawater; Fig. 1) and affixed to the left side of the dorsal fin with plastic cable ties and a galvanic timed release (International Fishing Devices, Inc., Northland, New Zealand; Whitmore et al., 2016). After a predesignated period of time (12–72 h), the galvanic release dissolved in seawater, releasing the ADL package and allowing it to float to the surface for recovery. Floating tag packages were detected with a hand-held VHF receiver (R4520C; Advanced Telemetry Systems, Isanti, MN), then retrieved by vessel; for more information on tagging and recovery methods see Lear and Whitney (2016) and Whitmore et al. (2016).

ADL data processing and analysis

Data from the ADLs were analyzed with Igor Pro software, vers. 6.22 (WaveMetrics, Inc., Lake Oswego, OR) and Ethographer (Sakamoto et al., 2009). Data for each individual's ADL were visually inspected for postrelease mortality, indicated by a constant depth and cessation of tailbeats that were evidence of a lack of movement and, for an obligate ram-ventilating shark, ultimately death (Whitney et al., 2016). Erratic tailbeats could continue for several minutes but, for consistency, time of death was considered to be the final time that the shark came to rest on the seafloor. Using the data from the ADLs, we generated 58 metrics of swim performance according to Whitney et al. (2016). The metrics included tailbeat acceleration amplitude (TBAA), tailbeat cycle (TBC), overall dynamic body acceleration (ODBA; Wilson et al., 2006), and ODBA bursts, while from the depth information we derived number of dives, duration of dives, average depth, and average vertical velocity (VV) for each hour (Whitney et al., 2016). Because sharks are negatively buoyant, their swimming dynamics differ depending on their orientation and vertical direction of travel.

Figure 1

Photograph of a tag float package, which includes an acceleration data logger (ADL) and a very high frequency (VHF) transmitter with a 1-d galvanic release, attached to the dorsal fin of blacktip shark (*Carcharhinus limbatus*) S16, which was 112 cm in precaudal length and was 1 of 31 blacktip sharks caught and released off Florida between September 2011 and April 2013. The ADL was embedded on the opposite side of the tag float abutting the fin (not visible). The top of the float is painted orange for identification and recovery of the tag package at sea (Whitmore et al., 2016).

Therefore, we also divided data into descent, ascent, and level phases before statistical analysis (Whitney et al., 2016).

To determine possible recovery period, we took hourly means of each metric, and built asymptotic nonlinear mixed models using the nlme package in the open-source statistical software R, vers. 3.1.0 (R Core Team, 2014). Recovery period was defined as the amount of postrelease time it took for the metric value to gain 80% of the difference between the initial postrelease value and the fully recovered value, defined as the upper asymptote in the logistic equation (Whitney et al., 2016). Metrics shown to display a recovery period were then calculated for each individual (for a more detailed description of these analyses, see Whitney et al., 2016).

Statistical analysis

All statistical analyses were conducted in R, and all results were reported as means with SDs unless otherwise stated.

At-vessel capture metrics Chi-square tests were performed to test the effect of hook type on the location of hooking (jaw, mouth, gut), the presence of abrasions or bleeding, and the likelihood of the hook being removed by the fisherman (as opposed to the line being cut and the hook left attached to the shark).

Generalized linear models (GLMs) were used to determine which at-vessel capture metrics (temperature, dissolved oxygen, hook type, hooking location, fight time, handling time) affected blood biomarkers (pH, pCO_2, La^-), and an ordinal logistic regression (OLR) was used to determine which capture metrics impacted the BRCS. A full complement of all possible models (with the addition and removal of each term) was constructed and compared by using the MuMIn package, vers. 1.15.6, in R. The model with the lowest Akaike's information criterion (AIC) was considered the candidate model and the significance of each term was determined by using the F-statistic from an analysis of variance (ANOVA).

Postrelease outcome To investigate the ability of at-vessel metrics to determine postrelease outcome, the dimensionality of behavioral recovery periods was reduced by using 2 methods in order to minimize potential type-I error. With the first method, an average

time to recovery was determined for each individual by averaging the recovery periods across all swimming metrics. GLMs were used to determine which at-vessel metrics (blood biomarkers, environmental and capture metrics) predicted average time to recovery. As with blood biomarker models, a full complement of models was constructed and compared by using AIC, with the significance of the terms in the candidate model determined by an ANOVA.

However, reducing the dimensionality of the recovery period into 1 average negates the possibility that there are multiple ways in which an individual can recover, and these could be affected by different capture parameters. For the second method a principal components analysis (PCA) was conducted on the time to recovery for all swimming metrics. Using the envfit function in the vegan package, vers. 2.3-5, in R, we overlaid the at-vessel metrics on the recovery period ordination from the PCA.

Results

Between September 2011 and April 2013, 31 blacktip sharks were caught and tagged with ADLs (Cape Canaveral, n=2; Charlotte Harbor, n=29), providing a total of 838 h of acceleration data. The durations of individual ADL records on surviving sharks lasted between 7.1 and 71.7 h (mean: 30 h [SD 22]). Precaudal length of the tagged sharks ranged from 92 to 132 cm (mean: 107.5 cm [SD 11.2]), and girth ranged from 48 to 81 cm (mean: 61.2 cm [SD 7.4]). Fight times lasted between 2 and 16 min (mean: 7 min [SD 3]), and handling times lasted between 6 and 18 min (mean: 9.7 min [SD 2.9]) (Table 1). These times were largely consistent with those practiced by participating recreational captains during their typical charters to take photographs and remove fishing gear (Moore[4]; Rapp[5]).

At-vessel capture metrics

Individuals were captured on both circle (n=14) and J-hooks (n = 17), and hooking locations were jaw (n=22), mouth (n=4), and gut (n=3). Hook type did not affect where the shark was hooked (χ^2=0.92, df =2, P=0.62), how likely the hook was to be removed by the fisherman (χ^2=1.01, df=1, P=0.32), severity of abrasions (χ^2=0.02, df=1, P=0.89), observed bleeding (χ^2=0.05, df=1, P=0.82), or the BRCS (χ^2=3.34, df=3, P=0.36). Additionally, no capture-related variables (hook-type, fight time, La^-, pCO_2, and pH) significantly affected BRCS (OLR: P>0.08 for all predictors).

There was interindividual variability in observed blood biochemical markers (Table 1), yet pH correlated with pCO_2 (ρ= −0.44, $t_{1,29}$= −2.66, P=0.01) and La^- (ρ= −0.51, $t_{1,29}$ = −3.17, P=0.004); however, La^- was not correlated with pCO_2 (ρ= −0.31, $t_{1,29}$ = −1.76, P=0.09). Hook type, hooking location, and dissolved oxygen were not found to predict biochemical markers and, therefore, were not included in any final predictive models. La^- increased (coefficient of multiple determination [R^2]=0.57) with increasing fight times ($F_{1,28}$=12.12, P=0.002) and handling times ($F_{1,28}$=25.89, P<0.001) (Fig. 2, Table 2), whereas increasing handling time was found to significantly lower blood pH (R^2=0.18, $F_{1,29}$=6.44, P=0.02; Fig. 2, Table 2). Individuals captured at higher temperatures were found to have increased pCO_2 levels ($F_{1,28}$=4.96, P=0.034; Fig. 2, Table 2). The final model for pCO_2 included a negative relationship with fight time, however this was not significant ($F_{1,28}$=0.63, P=0.43).

Postrelease outcome

Mortality All sharks swam away after capture and handling and only 1 individual (S28; BRCS=4; Table 1) needed to be extensively revived (2–3 min until it swam under its own volition) before release. Three of the 31 tagged sharks died after being released as indicated from the acceleration and depth data (Fig. 3) representing a postrelease mortality rate of 9.7%. All mortalities occurred within 2 h of release (58, 76, and 103 min), all succumbing individuals were hooked in the jaw, and 2 of the 3 were caught on J-hooks. All 3 confirmed mortalities had a BRCS of "fair." Two of the dead sharks appeared to have been scavenged after the animals sank to the sea floor and had ceased movement for over 30 minutes. The ADLs prematurely released during a series of high intensity movement, an indication of scavenging, and one of the packages displayed bite marks upon recovery (e.g., Lear and Whitney, 2016). Two of the mortalities occurred at high temperatures, and these sharks also had low blood pH and high La^-. However, the third mortality occurred for an individual with blood stress values similar to sharks that survived (Fig. 4).

Quantifying sublethal effects Based on the data collected from the ADLs, we determined that 19 of 58 metrics of swimming behavior showed indications of a possible recovery period (for more detail, see Whitney et al., 2016, table 1). Overall, blacktip sharks recovered 10.5 h (SD 3.8) after release. Larger sharks had a significantly shorter average recovery time than smaller sharks ($F_{1,14}$=7.83, P=0.014, Fig. 5); our model also indicated that increasing pCO_2 decreases time to recovery, however this term was not significant ($F_{1,14}$=3.58, P=0.079).

The PCA of recovery period showed that the first 2 principal components (PC) accounted for 50.7% of the variance in the data. PC1 was correlated with recovery periods determined from average ODBA, TBC, TBAA and average VV, whereas PC2 was correlated with recovery periods determined from maximum ODBA,

[4] Moore, R. 2012. Personal commun. Florida Light Tackle Charters. 17044 Greenan Ave., Port Charlotte, FL 33948.

[5] Rapp, D. 2012. Personal commun. Sea Leveler Sport Fishing Charters. 505 Glen Cheek Dr., Cape Canaveral, FL 32920.

Table 1

Data records of individual blacktip sharks (*Carcharhinus limbatus*) caught and released between September 2011 and April 2013 at 2 sites off Florida: Charlotte Harbor and surrounding waters in the Gulf of Mexico and off Cape Canaveral in the Atlantic Ocean. Mortalities are in bold and italics. Sharks were measured in precaudal length. BRCS=behavioral release condition score; pCO_2=partial pressure of carbon dioxide. Recovery period is the averaged behavioral recovery period for that individual over all 19 behavioral metrics and was only calculated for sharks with recording periods over 12 h.

ID	Length (cm)	Temp (°C)	Hook type	Fight time (min)	Handling time (min)	BRCS	pH	pCO_2 (mmHg)	Lactate (mmol/L)	Recording period (h)	Recovery period (h)
S01	***129***	***29.6***	***J***	***13***	***18***	***2***	***7.1***	***5.06***	***8.57***	***10.4***	–
S02	97	29.9	C	6	12	1	7.18	6.01	5.67	11.4	–
S03	102	25.2	C	5	9	1	7.29	5.85	5.62	21.4	13.4
S04	92	25.0	C	3	14	3	7.18	4.44	7.53	35.9	14.0
S05	132	25.2	C	11	13	1	7.17	4.3	7.48	57.9	8.7
S06	***98***	***25.3***	***C***	***5***	***9***	***2***	***7.34***	***5.99***	***3.18***	***8.6***	–
S07	106	24.7	J	6	8	1	7.18	4.61	6.76	13.8	14.2
S08	93	24.7	C	4	10	1	7.15	4.73	8.27	27.8	12.5
S09†	95	25.3	J	2	10	1	7.06	6.29	3.62	54.6	8.4
S10	101	25.4	J	4	6	1	7.25	6.32	2.72	51.8	11.8
S11†	99	25.9	J	4	9	1	7.03	10.65	5.05	7.1	–
S12	92	25.9	J	4	10	1	7.09	10.28	4.4	7.4	–
S13	108	25.9	J	9	9	1	7.31	6.09	4.81	10.7	–
S14	128	25.1	J	6	8	1	7.34	4.4	4.08	19.9	7.0
S15	119	24.8	J	7	9	1	7.27	6.98	2.97	18.8	9.2
S16	112	29.8	C	16	9	2	7.14	4.82	8.77	9.5	–
S17	110	29.1	J	10	9	3	7.1	10.55	5.59	54.1	10.2
S18	***120***	***29.3***	***J***	***13***	***11***	***2***	***7.02***	***6.85***	***10.71***	***2.7***	–
S19	105	29.3	J	8	6	1	7.18	11.64	3.07	49.4	7.2
S20	120	28.9	C	5	6	1	7.28	4.91	3.34	10.7	–
S21†	105	27.0	J	10	10	2	7.26	5.88	4.74	71.7	9.0
S22	92	27.2	C	5	6	2	7.16	8.08	4.77	68.3	12.8
S23	114	27.1	C	10	9	1	7.22	6.03	4.53	67.7	12.2
S24	113	26.8	J	10	10	1	7.28	6.08	4.46	11.9	–
S25	100	26.2	J	4	6	1	7.26	5.61	4.42	67.3	15.9
S26	102	27.6	C	6	8	3	7.25	6.23	4.98	11.4	–
S27	103	27.4	C	5	7	2	7.14	11.37	4.02	9	–
S28	108	27.3	C	12	8	4	7.21	7.2	4.52	10.4	–
S29	108	27.3	J	12	10	3	7.24	6.87	4.92	10.7	–
S30	109	27.3	C	7	7	2	7.2	7.13	4.73	27.3	11.1
S31	122	27.2	J	11	7	1	7.36	4.82	3.83	27.2	9.4
Mean	107.5	26.9		7.5	9.1	1.6	7.20	6.65	5.23	28.0	11.0
SD	11.2	1.7		3.5	2.6	0.8	0.09	2.12	1.93	22.6	2.6

†Denotes a shark that was gut hooked. The hook was not removed in all 3 cases.

maximum vertical velocity, and the number of ODBA bursts. Increasing handling time and La^- corresponded with longer recovery periods along PC1, whereas decreasing temperature, and gut-hooking corresponded with longer recovery times along PC2 (Fig. 6). As found through GLM, increasing animal size correlated with shorter recovery times along PC1 and PC2. However, certain at-vessel capture metrics (pH, pCO2, BRCS and hook-type) correlated poorly with the first 2 recovery period PCs.

Discussion

In this study, we documented 3 postrelease mortalities out of 31 capture and releases (9.7% mortality) for blacktip sharks caught on rod and reel in the Florida recreational fishery. Our results are consistent with mortality rates for other elasmobranchs caught on rod and reel, such as 10% for Atlantic sharpnose sharks (*Rhizoprionodon terraenovae*; Gurshin and Szedlmayer, 2004), 10% for shortfin makos (*Isurus oxyrinchus*;

Table 2

Parameters and coefficients of determination (r^2) for models of capture metrics that predict blood biomarkers, lactate concentration, acidity (pH), and partial pressure of carbon dioxide (pCO_2), for blacktip sharks (*Carcharhinus limbatus*) caught and released off Florida during 2011–2013. Values are output of models, representing the equation for the line and the variance accounted for.

	Intercept	Fight time	Handling time	Temperature	r^2
Lactate	−0.6020	0.2092	0.4660	–	0.5758
pH	7.3377	–	−0.0150	–	0.1818
pCO_2	−7.3036	−0.2358	–	0.5853	0.1664

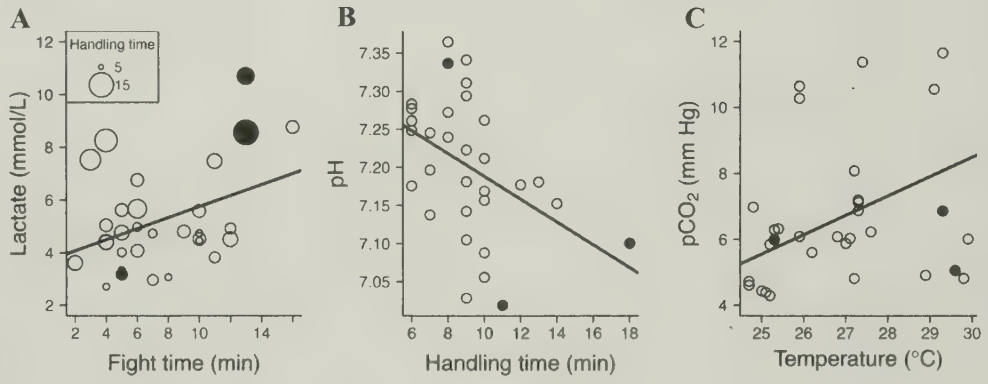

Figure 2

Significant relationships between blood biomarkers and capture metrics for blacktip sharks (*Carcharhinus limbatus*) caught and released between September 2011 and April 2013 at 2 sites off Florida: Charlotte Harbor and surrounding waters in the Gulf of Mexico and off Cape Canaveral in the Atlantic Ocean. Open circles represent sharks that lived, and closed circles represent sharks that died, and lines of best fit were determined by the selected model. (**A**) Lactate concentration correlated with fight time and handling time, which is represented by the size of the data points. (**B**) Blood pH decreased with increasing handling times. (**C**) partial pressure of carbon dioxide (pCO_2) increased with increasing temperature.

French et al., 2015), and 12.5% for juvenile lemon sharks (*Negaprion brevirostris*; Danylchuk et al., 2014). Kneebone et al. (2013) found a lower mortality rate of 1.2% for juvenile sand tigers (*Carcharias taurus*), whereas Heberer et al. (2010) found a rate of 26% for the common thresher shark (*Alopias vulpinus*). However, the feeding strategy of the common thresher shark is unique and mortality is highly dependent on the type of gear and fishing practice (mouth-hooked=0%, tail-hooked with trailing gear=66%; Sepulveda et al., 2015).

Our results were lower than many postrelease mortality rates observed for elasmobranchs captured by commercial fisheries: 24% for spiny dogfish (*Squalus acanthias*) in a trawl fishery (Mandelman and Farrington, 2007); 15–31% for species captured on longlines (Musyl et al., 2011; Marshall et al., 2015; Campana et al., 2016); 43% for great hammerheads (*Sphyrna mokarran*) and 26% for bull sharks (*Carcharhinus leucas*) captured on drum lines (mortality estimated on the basis of the failure of satellite tags to transmit data; Gallagher et al., 2014); or 48% for released silky sharks (*Carcharhinus falciformis*) captured in a purse siene (Poisson et al., 2014). In addition, we observed no at-vessel mortality, which can be as high as 88% for blacktip sharks caught by demersal longline (Morgan and Burgess, 2007). This finding suggests that the impact of recreational fishing is minimal, with a mortality rate <10%, and well below the 20% mortality threshold that is considered unacceptably high for recreational fisheries (Arlinghaus et al., 2007). Although even low rates of postrelease mortality can be detrimental to a stock, depending on its life history and overall fishing pressure, results from a recent assessment suggest that

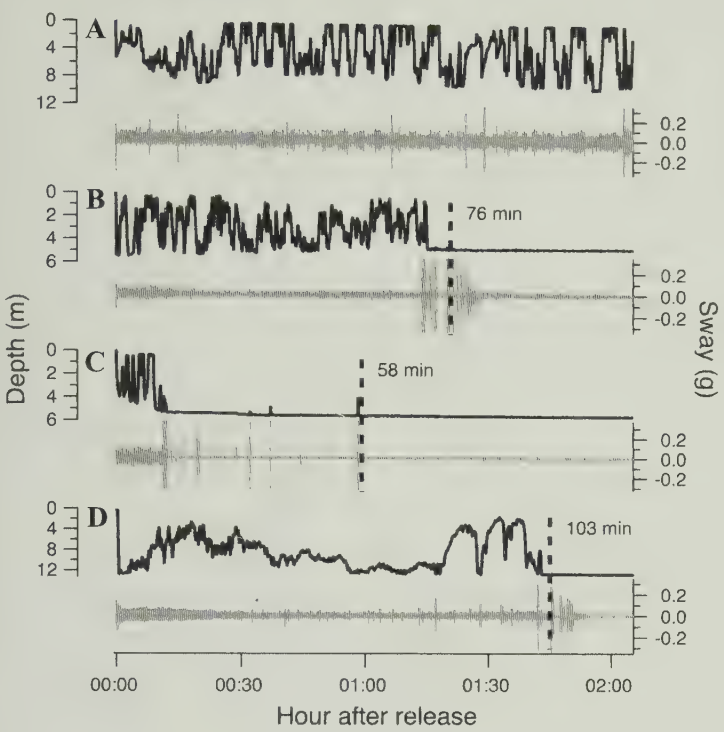

Figure 3

The differences in depth (black line) and dynamic acceleration (gray line) of the sway axis (tailbeats, measured in units of gravity [1 g=9.8 m/s^2]) for (**A**) a blacktip shark (*Carcharhinus limbatus*), S16, that lived) and for the 3 sharks for which fatalities were observed (**B**) S18, (**C**) S6, and (**D**) S1. Sharks were designated as mortalities on a stationary depth, representative of the seafloor and a cessation of consistent tailbeats. The final time that the shark landed on the seafloor was used to determine the time of death (dashed line). Sharks were caught and released off Florida between September 2011 and April 2013.

blacktip sharks in the Gulf of Mexico could sustain this level of mortality (SEDAR[6]).

Our mortality rate for blacktip sharks could be an underestimate because the sampling period was limited to 3 days after release; any postrelease mortalities that happened after this period were missed. The 3 gut-hooked animals may have been especially susceptible to delayed mortality. Alternatively, the longer handling times required for blood sampling and tag attachment may have increased the likelihood of mortality compared to standard fishing practices. However, we found that sharks behaviorally recovered within 24 h and all mortalities occurred within the first 2 h, suggesting that most mortalities happen shortly after release. This is a common finding from past studies, where a single sharpnose shark mortality occured ~40 min after release (Gurshin and Szedlmayer, 2004), and juvenile lemon shark mortalities occurred within a 15-min observation period (Danylchuk et al., 2014). Furthermore, for studies that have used longer-term pop-up satellite tags, mortality was reported to occur shortly after release: 87% of mortalities happened within 60 min for dusky sharks (*Carcharhinus obscurus*) and sandbar sharks (Marshall et al., 2015); 100% of mortalities occurred within 4 h for common thresher sharks (Heberer et al., 2010); >50% for blue sharks (*Prionace glauca*), shortfin makos, and porbeagles (*Lamna nasus*) died within 6 h of release (Campana et al., 2016); and >50% of silky sharks died within 1 day of release (Hutchinson et al., 2015).

Shark mortalities within 10 d of catch and release are largely attributed to capture-related causes, yet the majority of mortalities that occur within the first 6 h after release are likely the result of the direct physiological stress of capture (e.g., blood acidosis), or catastrophic hooking injuries (e.g., gill damage or puncture of the peritoneal cavity) (Epperly et al., 2012; Godin et al., 2012; Renshaw et al., 2012; Kneebone et al., 2013). This short time period is within the 11 h postrelease recovery period measured in our study. Similar duration for behavioral recovery (based on tailbeat frequency) have been observed with juvenile scalloped hammerheads (*Sphyrna lewini*) after tagging (Lowe, 2001). Furthermore, this behavioral recovery roughly corresponds with the duration of physiological recovery observed in captive sand tigers, whose blood biomarkers returned to baseline within 12 h (Kneebone et al., 2013).

Some elasmobranchs appear to be able to recover from the physiological stress of capture relatively quickly (<1 d). However, differences in physiology, life history, and habitat preference indicate that these results are species or population-specific, and managers should exercise caution before extrapolating such results to other stocks (Mandelman and Skomal, 2009). For instance, Gallagher et al. (2017) recently used accelerometers to show that blacktip sharks fight more intensely than nurse sharks (*Ginglymostoma cirratum*) and tiger sharks (*Galeocerdo cuvier*) upon being hooked, and this corresponded to higher La^- values.

Studies of blood chemistry of sharks have revealed that capture stress can manifest itself in changes in La^- (Hoffmayer and Parsons, 2001; Moyes et al., 2006; Skomal, 2007; Hyatt et al., 2012), hematocrit (Brill et al., 2008; Marshall et al., 2012), HCO_3 (Skomal, 2007; Hyatt et al., 2012), K+ (Mandelman and Farrington, 2007; Frick et al., 2010; Marshall et al., 2012), Ca^{2+}, Na^+ (Marshall et al., 2012), and pH (Hoffmayer and Parsons, 2001; Manire et al., 2001; Skomal, 2006; Mandelman

[6] SEDAR (Southeast Data, Assessment, and Review). 2012. SEDAR 29 stock assessment report: HMS Gulf of Mexico blacktip shark, 142 p. SEDAR, North Charleston, South Carolina. [Available from website.]

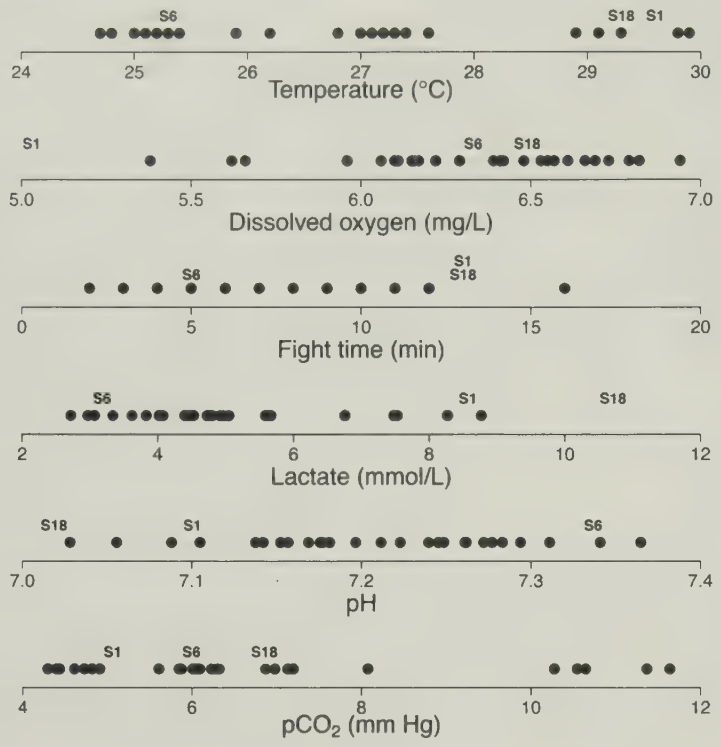

Figure 4

At-vessel capture metrics for all live (black circles) and dead (shark ID numbers) blacktip sharks (*Carcharhinus limbatus*) caught and released off Florida between September 2011 and April 201. Sharks were labeled according to the shark ID number from Table 1. Environmental metrics were temperature and dissolved oxygen; the behavioral metric was fight time; and biochemical metrics were lactate concentration, acidity (pH), and partial pressure of carbon dioxide (pCO_2).

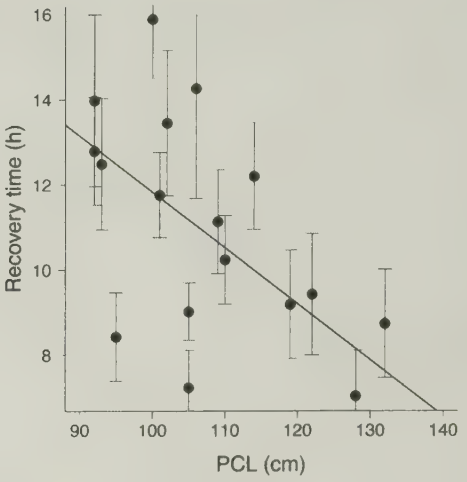

Figure 5

The relationship between precaudal length (PCL) and recovery period, determined with a generalized linear model, for blacktip sharks (*Carcharhinus limbatus*) caught and released off Florida between September 2011 and April 2013. The relationship is given by the equation 28.1 – (0.13×PCL) – (0.473×pCO_2). The average behavioral recovery period determined from all behavioral metrics was shorter with increasing shark length (coefficient of multiple determination=0.45). Error bars represent standard error of the mean; however, only the means were used in the regression.

and Farrington, 2007; Hyatt et al., 2012). Many studies have found significant differences in these physiological indicators between at-vessel moribund and healthy sharks and have used them to predict and extrapolate postrelease mortality. In general, the exhaustive exercise associated with rod and reel capture caused acid-base disruptions in blacktip sharks that increased in magnitude with increasing fight time (decreasing pH; Fig. 2). Concomitant rises in La^- and pCO_2 indicate that acidemia was of both metabolic and respiratory origin, respectively (Fig. 2). Although these physiological perturbations in acid-base status did not impact survivorship in most of the blacktip sharks sampled, 2 of the 3 mortalities may be linked to these changes in blood chemistry. These 2 sharks were exposed to high water temperatures (>29°C) and long fight times (13 min), and exhibited the highest La^- levels, which would indicate blood acidemia driven by metabolic acidosis. This result suggests that higher water temperatures exacerbate the stress response of blacktip sharks and could cause higher levels of postrelease mortality if fight times are extended. However, the third shark that died after release was not exposed to high water temperatures (25.3°C), had a relatively short fight time (5 min) and handling time (8 min), and was not experiencing acidemia as indicated by a relatively high pH and the fourth lowest La^- level measured in this study (Fig. 4). This finding suggests that the disruption of acid-base homeostasis may not be the only cause of death after exposure to rod and reel angling.

Previous studies have been able to predict postrelease mortality from blood biochemistry (Moyes et al., 2006; Renshaw et al., 2012); however, because of the small sample size, the low mortality rate, and high variability observed in blood gas values, we were unable to predict postrelease outcome from blood gas analytes. Furthermore, blood biomarkers did not correlate with observed behavioral recovery periods, although larger sharks did display shorter recovery periods. This reduced recovery time could be due to the fact that larger individuals have a lower cost of transport (lower energy requirement for recovery, e.g., Parsons, 1990).

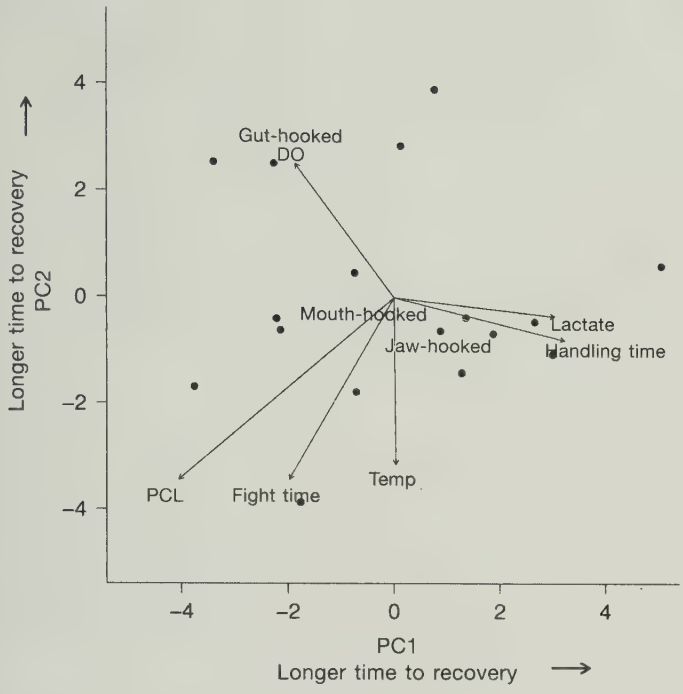

Figure 6

Principal component analysis of the recovery period of blacktip sharks (*Carcharhinus limbatus*) caught and released off Florida between September 2011 and April 2013. Increasing values along both principal components (PCs) correspond to longer times to recovery. Black circles represent individual sharks. PC1 corresponds to behavioral recovery metrics calculated from averages (average overall dynamic body acceleration [ODBA], tailbeat cycle, tailbeat amplitude, and vertical velocity), and PC2 corresponds to maximum behavioral exertion metrics (maximum ODBA, maximum vertical velocity, and ODBA bursts). Capture metrics, such as dissolved oxygen (DO) of the water at capture location and precaudal length (PCL), are fit onto the recovery period ordination and are displayed as arrows. The direction of the arrow shows the direction and magnitude of its correlation with the behavioral recovery metrics.

In this study, hook type did not affect where a shark was hooked, animal condition, or the likelihood of the fisherman removing the hook. In other recreational fisheries, the use of circle-hooks has been found to increase the likelihood of common thresher sharks and shortfin makos being "mouth hooked" as opposed to "gut or foul hooked" (hooked on the fins or trunk) (French et al., 2015; Sepulveda et al., 2015), as well as increasing the likelihood of jaw-hooking across a range of recreationally caught shark species (Willey et al., 2016). Studies on elasmobranchs captured in commercial fisheries have reported a lower incidence of gut-hooking with circle-hooks than with J-hooks (Kerstetter and Graves, 2006), and lower at-haulback mortality with circle-hooks (Campana et al., 2009), although the magnitude of this discrepancy is also species-specific.

Overall, we found a relatively low rate of postrelease mortality (<10%) and most individuals recovered from capture stress after approximately 11 h. Catch-and-release recreational fisheries may have a low impact on blacktip shark survivorship if animals are kept in the water and have not sustained serious injury.

Acknowledgments

This study would not have been possible without the expertise and dedication of Captain R. Moore. The authors also thank Captains G. Rapp and D. Rapp for their support, C. Capizzano, H. Marshall, J. Morris, G. Schwieterman, J. Tyminski, and numerous interns and volunteers for their help with fieldwork and other logistics, and K. Heym, S. Coy, V. Wright-Placeres, and K. Casey (Florida Aquarium) for their support in equipment maintenance and accounting. This study was funded by the NOAA Cooperative Research Program, grant no. NA11NMF4540120. This report serves as Sea Research Foundation publication No. 275.

Literature cited

Arlinghaus, R., S. J. Cooke, J. Lyman, D. Policansky, A. Schwab, C. Suski, S. G. Sutton, and E. B. Thorstad.
2007. Understanding the complexity of catch-and-release in recreational fishing: an integrative synthesis of global knowledge from historical, ethical, social, and biological perspectives. Rev. Fish. Sci. 15:75–167.

Bartholomew, A., and J. A. Bohnsack.
2005. A review of catch-and-release angling mortality with implications for no-take reserves. Rev. Fish Biol. Fish. 15:129–154.

Brill, R., P. Bushnell, S. Schroff, R. Seifert, and M. Galvin.
2008. Effects of anaerobic exercise accompanying catch-and-release fishing on blood-oxygen affinity of the sandbar shark (*Carcharhinus plumbeus*, Nardo). J. Exp. Mar. Biol. Ecol. 354:132–143.

Campana, S. E., W. Joyce, M. P. Francis, and M. J. Manning.
2009. Comparability of blue shark mortality estimates for the Atlantic and Pacific longline fisheries. Mar. Ecol. Prog. Ser. 396:161–164.

Campana, S. E., W. Joyce, M. Fowler, and M. Showell.
2016. Discards, hooking, and post-release mortality of porbeagle (*Lamna nasus*), shortfin mako (*Isurus oxyrinchus*), and blue shark (*Prionace glauca*) in the Canadian pelagic longline fishery. ICES J. Mar. Sci. 73:520–528.

Cooke, S. J., and C. D. Suski.
2004. Are circle hooks an effective tool for conserving marine and freshwater recreational catch-and-release fisheries? Aquat. Conserv. 14:299–326.

Cooke, S. J., and H. L. Schramm.
2007. Catch-and-release science and its application to conservation and management of recreational fisheries. Fish. Manage. Ecol. 14:73–79.
Danylchuk, A. J., C. D. Suski, J. W. Mandelman, K. J. Murchie, C. R. Haak, A. M. Brooks, and S. J. Cooke.
2014. Hooking injury, physiological status and short-term mortality of juvenile lemon sharks (*Negaprion bevirostris*) following catch-and-release recreational angling. Conserv. Physiol. 2:cot036.
Davis, M. W.
2002. Key principles for understanding fish bycatch discard mortality. Can. J. Fish. Aquat. Sci. 59:1834–1843.
Ellis, J. R., S. R. McCully Phillips, and F. Poisson.
2017. A review of capture and post-release mortality of elasmobranchs. J. Fish Biol. 90:653–722.
Epperly, S. P., J. W. Watson, D. G. Foster, and A. K. Shah.
2012. Anatomical hooking location and condition of animals captured with pelagic longlines: the grand banks experiments 2002–2003. Bull. Mar. Sci. 88:513–527.
Ferretti, F., B. Worm, G. L. Britten, M. R. Heithaus, and H. K. Lotze.
2010. Patterns and ecosystem consequences of shark declines in the ocean. Ecol. Lett. 13:1055–1071.
French, R. P., J. L. Lyle, S. Tracey, S. Currie, and J. M. Semmens.
2015. High survivorship after catch-and-release fishing suggests physiological resilience in the endothermic shortfin mako shark (*Isurus oxyrinchus*). Conserv. Physiol. 3:cov044.
Frick, L. H., R. D. Reina, and T. I. Walker.
2010.vStress related physiological changes and post-release survival of Port Jackson sharks (*Heterodontus portusjacksoni*) and gummy sharks (*Mustelus antarcticus*) following gill-net and longline capture in captivity. J. Exp. Mar. Biol. Ecol. 385:29–37.
Gallagher, A. J., J. E. Serafy, S. J. Cooke, and N. Hammerschlag.
2014. Physiological stress response, reflex impairment, and survival of five sympatric shark species following experimental capture and release. Mar. Ecol. Prog. Ser. 496:207–218.
Gallagher, A. J., E. R. Staaterman, S. J. Cooke, and N. Hammerschlag.
2017. Behavioural responses to fisheries capture among sharks caught using experimental fishery gear. Can. J. Fish. Aquat. Sci. 74:1–7.
Godin, A. C., J. K. Carlson, and V. Burgener.
2012. The effect of circle hooks on shark catchability and at-vessel mortality rates in longlines fisheries. Bull. Mar. Sci 88:469–483.
Gurshin, C. W. D., and S. T. Szedlmayer.
2004. Short-term survival and movements of Atlantic sharpnose sharks captured by hook-and-line in the north-east Gulf of Mexico. J. Fish Biol. 65:973–986.
Heberer, C., S. A. Aalbers, D. Bernal, S. Kohin, B. DiFiore, and C. A. Sepulveda.
2010. Insights into catch-and-release survivorship and stress-induced blood biochemistry of common thresher sharks (*Alopias vulpinus*) captured in the southern California recreational fishery. Fish. Res. 106:495–500.
Hoenig, J. M., and S. H. Gruber.
1990. Life-history patterns in the elasmobranchs: implications for fisheries management. *In* Elasmobranchs as living resources: advances in the biology, ecology, systematics, and the status of fisheries (H. L. Pratt Jr., S. H. Gruber, and T. Taniuchi, eds.), p. 1–16. NOAA Tech. Rep. NMFS 90.
Hoffmayer, E. R., and G. R. Parsons.
2001. The physiological response to capture and handling stress in the Atlantic sharpnose shark, *Rhizoprionodon terraenovae*. Fish Physiol. Biochem. 25:277–285.
Hueter, R. E., C. A. Manire, J. P. Tyminski, J. M. Hoenig, and D. A. Hepworth.
2006. Assessing mortality of released or discarded fish using a logistic model of relative survival derived from tagging data. Trans. Am. Fish. Soc. 135:500–508.
Hutchinson, M. R., D. G. Itano, J. A. Muir, and K. N. Holland.
2015. Post-release survival of juvenile silky sharks captured in a tropical tuna purse seine fishery. Mar. Ecol.: Prog. Ser. 521:143–154.
Hyatt, M. W., P. A. Anderson, P. M. O'Donnell, and I. K. Berzins.
2012. Assessment of acid–base derangements among bonnethead (*Sphyrna tiburo*), bull (*Carcharhinus leucas*), and lemon (*Negaprion brevirostris*) sharks from gillnet and longline capture and handling methods. Comp. Biochem. Physiol. A 162:113–120.
Kawabe, R., K. Nashimoto, T. Hiraishi, Y. Naito, and K. Sato.
2003. A new device for monitoring the activity of freely swimming flatfish, Japanese flounder *Paralichthys olivaceus*. Fish. Sci. 69:3–10.
Kerstetter, D. W., and J. E. Graves.
2006. Effects of circle versus J-style hooks on target and non-target species in a pelagic longline fishery. Fish. Res. 80:239–250.
Kieffer, J. D.
2000. Limits to exhaustive exercise in fish. Comp. Biochem. Physiol. A 126:161–179.
Kneebone, J., J. Chisholm, D. Bernal, and G. Skomal.
2013. The physiological effects of capture stress, recovery, and post-release survivorship of juvenile sand tigers (*Carcharias taurus*) caught on rod and reel. Fish. Res. 147:103–114.
Lear, K. O., and N. M. Whitney.
2016. Bringing data to the surface: recovering data loggers for large sample sizes from marine vertebrates. Anim. Biotelem. 4:12.
Lowe, C.
2001. Metabolic rates of juvenile scalloped hammerhead sharks (*Sphyrna lewini*). Mar. Biol. 139:447–453.
Mandelman, J. W., and M. A. Farrington.
2007. The estimated short-term discard mortality of a trawled elasmobranch, the spiny dogfish (*Squalus acanthias*). Fish. Res 83:238–245.
Mandelman, J. W., and G. B. Skomal.
2009. Differential sensitivity to capture stress assessed by blood acid–base status in five carcharhinid sharks. J. Comp. Physiol., B 179:267–277.
Manire, C., R. Hueter, E. Hull, and R. Spieler.
2001. Serological changes associated with gill-net capture and restraint in three species of sharks. Trans. Am. Fish. Soc. 130:1038–1048.
Marshall, H., L. Field, A. Afiadata, C. Sepulveda, G. Skomal, and D. Bernal.
2012. Hematological indicators of stress in longline-captured sharks. Comp. Biochem. Physiol. A 162:121–129.
Marshall, H., G. Skomal, P. G. Ross, and D. Bernal.
2015. At-vessel and post-release mortality of the dusky (*Carcharhinus obscurus*) and sandbar (*C. plumbeus*) sharks after longline capture. Fish. Res. 172:373–384.

Milligan, C. L.
1996. Metabolic recovery from exhaustive exercise in rainbow trout. Comp. Biochem. Physiol. A 113:51–60.
Morgan, A., and G. H. Burgess.
2007. At-vessel fishing mortality for six species of sharks caught in the Northwest Atlantic and Gulf of Mexico. Gulf Caribb. Res. 19:123–129.
Moyes, C. D., N. Fragoso, M. K. Musyl, and R. W. Brill.
2006. Predicting postrelease survival in large pelagic fish. Trans. Am. Fish. Soc. 135:1389–1397.
Musyl, M. K., R. W. Brill, D. S. Curran, N. M. Fragoso, L. M. McNaughton, A. Nielsen, B. S. Kikkawa, and C. D. Moyes.
2011. Postrelease survival, vertical and horizontal movements, and thermal habitats of five species of pelagic sharks in the central Pacific Ocean. Fish. Bull. 109:341–368.
National Research Council.
2011. Guide for the care and use of laboratory animals, 8th ed, 220 p. National Academies Press, Washington, DC.
Parsons, G. R.
1990. Metabolism and swimming efficiency of the bonnethead shark *Sphyrna tiburo*. Mar. Biol. 104:363–367.
Poisson, F., J. D. Filmalter, A.-L. Vernet, and L. Dagorn.
2014. Mortality rate of silky sharks (*Carcharhinus falciformis*) caught in the tropical tuna purse seine fishery in the Indian Ocean. Can. J. Fish. Aquat. Sci. 71:795–798.
R Core Team.
2014. R: a language and environment for statistical computing. R Foundation for Statistical Computing, Vienna, Austria. [Available from website, accessed June 2014.]
Raby, G. D., J. R. Packer, A. J. Danylchuk, and S. J. Cooke.
2014. The understudied and underappreciated role of predation in the mortality of fish released from fishing gears. Fish Fish. 15:489–505.
Renshaw, G. M. C., A. K. Kutek, G. D. Grant, and S. Anoopkumar-Dukie.
2012. Forecasting elasmobranch survival following exposure to severe stressors. Comp. Biochem. Physiol. A 162:101–112.
Sakamoto, K. Q., K. Sato, M. Ishizuka, Y. Watanuki, A. Takahashi, F. Daunt, and S. Wanless.
2009. Can ethograms be automatically generated using body acceleration data from free-ranging birds? PloS ONE 4(4):e5379.
Sepulveda, C. A., C. Heberer, S. A. Aalbers, N. Spear, M. Kinney, D. Bernal, and S. Kohin.
2015. Post-release survivorship studies on common thresher sharks (*Alopias vulpinus*) captured in the southern California recreational fishery. Fish. Res. 161:102–108.
Serafy, J. E., D. W. Kerstetter, and P. H. Rice.
2009. Can circle hook use benefit billfishes? Fish Fish. 10: 132–142.
Serafy, J. E., S. J. Cooke, G. A. Diaz, J. E. Graves, M. Hall, M. Shivji, and Y. Swimmer.
2012. Circle hooks in commercial, recreational, and artisanal fisheries: research status and needs for improved conservation and management. Bull. Mar. Sci. 88:371–391.
Shepard, E. L. C., R. P. Wilson, L. G. Halsey, F. Quintana, A. Gómez Laich, A. C. Gleiss, N. Liebsch, A. E. Myers, and B. Norman.
2008. Derivation of body motion via appropriate smoothing of acceleration data. Aquat. Biol. 4:235–241.
Skomal, G. B.
2006. The physiological effects of capture stress on post-release survivorship of sharks, tunas, and marlin. Ph.D. diss., 311 p. Boston Univ., Boston, MA.
2007. Evaluating the physiological and physical consequences of capture on post-release survivorship in large pelagic fishes. Fish. Manage. Ecol. 14:81–89.
Skomal, G., and D. Bernal.
2010. Physiological responses to stress in sharks. *In* Sharks and their relatives II: biodiversity, adaptive physiology, and conservation (J. C. Carrier, J. A. Musick, and M. R. Heithaus, eds.), p. 459–490. CRC Press, Boca Raton, FL.
Skomal, G. B., and J. W. Mandelman.
2012. The physiological response to anthropogenic stressors in marine elasmobranch fishes: a review with a focus on the secondary response. Comp. Biochem. Physiol. A 162:146–155.
Skomal, G. B., B. C. Chase,and E. D. Prince.
2002. A comparison of circle hook and straight hook performance in recreational fisheries for juvenile Atlantic bluefin tuna. Am. Fish. Soc. Symp. 30:57–65.
Wells, R. M. G., R. H. McIntyre, A. K. Morgan, and P. S. Davie.
1986. Physiological stress responses in big gamefish after capture: observations on plasma chemistry and blood factors. Comp. Biochem. Physiol. A 84:565–571.
Whitmore, B. M., C. F. White, A. C. Gleiss, and N. M. Whitney.
2016. A float-release package for recovering data-loggers from wild sharks. J. Exp. Mar. Biol. Ecol 475:49–53.
Whitney, N. M., Y. P. Papastamatiou, and A. C. Gleiss.
2012. Integrative multisensor tagging: emerging techniques to link elasmobranch behavior, physiology, and ecology. *In* Biology of sharks and their relatives, 2nd ed. (J. C. Carrier, J. A. Musick, and M. R. Heithaus, eds.), p. 265–260. CRC Press, Boca Raton, FL.
Whitney, N. M., C. F. White, A. C. Gleiss, G. D. Schwieterman, P. Anderson, R. E. Hueter, and G. B. Skomal.
2016. A novel method for determining post-release mortality, behavior, and recovery period using acceleration data loggers. Fish. Res. 183:210–221.
Willey, A. L., L. S. Barker, and M. Sampson.
2016. A comparison of circle hook and J hook performance in the recreational shark fishery off Maryland. Fish. Bull. 114:370–373.
Wilson, R. P., C. R. White, F. Quintana, L. G. Halsey, N. Liebsch, G. R. Martin, and P. J. Butler.
2006. Moving towards acceleration for estimates of activity-specific metabolic rate in free-living animals: the case of the cormorant. J. Anim. Ecol. 75:1081–1090.
Wood, C. M.
1991. Acid-base and ion balance, metabolism, and their interactions, after exhaustive exercise in fish. J. Exp. Biol. 160:285–308.

National Marine
Fisheries Service
NOAA

Fishery Bulletin
established in 1881

Spencer F. Baird
First U.S. Commissioner
of Fisheries and founder
of *Fishery Bulletin*

Residency, partial migration, and late egress of subadult Chinook salmon (*Oncorhynchus tshawytscha*) and coho salmon (*O. kisutch*) in Puget Sound, Washington

Anna N. Kagley (contact author)[1]
Joseph M. Smith[2]
Kurt L. Fresh[1]
Kinsey E. Frick[1]
Thomas P. Quinn[2]

Email address for contact author: anna.kagley@noaa.gov

[1] Northwest Fisheries Science Center
National Marine Fisheries Service, NOAA
2725 Montlake Boulevard East
Seattle, Washington 98112

[2] School of Aquatic and Fishery Sciences
University of Washington
Box 355020
Seattle, Washington 98195

Abstract—Migratory behavior affects growth, survival, and fitness of individual fish, the dynamics and resilience of populations, and the ecosystems that fish occupy. Many salmonids are anadromous but individuals vary in the duration and spatial extent of marine migrations. We used telemetry to investigate movements of Chinook salmon (*Oncorhynchus tshawytscha*) that remained in Puget Sound (residents) rather than migrated to the Pacific Ocean. Most tagged Chinook salmon (26 of 37=70%) remained in Puget Sound for a substantial period, staying in the region where captured. However, 30% of tagged individuals, termed "transients," subsequently left Puget Sound. Residents and transients did not differ in tagging date, body size, or origin (hatchery or wild). Compared with sympatric coho salmon (*O. kisutch*) where 80% remained as residents according to similar data, Chinook salmon tended to be detected closer to shore, in shallower water, and on fewer different receivers. For both species, residents showed limited movement within Puget Sound. We conclude that Chinook and coho salmon display resident and transient movement patterns across a behavioral continuum rather than within discrete migrational categories. These movement patterns are important because they affect the role of salmon in the ecosystem, their vulnerability to fisheries, and their accumulation of chemical contaminants.

Manuscript submitted 11 January 2017.
Manuscript accepted 24 August 2017.
Fish. Bull. 115:544–555 (2017).
Online publication date: 14 September 2017.
doi: 10.7755/FB.115.4.10

The views and opinions expressed or implied in this article are those of the author (or authors) and do not necessarily reflect the position of the National Marine Fisheries Service, NOAA.

Many of the world's most abundant fish species are migratory within fresh or marine waters or between these distinct environments (Lucas and Baras, 2001; Secor, 2015). However, species and populations often vary greatly in the prevalence, duration, and spatial extent of their migrations (Quinn and Brodeur, 1991; Chapman et al., 2012a; Chapman et al., 2012b). Such variation (e.g., partial and differential migration) can affect the population's stability through alterations in exposure to predators, fisheries, and contaminants (Kerr et al., 2010; Gahagan et al., 2015). Consequently, a full understanding of variation in movement patterns is important for management of these populations, such as conservation planning and the measurement of survival.

Among fishes, salmonids show a particularly wide variety of migration patterns (Jonsson and Jonsson, 1993; Klemetsen et al., 2003; Quinn and Myers, 2004). These patterns have been studied extensively owing to the importance of salmonids in commercial and recreational fisheries, ecosystem function, and biodiversity (NRC, 1996). Many studies have investigated the ecological and evolutionary basis of anadromy and nonanadromy (Wood and Foote, 1996; Dodson et al., 2013; Kendall et al., 2015) but there is also great variation in the extent of migration among anadromous individuals, especially for Chinook salmon (*Oncorhynchus tshawytscha*). The tendency to use different marine environments (coastal and open ocean) varies markedly among populations, as does the tendency to migrate northward or southward along the coast of North America (Myers et al., 1998; Trudel et al., 2009; Weitkamp, 2010; Sharma and Quinn, 2012). In addition, some individuals do not migrate into the North Pacific Ocean but rather spend all or most of their

marine period within protected waters of southeastern Alaska (Orsi and Jaenicke, 1996) and British Columbia (Healey and Groot, 1987). It has also been known for decades that some Chinook salmon, termed "residents," are found throughout the year within Puget Sound, the Strait of Georgia, and associated inlets (Pressey[1]; Haw et al.[2]; Buckley, 1969). It has been unclear to what extent these salmon move within the inland marine waters, collectively known as the Salish Sea, and whether they leave for the coast at some point. Brannon and Setter (1989) inferred from coded wire tagging data that both maturing and immature Chinook salmon may make annual "loop" migrations from Puget Sound north into the Strait of Georgia in spring and summer and then back south into Puget Sound. However, there is no direct evidence of individual fish making such migrations.

Resident salmon seem to constitute a persistent and substantial fraction of the entire Puget Sound population of Chinook salmon. Analysis of coded-wire tag data indicated that an estimated 29% of hatchery Chinook salmon subyearlings and 45% of yearlings entering Puget Sound remained as residents (O'Neill and West, 2009). Subsequent analyses based on similar data but reflecting a different analytical approach also revealed that many Puget Sound Chinook salmon adopt a resident marine distribution pattern (Chamberlin et al., 2011). This pattern occurs but is less common with coho salmon (*O. kisutch*; Rohde et al., 2014). However, because coded wire tags document only the location where fish are captured, and not movement patterns, movements of individual fish cannot be determined with these tags. Research using hydroacoustic transmitters revealed differences between coho and Chinook salmon depth distributions and diel vertical migrations but did not provide information on movement throughout the basins in Puget Sound and the Salish Sea (Smith et al., 2015). Four Chinook salmon distribution patterns were observed in the Salish Sea (Arostegui et al., 2017), but information on resident Chinook salmon movements in the main basins of Puget Sound is still very limited.

The Chinook salmon evolutionarily significant unit in Puget Sound is listed as threatened under the U.S. Endangered Species Act (Federal Register, 2005). A better understanding of the movements of these fish between Puget Sound and the coastal ocean, and within Puget Sound, will help to identify patterns in habitat use, to evaluate fishery management objectives across jurisdictional boundaries, and even help to determine pathways to contaminant exposure. Resident Chinook salmon, for example, have higher accumulations of polychlorinated biphenyls (PCBs) than conspecifics that migrate to the coastal ocean (O'Neill and West, 2009). As a prey item these salmon contain high enough levels of persistent organic pollutants to have possible health effects on ESA-listed killer whales (Hickie et al., 2007; Cullon et al., 2009) and to require human health advisories (WDOH[3]).

In this study, individual Chinook salmon were implanted with hydroacoustic tags at a time after the majority of salmon had typically left Puget Sound for ocean feeding grounds (Healey, 1991). The detections of these presumably resident Chinook salmon were used to determine: 1) whether these individuals remained within Puget Sound, and 2) whether origin (wild or hatchery), body size, or season of tagging influenced their tendency to remain in Puget Sound. For the fish that stayed as residents within Puget Sound, we also determined 3) whether resident salmon remained in the same region where they were tagged or moved throughout Puget Sound and parts of the Salish Sea, and 4) whether detections depended on the receiver location's water depth and proximity to shore.

Finally, we compared the location features of receivers that recorded Chinook salmon with those features that were recorded with receivers that detected coho salmon collected and tagged at the same locations and times (Rohde et al., 2013). Coho and Chinook salmon in Puget Sound are ecologically similar and both exhibit partial migration (i.e., residency). The factors affecting residency, inferred from coded wire tagging data, were similar for the 2 species (Chamberlin et al., 2011; Rohde et al., 2014), and both species tended to be caught as residents in the natal basin where they entered Puget Sound. We therefore combined data from this study and that by Rohde et al. (2013) to compare directly the movement patterns of individual residents of these species in Puget Sound.

Materials and methods

Tagging

On 9 dates in June (2006 and 2007), November (2006), and December (2006, 2007, and 2008), 87 Chinook salmon were caught with a commercial purse seine in central Puget Sound (tagging area, Fig. 1). On the basis of the dates, locations, and sizes (range: 208–370 mm in fork length) of these salmon, all were assumed to be residents at the time of capture. To determine residency we presumed that fish of this size would have entered salt water as smolts the previous spring or summer and were still in Puget Sound about a year later at a time when migratory individuals would be moving along the coast or in offshore waters of the North Pacific Ocean (Trudel et al., 2009).

[1] Pressey, R. T. 1953. The sport fishery for salmon on Puget Sound. Wash. Dep. Fish., Fish. Res. Pap. 1:33–48.

[2] Haw, F., H. O. Wendler, and G. Deschamps. 1967. Development of Washington State salmon sport fishery through 1964. Wash. Dep. Fish., Res. Bull. 7, 192 p. [Available from website.]

[3] WDOH (Washington State Department of Health). 2006. Human health evaluation of contaminants in Puget Sound fish, 136 p. Div. Environ. Health, Wash. State Dep. Health, Olympia, WA. [Available from webiste.]

Figure 1

Map of the study area showing the locations in Puget Sound, Washington, where Chinook salmon (*Oncorhynchus tshawytscha*) were caught and tagged (shaded rectanglar area) during 2006–2008 and the locations of active stationary receivers. The major basins in Puget Sound are outlined by dotted lines.

Study fish were transferred from the seine into a live well with aerated flowthrough seawater at ambient temperature (10–12°C) and salinity. Compressed air was pumped into the tank and dissolved oxygen levels were periodically checked. Fish with visible distress or with scale losses greater than 10% were excluded from being tagged. Weights (measured in grams) and lengths (measured in millimeters) were recorded for selected animals before tagging. Fish were transferred to a small cooler with 65 mg/L tricaine methanesulfonate and anesthetized to a point that induced loss of equilibrium but still allowed opercular movement. Each fish was checked for an adipose fin clip and codedwire tag, either of which would indicate hatchery origin. The fish was then transferred to a surgical table of closedcell foam shaped to allow the fish to be positioned on its dorsum. A supply of water infused with anesthetia was fed by gravity through a tube and delivered to the gills.

An individually coded V9 (i.e., one of the following: V9-1L at 24 mm, V9-2L at 29 mm, and V9-6L at 21 mm in length) acoustic transmitter (VEMCO,[4] Bedford, Nova Scotia, Canada) was inserted into the peritoneal cavity through a small incision (15–20 mm) just off center of the linea alba of the abdomen and anterior to the pelvic fins. Tag-to-body-weight ratio did not exceed 2%, well below that recommended by Hall et al. (2009) to minimize tag effects. All tags had a power output of 145 dB, a variable ping rate, and a projected battery life of 79–537 d. The incision was closed by using absorbable surgical thread (coated Vicryl 60; Ethicon, Somerville, NJ) and sutured with a tapered RB-1 needle and using 2 surgeon knots. Including time under anesthesia, each fish was handled for an average of 6 min of which the surgery took approximately 2 min. After surgery the fish were placed in a recovery tank until they were upright and swimming independently (ca. 15 min); they were then released near the capture site.

Data collection

Since 2004, hydroacoustic tags have been extensively used in Puget Sound, the Strait of Georgia, and nearby water bodies to study movements of many fish species (Melnychuk et al., 2007; Welch et al., 2009; Moore et al., 2010; Hayes et al., 2011; Andrews and Quinn, 2012). Receivers were deployed in Puget Sound and maintained by several investigative teams (Hood Canal=119 receivers, Admiralty Inlet=61, central Puget Sound=271, Whidbey Basin=140 and south Puget Sound=50; Fig. 1). These studies also coincided with the Pacific Ocean Shelf Tracking Project, an international monitoring effort using the same technology to deploy arrays of receivers along the continental shelf from California to Alaska. Combined, these individual and arrayed receivers provided the means to detect fish migrating to the Pacific Ocean via the Strait of Juan de Fuca and Johnstone Strait, British Columbia, Canada, as well as fish moving within the San Juan Islands (Fig. 1; Arostegui et al., 2017). Combined, there were over 800 active receivers within the Salish Sea and an additional 55 along the Washington State coast (including the Willapa Bay subarray; Reichisky et al., 2013) in the Pacific Ocean during the study. The amount of

[4] Mention of trade names or commercial companies is for identification purposes only and does not imply endorsement by the National Marine Fisheries Service, NOAA.

time that each receiver was active varied from a few months to years (median: 155 d) according to the primary focus of the study for which they were deployed (detailed receiver location and status information are available from the Ocean Tracking Network website and Hydraphone Data Repository website). The number of receivers deployed in each basin varied through time but was always more than would be feasible for any single study.

Data analysis

Fish last detected crossing uninterrupted receiver arrays in Admiralty Inlet, the Strait of Juan de Fuca, or Johnstone Strait, or detected on individual receivers along the Washington State coast without exiting detections, were classified as transients because these detections indicated that they left Puget Sound. In contrast, fish last detected within Puget Sound (Whidbey Basin, Admiralty Inlet, Hood Canal, central or southern Puget Sound) and having no coastal or Strait of Georgia detections were classified as residents. Based on acoustic detections, the minimum amount of time it took a tagged fish to leave central Puget Sound and reach the Strait of Juan de Fuca was 6 d. Consequently, we excluded from analysis any fish with final receiver detections within 6 days of tagging because the tracking duration was not sufficient to detect a departure. Given the distribution of receivers (Fig. 1), our probability of detecting a fish exiting the study area for coastal waters was high, but detection of an individual remaining in Puget Sound depended upon the movements and location of that fish. A Welch's *t*-test was used to determine whether fork length differed between fish that were included and excluded from the analysis. A chi-square test was used to determine whether there was a difference in proportion of wild vs. hatchery fish for fish included and excluded from the analysis. A chisquare test was employed to determine whether remaining a resident was independent of origin (hatchery or wild) or month of tagging. Welch's *t*-tests were used to evaluate whether fork length or condition index (Anderson and Neumann, 1996) had any influence on whether or not fish remained a resident within Puget Sound. Linear regression analysis allowed us to determine whether the total detection time for fish that remained in Puget Sound was influenced by fork length of the fish. We also calculated the total distance fish moved per number of days with obtained detections, and we used a Welch's *t*-test to determine whether the total distance traveled per day was different for fish that remained as residents and those that left Puget Sound.

To investigate the use of different areas of Puget Sound by Chinook salmon that remained resident (excluding transient fish), a "site-use rank sum metric" was calculated as a composite variable for each stationary receiver. This variable was created by using 4 metrics similar to those used by Rohde et al. (2013): 1) number of unique fish detected at each receiver, 2) number of days that a receiver detected at least 1 fish, 3) total amount of time spent at each receiver by all fish, divided by the number of individuals detected there (i.e., average time spent per detected fish), and 4) total number of visits to each receiver, divided by the number of individuals detected there. These 4 metrics were combined by summing the rank scores of each variable for each receiver. Low values of the site-use rank sum metric corresponded with low values of the 4 variables and high values of the metric corresponded with high values of the 4 variables. The amount of time spent by each fish at each receiver was calculated as the time between the first and last detections. If a fish was not detected for more than 1 h or the fish visited another receiver the duration period was terminated. A minimum of 2 detections within 1 h were needed to create a duration period.

To characterize areas where fish spent time, the maximum depth within the listening distance (a 520-m radius— an estimate of receiver range based on favorable environmental conditions and the tag output and settings) and the distance to shore were determined for each receiver (Smith et al., 2015). Receivers were then categorized as onshore-shallow (<1 km from shore and <95 m deep), onshore-deep (<1 km from shore and >95 m deep), or offshore-deep (>1 km from shore and >95 m deep). These categories were chosen because there was a clear break between the data at these cutoffs; no receivers were located offshore in shallow water (Fig. 2).

To determine whether site use (measured as the site-use rank sum metric) differed among receiver types (onshore-shallow, onshore-deep, offshore-deep), an analysis of variance (ANOVA) was used. Univariate normality of the residuals was examined with a quantile-quantile plot, homogeneity of variances was examined by plotting standardized residuals against fitted values, and independence was examined by plotting the residuals by each factor of receiver type. A post-hoc Tukey's honestly significant difference (HSD) multiple comparison test was used to determine which receiver types were significantly different.

Diel patterns of receiver recordings of fish that remained as residents were examined by determining the number of discrete movements and presence of fish during each hour of the day. Following Chamberlin et al. (2011), we defined movements as discrete detections between individual receivers. These movement data were summarized by receiver type (offshore-deep, onshore-deep, and onshore-shallow) and tested for circular uniformity among hours by using Rayleigh tests with R package circular, vers. 0.4-7 (Agostinelli and Lund, 2013).

Additionally, the movements of individually tagged Chinook salmon were compared with those of tagged coho salmon (Rohde et al., 2013) by categorizing receivers as detecting 1) both Chinook and coho salmon, 2) only Chinook salmon, or 3) only coho salmon. We examined whether the proportion of fish among these

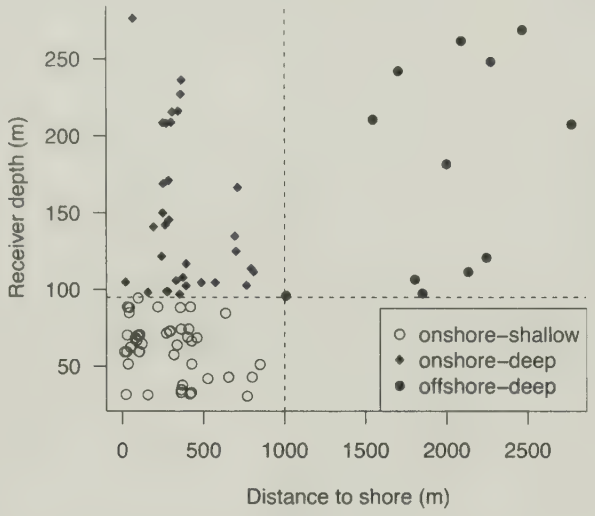

Figure 2

Scatterplot showing by depth (m) and distance to shore (m) the distribution of receivers used to track Chinook salmon (*Oncorhynchus tshawytscha*) in Puget Sound, Washington. The 3 categories used to group receivers were onshore-shallow (white circles; <1 km from shore and <95 m deep), onshore-deep (black diamonds; <1 km from shore and >95 m deep), and offshore-deep (black circles; >1 km from shore and >95 m deep).

categories differed by receiver type across all basins by using a chi-square test. Spearman's rank correlation analysis was used to determine whether the number of individual Chinook salmon detected correlated with the number of individual coho salmon detected at receivers that detected both species. Similarly, Spearman's rank correlation analysis was used to compare the number of days Chinook and coho salmon were detected. All data analyses were performed in R, vers. 3.2.1 (R Core Team, 2015).

Results

Of the 87 fish tagged, 50 were excluded, having final detections less than 6 d after tagging (the minimum time it took fish to reach the Strait of Juan de Fuca), a period insufficient to detect departure. Given the expansive area not covered by receivers we do not presume to provide natural or tag-related mortality for these fish, but the lack of a prolonged detection history precluded us from categorizing them as transient or resident. The 37 fish included in the analysis (for which we had detections more than 6 days after tagging) had longer fork lengths (FLs) than the excluded fish (mean: 273 vs 245 mm FL, t=–3.60, P<0.01). The proportions of natural and hatchery origin individuals did not differ for included fish (11 of 37 wild; 30%) and excluded fish (16 of 50 wild, 32%) (χ^2<0.01, df=1, P=1.00).

Movement from Puget Sound

The 37 fish analyzed were considered resident at the time of tagging, but 11 (30%) subsequently left Puget Sound and were reclassified as transients, and 26 remained as residents. Eleven of the 37 were of natural origin and 26 were of hatchery origin. The origins of the transients (27% natural) and residents (31% natural) did not differ (χ^2<0.01, df=1, P=1.00). Transients were detected in Puget Sound for as little as 1 d to as much as 124 d before exiting. There were too few individual departures for rigorous statistical analyses, but departures occurred throughout the year (January=1, April=2, June=3, July=2, November=2, December=1).

The time of year when fish were tagged did not affect the likelihood of a fish staying as a resident. Of the 37 fish included in analyses, 16 of 20 (80%) fish tagged in June (summer) remained resident in Puget Sound, and 10 of 17 (59%) tagged in the fall through November–December (χ^2=1.09, df=1, P=0.30). Fish that remained resident and those that left Puget Sound did not differ in fork length (mean: 278 vs. 262 mm, t=0.99, P=0.34) or condition factor (mean: 1.21 vs. 1.23, t= –0.57, P=0.58). The total duration of detection for fish that stayed as residents within Puget Sound was not significantly influenced by fish length (coefficient of determination [r^2]=0.12, P=0.08).

Movement among basins

Detection data indicated that fish remaining as residents seldom moved between basins. Twenty-six fish remained residents: 10 individuals (fish 1–10, Fig. 3) were never detected outside central Puget Sound; 9 individuals moved only between Admiralty Inlet and central Puget Sound (fish 11–19, Fig. 3); 6 individuals moved between central Puget Sound, Admiralty Inlet, and the Whidbey Basin (fish 20–25, Fig. 3); and 1 fish moved between central Puget Sound, Admiralty Inlet, and Hood Canal (fish 26, Fig. 3). The 11 fish that left Puget Sound had different movement patterns (fish 27–37, Fig. 3). The last known locations varied for waters within Lime Kiln State Park on San Jun Island (fish 27–28, Fig. 3; Arostegui et al. 2017), the Strait of Juan de Fuca (fish 29–31, 33–35, 37, Fig. 3), waters off northwestern Vancouver Island near Lippy Point (Rechisky et al., 2013; fish 32, Fig. 3), and the Washington State coast at Willapa Bay (fish 36, Fig. 3). Interestingly, these fish were not detected on the Canadian Northern Strait of Georgia or Queen Charlotte subarrays. Hood Canal had 119 receivers active during at least part of the study period but only 2 individuals (fish 26 and 30, Fig. 3) were detected there. Similarly, south Puget Sound had 50 active receivers and only 1 fish was detected there (fish 27, Fig. 3).

Movement within Puget Sound

The site-use rank sum metric was used to measure fish use within Puget Sound. Fish that remained within

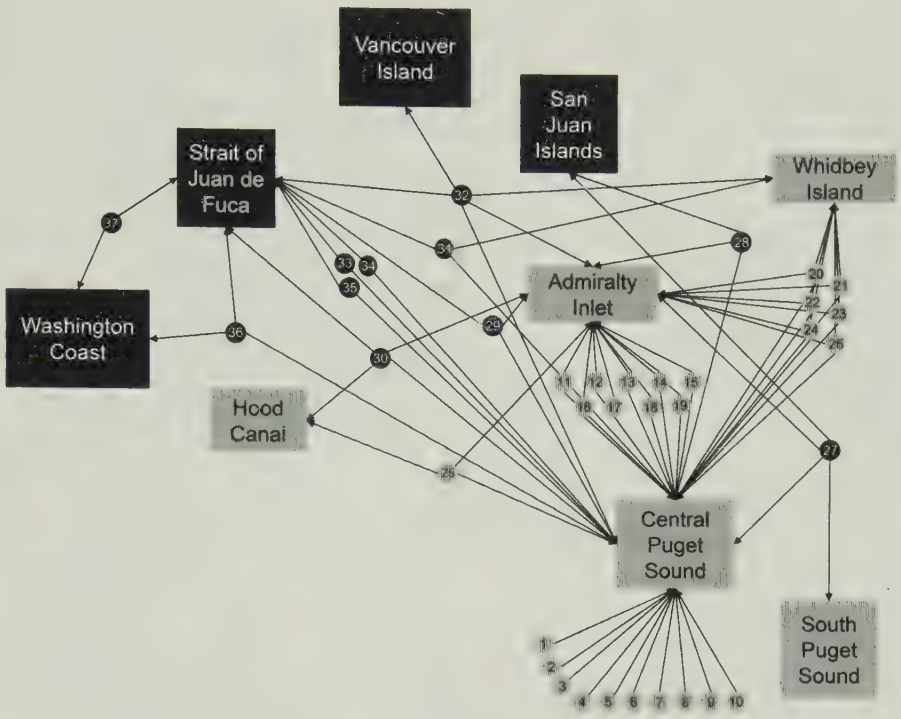

Figure 3

Diagram indicating the network of major basins within Puget Sound (gray rectangles), Washington, basins outside of Puget Sound (black rectangles), and individually tagged Chinook salmon (*Oncorhynchus tshawytscha*) that remained resident within Puget Sound (gray circles) and those that left Puget Sound (black circles). Numbers in the circles identify individual fish. Arrows indicate movement between basins by individual fish. For example, fish 1–10 were detected only where tagged in central Puget Sound, but fish 26 was detected in Admiralty Inlet and Hood Canal.

Puget Sound used offshore-deep, onshore-deep sites and onshore-shallow sites differently (ANOVA: $F_{2,\ 51}$=4.11, P=0.02). A Tukey's HSD post-hoc multiple comparison test indicated that site use was greater at offshore-deep sites (mean: 120.27) and onshore-deep sites (mean: 126.67) than at onshore-shallow sites (mean: 85.17).

Fish presence at receivers showed a 24h periodicity only at onshore-shallow receiver locations (mean: 08:40 h, z=0.12, P=0.047, Fig. 4). Offshore-deep and onshore-deep sites showed no peak in the hour of presence of tagged fish. Fish movement was distributed uniformly among hours regardless of receiver type (Fig. 4).

The total distance moved per day (an indicator of gross movement and not necessarily directionality) was farther for fish that left Puget Sound than for fish that remained as residents (mean: 6.09 vs. 2.69 km/d, t= –2.19, P=0.05). For Chinook salmon within Puget Sound, the total distance moved provided only a limited picture of fish behavior, and fish showed a range of patterns. For example, one fish was tagged in central Puget Sound on 1 November 2006, detected leaving Puget Sound through the Strait of Juan de Fuca on 16 November, and detected along the coast of Washington on 3 December, having moved about 280 km in 17 d or 16.5 km/d (Fig. 5A). This fish continued along the coast west of Willapa Bay through 1 January 2007 but was detected again at the Strait of Juan de Fuca on 14 March 2007. Therefore, had it been caught, on the basis of its locations, it would have been considered a resident in November, a migrant to the coast in December, and a resident in March. In contrast, a resident fish was tagged in central Puget Sound on 7 June 2007 and then detected repeatedly over 8 months moving between 14 nearby receivers (within an extent of only 45 km N to S and 21 km E to W; Fig. 5B). Other individuals fell within this range of movement; most were detected moving among receivers within central Puget Sound.

Comparison with coho salmon movements

To compare the behavior of Chinook and coho salmon, receivers were identified that detected the 37 Chinook salmon from this study and the 35 coho salmon reported by Rohde et al. (2013). Seventy-four receivers throughout all basins detected both species, of which 30 receivers

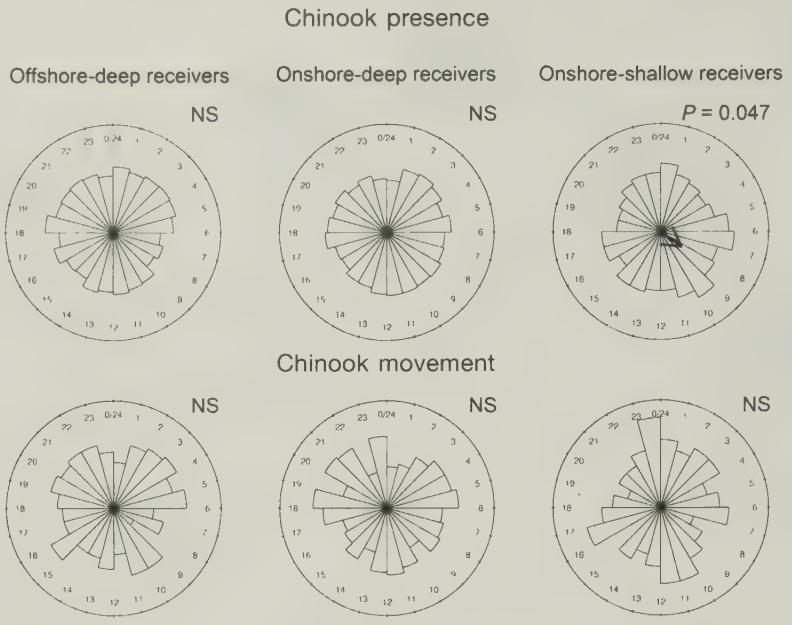

Figure 4

Circular histograms showing the diel patterns of presence (top) and movement (bottom) of Chinook salmon (*Oncorhynchus tshawytscha*) at offshore-deep (>1 km from shore and >95 m deep), onshore-deep (<1 km from shore and >95 m deep), and onshore-shallow (<1 km from shore and <95 m deep) receivers in Puget Sound, Washington. The *P*value indicates significance from a Rayleigh test of uniformity (NS=not significant). The arrow on the significant plot indicates the mean time vector with length rho, a measure of the concentration of data.

detected only Chinook salmon, and 51 receivers detected only coho salmon. Chinook salmon were detected on 104 receivers and coho salmon on 125 receivers. The species detected (both, Chinook salmon only, coho salmon only) varied with receiver type (offshore-deep, onshore-deep, onshore-shallow: χ^2=21.88, df=4, P<0.01). The receivers that detected only Chinook salmon were mostly onshore-shallow receivers (70%), followed by onshore-deep receivers (23%), and offshore-deep receivers (7%) whereas the receivers that detected only coho salmon were mostly offshore-deep (45%), followed by onshore-shallow (33%), and onshore-deep (22%). The receivers that detected both species were more evenly distributed (38% offshore-deep, 35% onshore-deep, and 27% onshore-shallow). The 44 receivers within Puget Sound that detected both Chinook and coho salmon showed positive correlations with the numbers of individual fish (coefficient of correlation [r]=0.47, P<0.01) and days with detections (r=0.54, P<0.01).

Discussion

All the Chinook salmon tagged in this study were categorized initially as residents because they were still in Puget Sound late in their first or in their second year in salt water. Had all of them remained within Puget Sound, we would have inferred a clear distinction between these resident fish and the typical migrants that leave Puget Sound after a few months to feed in the coastal or open ocean waters until they return to spawn. However, 30% of the tagged fish later left Puget Sound, and so were termed transients. If they had been caught in fisheries along the coast, there is no way to know that they had spent significant time in Puget Sound. Indeed, some fish were tracked out to the coast and then back into Puget Sound, further illustrating the flexibility of residency and coastal migrations.

There was no effect of size, origin (hatchery or wild), tagging location, or tagging season on whether a fish remained resident or became a transient, although the small sample sizes limited our effort to detect effects. For example, we included only fish with a minimum of 6 d of detection data (sufficient to detect possible departure). The Chinook salmon detected for more than 6 d after tagging were larger than those omitted for lack of ample detection data. This observation is consistent with size-selective natural mortality or an effect of handling, although 2 laboratory studies found little or no size effects on survival for Chinook salmon with

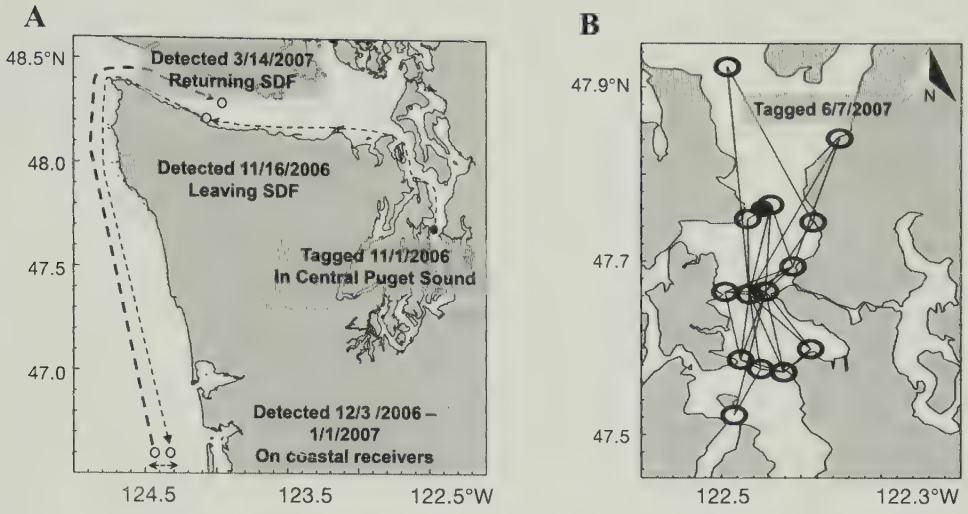

Figure 5

Examples of movement by individual Chinook salmon (*Oncorhynchus tshawytscha*) classified as (**A**) transient and (**B**) resident. The solid black circle in each panel indicates the tagging location, and open circles indicate receivers with that detected fish. The transient Chinook salmon (fish 37), tagged in central Puget Sound, left through the Strait of Juan de Fuca, was detected on the southern coast of Washington, and then returned to the Strait of Juan de Fuca. The resident Chinook salmon (fish 11) was tagged in central Puget Sound and detected at 14 receivers within central Puget Sound. The lines in panel B indicate movement of fish 11 between receivers.

surgically implanted acoustic tags (Hall et al., 2009; Rechisky and Welch[5]). The detected fish did not represent a different age-group and were assumed to be broadly representative of the tagged fish, however the movements and fate of the undetected fish were unknown. Interpretation of the detection data was further complicated by the uncertain origin of the individual fish, some of which may have originated outside Puget Sound. However, the transients did not leave Puget Sound synchronously, rather they departed at seemingly random times over much of the year. This variation in departure timing and the small size of fish suggests that individuals tagged that subsequently left did not do so as part of a spawning migration to rivers outside Puget Sound, but more likely as part of feeding migrations.

Chinook salmon in our study showed behavior similar to that of Puget Sound coho salmon studied similarly by Rohde et al. (2013). Of the Chinook salmon tagged and detected, 30% were classified as transients, and of the coho salmon tagged and detected, 20% were classified as transients according to the same criteria. Both species left Puget Sound throughout the year, showing no clear modal season, and for neither species did residents and transients differ in size, wild-hatchery origin, or time of year when tagged. Moreover, indices of site use at common receiver sites (numbers of fish detected, days with detections) were significantly correlated between the two species. In addition, coho and Chinook salmon that remained in Puget Sound as residents seldom moved from the central basin where they were tagged. Receivers in south Puget Sound and Hood Canal detected only 1 and 2 tagged fish, respectively. Few detections occurred in the Whidbey Basin as well. These areas are not devoid of resident Chinook salmon (Chamberlin et al., 2011) or coho salmon (Rohde et al., 2014), but both species tend to remain in one basin unless they leave Puget Sound entirely.

There were several significant differences between the movements of the 2 salmon species. Chinook salmon were detected on fewer different receivers, suggesting less overall movement than that of coho salmon, and Chinook salmon were also detected more often than coho salmon at receivers onshore and in shallower water. In addition, Chinook salmon showed weak and inconsistent diel activity patterns. In contrast, coho salmon were most active at shallow, onshore sites at night and deep, offshore sites during the day and were most often detected onshore near dawn and offshore in the afternoon (Rohde et al., 2013). These differences are also consistent with the pronounced differences in depth distributions and diel vertical movement reported by Smith et al. (2015) for coho and Chinook salmon in Puget Sound.

[5] Rechisky, E. L., and D. W. Welch. 2010. Surgical implantation of acoustic tags: influence of tag loss and tag-induced mortality on free-ranging and hatchery-held spring Chinook salmon (*Oncorhynchus tshawytscha*) smolts. *In* PNAMP Special Publication: Tagging, telemetry, and marking measures for monitoring fish populations: a compendium of new and recent science for use in informing technique and decision modalities (K. S. Wolf and J. S. O'Neal, eds.), p. 69–94. PNAMP Spec. Publ. 2010-002. Pacific Northwest Aquatic Monitoring Partnership, Duvall, WA. [Available from website]

Similar to the analysis of acoustically tagged coho and Chinook salmon, analysis of coded-wire tagging data also revealed differences and similarities that shed light on the phenomenon of residency (partial migration) of salmon. Residency seems much more prevalent with Chinook salmon (O'Neill and West, 2009; Chamberlin et al., 2011) than with coho salmon (Rohde et al., 2014), although it is not possible to precisely estimate the fraction for either species that adopts this behavior. However, the proportions of subyearling and yearlings adopting resident behavior were positively correlated between the two species among years, as well correlated with environmental variables (Rohde et al., 2014), suggesting common influences on behavior. In addition, salmon of both species that remain as residents in Puget Sound tend to be caught in natal basins more often than would happen by chance, although some movement certainly occurs (Chamberlin and Quinn, 2014; Rohde et al., 2014). Taken together, the combination of tagging and tracking studies for both species indicate that commonalities exceeded differences, and that the main difference was the greater prevalence of residency and somewhat more restricted movements within Puget Sound for Chinook salmon.

A number of diadromous species also exhibit alternative migratory behaviors that include resident forms of behavior similar to those of Puget Sound coho and Chinook salmon (Chapman et al., 2012a, Chapman et al. 2012b). Striped bass (*Morone saxatilis*) have both resident fish that do not leave the natal river or estuary and migratory fish that travel long distances in coastal waters. Clarke (1968) referred to these fish as contingents within populations, defined as "a group of fish that engage in a common pattern of seasonal migration between feeding areas, wintering areas, and spawning areas" (p. 320). Subsequent research with otolith microchemistry has revealed 3 distinct contingents: a resident group that remains in fresh water, a mesohaline group that occupies estuarine waters, and a migratory group that uses the coastal Atlantic Ocean (Secor, 1999). White perch (*M. americana*) displays 2 contingents; the great majority use estuarine habitats and a small fraction reside in rivers (Kerr et al., 2009). Individual white perch adopt one pattern or the other and do not switch patterns, whereas striped bass can shift between patterns (Zlokovitz et al., 2003).

The widespread occurrence of residency in diadromous species, such as salmonids, suggests advantages for having a portion of the population not undergo extensive ocean migrations. One explanation for the phenomenon is that resident fish, compared to ocean migrants, might be exposed to fewer predators (Emmett and Schiewe, 1997). However, one consequence of residency is slower growth than that of members of the cohort feeding in the ocean, as evidenced by smaller size at age in coho salmon (Milne, 1950; Pressey[1]; Rohde et al., 2014) and pink salmon (Pressey[1]), and the smaller size of resident Chinook salmon (Pressey[1]). Therefore, any hypothesis to explain residency must address this growth differential, as well as the greater prevalence of residency among Chinook than among coho salmon. Perhaps, because coho salmon tend to spend only a single winter at sea, the need to grow fast is greater than it is for Chinook salmon (Sandercock, 1991; Pearcy, 1992), which delay maturation and the corresponding return to spawn when growth is reduced (Healey, 1991).

In Puget Sound, the incidence of transients, some of which later return from the coast and resume residency in the sound, implies behavioral patterns that reflect modes along a continuum rather than discrete variants. This variability contributes to the "portfolio effect" (where diversification minimizes the risk of instability) for Chinook salmon and coho salmon, although in the face of broad regime shifts and anthropogenic effects across the entire region, it has not precluded declines in the species. The processes affecting migratory decisions, whether physiological (e.g., growth rate, lipid deposition, hormone levels) or environmental (e.g., water temperature, prey availability) remain unknown. However, the contribution of these drivers differs for coho salmon, because residency is less often displayed, compared with Chinook salmon. Regardless, although not likely accounting for a large portion of Salish Sea salmonids, partial migration and late migration strategies could justify adjustment to calculations of early marine mortality in Chinook salmon survival studies such as that of Neville et al. (2015), and the concept could be explored for other species, such as sockeye salmon (*Oncorhynchus nerka*) (Wood et al., 2012).

In summary, Chinook salmon display a wide range of alternative migration patterns. These patterns include those of nonanadromous males that mature as parr (Gebhards, 1960; Pearsons et al., 2009; Johnson et al., 2012), of juveniles that migrate to sea in their first or second year of life (Taylor, 1990; Healey, 1991), and of anadromous fish that remain as residents in protected marine waters (Pressey[1]) or that migrate to the coast or the open North Pacific Ocean (Healey, 1983; Sharma and Quinn, 2012). This list should also include variants, such as those termed transients, fish initially adopting residency and then moving to the outer coast, and some that return to Puget Sound before maturation. Although the sample size and approach used in our study cannot precisely quantify the degree of prevalence of late migration and partial migration strategies, these are behaviors clearly adopted by a portion of the population as a whole.

Alternative patterns of migration, as well as the presence of nonmigratory and migratory animals, can enhance the resilience of populations (Kerr et al., 2010) because the fish experience different regimes of growth and mortality. The reduced growth of resident salmon compared with those feeding along the coast is balanced against the higher survival rates of resident fish. Survival rates of coho salmon entering the Salish Sea are higher on average than coho salmon of coastal populations but the survival rates in these regions have shown different trajectories over the past decades (Zimmerman et al., 2015). Assuming similar patterns

with Chinook salmon, the resident component of the population complex might enjoy higher overall fitness in some regimes and lower in others, effectively buffering the complex as a whole. If so, variants in migratory patterns may contribute to the capacity of Chinook salmon to persist during periods when environmental conditions in some marine habitats are less favorable.

Acknowledgments

We appreciate K. Dobszynski, J. Chamberlin, J. Hall, and T. Sandell, among many others for aid with fieldwork and F. Goetz, Washington Department of Fish and Wildlife, the U.S. Army Corps of Engineers, Seattle Aquarium, Seattle City Light, the Nisqually and Squaxin Tribes, Beam Reach, and the Pacific Ocean Shelf Tracking Project. D. Spilsbury-Pucci, S. Moore and S. O'Neill gave invaluable input and interpretation. Partial funding for this project was provided by the State of Washington's Salmon Recovery Funding Board, National Marine Fisheries Service, and others.

Literature cited

Agostinelli, C., and U. Lund.
2013. R package 'circular': circular statistics (version 0.4-7). [Available from website.]

Arostegui, M. C., J. M. Smith, A. N. Kagley, D. Spilsbury-Pucci, K. L. Fresh, and T. P. Quinn.
2017. Spatially clustered movement patterns and segregation of subadult Chinook salmon within the Salish Sea. Mar. Coast. Fish. 9:1–12.

Anderson, R. O., and R. M. Neumann.
1996. Length, weight, and associated structural indices. *In* Fisheries Techniques, 2nd ed. (B. R. Murphy, and D. W. Willis, eds.), p. 447–481. Am. Fish. Soc., Bethesda, MD.

Andrews, K. S., and T. P. Quinn.
2012. Combining fishing and acoustic monitoring data to evaluate the distribution and movements of spotted ratfish *Hydrolagus colliei*. Mar. Biol. 159:769–782.

Brannon, E., and A. Setter.
1989. Marine distribution of a hatchery fall Chinook salmon population. *In* Proceedings of the salmonid migration and distribution symposium; Trodheim, Norway, 23–25 June 1987 (E. Brannon and B. Jonsson, eds.), p. 63–69. Univ. Washington, Seattle, WA.

Buckley, R. M.
1969. Analysis of the Puget Sound sport fishery for resident coho salmon, *Oncorhynchus kisutch* (Walbaum). M.S. thesis, 73 p. Univ. Wash., Seattle, WA.

Chamberlin, J. W., and T. P. Quinn.
2014. Effects of natal origin on localized distributions of Chinook salmon, *Oncorhynchus tshawytscha*, in the marine waters of Puget Sound, Washington. Fish. Res. 153:113–122.

Chamberlin, J. W., T. E. Essington, J. W. Ferguson, and T. P. Quinn.
2011. The influence of hatchery rearing practices on salmon migratory behavior: Is the tendency of Chinook salmon to remain within Puget Sound affected by size and date of release? Trans. Am. Fish. Soc. 140:1398–1408.

Chapman, B. B., K. Hulthén, J. Brodersen, P. A. Nilsson, C. Skov, L.-A. Hansson, and C. Brönmark.
2012a. Partial migration in fishes: causes and consequences. J. Fish Biol. 81:456–478.

Chapman, B. B., C. Skov, K. Hulthén, J. Brodersen, P. A. Nilsson, L.-A. Hansson, and C. Brönmark.
2012b. Partial migration in fishes: definitions, methodologies and taxonomic distribution. J. Fish Biol. 81:479–499.

Clark, J.
1968. Seasonal movements of striped bass contingents of Long Island Sound and the New York Bight. Trans. Am. Fish. Soc. 97:320–343.

Cullon, D. L., M. B. Yunker, C. Alleyne, N. J. Dangerfield, S. O'Neill, M. J. Whiticar, and P. S. Ross.
2009. Persistent organic pollutants in Chinook salmon (*Oncorhynchus tshawytscha*): implications for resident killer whales of British Columbia and adjacent waters. Environ. Toxicol. Chem. 28:148–161.

Dodson, J. J., N. Aubin-Horth, V. Thériault, and D. J. Páez.
2013. The evolutionary ecology of alternative migratory tactics in salmonid fishes. Biol. Rev. Camb. Philos. Soc. 88:602–625.

Emmett, R. L., and M. H. Schiewe (eds.).
1997. Estuarine and ocean survival of northeastern Pacific salmon: proceedings of the workshop. NOAA Tech. Memo. NMFS-NWFSC-29, 313 p.

Federal Register.
2005. Endangered and threatened species: final listing determinations for 16 ESUs of West Coast salmon, and final 4(d) protective regulations for threatened salmonid ESUs. Fed. Regist. 70:37160–37204. [Available from website.]

Gahagan, B. I., D. A. Fox, and D. H. Secor.
2015. Partial migration of striped bass: revisiting the contingent hypothesis. Mar. Ecol. Prog. Ser. 525:185–197.

Gebhards, S. V.
1960. Biological notes on precocious male Chinook salmon parr in the Salmon River drainage, Idaho. Prog. Fish-Cult. 22:121123.

Hall, J. E., J. Chamberlin, A. N. Kagley, C. Greene, and K. L. Fresh.
2009. Effects of gastric and surgical insertions of dummy ultrasonic transmitters on juvenile Chinook salmon in seawater. Trans. Am. Fish. Soc. 138:52–57.

Hayes, M. C., S. P. Rubin, R. R. Reisenbichler, F. A. Goetz, E. Jeanes, and A. McBride.
2011. Marine habitat use by anadromous bull trout from the Skagit River, Washington. Mar. Coast. Fish. 3:394–410.

Healey, M. C.
1983. Coastwide distribution and ocean migration patterns of stream- and ocean-type Chinook salmon, *Oncorhynchus tshawytscha*. Can. Field-Nat. 97:427–433.
1991. Life history of Chinook salmon (*Oncorhynchus tshawytscha*). *In* Pacific salmon life histories (C. Groot and L. Margolis, eds.), p. 311–393. UBritishC Press, Vancouver, Canada.

Healey, M. C., and C. Groot.
1987. Marine migration and orientation of oceantype Chinook and sockeye salmon. Am. Fish. Soc. Symp. 1:298–312.

Hickie, B. E., P. S. Ross, R. W. MacDonald, and J. K. B. Ford.
2007. Killer whales (*Orcinus orca*) face protracted health risks associated with lifetime exposure to PCBs. Environ. Sci. Technol. 41:6613–6619.

Johnson, J., T. Johnson, and T. Copeland.
2012. Defining life histories of precocious male parr, minijack, and jack Chinook salmon using scale patterns. Trans. Am. Fish. Soc. 141:1545–1556.

Jonsson, B., and N. Jonsson.
1993. Partial migration: niche shift versus sexual maturation in fishes. Rev. Fish Biol. Fish. 3:348–365.

Kendall, N. W., J. R. McMillan, M. R. Sloat, T. W. Buehrens, T. P. Quinn, G. R. Pess, K. V. Kuzishchin, M. M. McClure, and R. W. Zabel.
2015. Anadromy and residency in steelhead and rainbow trout (*Oncorhynchus mykiss*): a review of the processes and patterns. Can. J. Fish. Aquat. Sci. 72:319–342.

Kerr, L. A., D. H. Secor, and P. M. Piccoli.
2009. Partial migration of fishes as exemplified by the estuarine-dependent white perch. Fisheries 34:114–123.

Kerr, L. A., S. X. Cadrin, and D. H. Secor.
2010. The role of spatial dynamics in the stability, resilience, and productivity of an estuarine fish population. Ecol. Appl. 20:497–507.

Klemetsen, A., P.-A. Amundsen, J. B. Dempson, B. Jonsson, N. Jonsson, M. F. O'Connell, and E. Mortensen.
2003. Atlantic salmon *Salmo salar* L., brown trout *Salmo trutta* L. and Arctic charr *Salvelinus alpinus* (L.): a review of aspects of their life histories. Ecol. Freshw. Fish. 12:1–59.

Lucas, M. C., and E. Baras.
2001. Migration of freshwater fishes, 440 p. Blackwell Science, Ltd., Oxford, UK.

Melnychuk, M. C., D. W. Welch, C. J. Walters, and V. Christensen.
2007. Riverine and early ocean migration and mortality patterns of juvenile steelhead trout (*Oncorhynchus mykiss*) from the Cheakamus River, British Columbia. Hydrobiologia 582:55–65.

Milne, D. J.
1950. The difference in the growth rate of coho salmon on the east and west coasts of Vancouver Island in 1950. Fish. Res. Board Can., Prog. Rep. Pacific Coast Stn. 85:80–82.

Moore, M. E., B. A. Berejikian, and E. P. Tezak.
2010. Early marine survival and behavior of steelhead smolts through Hood Canal and the Strait of Juan de Fuca. Trans. Am. Fish. Soc. 139:49–61.

Myers, J. M., R. G. Kope, G. J. Bryant, D. Teel, L. J. Lierheimer, T. C. Wainwright, W. S. Grant, F. W. Waknitz, K. Neely, S. T. Lindley, and R. S. Waples.
1998. Status review of Chinook salmon from Washington, Idaho, Oregon, and California. NOAA Tech. Memo. NMFSNWFSC35, 443 p.

Neville, C. M., R. J. Beamish, and C. M. Chittenden.
2015. Poor survival of acoustically-tagged juvenile Chinook salmon in the Strait of Georgia, British Columbia, Canada. Trans. Am. Fish. Soc. 141:25–33.

NRC (National Research Council).
1996. Upstream: salmon and society in the Pacific Northwest, 452 p. The National Academies Press, Washington, DC.

O'Neill, S. M., and J. E. West.
2009. Marine distribution, life history traits, and the accumulation of polychlorinated biphenyls in Chinook salmon from Puget Sound, Washington. Trans. Am. Fish. Soc. 138:616–632.

Orsi, J. A., and H. W. Jaenicke.
1996. Marine distribution and origin of prerecruit Chinook salmon, *Oncorhynchus tshawytscha*, in southeastern Alaska. Fish. Bull. 94:482–497.

Pearcy, W. G.
1992. Ocean ecology of North Pacific salmonids, 179 p. Univ. Wash. Press, Seattle, WA.

Pearsons, T. N., C. L. Johnson, B. B. James, and G. M. Temple.
2009. Abundance and distribution of precociously mature male spring Chinook salmon of hatchery and natural origin in the Yakima River. North Am. J. Fish. Manage. 29:778–790.

Quinn, T. P., and R. D. Brodeur.
1991. Intraspecific variations in the movement patterns of marine animals. Am. Zool. 31:231–241.

Quinn, T. P., and K. W. Myers.
2004. Anadromy and the marine migrations of Pacific salmon and trout: Rounsefell revisited. Rev. Fish Biol. Fish. 14:421–442.

R Core Team.
2015. R: a language and environment for statistical computing. R Foundation for Statistical Computing, Vienna, Austria. [Available from website, accessed June 2015].

Rechisky, E. L., D. W. Welch, A. D. Porter, M. C. Jacobs-Scott, and P. M. Winchell.
2013. Influence of multiple dam passage on survival of juvenile Chinook salmon in the Columbia River estuary and coastal ocean. Proc. Nat. Acad. Sci. USA 110:6883–6888.

Rohde, J., A. N. Kagley, K. L. Fresh, F. A. Goetz, and T. P. Quinn.
2013. Partial migration and diel movement patterns in Puget Sound coho salmon. Trans. Am. Fish. Soc. 142:1615–1628.

Rohde, J., K. L. Fresh, and T. P. Quinn.
2014. Factors affecting partial migration in Puget Sound coho salmon. North Am. J. Fish. Manage. 34:559–570.

Sandercock, F. K.
1991. Life history of coho salmon (*Oncorhynchus kisutch*). *In* Pacific salmon life histories (C. Groot and L. Margolis, eds.), p. 395–445. Univ. British Columbia Press, Vancouver, Canada.

Secor, D. H.
1999. Specifying divergent migrations in the concept of stock: the contingent hypothesis. Fish. Res. 43:13–34.
2015. Migration ecology of marine fishes, 304 p. Johns Hopkins Univ. Press, Baltimore, MD.

Sharma, R., and T. P. Quinn.
2012. Linkages between life history type and migration pathways in freshwater and marine environments for Chinook salmon, *Oncorhynchus tshawytscha*. Acta Oecol. 41:1–13.

Smith, J. M., K. L. Fresh, A. N. Kagley, and T. P. Quinn.
2015. Ultrasonic telemetry reveals seasonal variation in depth distribution and diel vertical migrations of subadult Chinook and coho salmon in Puget Sound. Mar. Ecol. Prog. Ser. 532:227–242.

Taylor, E. B.
1990. Environmental correlates of life-history variation in juvenile Chinook salmon, *Oncorhynchus tshawytscha* (Walbaum). J. Fish Biol. 37:1–17.

Trudel, M., J. Fisher, J. A. Orsi, J. F. T. Morris, M. E. Thiess, R. M. Sweeting, S. Hinton, E. A. Fergusson, and D. W. Welch.
2009. Distribution and migration of juvenile Chinook salmon derived from coded wire tag recoveries along the continental shelf of western North America. Trans. Am. Fish. Soc. 138:1369–1391.

Weitkamp, L. A.
2010. Marine distributions of Chinook salmon from the west coast of North America determined by coded wire tag recoveries. Trans. Am. Fish. Soc. 139:147–170.

Welch, D. W., M. C. Melnychuk, E. R. Rechisky, A. D. Porter, M. C. Jacobs, A. Ladouceur, R. S. McKinley, and G. D. Jackson.
2009. Freshwater and marine migration and survival of endangered Cultus Lake sockeye salmon (*Oncorhynchus nerka*) smolts using POST, a large-scale acoustic telemetry array. Can. J. Fish. Aquat. Sci. 66:736–750.

Wood, C. C., and C. J. Foote.
1996. Evidence for sympatric genetic divergence of anadromous and nonanadromous morphs of sockeye salmon (*Oncorhynchus nerka*). Evolution 50:1265–1279.

Wood, C. C., D. W. Welch, L. Godbout, and J. Cameron.
2012. Marine migratory behavior of hatchery-reared anadromous and wild non-anadromous sockeye salmon revealed by acoustic tags. Am. Fish. Soc. Symp. 76:289–311.

Zimmerman, M. S., J. R. Irvine, M. O'Neill, J. H. Anderson, C. M. Greene, J. Weinheimer, M. Trudel, and K. Rawson.
2015. Spatial and temporal patterns in smolt survival of wild and hatchery coho salmon in the Salish Sea. Mar. Coast. Fish. 7:116–134.

Zlokovitz, E. R., D. H. Secor, and P. M. Piccoli.
2003. Patterns of migration in Hudson River striped bass as determined by otolith microchemistry. Fish. Res. 63:245–259.

National Marine
Fisheries Service
NOAA

Fishery Bulletin
established in 1881

Spencer F. Baird
First U.S. Commissioner
of Fisheries and founder
of *Fishery Bulletin*

Diel differences in abundance and diversity of fish species and blue crab (*Callinectes sapidus*) in the sandy beach shore zone of lower Delaware Bay

Michael P. Torre (contact author)
Danielle M. Lifavi
Timothy E. Targett

Email address for contact author: torrem27@gmail.com

School of Marine Science and Policy
University of Delaware
112 Smith Laboratory
Lewes, Delaware 19958
Present address for contact author: School of Marine Sciences
University of Maine
223 Libby Hall
Orono, Maine 04469

Abstract—Diel sampling was conducted during June–September 2013, in the shore zone and adjacent nearshore zone of Delaware Bay, Delaware, to identify day and night changes in nekton density, species richness, and the species assemblage. Mean species richness and total nekton density in the shore zone were higher at night. A detailed examination of abundant species revealed that bay anchovy (*Anchoa mitchilli*), weakfish (*Cynoscion regalis*), spot (*Leiostomus xanthurus*), and blue crab (*Callinectes sapidus*) occurred in higher densities in the shore zone at night than during the day. Bluefish (*Pomatomus saltatrix*) occurred in higher densities during the day. Additionally, small (<20 mm in fork length) Atlantic silverside (*Menidia menidia*) and bay anchovy, were observed in abundance in the shore zone only during daytime. Day and night differences in predator–prey dynamics were likely a primary driver of diel differences in nekton abundances observed in the shore zone. No diel differences in species richness, nekton density, or species assemblage were found in the adjacent nearshore area. Daytime sampling predominates in studies of shore-zone nekton and our results show the value of also sampling at night. Future research should include samples throughout the diel cycle and include tagging and movement data to allow a better understanding of diel dynamics of nekton along sandy beach shores.

Manuscript submitted 16 December 2016
Manuscript accepted 29 August 2017.
Fish. Bull. 115:556–565 (2017).
Online publication date: 19 September 2017.
doi: 10.7755/FB.115.4.11

The views and opinions expressed or implied in this article are those of the author (or authors) and do not necessarily reflect the position of the National Marine Fisheries Service, NOAA.

Estuarine and ocean shore zones are known to support high nekton densities worldwide (Whitfield, 1999; Félix et al., 2007; Gondolo et al., 2011). Sandy beaches dominate the world's shorelines and are productive habitats serving important functions as nursery areas and migration pathways (McLachlan and Brown, 2006; Marin Jarrin and Shanks, 2011; Rodrigues and Vieira, 2013). Estuaries along the east coast of the U.S. are no exception and support many ecologically and economically important species during one or more of their life stages and are essential for the maintenance of coastal fisheries (Beck et al., 2001; Able et al., 2010).

Nekton assemblages along sandy estuarine beaches and ocean surf zones vary spatially and temporally in response to the dynamic nature of these environments (Layman, 2000; Marin Jarrin and Shanks, 2011). These dynamics include day-night changes which are reflected in the abundance and diel movement of many of the dominant shore zone species (Gibson and Robb, 1996; Becker and Suthers, 2014; Bennett et al., 2015). Interaction between predator and prey species is a major process driving the distribution of estuarine nekton **as** prey alter their distribution to inhabit shallow water refuge areas (Becker and Suthers, 2014). Despite the importance of diel variation, most studies of sandy beach shore zones have been conducted during the daytime, a period that allows the capture of only a portion of assemblage dynamics (Rountree and Able, 1993; Becker and Suthers, 2014).

Previous studies of diel variation in shore zone nekton assemblages have generally reported increased species richness, catch per unit of effort (CPUE) or density during nighttime (or both) (Horn, 1980; Ross et al., 1987; Layman, 2000; Gaelzer and Zalmon, 2008; Vasconcellos et al., 2010, 2011; Yeoh et al., 2017). There have, however, also been reports of greater species richness or higher densities of shore zone fish species (or both) during the day (Godefroid et al., 1998; Pessanha and Araújo,

2003; Yeoh et al., 2017). In a recent work (Torre and Targett, 2016), we reported habitat-specific differences in the shore zone nekton assemblage between beach and riprap in Delaware Bay and noted diel differences in abundance for some, but not all, species.

We examined differences in abundance and diversity of fishes and blue crab (*Callinectes sapidus*) in the sandy beach shore zone and adjacent nearshore of Delaware Bay. Specifically, total nekton density, species richness, and the density of individual species during the day and night were compared. In addition, sampling occurred concurrently with research that identified feeding patterns of selected dominant species (Torre and Targett, 2017) and this concurrence provided an opportunity to assess the potential role of predator–prey dynamics of the shore zone nekton over the diel temporal range.

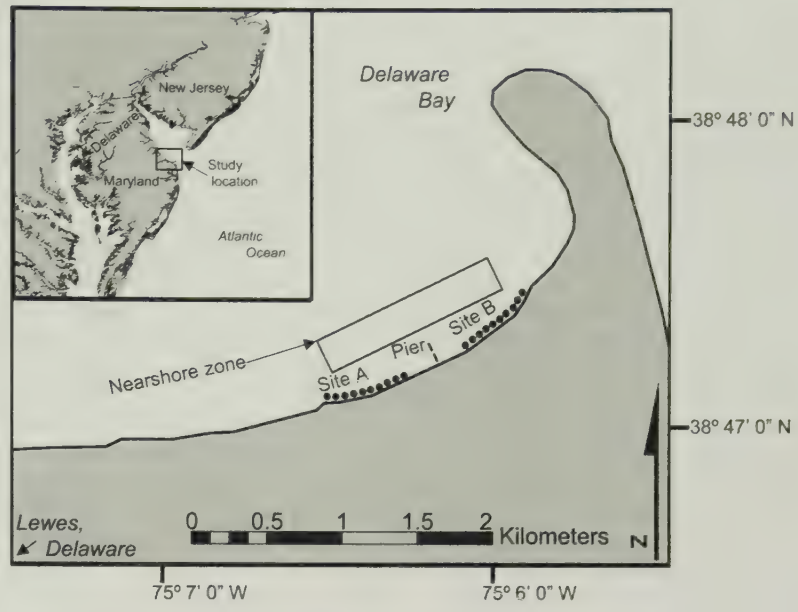

Figure 1

Map of the nearshore zone and the shore zone where sampling occurred during June–September 2013. Nearshore sampling occurred adjacent to the shore zone ~200–500 m from the shoreline. Shore sampling occurred along two ~400 m stretches of Delaware Bay beach. Black circles denote the 10 sampling locations at each shore zone site that were evenly spaced ~20 m from each other. Eight seining hauls (2 during the day and 2 at night) were conducted at 2 randomly chosen locations at site A and at site B each sampling week.

Materials and methods

Study area

Delaware Bay is a coastal plain estuary and one of the largest estuaries on the U.S. east coast (Bryant and Pennock, 1988; Pennock and Sharp, 1994). Unvegetated shore zones represent 74% of the bay's shoreline which is characterized by shallow, gradually sloping, sandy or muddy beaches that are often subject to wave erosion (de Sylva et al.[1]; Lathrop et al.[2]). The shore zone and nearshore waters support high densities of small forage and juvenile fish, and are feeding and spawning areas of adult fish (Shuster[3]; de Sylva et al.[1]; Able et al., 2007; Boutin, 2008). The fish fauna of Delaware Bay are dominated by species in the families Engraulidae, Atherinopsidae, Sciaenidae, Moronidae and Clupeidae (de Sylva et al.[1]; Bryant and Pennock, 1988; Torre and Targett, 2016). Blue crab are also abundant in Delaware Bay throughout their life history (Epifanio et al., 1984).

The study area in lower Delaware Bay (Fig. 1) included a gradually sloping beach area and a nearshore habitat composed of course sand and sandbars running parallel to shore ~200–500 m from low tide (tidal range ~1.4 m). Sampling sites were two ~400-m stretches of sandy beach and a single 300-m×1200-m area of nearshore habitat adjacent to the shore zone sites. The 2 stretches of beach (sites A and B; Fig. 1) were separated by a wooden pier, open beneath and perpendicular to the shoreline, and were >100 m from the pier. Each stretch of beach consisted of 10 potential seining locations, with their centers evenly spaced ~40 m apart (Fig. 1).

Macrofauna sampling

Shore zone sampling was conducted with a ~36-m bag seine (1.2 m high; 3.5-mm mesh) every 2 weeks from June through September 2013. Eight seine hauls were taken each sampling week, 2 during daytime and 2 at night, at each of the 2 sites (Fig. 1). Specific seining locations were randomly chosen from the 10 possible at each site (Fig. 1); and if the second location was adjacent to the first, a different one was randomly selected to minimize effects of spatial autocorrelation. Day sampling occurred between 1 h after sunrise and 1 h before sunset, and night sampling between 1 h after sunset

[1] de Sylva, D. P., F. A. Kalber Jr., and C. N. Shuster Jr. 1962. Fishes and ecological conditions in the shore zone of the Delaware River estuary, with notes on other species collected in the deeper water. Univ. Delaware Mar. Lab., Info. Ser. Publ. 5, 164 p. Dep. Biol. Sci., Univ. Delaware, Newark, DE. [Available from website.]

[2] Lathrop, R. G., Jr., M. Allen, and A. Love. 2006. Mapping and assessing critical horseshoe crab spawning habitats of Delaware Bay, 36 p. Cent. Remote Sens. Spatial Anal., Rutgers Univ., New Brunswick, NJ. [Available from website.]

[3] Shuster, C. N., Jr. 1959. A biological evaluation of the Delaware River estuary. Univ. Delaware Mar. Lab., Info. Ser. Publ. 3, 75 p. Dep. Biol. Sci., Univ. Delaware, Newark, DE. [Available from website.]

and 1h before sunrise, during mid-tide and separate 24-h periods. In total, 64 seine-hauls were conducted, 32 during daytime and 32 at night.

Seining covered the intertidal and shallow subtidal area to ~1.5 m depth. The following procedure (after Giordano) was used to quickly enclose the sampling area and minimize loss of large mobile fish: 1) One end of the net was held on the shoreline; 2) the other end was deployed quickly (<45 s) off the bow of a boat, along an elliptical path from that shore point, to enclose the area immediately adjacent to the ~27 m section of shore; 3) both ends of the net were then slowly moved together along the shore; and 4) once the ends were together the net was pulled in, forcing all enclosed fish and crabs into the bag. During nighttime sampling, headlamps were illuminated immediately after step 2 to facilitate the subsequent steps and to observe the catch as it was brought into the net.

The adjacent nearshore area (Fig. 1) was sampled once each month during day and night in July, August, and September. Each sampling effort consisted of 3 tows (10 min at 1–1.5 m/s) in 3–6 m depth with a 6-m otter trawl (10-mm mesh; 5-mm mesh bag liner) during day and night. In total 18 trawl tows were conducted, 9 during the day and 9 at night.

Fish and blue crab were counted and measured to the nearest millimeter (for species with >20 individuals, a random subsample of 20 was measured); fork length (FL) for fish with forked tails, total length (TL) for other species, and carapace width (CW) for blue crab. The area sampled was calculated to convert relative measures of abundance into density. For the shore zone the formula for a half ellipse was used:

$$Area = \frac{1}{2}\pi ab,$$

where a = half the length of the enclosed shoreline; and
b = the distance between shoreline and the apogee of the net.

Values for a and b were measured by setting the seine 5 times during a nonsampling trial and estimated values were a=13.5 m and b=10.0 m. For the nearshore, the following equation was used:

$$Area = wl,$$

where w = the estimated average width of trawl during operation (6 m); and
l = the tow length.

Water temperature and salinity at the time of sampling were measured 0.5 m below the water surface using a dissolved oxygen meter (YSI, Inc.[4], Yellow Springs, OH).

Data analyses

Mean density and species richness of fish and blue crab at both day and night were compared for both shore zone and nearshore samples. Potential differences in sampling efficiency and species selectivity between the seine net used in shore zone sampling and the otter trawl used in nearshore sampling precluded statistical comparisons between the 2 areas. Two-factor analysis of variance (ANOVA) was used to test for significant (α=0.05) diel and site differences in total nekton density and species richness in the shore zone. Significant diel and site differences in density of individual species that accounted for >1% of the total catch in the shore zone were tested with randomization tests for 2-factor ANOVA (α=0.01). The latter analysis is a nonparametric version of a 2-factor ANOVA that is more robust for the non-normally distributed data and frequent occurrence of zeros (Anderson and Braak, 2003) that resulted from subsetting total nekton density data into individual species. Student's t-tests were used to test for diel differences in total nekton density and species richness in the nearshore. Significant diel differences in the density of individual species that accounted for >1% of the total catch in the nearshore area were tested with a randomization test (α=0.01) in place of Student's t-test for the same reasons noted above (Tebbs and Bower, 2003). Randomization tests were carried out with R software, vers. 2.11.0 (R Core Development Team, 2010), and the critical level of significance was adjusted from α=0.05 to α=0.01 to account for multiple testing.

One-factor ANOVA was used to test for significant (α=0.01) diel differences in the length of species that accounted for >1% of total catch in shore zone and nearshore samples. When unequal variances violated the assumptions of the ANOVA, a Kruskal-Wallis H test was used instead and the critical level of significance was adjusted from α=0.05 to α=0.01 to account for multiple testing.

Differences in species assemblages between day and night in the shore zone and the nearshore were analyzed by using a multivariate approach with nonmetric multidimensional scaling (NMDS) and adonis procedures. The vegan package, vers. 1.13-8, within R software (vers. 2.11.0) was used for this analysis (Oksanen et al., 2008; R Core Development Team, 2010). This approach allows comparison of species assemblages by considering all species present and their abundances. Mean density of each species during day and night was calculated by pooling data from the 2 replicate seine hauls at each site to reduce variability in the analysis. Density data were square root transformed and similarity matrices were constructed for each site with the Bray–Curtis similarity measure. 2D plots depicting similarity of faunal assemblages between day and night were generated from similarity matrices generated with NMDS. Spider diagrams were overlaid upon 2D NMDS plots to show group centroids and spread. Significant variation in species assemblages was tested by using the adonis function in the vegan package (Oksanen et al., 2008). This function performs a permutational multiple analysis of variance (MANOVA) with Bray–Curtis similarity matrices to assign variation in

[4] Mention of trade names or commercial companies is for identification purposes only and does not imply endorsement by the National Marine Fisheries Service, NOAA.

Table 1

Frequency of occurrence and mean density (individuals/100 m^2), with standard error (SE), of dominant (>1% total catch for diel period) nekton species during day and night in the shore zone of lower Delaware Bay (see Fig. 1) from June through September 2013. Catch data from sites A and B are combined. Significant differences in mean density between day and night are indicated by asterisks according to the criteria: *=P<0.01, **=P<0.005, ***=P<0.001. The critical level of significance was adjusted from α=0.05 to α=0.01 to account for multiple testing. P-values are provided for differences between day and night; values for site interaction effect are not shown because no significant effects were detected. P-values are given for species that were not included in a species-specific test (>1% total catch for diel period). Species unique to the shore zone (not observed in the nearshore area) are denoted by $_s$. N/A=no statistical comparison was made because of low abundance.

	Total		Day		Night		
Species	Number	%catch	Frequency of occurrence	Mean density (SE)	Frequency of occurrence	Mean density (SE)	P-value: day vs. night
All species	6545	100.0	100.00	24.53 (4.63)	100.00	72.22 (11.82)	<0.001 ***
Menidia menidia $_s$	3368	51.3	96.88	17.97 (6.71)	100.00	32.23 (8.76)	0.03
Anchoa mitchilli	2129	32.4	59.38	2.18 (0.58)	96.88	31.05 (9.97)	<0.001 ***
Cynoscion regalis	275	4.2	12.50	0.47	56.25	7.10 (3.27)	<0.001 ***
Pomatomus saltatrix	154	2.3	65.63	2.94 (0.97)	37.50	0.90 (0.13)	<0.001 ***
Brevoortia tyrannus	110	1.7	18.75	8.10 (1.94)	15.63	0.66 (0.11)	0.06
Mugil cephalus $_s$	88	1.3	15.63	5.09 (1.02)	34.38	1.46 (0.20)	0.27
Callinectes sapidus	85	1.3	25.00	0.53 (0.04)	59.38	1.89 (0.37)	<0.001 ***
Leiostomus xanthurus	70	1.1	12.50	0.59 (0.06)	43.75	2.19 (0.59)	<0.001 ***
Trachinotus carolinus	55	0.8	31.25	1.08 (0.12)	25.00	1.89 (0.32)	N/A
Micropogonias undulatus	51	0.8	9.38	0.79 (0.07)	40.63	1.67 (0.61)	N/A
Strongylura marina $_s$	39	0.6	3.13	0.47	34.38	1.63 (0.41)	N/A
Bairdiella chrysoura	35	0.5	15.63	2.64 (0.08)	15.63	0.66 (0.06)	N/A
Menticirrhus saxatilis	34	0.5	18.75	0.86 (0.12)	37.50	0.90 (0.15)	N/A
Paralichthys dentatus	10	0.2	3.13	0.47	21.88	0.61 (0.05)	N/A
Selene vomer	7	0.1	12.50	0.47	9.38	0.47 (0.05)	N/A
Fundulus heteroclitus $_s$	6	0.1	0.00	0.00	9.38	0.94 (<0.01)	N/A
Sphoeroides maculatus $_s$	6	0.1	6.25	0.47	9.38	0.63 (<0.01)	N/A
Fundulus majalis $_s$	4	0.1	6.25	0.71 (0.08)	3.13	0.47 (0.06)	N/A
Pseudopleuronectes americanus	4	0.1	6.25	0.47	6.25	0.47	N/A
Chilomycterus schoepfii	3	0.0	0.00	0.00	9.38	0.47	N/A
Pogonias cromis	3	0.0	6.25	0.47	3.13	0.47	N/A
Astroscopus guttatus $_s$	2	0.0	0.00	0.00	6.25	0.47	N/A
Clupea harengus $_s$	1	0.0	0.00	0.00	3.13	0.47	N/A
Dasyatis americana $_s$	1	0.0	0.00	0.00	3.13	0.47	N/A
Hyporhamphus meeki $_s$	1	0.0	3.13	0.47	0.00	0.00	N/A
Lagodon rhomboides $_s$	1	0.0	0.00	0.00	3.13	0.47	N/A
Ophidion marginatum $_s$	1	0.0	0.00	0.00	0.00	0.47	N/A
Peprilus triacanthus	1	0.0	0.00	0.00	3.13	0.47	N/A
Syngnathus fuscus	1	0.0	3.13	0.47	0.00	0.00	N/A

species assemblage data that was due to explanatory variables (day and night). The number of permutations used was 999.

Results

Shore zone and nearshore temperature ranged from ~20.5–25.0°C during June through September 2013. Slightly higher temperatures were measured in the shore zone during the day (20.6–25.0°C) than at night (20.7–23.4°C). Nearshore temperatures were also slightly higher during the day (22.0–23.5°C) than at night (20.0–23.1°C). Salinity values ranged from ~21–29 and were similar between day and night and between the shore zone and nearshore areas.

A total of 9719 fish and blue crab were captured in the shore zone and nearshore area, representing 38 species. The assemblage comprised members of the families Atherinopsidae, Engraulidae, Sciaenidae, Pomatomidae, Clupeidae, Mugilidae, and Portunidae.

Fish density in the shore zone (Table 1) was dominated by Atlantic silverside (*Menidia menidia*, 51%), bay anchovy (*Anchoa mitchilli*, 32%), weakfish (*Cynoscion regalis*, 4%), and bluefish (*Pomatomus saltatrix*, 2%). Total nekton density in the shore zone was

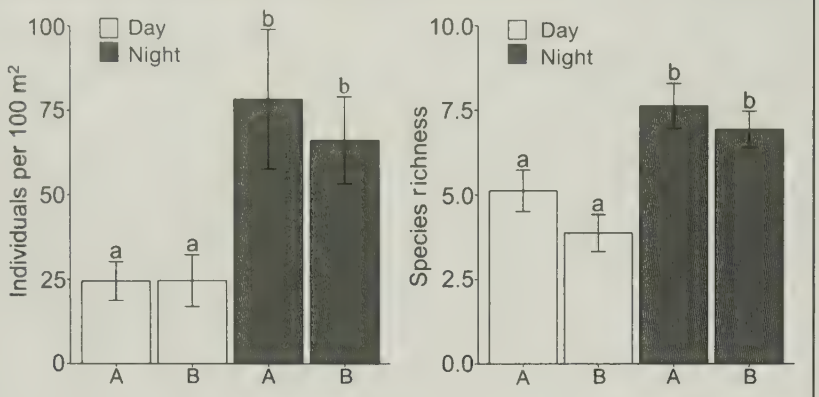

Figure 2

Mean density (individuals/100 m^2) and mean species richness of nekton per seine haul at shore zone sampling sites A and B (Fig. 1) during day and night in lower Delaware Bay in June–September 2013. Columns with the same letter are not significantly different from each other (P<0.05). Error bars indicate standard errors of the means.

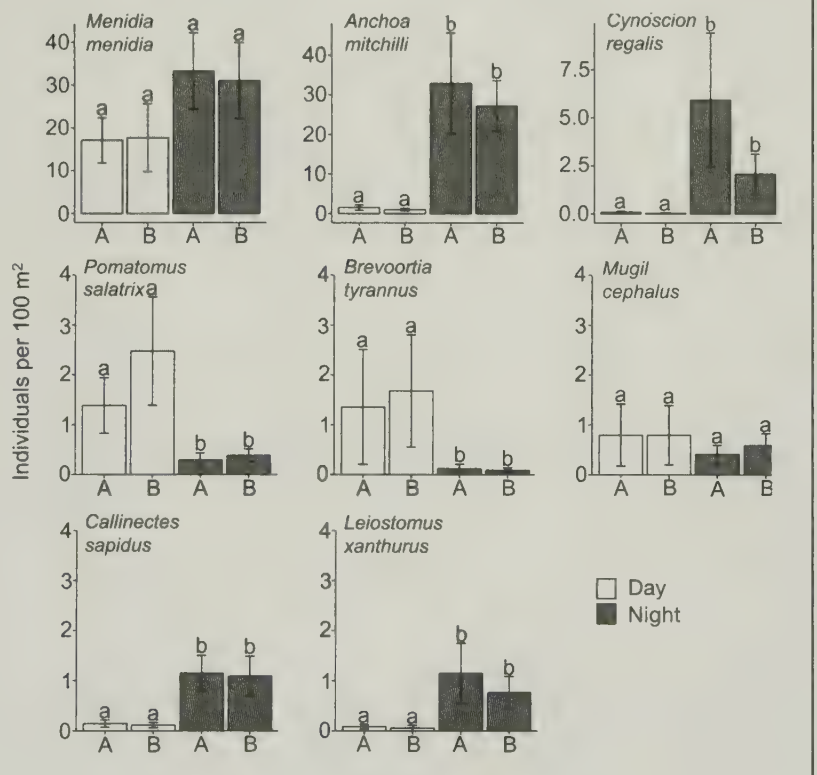

Figure 3

Mean density (individuals/100 m^2) of dominant species (>1% of total catch) per seine haul at shore zone sites A and B (Fig. 1) during day and night in lower Delaware Bay in June–September, 2013. Columns with the same letter are not significantly different from each other (P<0.05). Error bars indicate standard errors of the means.

94% higher at night than during the day (P<0.001) and was similar between the 2 sampling sites (P=0.750), with no interaction between time of day and site (P=0.829; Table 1, Fig. 2). Diel density differences were also found for a number of dominant shore zone species but there were no significant differences between sites or interaction effects. Bay anchovy, weakfish, spot (*Leiostomus xanthurus*), and blue crab occurred in the shore zone in significantly higher densities at night, whereas bluefish had significantly higher density during the day (Fig. 3). Mean species richness per seine haul in the shore zone was 62% higher (P<0.001) at night (7.3 [standard error (SE) 0.8]) than during the day (4.5 [SE 0.8]) and was similar for the 2 sampling sites (P=0.108), with no interaction (P=0.637; Fig. 2).

In the adjacent nearshore sampling area (Table 2), density was dominated by bay anchovy (73%), spot (11%), and weakfish (9%). Several species were unique to either the shore zone or nearshore sampling areas (Tables 1 and 2). Nearshore fish density was not significantly different during day and night (P=0.19, Table 2) and no species-specific differences in day and night densities were found (Table 2). Species richness per tow in the adjacent nearshore sampling area was not statistically different (P=0.14) during the night (8.8 [SE 0.9]) and day (6.7 [SE 0.8]).

The size range of dominant species was generally similar during the day and night in the shore zone and nearshore (Table 3), with the exception of the size range of Atlantic menhaden (*Brevoortia tyrannus*, P=0.002) and striped mullet (*Mugil cephalus*, P<0.001). Larger Atlantic menhaden were present in the shore zone during day and not at night and larger striped mullet were present in the shore zone during the night and not during the day (Table 3). It is noted, however, that only 4 Atlantic menhaden were captured during night sampling.

Ordination of shore zone and nearshore density data by NMDS shows diel differences in the species assemblage in the shore zone but not in the nearshore area (Fig. 4). Permutational MANOVA shows that the diel period significantly explained 17%

Table 2

Frequency of occurrence and mean density (individuals/100 m^2), with standard error (SE), of dominant (>1% total catch for diel period) nekton taxa during day versus night in the nearshore area of lower Delaware Bay (see Fig. 1) from June through September 2013. Significant differences in mean density between day and night are indicated by asterisks according to the criteria: *=P<0.01, **=P<0.005, ***=P<0.001. The critical level of significance was adjusted from α=0.05 to α=0.01 to account for multiple testing. Taxa unique to the nearshore area (not observed in the shore zone) are denoted by $_n$. N/A=no statistical comparison was made because of low abundance.

	Total		Day		Night		
Species (or family)	Number	%catch	Frequency of occurrence	Mean density (SE)	Frequency of occurrence	Mean density (SE)	P-value: day vs. night
All taxa	3153	100.00	100.0	4.38 (1.20)	100.0	3.07 (0.65)	0.71
Anchoa mitchilli	2300	72.95	100.0	3.59 (1.26)	100.0	1.86	0.11
Leiostomus xanthurus	346	10.97	77.8	0.41 (0.25)	100.0	0.49	0.28
Cynoscion regalis	285	9.04	66.7	0.28 (0.15)	77.8	0.61	0.11
Peprilus triacanthus	57	1.81	66.7	0.11 (0.04)	55.6	0.12	0.44
Micropogonias undulatus	40	1.27	66.7	0.13 (0.03)	33.3	0.05	0.03
Callinectes sapidus	28	0.89	44.4	0.04 (0.01)	88.9	0.05	N/A
Pomatomus saltatrix	16	0.51	44.4	0.05 (0.01)	55.6	0.03	N/A
Selene vomer	16	0.51	44.4	0.04 (0.01)	33.3	0.06	N/A
Mustelus canis $_n$	13	0.41	33.3	0.02 (<0.01)	66.7	0.03	N/A
Trinectes maculatus $_n$	9	0.29	22.2	0.08 (0.03)	11.1	0.02	N/A
Pogonias cromis	8	0.25	11.1	0.02	33.3	0.05	N/A
Urophycis regia $_n$	8	0.25	22.2	0.05 (0.01)	44.4	0.02	N/A
Bairdiella chrysoura	6	0.19	11.1	0.11	22.2	0.02	N/A
Menticirrhus saxatilis	4	0.13	11.1	0.02	11.1	0.06	N/A
Paralichthys dentatus	3	0.10	0.0	0.00	33.3	0.02	N/A
Gymnuridae $_n$	2	0.06	0.0	0.00	22.2	0.02	N/A
Prionotus carolinus $_n$	2	0.06	0.0	0.00	22.2	0.02	N/A
Syngnathus fuscus	2	0.06	11.1	0.02	11.1	0.02	N/A
Brevoortia tyrannus	1	0.03	11.1	0.02	0.0	0.00	N/A
Chilomycterus schoepfii	1	0.03	0.0	0.00	11.1	0.02	N/A
Pseudopleuronectes americanus	1	0.03	0.0	0.00	11.1	0.02	N/A
Raja eglanteria $_n$	1	0.03	0.0	0.00	11.1	0.02	N/A
Trachinotus carolinus	1	0.03	11.1	0.02	0.0	0.00	N/A

of the variation in species assemblage in the shore zone (F=5.871, coefficient of multiple determination [R^2]=0.170, P<0.001), whereas site (F=0.336, R^2=0.009, P=0.956) and interaction (F=0.289, R^2=0.008, P=0.968) were not significant. No difference in the species assemblage was identified in relation to day and night in the adjacent nearshore area (F=1.506, R^2=0.086, P=0.185).

Discussion

We observed clear diel differences in nekton assemblage along the sandy beach shore zone in Delaware Bay and greater nekton density and higher species richness at night. Diel patterns were also evident in many of the most abundant species; higher densities were found at night in most cases. Ordination plots revealed distinct day and night groups (see Fig. 4) but showed a large spread within groups, which can be explained by seasonal variation in species assemblages, and which could be reduced with a shorter sampling period. These results expand on those noted by Torre and Targett (2016) and highlight the importance of investigating assemblage dynamics across the diel cycle.

Interaction between predators and prey is a major process driving the distribution of shallow water estuarine nekton (Baker and Sheaves, 2007; Becker and Suthers, 2014; Yeoh et al., 2017). Responding to predation pressure, prey species and small juveniles of larger species alter their distribution to inhabit shallow water refuge areas where low abundance of large, primarily piscivorous fishes is generally thought to decrease predation (Baker and Sheaves, 2007; Becker and Suthers, 2014). Predator–prey interactions are dynamic over the diel cycle because many piscivorous fishes use sight to locate and capture prey (Horodysky et al., 2008; Yeoh et al., 2017). On the basis of this concept and because abiotic conditions were similar for day and night, we believe the diel differences in shore-zone nekton observed in our study are largely driven by day and night differences in predator–prey dynamics.

Table 3

Size range and mean size, with standard error (SE), of dominant (>1% total catch) nekton species during day versus night in the shore zone and nearshore area of lower Delaware Bay (see Fig. 1) during June, July, and August 2013. Size was measured in fork length (FL), total length (TL), or carapace width (CW). Length comparisons (*P*-value column) are from one-factor analysis of variance (ANOVA) or Kruskal-Wallis *H* test, when unequal variances violated assumptions of the ANOVA. The critical level of significance was adjusted from α=0.05 to α=0.01 to account for multiple testing.

	Day		Night		
Species	Size range (mm)	Mean size (SE)	Size range (mm)	Mean size (SE)	*P*-value: day vs. night
Shore zone					
Anchoa mitchilli	FL: 30–115	60.23 (17.33)	35–94	58.92 (8.00)	0.090
Brevoortia tyrannus	FL: 68–112	84.79 (11.54)	55–89	70.57 (14.06)	0.002**
Callinectes sapidus	CW: 30–170	132.22 (44.38)	15–180	135.5 (27.55)	0.230
Cynoscion regalis	TL: 38–74	52.5 (15.33)	47–294	65.17 (28.14)	0.050
Leiostomus xanthurus	FL: 70–196	111.8 (49.44)	65–219	136.4 (49.01)	0.970
Menidia menidia	FL: 35–125	76.62 (10.76)	34–138	74.03 (11.86)	0.100
Mugil cephalus	FL: 57–187	88.02 (33.81)	65–158	128.15 (25.8)	<0.001***
Pomatomus saltatrix	FL: 24–155	100.82 (23.67)	89–205	123.65 (29.67)	0.030
Nearshore area					
Anchoa mitchilli	FL: 30–111	66.04 (14.08)	26–110	68.36 (11.38)	0.080
Cynoscion regalis	TL: 43–215	141.75 (30.62)	45–232	136.26 (37.37)	0.143
Leiostomus xanthurus	FL: 98–188	142.57 (18.66)	60–193	139.54 (24.05)	0.117
Micropogonias undulatus	TL: 155–227	195.18 (16.34)	147–195	181.86 (16.78)	0.050
Peprilus triacanthus	FL: 32–143	103.53 (31.51)	95–135	115.33 (9.41)	0.060

Concurrent sampling of stomach contents was conducted to identify feeding patterns of selected dominant species (Torre and Targett, 2017), providing an opportunity to consider the potential role of predator–prey dynamics in the diel differences seen in shore-zone nekton. Stomach content data from juvenile bluefish (mean: ~100 mm FL) collected in the shore zone during daytime (Torre and Targett, 2017) showed that they were feeding exclusively on juvenile (<20 mm FL) Atlantic silverside and bay anchovy. Although these prey were too small to be quantitatively sampled by the seine net, we saw large numbers of both species in this size range temporarily retained in the net during daytime sampling, but not at night, despite clear nighttime visibility provided by headlamps. A small number of these fish species were in the net when it was brought onto the beach but were not retained as the net was being moved to where the contents were counted. It is important to note that these small Atlantic silverside and bay anchovy showed a different diel abundance pattern than that of larger individuals (mean: Atlantic silverside, ~75 mm FL; bay anchovy, ~60 mm FL) that were vulnerable to the seine net and which were either not significantly different in abundance during day and during night (Atlantic silverside) or were higher in abundance at night (bay anchovy).

We speculate that the small Atlantic silverside and bay anchovy were abundant in the shore zone during the day because the shallow waters are a relative predation refuge (Torre and Targett, 2017). The bluefish is characterized as a daytime active predator on account of their visual capabilities (Horodysky et al., 2008), and Buckle and Conover (1997) observed that gut fullness of young-of-the-year bluefish in the Hudson River estuary was highest during the day. These small Atlantic silverside and bay anchovy were preyed upon by the small bluefish in the shore zone because bluefish become piscivorous relatively early in life (Scharf et al., 2009); however, predation mortality would still be reduced in comparison with that in adjacent deeper water with higher numbers of larger piscivorous fishes (Baker and Sheaves, 2007). Additionally, Yeoh et al. (2017) reported increased abundance of atherinids (silversides) and other small pelagic fishes in the shore zone during the day.

In contrast, juvenile weakfish were present in greater density in the shore zone at night and stomach content analysis of these individuals (Torre and Targett, 2017) showed that they were feeding almost exclusively on mysid shrimp (*Neomysis americana*). Weakfish are crepuscular and nocturnal predators (Horodysky et al., 2008) and this mysid species is known to undergo migration into surface or shallow waters during night (Hulburt, 1957; Hopkins, 1965). Grecay and Targett (1996) found that although feeding by juvenile weakfish was significantly reduced under dark conditions in the laboratory, fish were able to feed effectively if mysids occurred at sufficiently high density. Therefore, it is possible that weakfish moved into the shore zone at night in response to the higher concentrations of mysid shrimp.

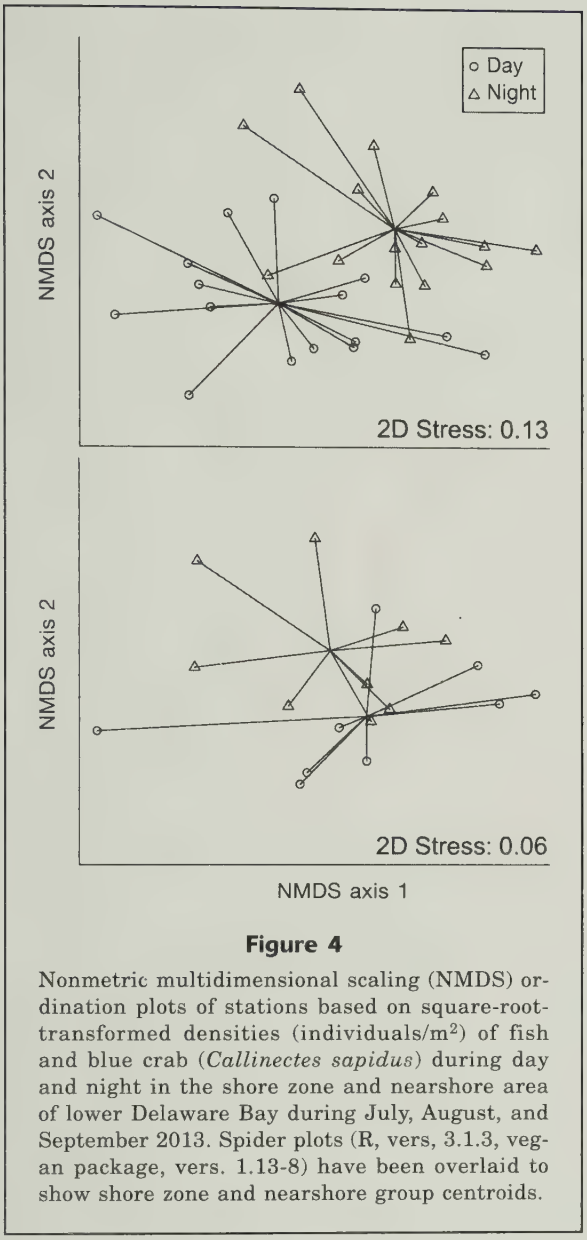

Figure 4

Nonmetric multidimensional scaling (NMDS) ordination plots of stations based on square-root-transformed densities (individuals/m^2) of fish and blue crab (*Callinectes sapidus*) during day and night in the shore zone and nearshore area of lower Delaware Bay during July, August, and September 2013. Spider plots (R, vers, 3.1.3, vegan package, vers. 1.13-8) have been overlaid to show shore zone and nearshore group centroids.

Avian predators may restrict some species to deeper water during the day because birds are higher-order predators in estuarine systems and can exert significant top-down pressure on nekton assemblages (Steinmetz et al., 2003; Yeoh et al., 2017). Bay anchovy are known to exhibit diel vertical movement, inhabiting deeper water during day (Vouglitoisa et al., 1987) and moving upward or into shallow water at night (Hagan and Able, 2008). Although we saw large numbers of small (<20 mm FL) bay anchovy in the shore zone during the day, larger individuals (mean: ~60 mm FL) were more dense in the shore zone at night, possibly as a response to both increased foraging opportunity on mysid shrimp, a staple of their diet (Hartman et al., 2004), and because of reduced avian predation.

Gear avoidance could affect sampling efficiency of mobile fish species (Říha et al., 2008) and contribute to differences in density and species richness between day and night samples. However, the seining methods used in our study were designed to rapidly enclose the sampling area and minimize escape of mobile species (Torre and Targett, 2016, 2017). Furthermore, Říha et al. (2008) reported either similar or higher sampling efficiency during daytime than at night with 10–50 m seine nets. Therefore, it seems unlikely that gear avoidance greatly impacted the observed diel differences in species densities in the shore zone.

As described above, several species were significantly more abundant in the shore zone during either day or night, a finding that would suggest onshore–offshore diel migrations; however, no diel patterns were evident in the adjacent nearshore habitat. Lack of diel changes in the nearshore could be a result of sufficiently different predator-dynamics in the shore zone than in the more extensive and deeper nearshore. Differences in water depth, over a relatively small horizontal distance, create advantages and disadvantages for predators and prey in the shallow shore zone. Prey fishes moving into and out of the shore zone on a diel basis can take advantage of a refuge from predation resulting from the size-specific spatial distribution patterns of piscivorous fish predators (Baker and Sheaves, 2007) and the associated predation constraints imposed on large fishes in very shallow water. There are also diel movements of invertebrate prey, such as mysids, creating potential foraging opportunities for some fish species (Hulburt, 1957; Hopkins, 1965), increased potential vulnerability to avian predation in shallow water (Steinmetz et al., 2003; Yeoh et al., 2017), and the interaction of all these processes with differences in visibility caused by the diel light cycle.

Clear diel differences in the species assemblage in the shore zone and distinct diel patterns in the abundance of several dominant species highlight that day sampling alone does not give a true reflection of the nekton assemblage in the sandy beach shore zone of Delaware Bay. The way we perceive habitat value and its functional role for fishes, including predator–prey interactions, are affected by a reliance on only daytime sampling and observations. Our results show the value of investigating shore-zone nekton dynamics over the diel cycle. Future research should include the following: sampling throughout the diel cycle and incorporating tagging and movement studies (Gibson et al., 2011; Yeoh et al., 2017); and assessment of the influence of lunar, tidal, and seasonal cycles (Gibson et al., 1998) to more fully understand diel movement dynamics of nekton along sandy beach shores.

Acknowledgments

We thank R. Dixon, M. Davidson, P. Kaestner, and A. Gruszkiewicz for field and laboratory assistance. We thank D. Miller for statistical advice and D. Taylor for

helpful comments on a thesis draft. We also thank 3 anonymous reviewers for their helpful comments. This research was supported by a grant from NOAA, National Centers for Coastal Ocean Science, Center for Sponsored Coastal Ocean Research (award number NA09NOS4780219) to T. Targett. This short contribution is publication no. 16-003 of the NOAA/CSCOR Mid-Atlantic Shorelines project.

Literature cited

Able, K. W., J. H. Balletto, S. M. Hagan, P. R. Jivoff, and K. Strait.
2007. Linkages between salt marshes and other nekton habitats in Delaware Bay, USA. Rev. Fish. Sci. 15:1–61.

Able, K. W., D. H. Wilber, A. Muzeni-Corino, and D. G. Clarke.
2010. Spring and summer larval fish assemblages in the surf zone and nearshore off northern New Jersey, USA. Est. Coast. 33:211–222.

Anderson, M., and C. T. Braak.
2003. Permutation tests for multi-factorial analysis of variance. J. Stat. Comput. Sim. 73:85–113.

Baker, R., and M. Sheaves.
2007. Shallow-water refuge paradigm: Conflicting evidence from tethering experiments in a tropical estuary. Mar. Ecol. Prog. Ser. 349:13–22.

Beck, M. W., K. L. Heck, K. W. Able, D. L. Childers, D. B. Eggleston, B. M. Gillanders, B. Halpern, C. G. Hays, K. Hoshino, T. J. Minello, et al.
2001. The identification, conservation, and management of estuarine and marine nurseries for fish and invertebrates: a better understanding of the habitats that serve as nurseries for marine species and the factors that create site-specific variability in nursery quality will improve conservation and management of these areas. BioScience 51:633–641.

Becker, A., and I. M. Suthers.
2014. Predator driven diel variation in abundance and behaviour of fish in deep and shallow habitats of an estuary. Est. Coast. Shelf Sci. 144:82-88.

Bennett, R. H., P. D. Cowley, A.-R. Childs, and T. F. Næsje.
2015. Movements and residency of juvenile white steenbras *Lithognathus lithognathus* in a range of contrasting estuaries. Est. Coast. Shelf Sci. 152:100–108.

Boutin, B. P.
2008. Tidal tributaries and nearshore areas as nursery habitat for juvenile sciaenid fishes and other estuarine nekton in Delaware Bay and the Delaware coastal bays. Ph.D. diss., 172 p. Univ. Delaware, Newark, DE.

Bryant, T. L., and J. R. Pennock.
1988. The Delaware estuary: rediscovering a forgotten resource, 144 p. Sea Grant Coll. Program, Univ. Delaware, Newark, DE.

Buckle, J. A., and D. O. Conover.
1997. Movements, feeding periods, and daily ration of piscivorus young-of-the-year bluefish, *Pomatomus salatrix*, in the Hudson River estuary. Fish. Bull. 95:665–679.

Epifanio, C. E., C. C. Valenti, and A. E. Pembroke.
1984. Dispersal and recruitment of blue crab larvae in Delaware Bay, U.S.A. Est. Coast. Shelf Sci. 18:1–12.

Félix, F. C., H. L. Spach, P. S. Moro, R. Schwarz Jr., C. Santos, C. W. Hackradt, and M. Hostim-Silva.
2007. Utilization patterns of surf zone inhabiting fish from beaches in Southern Brazil. Pan-Am. J. Aquat. Sci. 2:27–39.

Gaelzer, L. R., and I. R. Zalmon.
2008. Diel variation of fish community in sandy beaches of southeastern Brazil. Braz. J. Oceanogr. 56:23–29.

Gibson, R. N., and L. Robb.
1996. Piscine predation on juvenile fishes on a Scottish sandy beach. J. Fish Biol. 49:120–138.

Gibson, R. N., L. Pihl, M. T. Burrows, J. Modin, H. Wennhage, and L. A. Nickell.
1998. Diel movements of juvenile plaice *Pleuronectes platessa* in relation to predators, competitors, food availability and abiotic factors on a microtidal nursery ground. Mar. Ecol. Prog. Ser. 165:145–159.

Gibson, R. N., M. T. Burrows, and L. Robb.
2011. Field experiments on depth selection by juvenile plaice *Pleuronectes platessa*. Mar. Ecol. Prog. Ser. 430:197–205.

Godefroid, R. S., M. Hofstaetter, and H. L. Spach.
1998. Moon, tidal and diel influences on catch composition of fishes in the surf zone of Pontal do Sul beach, Paraná. Rev. Bras. Zool. 15:697–701.

Gondolo, G. F., G. M. T. Mattox, and P. T. M. Cunningham.
2011. Ecological aspects of the surf-zone ichthyofauna of Itamambuca Beach, Ubatuba, SP. Biota Neotrop. 11:183–192.

Grecay, P. A., and T. E. Targett.
1996. Effects of turbidity, light level and prey concentration on feeding of juvenile weakfish *Cynoscion regalis*. Mar. Ecol. Prog. Ser. 131:11–16.

Hagan, S. M., and K. W. Able.
2008. Diel variation in the pelagic fish assemblage in a temperate estuary. Est. Coast. 31:33–42.

Hartman, K. J., J. Howell, and J. A. Sweka.
2004. Diet and daily ration of bay anchovy in the Hudson River, New York. Trans. Am. Fish. Soc. 133:762–771.

Hopkins, T. L.
1965. Mysid shrimp abundance in surface waters of Indian River Inlet, Delaware. Chesapeake Sci. 6:86–91.

Horn, M. H.
1980. Diel and seasonal variation in abundance and diversity of shallow-water fish populations in Morro Bay, California. Fish. Bull. 78:759–770.

Horodysky, A. Z., R. W. Brill, E. J. Warrant, J. a Musick, and R. J. Latour.
2008. Comparative visual function in five sciaenid fishes inhabiting Chesapeake Bay. J. Exp. Biol. 211:3601–3612.

Hulburt, E. M.
1957. The distribution of *Neomysis americana* in the estuary of the Delaware River. Limnol. Oceanogr. 2:1–11.

Layman, C. A.
2000. Fish assemblage structure of the shallow ocean surf-zone on the eastern shore of Virginia Barrier Islands. Est. Coast. Shelf Sci. 51:201–213.

Marin Jarrin, J. R., and A. L. Shanks.
2011. Spatio-temporal dynamics of the surf-zone faunal assemblages at a southern Oregon sandy beach. Mar. Ecol. 32:232–242.

McLachlan, A., and A. C. Brown.
2006. The ecology of sandy shores, 2nd dd, 392 p. Academic Press, Amsterdam, Netherlands.

Oksanen, J., R. Kindt, P. Legendre, B. O'Hara, G. L. Simpson, M. H. H. Stevens, and H. Wagner.
2008. Vegan: community ecology package, vers. 1.13-8. [Available from website.]
Pennock, J. R., and J. H. Sharp.
1994. Temporal alternation between light- and nutrient-limitation of phytoplankton production in a coastal plain estuary. Mar. Ecol. Prog. Ser. 111:275–288.
Pessanha, A. L. M., and F. G. Araújo.
2003. Spatial, temporal and diel variations of fish assemblages at two sandy beaches in the Sepetiba Bay, Rio de Janeiro, Brazil. Est. Coast. Shelf Sci. 57:817–828.
R Core Development Team.
2010. R: a language and environment for statistical computing. R Foundation for Statistical Computing, Vienna, Austria. [Available from website, accessed April 2010.]
Říha, M., J. Kubečka, T. Mrkvička, M. Prchalová, M. Čech, V. Draštík, J. Frouzová, M. Hladík, E. Hohausová, O. Jarolím. et al.
2008. Dependence of beach seine net efficiency on net length and diel period. Aquat. Living Resour. 21:411–418.
Rodrigues, F. L., and J. P. Vieira.
2013. Surf zone fish abundance and diversity at two sandy beaches separated by long rocky jetties. J. Mar. Biol. Assoc. U.K. 93:867–875.
Ross, S. T., R. H. McMichael Jr., and D. L. Ruple.
1987. Seasonal and diel variation in the standing crop of fishes and macroinvertebrates from a Gulf of Mexico surf zone. Est. Coast. Shelf Sci. 25:391–412.
Rountree, R. A., and K. W. Able.
1993. Diel variation in decapod crustacean and fish assemblages in New Jersey polyhaline marsh creeks. Est. Coast. Shelf Sci. 37:181–201.
Scharf, F. S., J. A. Buckel, and F. Juanes.
2009. Contrasting patterns of resource utilization between juvenile estuarine predators: the influence of relative prey size and foraging ability on the ontogeny of piscivory. Can. J. Fish. Aquat. Sci. 66:790–801.
Steinmetz, J., S. L. Kohler, and D. A. Soluk.
2003. Birds are overlooked top predators in aquatic food webs. Ecology 84:1324–1328.
Tebbs, J. M., and K. M. Bower.
2003. Some comments on the robustness of Student *t* procedures. J. Eng. Educ. 92:91–94.
Torre, M. P., and T. E. Targett.
2016. Nekton assemblages along riprap-altered shorelines in Delaware Bay, USA: comparisons with adjacent beach. Mar. Ecol. Prog. Ser. 548:209–218.
2017. Feeding by bluefish and weakfish along riprap-hardened shorelines: comparisons with adjacent sandy beach in Delaware Bay, USA. Trans. Am. Fish. Soc. 146:341–348.
Vasconcellos, R. M., F. G. Araújo, J. N. de Sousa Santos, and M. de Araújo Silva.
2010. Short-term dynamics in fish assemblage structure on a sheltered sandy beach in Guanabara Bay, Southeastern Brazil. Mar. Ecol. 31:506–519.
Vasconcellos, R. M., F. G. Araujo, J. N. de Sousa Santos, and M. de Araújo Silva.
2011. Diel seasonality in fish biodiversity in a sandy beach in south-eastern Brazil. J. Mar. Biol. Assoc. U.K. 91:1337–1344.
Vouglitoisa, J. J., K. W. Able, R. J. Kurtz, and K. A. Tighe.
1987. Life history and population dynamics of the bay anchovy in New Jersey. Trans. Am. Fish. Soc. 116:141–153.
Whitfield, A. K.
1999. Ichthyofaunal assemblages in estuaries: a South African case study. Rev. Fish Biol. Fish. 9:151–186.
Yeoh, D. E., F. J. Valesini, C. S. Hallett, D. A. Abdo, and J. Williams.
2017. Diel shifts in the structure and function of nearshore estuarine fish communities. J. Fish Biol. 90:1214–1243.

National Marine
Fisheries Service
NOAA

Fishery Bulletin
established in 1881

Spencer F. Baird
First U.S. Commissioner
of Fisheries and founder
of *Fishery Bulletin*

Recovery of visual function in Pacific halibut (*Hippoglossus stenolepis*) after exposure to bright light

Christopher Magel (contact author)[1]
Clifford Ryer[1]
Richard Brill[2]

Email address for contact author: chris.magel@noaa.gov

[1] Alaska Fisheries Science Center
National Marine Fisheries Service, NOAA
2030 S. Marine Science Drive, Building RSF951
Newport, Oregon 97365-5296

[2] Northeast Fisheries Science Center
National Marine Fisheries Service, NOAA
P.O. Box 1346
Gloucester Point, Virginia 23062-1346

Abstract—Commercial fishing exposes Pacific halibut (*Hippoglossus stenolepis*) to a myriad of stressors during capture, processing, and discarding, including exposure to direct sunlight that causes diminished retinal sensitivity. It is unknown, however, whether recovery occurs. We therefore employed both electroretinography and a behavioral assay to measure recovery of retinal sensitivity and visual function in halibut exposed to 15 min of simulated sunlight. We used electroretinography to measure changes in retinal light sensitivity after recovery periods of 2, 4, 6 and 10 weeks and a behavioral assay to measure responsiveness to simulated prey (i.e., in behavioral trials) to measure visual function after recovery periods of 2 to 6 d. Exposure to simulated sunlight significantly reduced retinal sensitivity to light with no apparent recovery after 10 weeks. Although retinal sensitivity was reduced, fish exposed to direct sunlight displayed no demonstrable deficits in visual function during behavioral trials.

Manuscript submitted 24 January 2017.
Manuscript accepted 7 September 2017.
Fish. Bull. 115:566–575 (2017).
Online publication date: 20 September 2017.
doi: 10.7755/FB.115.4.12

The views and opinions expressed or implied in this article are those of the author (or authors) and do not necessarily reflect the position of the National Marine Fisheries Service, NOAA.

One-quarter of the catch of worldwide fisheries comprises nontarget species (i.e., as bycatch or incidental catch) that are often discarded (Alverson et al., 1994). Fish may be dead when discarded, or may subsequently expire as a consequence of physical injury and stress incurred during capture and release. Mortality rates for discarded fish are, however, rarely known and represent a large source of uncertainty in fisheries models (Davis, 2002). In some instances, compromised fish succumb to predation hours or days after being discarded (Davis, 2002). For example, juvenile walleye pollock (*Gadus chalcogrammus*) and sablefish (*Anoplopoma fimbria*) subjected to stressors simulating escape through trawl codend meshes have been shown to be more vulnerable than control fish to predation in staged predator encounters (Ryer, 2002, 2004). In other instances, fish may recover but experience lower fitness as a consequence of injuries or stress. Atlantic cod (*Gadus morhua*) stressed through simulated trawl avoidance produced poor quality eggs and larvae (Morgan et al., 1999); and sockeye salmon (*Oncorhynchus nerka*) that escaped gill nets incurred physical injuries and physiological impairments that reduced spawning success by 50% (Baker and Schindler, 2009). Reduced growth and body size may also impact reproduction. Using a bioenergetics model, Meka and Margraf (2007) estimated that catch-and-release can reduce growth of rainbow trout (*Oncorhynchus mykiss*) up to 15% when there is no physical injury, and up to 164% where debilitating hook injuries are incurred. Although these studies have documented outcomes of bycatch stress, they rarely address the mechanisms that cause the stress. In particular, scant information exists on how capture and release may impair sensory systems such as vision, which fish rely on to locate food and avoid predation.

Pacific halibut (*Hippoglossus stenolepis*) are captured in trawl and longline fisheries targeting groundfishes along the contiguous United States and Canada (Davis and Olla,

2001). Trawl fisheries are, however, required to discard all Pacific halibut, thus subjecting a significant portion of the Bering Sea and Gulf of Alaska population to capture stress (Williams and Wilderbuer[1]). Methods to determine health and condition of Pacific halibut destined for discard are based on the physical condition of the fish and variables related to the actual fishing process (Kaimmer and Trumble, 1998). Information on fish condition, stress, and variables related to the fishing process are collected by fisheries observers, but these data can vary greatly owing to subjective differences in assessment of fish condition and trawl tow characteristics (e.g., catch weight, depth of tow, tow speed) (Pikitch et al.[2]). Therefore, the amount of time on deck may be a better indicator of condition at release than the means of capture (i.e., trawl or longline) (Davis and Schreck, 2005).

Recent studies indicate that Pacific halibut biomass remains relatively stable, although recruitment remains weak (Stewart and Hicks[3]), and bycatch mortality is approximately 20% within directed groundfish fisheries (Benaka et al., 2014). Also, bycatch has been slowly decreasing, although rates fluctuate depending on the location of the fishery itself (Dykstra[4]). Continued reductions in bycatch mortality could be facilitated by a better understanding of both the physiological and behavioral mechanisms that are compromised at the time of release of bycatch and affect survival.

Pacific halibut are visual predators (Hurst et al., 2007) and frequently live in turbid coastal waters at depths ranging from 90 to 900 m (i.e., on the continental shelf) (IPHC[5]) and therefore under low ambient light levels. After capture in trawl fisheries, individual fish are often left on deck for tens of minutes before they are discarded (Trumble et al., 1995; Davis and Olla, 2001). During this time, they can be exposed to direct sunlight (i.e., at light levels orders of magnitude above ambient levels on the seafloor) that potentially causes impaired visual function (Loew, 1976; Meyer-Rochow, 1994; Wu et al., 2006). Previous research has documented a reduction in retinal sensitivity to light in Pacific halibut after 15 min of exposure to simulated sunlight (Brill et al, 2008). This reduction in sight could have consequences for foraging success after release by diminishing the ability of a fish to perceive and capture prey. It is unknown, however, whether this deficit is permanent or whether it reduces the ability of Pacific halibut to detect and capture prey. Our objective was to extend previous research (Brill et al., 2008) and to assess specifically whether retinal sensitivity and overall visual function can recover after exposure to simulated sunlight.

We addressed these objectives by using both electroretinography (ERG) and behavioral methods. ERG measures the summed potential of electrical signals within the retina, providing a technique for rapidly and quantitatively assessing retinal function (Brown, 1968). An evaluation of the behavior of Pacific halibut subjected to bright light, namely an evaluation of their ability to accomplish essential tasks, such as perceiving and capturing prey, will help determine the effects of bycatch on somatic growth, fecundity, and survival.

Materials and methods

All fish capture, maintenance, handling, and experimental procedures followed accepted protocols and were in compliance with all relevant laws and regulation. Age-0 Pacific halibut (40–70 mm in total length [TL]) were acquired by trawl net in Chiniak Bay, Kodiak Island, Alaska (57°40′N, 152°30′W) and delivered to the Hatfield Marine Science Center, Newport, Oregon. Pacific halibut were kept in 3.1-m diameter fiberglass tanks (at a 1-m depth) with flowing seawater at 8–10°C degrees for 2 or 3 years before use in the experiments. The tanks were maintained under low-illumination fluorescent lighting (photon flux density of 0.01 $\mu mol \cdot m^{-2} \cdot s^{-1}$) and day time and night time were set on a 12-h photoperiod. Fish were fed 3 times per week during the first year and twice per week during the second year with a gel food consisting of gelatin, vitamins, amino acid supplements, krill (*Euphausia superba*), pelleted food, Pacific herring (*Clupea pallasii*), and squid.

Exposure to bright light

Individual 2-year-old Pacific halibut (13–17 cm TL) fish were lifted by dip net from their holding tank, lightly anesthetized with a tricaine methanosufonate (Tricaine-S[6] [MS-222], Western Chemical, Inc., Ferndale, WA) solution of ~5 mg/L to reduce movement and stress, and held in a shallow seawater bath (12°C). They were

[1] Williams, G. H., and T. Wilderbuer. 1992. Revised estimates of Pacific halibut discard mortality rates in the 1990 groundfish fisheries off Alaska. *In* Int. Pac. Halibut Comm. report of assessment and research activities 1991, p. 191–209. Int. Pac. Halibut Comm., Seattle, WA. [Available from website.]

[2] Pikitch, E. K., D. L. Erickson, C. K. Mitchell, and J. R. Wallace. 1997. Practical applications of fishing and handling techniques in estimating the mortality of discarded trawl-caught Pacific halibut (*Hippoglossus stenolepis*). ICES C.M. 1997/FF:05, 18 p. [Available from website.]

[3] Stewart, I. J., and A. C. Hicks. 2017. Assessment of the Pacific halibut stock at the end of 2016. *In* Int. Pac. Halibut Comm. report of assessment and research activities 2006. IPHC-2016-RARA-26-R, p. 365–394. Int. Pac. Halibut Comm., Seattle, WA. [Available from website.]

[4] Dykstra, C. L. 2017. Incidental catch and mortality of Pacific halibut, 1990–2016. *In* Int. Pac. Halibut Comm. report of assessment and research activities 2006. IPHC-2016-RARA-26-R, p. 71–89. Int. Pac. Halibut Comm., Seattle, WA. [Available from website.]

[5] IPHC (International Pacific Halibut Commission). 1998. The Pacific halibut: biology, fishery, and management. Tech. Rep. 40, 64 p. Intl. Pac. Halibut Comm., Seattle, WA. [Available from website.]

[6] Mention of trade names or commercial companies is for identification purposes only and does not imply endorsement by the National Marine Fisheries Service, NOAA.

then exposed to simulated sunlight for 15 min by using a light source and a fiber optic guide aimed at the right eye of a fish. The left eye was covered with a light-blocking cloth. The 15-min simulated sunlight exposure was chosen to correspond with the time fish are left on deck during commercial trawl sorting operations (Davis and Olla, 2001; Davis and Schreck, 2005). Control fish were treated in kind, except that the light source was not turned on. Fish were subsequently returned to their holding tanks and separated with a barrier to allow both control and light exposed fish to be held under identical conditions.

Sunlight was simulated by using a high-intensity xenon lamp (Spectral Products, Putnam, CT) and its spectral range was ~320–700 nm, which approximates the visible (400–700 nm) and the UV range of sunlight directly overhead at sea level (Lalli and Parsons, 1997). Light intensity exiting the fiber optic light guide was ~2000 $\mu mol \cdot m^{-2} \cdot s^{-1}$ (measured over 400–700 nm of spectral range) and simulated sunlight (2010 $\mu mol \cdot m^{-2} \cdot s^{-1}$) and measured at Newport, Oregon, under ideal clear conditions at 1200 noon PST on 5 October 2007 and by using a IL 1700 Research Radiometer (International Light Technologies, Inc., Peabody, MA) equipped with a photosynthetically active radiation-filtered waterproof sensor.

Evaluation of visual function with the use of an ERG

To evaluate visual function by using ERG, fish were moved into a dark room in a light-proof container. Individuals were then lightly anesthetized with a buffered MS-222 solution (~5-mg/L) and the neuromuscular blocking drug gallamine triethiodide (Flaxedil, Sigma Chemical Co., St. Louis, MO, dose ~20 mg/kg) injected into the caudal vein to reduce movement. Fish were then placed on a sling and enclosed in a light-blocking container placed in an acrylic box. The body of the fish was submerged in a manner such that only a small portion of the head and the eye would remain above water to receive the light stimulus. The container was supplied with flow-through seawater (12°C) and the gills of the fish remained aerated by means of a small submersible pump for water circulation. Fish were adapted to darkness for a minimum of 1 h before physiological measurements were taken.

Teflon-coated silver wire electrodes with a silver chloride electroplated coating, were used to record the ERG responses The recording electrode was placed lightly on the corneal surface and the reference electrode was placed on the skin over the head of the fish. The recording chamber was illuminated with a dim red light (peak wavelength 660 nm) produced by light-emitting diodes (LEDs); these remained on while the electrodes were positioned. The recording system was grounded by using a stainless-steel plate within the experimental apparatus. ERG signals were amplified (10,000× gain) with 1-Hz high pass and 1-kHz low-pass filter settings on a DAM50 amplifier (World Precision Instruments, Inc., Sarasota, FL). The signal was also filtered with a HumBug active electronic noise eliminator (Quest Scientific Instruments, Inc., North Vancouver, Canada) that removed 60-Hz noise and was digitized at a 1-kHz sampling frequency with a multifunction data acquisition card (DAQCard-6024E, National Instruments Corp., Austin, TX). Light stimuli and all data were controlled by a custom program developed by Eric Warrant (University of Lund, Lund, Sweden) for use in the LabVIEW graphical programming system for measurement and automation (National Instruments Corp.).

A circular (3.8-cm diameter) light source (SL2420 spot light, Advanced Illumination, Inc., Rochester, VT) was used to produce a white LED light stimulus, and a thin diffuser and collimating lens were used to produce an even field of illumination (±10%). An intensity controller (CS410, Advanced Illumination, Inc.) was used to control light output. The intensity controller was connected and controlled by the analog output of the data acquisition card. To extend the range of available light levels, a series of neutral density filters (Kodak Optical Products, Eastman Kodak Co., Rochester, NY) were used to dim the light stimulus.

As in previous studies (e.g., Brill et al., 2008), we examined changes in retinal sensitivity to light resulting from exposure to simulated sunlight by recording the summed potential of electrical signal in response (in volts [V]) to a range of light intensities (I) and subsequently used the data to construct voltage in relation to log light intensity response curves (V-log I). Light intensities were increased by 0.2 log-unit steps from a level with no measurable response, to a level that produced a max response. A light stimulus consisted of a train of five 200-ms light flashes delivered 200 ms apart. This stimulus was presented every 5 s and repeated 5 times at each light intensity. The ERG responses to the final flash of each train were recorded and averaged. At the conclusion of an experiment, fish were euthanized with either a massive overdose (>300 mg/kg) of sodium pentobarbital (Beuthanasia-D, Merck Animal Health, Madison, NJ) injected into the caudal vein, or by immersion in a bath of clove oil where the clove oil solution was circulated over the gills by a small submersible pump.

Initially, we compared ERG data for the left and right eyes of control fish (n=4) that had not been exposed to simulated sunlight. Preliminary analysis indicated that right eyes produced a consistently stronger voltage signal than left eyes. Our original intention had been to use unexposed left eyes as 'within-fish' controls for the exposed right eyes in the exposure recovery experiment. However, because of the difference in signal strength between left and right eyes, we abandoned this strategy and relied instead upon a comparison of right eyes between control fish and sunlight exposed fish after various periods of recovery. Fish exposed to simulated sunlight were divided in groups with recovery times of 2, 4, 6, and 10 weeks. Each group consisted of 8–10 individuals.

In addition to voltage response data we also calculated voltage percent maximum (p-max) data; for each

fish, namely the percentage of maximal response at each tested light intensity. Finally, the data from each individual ERG curve was fitted by using a second-order polynomial equation with SYSTAT software, vers. 13 (Systat Software, Inc., San Jose, CA) or Microsoft Office 2013 (Microsoft Corp., Redmond, WA), because the ERG response curves generally were of a sigmoid shape. To provide a summary measure of visual impairment, we calculated log-scale illumination required to produce a 50% p-max response from each fish. In the left and right eye, and exposure recovery experiments, ERG responses presented as voltages and p-max responses were examined with repeated measures analysis of variance (ANOVA) (Sokal and Rohlf, 1969). For examination of the light level required to produce a 50% p-max response, we compared treatment groups, using one-way ANOVA (Sokal and Rohlf, 1969). Where appropriate, we employed a Tukey's honestly significant difference (HSD) test (Sokal and Rohlf, 1969) to examine differences in treatment means. Tests were considered significant at the $P<0.05$ level.

Behavioral evaluation of fish in relation to visual function

Individual 3-year-old Pacific halibut (21–27 cm TL) were anesthetized with MS-222 as described above, but in this case both eyes were subjected to a 15-min exposure to simulated sunlight before behavioral experiments. After light exposure, pairs of fish were moved into 1.9-m diameter × 80-cm deep circular tanks to recover. The tanks were located within a light-controlled laboratory and supplied with constantly flowing seawater at ~9°C.

Experiments were conducted with 8–10 pairs of fish at six light intensities simulating environmental conditions typical for Pacific halibut (~90–900 m): 1×10^{-3}, 1×10^{-4}, 1×10^{-5}, and 1×10^{-6}, 1×10^{-7} $\mu mol\cdot m^{-2}\cdot s^{-1}$, and complete darkness ($<0.01\times10^{-7}$). Light levels were measured on the bottom of the experimental tank with a IL1700 Research Radiometer equipped with a photosynthetically active radiation-filtered waterproof sensor. To reduce shadows, all lighting was attached to an overhead ring suspended 1.8 m above the tank bottom and approximately 0.7 m outside the tank circumference. Four cone lamps with green LED (~555-nm) clusters were mounted on the ring. The LED clusters were linked to a rheostat that was used to vary light intensity. The lights were placed directed perpendicular to the tanks to avoid glare and hot spots.

We recorded fish movements with an overhead video camera (Ikegami Electronics, Inc., Mahwah, NJ) and under infrared illumination. Infrared illumination ranged from 760–880 nm, which is a range undetectable by Pacific halibut (John, 1964; Higgs and Fuiman, 1996; Brill et al., 2008). Infrared lights were placed below the bottom of the tank and provided a silhouette of the fish; these lights were left on for all experimental trials, regardless of the light treatment being used. Each experimental tank had a clear Plexiglas tube placed in the middle that held a white fishing jig that was attached to the ceiling with a counter-weighted line and to the bottom of the tank with an elastic band. The bottom 20 cm of the Plexiglas tubes were covered with black tape, such that the jig would not be visible to the fish when not in use.

Fish were allowed to recover for at least 48 h after exposure to simulated sunlight before use in further trials. Each pair of fish was tested at all 6 levels of illumination: 2 illumination levels on each of the first 2 days, and a single illumination level on the last day. The illumination level was set with the rheostat and fish were allowed to acclimate for 2 h before the trial began, 2 h were allowed between trials, and the order of testing with respect to illumination level was randomized. A trial at each illumination level consisted of two 5-min periods before and after presentation of the visual stimulus (white jig). After the first 5-min period, the jig was moved up and down rapidly (within the Plexiglas tube) for 60 s and then allowed to sink back below the masked bottom of the Plexiglas tubes, where it was out of sight. Each minute was split into 10-s intervals and scored as to whether the pair of fish reacted to the visual stimuli. A reaction was considered positive if the fish either 1) moved one body length, 2) made oral contact with the column while attempting to bite at the jig, or 3) re-oriented itself such that the long axis of the fish was pointing toward the jig (~10°).

Scoring behavior of fish

Scores were recorded as either 0 (no reaction by either fish), 1 (reaction by one fish), or 2 (reaction by both fish). For each 1-min trial, the 10-s scores were summed to arrive at an activity index. We compared activity indexes of fish exposed to simulated sunlight and control fish over time at each light level by using repeated measures ANOVA (n=6-9). Where ANOVA results indicated significant differences, a Tukey's HSD was used to determine differences between group means. During the scoring process and in preliminary analysis it became apparent there was no difference between the lowest light levels (1×10^{-5}, 1×10^{-6}, and 1×10^{-7} $\mu mol\cdot m^{-2}\cdot s^{-1}$ and complete darkness). Hence, we decided to show only the highest 4 light intensities (1×10^{-3}, 1×10^{-4}, 1×10^{-5}, and 1×10^{-6} $\mu mol\cdot m^{-2}\cdot s^{-1}$).

Results

Electroretinography experiment

At the same light intensities, voltages measured on the corneal surface of the right eyes of control fish were significantly higher than those measured on the corneal surface of left eyes. This finding was manifest by a significant interaction between eye (left vs. right) and light intensity in our ANOVA ($F_{[16, 32]}=4.18$, $P<0.0001$). The difference in the responses of right and left eyes increased with increasing light intensities (Fig. 1). When voltage data for each fish were converted to p-

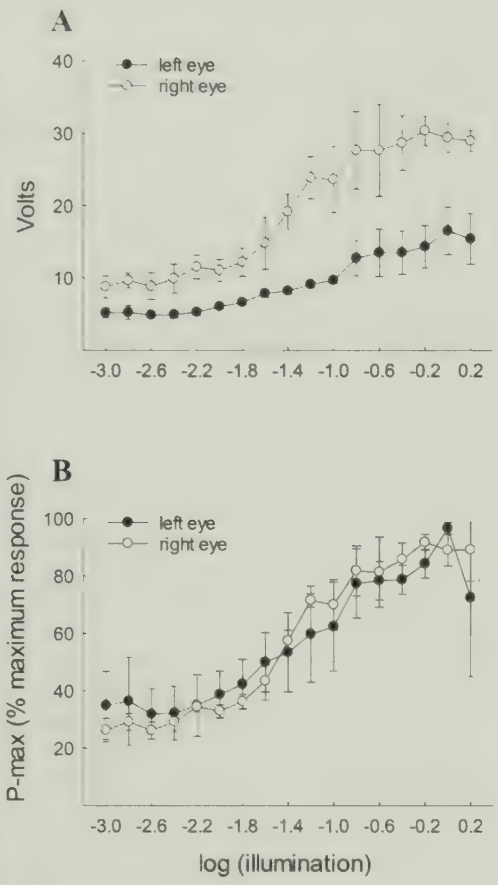

Figure 1

Comparison of responses to increasing illumination or light intensities (I, measured in log candela/m^2 by using electroretinography) between right and left eyes of previously unexposed Pacific halibut (*Hippoglossus stenolepis*) (n=4). To construct voltage in relation to log light intensity (V-log I) response curves, light intensities were increased in 0.2 log units from levels that produced no measurable responses to those that produced maximal responses. The data are reported either as voltage or as log-normalized by expressing the average response to an intensity step as a percentage of the maximum observed average response (p-max). V-log I response curves were created with both (**A**) voltage data and (**B**) log-normalized data expressed by the average response to an intensity step as a percentage of the maximum observed average response. Data points represent mean values, and error bars indicate standard errors of the means.

max, a significant difference was no longer present between left and right eyes ($F_{[1, 2]}$=0.00, P=0.963), nor was there a significant interaction between eye and light intensity ($F_{[16, 32]}$=0.90, P=0.575). P-max continued to increase with increasing test light level ($F_{16, 32]}$ =17.68, P<0.001).

Exposure to simulated sunlight for 15 min resulted in a visual deficit that did not improve during the 10 weeks of recovery. Voltages measured from the right eyes of control fish (i.e., no exposure to simulated sunlight) were generally greater than those of the right eyes of fish that were exposed to simulated sunlight and allowed to recover for 2–10 weeks. This was particularly evident at lower test light levels, as evidenced by a significant interaction between treatment and light intensity (Fig. 2A; $F_{[64,272]}$=1.55, P=0.009). Conversion of voltages to p-max did not appreciably change this relationship (Fig. 2B). Again, there was a significant interaction between treatment and light intensity ($F_{[64,272]}$=2.04, P<0.001).

There were significant differences in light intensities required to produce a response 50% of maximum ($F_{[4,17]}$=11.4, P<0.001) between treatments (control, and 2, 4, 6 and 10-weeks recovery) (Fig. 3). The light intensity required to produce a response 50% of maximum was significantly lower for control fish, than for fish in any of the recovery treatments (Tukey's HSD: P<0.05). Among the recovery treatments, the light intensity required to produce a response 50% of maximum increased over the 10-week recovery period and was lower at week 2 than at week 10 (Tukey's HSD: P<0.05). The light intensity required to produce a response 50% of maximum at week 2 did not differ from those at either weeks 4 or 6, and similarly, the response at week 10 did not differ from responses at weeks 4 or 6 (Tukey's HSD: P<0.05). In context, it took approximately 17 times the photons to produce a response of 50% of maximum in fish exposed to simulated sunlight after 10 weeks than it did for control fish.

Behavioral experiment

There was no effect of exposure to simulated sunlight on the behavioral response of Pacific halibut to the visual cues associated with a simulated prey ($F_{[27,324]}$ =0.40, P=0.539). This lack of difference between control and treated fish was consistent throughout the trials, as well as across ambient light levels, because ANOVA showed no significant interactions between treatment (control vs fish exposed to simulated sunlight) and any of the other factors (e.g., time, ambient light level). Pacific halibut were generally active and responded strongly to the appearance of prey (presented at the beginning of minute 6) at the highest ambient illumination (3×10^{-3} $\mu mol \cdot m^{-2} \cdot s^{-1}$), but responsiveness progressively declined at lower ambient light levels (Fig. 4). This finding is supported by a significant interaction between time and ambient light level in our ANOVA for Pacific halibut activity ($F_{[27,324]}$=4.16, P<0.001). At the 2 highest ambient light levels, fish would orient themselves toward the simulated prey when it appeared, swim toward it, and repeatedly strike at the sides of the Plexiglas tube containing the simulated prey. This behavior was characterized by a sharp in-

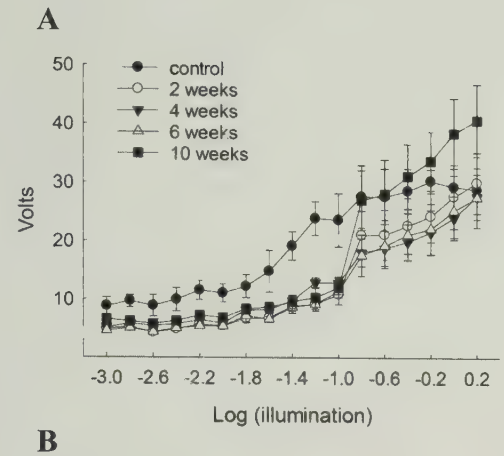

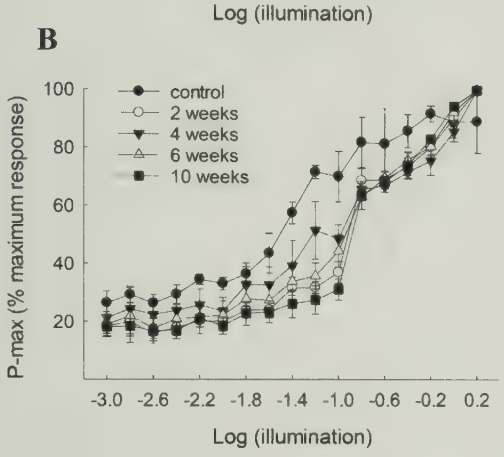

Figure 2

Comparison of responses to increasing illumination or light intensities (I, measured in log candela/m^2 by using electroretinography) between a control group of Pacific halibut (*Hippoglossus stenolepis*) and another group of Pacific halibut 2, 4, 6, and 10 weeks after light exposure (n=8–10). To construct voltage in relation to log light intensity (V-log I) response curves, light intensities were increased in 0.2 log-unit steps from levels that produced no measurable responses to those that produced maximal responses (p-max). The data are reported both as voltage and log-normalized by expressing the average response to an intensity step as a percentage of the maximum observed average response. V-log I response curves were created by using voltage data and log-normalized data expressed by the average response to an intensity step as a fraction of the maximum observed average response. All data points are those recorded from the right eye. Data points represent means ± standard error.

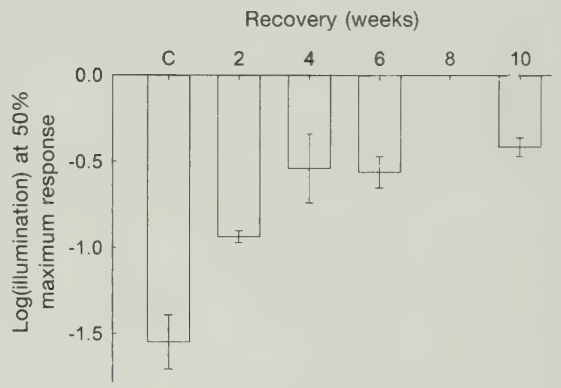

Figure 3

Comparison of responses to increasing illumination or light intensities (I, measured in log candela/m^2) by using electroretinography [ERG] between a control group of Pacific halibut (*Hippoglossus stenolepis*) and another group of Pacific halibut after 2, 4, 6, and 10 weeks of recovery from light exposure (n=8–10). To construct voltage in relation to log light intensity (V-log I) response curves, light intensities were increased in 0.2 log-unit steps from levels that produced no measurable responses to those that produced maximal responses. The data were log normalized by expressing the average response to an intensity step as a fraction of the maximum observed average response. Each curve was then fitted with a second-order polynomial equation because the ERG response curves generally indicated a sigmoid response to light intensities. Light intensities required to produce a response 50% of the maximum response were taken from the predicted values produced from the quadratic equation for each model. All data points were those recorded from the right eye. Data points represent means, and error bars indicate standard errors of the means.

crease in activity from minute 5 to 6 (Tukey's HSD: P<0.05, for 3×10^{-3} and 3×10^{-4} µmol·m^{-2}·s^{-1}) (Fig 4, A and B). This response diminished as ambient light levels decreased, and no significant increase in activity was observed from minute 5 to 6 at the 2 lowest ambient light levels (Tukey's HSD: P>0.05, for 3×10^{-5} and 3×10^{-6} µmol·m^{-2}·s^{-1}) (Fig 4, C and D).

Discussion

Prior research (Brill et al., 2008) has shown that exposure to simulated sunlight (i.e., imitating the situation experienced on the deck of a vessel) impairs the retinal function of Pacific halibut. The authors speculated that exposure to simulated sunlight resulted in damage and apoptosis of photoreceptor cells containing the longer wavelength (520–540-nm) absorbing visual pigments. A predominance of receptors with maximal sensitivity in the green wavelengths is characteristic of coastal and continental shelf species (Levine and MacNichol, 1979; Bowmaker, 1990). If permanent, a deficit in these retinal receptors could have negative consequences for post release foraging success, somatic growth, reproductive success, and ultimately survival.

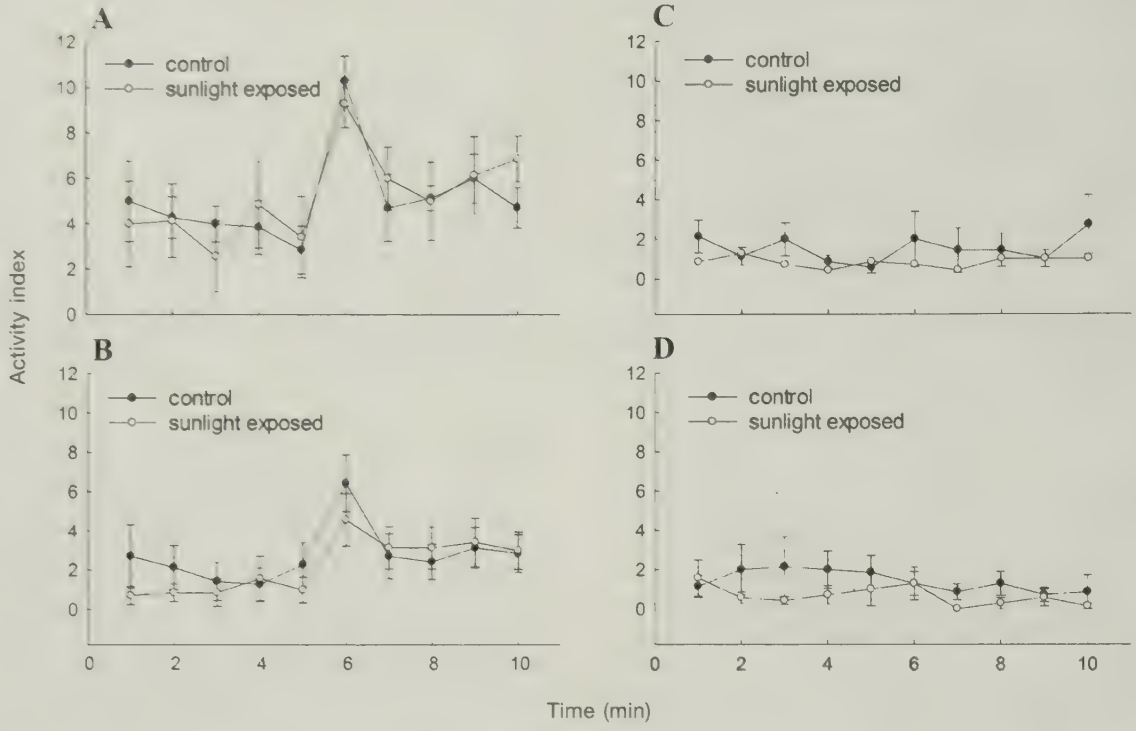

Figure 4

Results of the behavioral experiment quantifying responses of pairs of Pacific halibut (*Hippoglossus stenolepis*) to a visual stimulus (i.e., a white jig that simulated prey) at 4 ambient light levels (photon flux density): (**A**) 1×10^{-3}, (**B**) 1×10^{-4}, (**C**) 1×10^{-5}, and (**D**) 1×10^{-6} $\mu mol \cdot m^{-2} \cdot s^{-1}$. For each experiment, ambient light level was set with a rheostat and fish were allowed to acclimate for 2 h before the next trial began. Each trial consisted of a 5-min period before and a 5-min period after presentation of the visual stimulus. After the initial 5-min period, the jig was rapidly moved up and down within a Plexiglas column for 60 s and then allowed to sink back to the level at which it was out of sight of the fish (i.e., to the masked bottom of the column). A reaction was considered positive if the fish 1) moved one body length, 2) made oral contact with the column as it attempted to bite at the jig, or 3) reoriented itself such that its long axis was directly pointing toward the jig. Scores were recorded at 10-s intervals as either 0 (no reaction by either fish in the pair), 1 (reaction by one fish), and 2 (reaction by both fish). For each minute, the scores were summed to arrive at an activity index.

Using both ERG and a behavioral assay, we tested the hypothesis that Pacific halibut recover from retinal damage and visual function resulting from exposure to direct sunlight. Our ERG data indicated damage to the Pacific halibut visual system and no significant recovery during the 10 weeks after exposure. Even after 10 weeks, it took approximately 17 times the light intensity to elicit a response 50% of maximum than with control fish. This result equates to an approximate 94% reduction in retinal sensitivity. In contrast, our behavior assay (which occurred 2–6 d after exposure to simulated sunlight) could not reveal impairment of the ability of Pacific halibut to detect visual cues associated with simulated prey across a broad range of ambient light levels.

Electroretinography is a procedure in which the summed electrical responses from the retinal photoreceptors are recorded by placing electrodes on the corneal surface and skin adjacent to the eye. In our study, we exposed fish to 15 min of simulated sunlight, an intensity equivalent to ambient sunlight under clear skies at noon (Newport, Oregon, 5 October 2007; the same exposure used by Brill et al., 2008). Light-exposed fish required approximately 5 times the amount of light to generate an ERG response equal to control fish. This was manifest as a depression in both voltage and p-max voltage plotted against log illumination. These curves remained depressed over a 10-week post exposure period, compared with controls that indicated no recovery of retinal sensitivity. Brill et al. (2008) speculated that the mechanism of damage was disruption of photoreceptor cells and predicted that the process would be progressive and permanent. Our ERG data support this contention. The illumination required to stimulate a 50% maximum response, shows that vision deteriorated from 2 weeks to 10 weeks

after exposure, indicating a progressive worsening of Pacific halibut retinal sensitivity over time. In an environmental context, a sunlight exposed Pacific halibut would have to move to water that is 18 m shallower to have the same visual acuity as that of an unexposed fish, assuming a light extinction coefficient of 0.15 (e.g., simulating typical conditions in the Gulf of Alaska). This level of illumination would potentially result in a shoaling effect among fish discarded as bycatch. Our data further indicate that the visual deficit associated with sunlight exposure was most pronounced at the low end of the Pacific halibut visual range. As a consequence, fish captured in and subsequently returned to relatively shallow well-lit waters may be less affected than fish captured from and then returned to deeper water, where impaired fish may be at the limit of their range of visual sensitivity. Whether or not discarded Pacific halibut move to shallower water to mitigate visual impairments could be tested in future research with mark-recapture techniques. It should be noted that Pacific halibut size generally increases with depth. The fish used in our ERG were 2 year olds and therefore were smaller than most fish encountered in commercial fisheries. Although we have no reason to believe that the visual systems of our fish differed from those of larger Pacific halibut, future work in this area would benefit from an examination of a wider range of fish sizes.

The impairment of retinal sensitivity revealed by ERG contrasts with the results from our behavioral assay that produced no statistical evidence of significant visual impairment associated with exposure to simulated sunlight. The simulated prey bobbed up and down within a clear Plexiglass tube that minimized cues associated with water movements and the possibility that Pacific halibut would respond to nonvisual cues. The fact that the responsiveness of fish, as measured by activity, decreased with decreasing ambient light levels clearly indicates that Pacific halibut use vision to detect prey. Yet, across the range of ambient light levels there were no consistent statistical differences between control fish and those exposed to simulated sunlight, with the possible exception of a slight reduction of behavioral activity (i.e. movement, bait strike, etc) among the latter at an ambient light level of 1×10^{-4} $\mu mol \cdot m^{-2} \cdot s^{-1}$ (Fig. 4B). Pacific halibut are visual predators and at light levels of 1×10^{-4} $\mu mol \cdot m^{-2} \cdot s^{-1}$ primarily use visual cues to locate and attack prey, shifting to tactile and olfactory cues as light levels fall below 1×10^{-5} $\mu mol \cdot m^{-2} \cdot s^{-1}$ (Hurst et al., 2007). For immobile baits, Pacific halibut feeding performance is likewise facilitated by vision (Stoner, 2003). We initially reasoned that the threshold ambient light level for visual foraging would be that at which a deficit would be most pronounced. It is possible that we performed tests over too wide a range of ambient light levels. For example, we might have seen a difference between sunlight-exposed and control fish by testing over finer gradations of ambient light levels between 1×10^{-5} to 1×10^{-4} $\mu mol \cdot m^{-2} \cdot s^{-1}$). Additionally, conditions in this behavioral assay were designed to maximize the probability of prey detection. The Pacific halibut were in close proximity to the simulated prey in clear water. Had the distance between Pacific halibut and simulated prey been greater, or the water more turbid, the demands upon the visual system may have been magnified in such a way that more clearly showed impairment.

An ancillary discovery from our work was the difference between left and right eye function in Pacific halibut. Left eyes had consistently depressed V-log I curves than right eyes (i.e., the former are less light sensitive than the latter). Pacific halibut are right-eyed flounders; the left eye migrates to the right side of the head during larval development and metamorphosis. This "tortured ontogeny" in flatfish may add constraints to optic nerve function. To our knowledge, however, little research exists on retinal anatomy or physiology in larval flatfish, beyond documentation of eye development of Atlantic halibut (*Hippoglossus hippoglossus*) and other flatfish at settlement (Kvenseth et al., 1996; Friedman, 2008). Although V-log I curves differed between left and right eyes, there were no apparent differences when responses were transformed to p-max response curves. Therefore, although voltage responses to brief light flashes from the left eyes are lower, both left and right eyes appear to otherwise function comparably. In brief, both eyes show comparable light sensitivities, although the smaller ERG response from the left eye (compared with that of the right eye) at the same light intensities implies anatomical and perhaps functional differences at the central nervous system level. Additionally, because of their unique dextral morphological features as adults, Pacific halibut may be more susceptible to injuries to their right eyes owing to hooking injuries in long-line commercial fisheries because the right eye is closer than the left eye to the jaw. This conclusion would warrant future research in hook-induced eye damage and handling practices specific to hook-and-line fisheries.

Hook-and-line fisheries, whether recreational or commercial, generally result in the rapid return of discarded fish to the water so that there is a concomitant minimal exposure to direct sunlight. In contrast, in trawl fisheries Pacific halibut may remain on deck for up 30 min and experience significant mortality (Trumble et al., 1995), although new deck sorting methods have decreased that time. For those fish that survive aerial exposure, it was postulated that sublethal effects on visual sensitivity arising from sunlight exposure could further reduce growth and survival (Brill et al., 2008). Because flicker fusion frequency (i.e., the speed of vision or the ability to detect moving objects) and light sensitivity of the Pacific halibut visual system are adapted to low-light environments (Warrant, 1999), Pacific halibut, in particular, are susceptible to retinal damage from exposure to direct sunlight than are shallow-water fish species. Our ERG data support these conclusions and are consistent with the data from Brill et al. (2008) in that we found that exposure to simulated sunlight exposure reduces retinal light sen-

sitivity in Pacific halibut across a broad range of illuminations, and the ~94% reduction in light sensitivity does not recover for during 10 weeks. Visual sensitivity appeared to be most affected at low ambient light levels. If this impairment is permanent, we speculate that fish may either make the best of a bad situation if they are released into deep waters, or attempt to move to shallower water to compensate for their visual deficit. However, these conclusions from our ERG data conflict with our behavioral data and observations, where no clear impairment in simulated prey detection was observed. We suspect that our behavioral assay may not have been ideally designed to show differences in visual sensitivity. We are not aware of any other studies that have attempted to link visual function, as measured by methods such as ERG, with behavioral performance, which ultimately determines the fitness of a species with visual deficits. This is an area of research that will be needed to assess the consequences of damage to the visual system resulting from conditions onboard vessels before discard of bycatch (Pacific halibut and other fish species), and to assess the implications of such damage for fisheries management.

Acknowledgments

We thank P. Iseri, M. Ottmar, and S. Haines for assistance with the collection, care, and husbandry of fish. We also wish to acknowledge 3 anonymous reviewers for their insightful comments and editorial assistance on an early version of the manuscript.

Literature cited

Alverson, D. L., M. H. Freeberg, S. A. Murawski, and J. G. Pope.
1994. A global assessment of fisheries bycatch and discards. FAO Fish. Tech. Pap.339, 233 p. FAO, Rome.

Baker, M. R., and D. E. Schindler.
2009. Unaccounted mortality in salmon fisheries: non-retention in gillnets and effects on estimates of spawners. J. Appl. Ecol. 46:752–761.

Benaka, L. R., L. Sharpe, L. Anderson, K. Brennan, J. E. Budrick, C. Lunsford, E. Meredith, M. S. Mohr, and C. Villafana.
2014. Fisheries release mortality: identifying, prioritizing, and resolving data gaps. NOAA Tech. Memo. NMFS-F/SPO-142, 55 p.

Bowmaker, J. K.
1990. Visual pigments of fishes. *In* The visual system of fish (R. Douglas and M. Djamgoz, eds.), p. 81–107. Chapman and Hall, London.

Brill, R., C. Magel, M. Davis, R. Hannah, P. Rankin.
2008. Effects of rapid decompression and exposure to bright light on visual function in black rockfish (*Sebastes melanops*) and Pacific halibut (*Hippoglossus stenolepsis*). Fish. Bull. 106:427–437.

Brown, K. T.
1968. The electroretinogram: its components and their origin. Vision Res. 8:633–677.

Davis, M. W.
2002. Key principles for understanding fish bycatch discard mortality. Can. J. Fish. Aquat. Sci. 59:1834–1843.

Davis, M. W., and B. L. Olla.
2001. Stress and delayed mortality induced in Pacific halibut by exposure to hooking, net towing, elevated seawater temperature and air: implications for management of bycatch. North Am. J. Fish. Manage. 21:725–732.

Davis M. W., and C. B. Schreck.
2005. Responses by Pacific halibut to air exposure: lack of correspondence among plasma constituents and mortality. Trans. Am. Fish. Soc. 134:991–998.

Friedman, M.
2008. The evolutionary origin of flatfish asymmetry. Nature 454:209–212.

Higgs, D. M., and L. A. Fuiman.
1996. Light intensity and schooling behaviour in larval gulf menhaden. J. Fish. Biol. 48:979–991.

Hurst T. P., C. H. Ryer, J. M. Ramsey, and S. A. Haines.
2007. Divergent foraging strategies of three co-occurring north Pacific flatfishes. Mar. Biol. 151:1087–1098.

John, K. R.
1964. Illumination, vision, and schooling of *Astyanax mexicanus* (Filipi). J. Fish. Res. Board Can. 21:1453–1473.

Kaimmer, S. M., and R. J. Trumble.
1998. , condition, and mortality of Pacific halibut bycatch following careful release by Pacific cod and sablefish longline fisheries. Fish. Res. 38:131–144.

Kvenseth, A., M., K. Pittman, and J. V. Helvik.
1996. Eye development in Atlantic halibut (*Hippoglossus hippoglossus*): differentiation and development of the retina from early yolk sac stages through metamorphosis. Can. J. Fish. Aquat. Sci. 53:2524–2532.

Lalli, C. M., and T. R. Parsons.
1997. Biological oceanography: an introduction, 2nd ed., 324 p. Elsevier Butterworth-Heineman, Oxford, UK.

Levine, J. S., and E. F. MacNichol Jr.
1979. Visual pigments in teleost fishes: effects of habitat, microhabitat, and behavior on visual system evolution. Sens. Process. 3:95–131.

Loew, E. R.
1976. Light, and photoreceptor degeneration in the Norway lobster, *Nephrops norvegicus*. Proc. R. Soc. Lond., B. 193:31–44.

Meka, J. M., and F. J. Margraf.
2007. Using a bioenergetic model to assess growth reduction from catch-and-release fishing and hooking injury in rainbow trout, Oncorhynchus mykiss. Fish. Manage. Ecol. 14:131–139.

Meyer-Rochow, V. B.
1994. Light-induced damage to photoreceptors of spiny lobsters and other crustaceans. Crustaceana 67:95–109.

Morgan, M. J., C. E. Wilson, and L. W. Crim.
1999. The effect of stress on reproduction in Atlantic cod. J. Fish Biol. 54:477–488.

Ryer, C. H.
2002. Trawl stress and escapee vulnerability to predation in juvenile walleye pollock: is there an unobserved bycatch of behaviorally impaired escapees? Mar. Ecol. Prog. Ser. 232:269–279.
2004. Laboratory evidence for behavioural impairment of fish escaping trawls: a review. ICES J. Mar. Sci. 61:1157–1164.

Sokal, R. R., and F. J. Rohlf.
1969. Biometry, 776 p. W.H. Freeman and Co., San Francisco, CA.
Stoner, A. W.
2003. Hunger and light level alter response to bait by Pacific halibut: laboratory analysis of detection, location, and attack. J. Fish Biol. 62:1176–1193.
Trumble, R. J., G. H. Williams, and S. E. Hughes.
1995. Methods to improve survival of Pacific halibut bycatch discarded from a factory trawler. *In* Proceedings of the international symposium on North Pacific flatfish. Alaska Sea Grant College Program Rep. AK-SG-95-04, p. 591–610, Univ. Alaska Fairbanks, Fairbanks, AK.
Warrant, E. J.
1999. Seeing better at night: life style, eye design and the optimum strategy of spatial and temporal summation. Vision Res. 39:1611–1630.
Wu, J., S. Seregard, and P. V. Algvere.
2006. Photochemical damage of the retina. Surv. Ophthalmol. 51:461–481.

Acknowledgment of reviewers

The editorial staff of the *Fishery Bulletin* would like to acknowledge the scientists who reviewed manuscripts during 2016–17. Their contributions have helped ensure the publication of quality science.

Antonio Agüera
Carmen Alejo-Plata
Jahson Alemu
Michael Allen
Matthew Altenritter
Rebecca Anderson
Mayumi Arimitsu
Alexander Arkhipkin
Anibal Aubone

Robin Baird
Alistair Becker
Rhett Bennett
Joanna Borucinska
Shannon Bower
J. Matias Braccini
Patricia Brandes
Richard Brill
Lyle Britt
Richard Brodeur
Omri Bronstein
Stephen Brouwer
Nancy Brown-Peterson

Noel Cadigan
Gregor Cailliet
Steven Campana
Matthew Campbell
Jie Cao
Christian Capapé
John Carlson
James Carretta
Jose Castro
Leonardo Castro
Joshua Chamberlin
R. Christopher Chambers
Corrado Costa
Eudriano Costa
Paul Cowley
Kevin Craig
Nancie Cummings

Mike Dadswell
Luciano Dalla Rosa
Heather Dawson
Michael Domeier

Thomas Ebert
Keith Evans

Mary Fabrizio
Atle Foss
Chris Francis
James Franks
Emmanuel Frimpong
Rainer Froese

Austin Gallagher
Felipe Galván-Magaña
Konstantinos Ganias
Bruno Gianasi
John Gold
Jim Gower
Romana Gračan
John Graves
Correigh Greene
Vincent Guida
Simon Gulak
Christopher Gurshin

Toshihide Hamazaki
Owen Hamel
Nils Handegard
Jon Hare
Ian Harrison
Alastair Harry
Deborah Hart
Sean Hayes
Melissa Head
Mikko Heino
Gerald Hoff
Eric Hoffmayer
Christine Huffard
Peter Hulson

Abua Ikem

Barbara Javor
J. Michael Jech
Malcom Jobling
Catherine Johnston
Shoou-Jeng Joung

J. Kohl Kanwit
James Kennedy
David Kerstetter
Nikolai Klibansky
Amy Knowlton
Alexandros Kokkalis
Syd Kraul
Boyd Kynard

Tom Laidig
John Lawrence
Francisco Leitão
P. Michael Link
Brian Linton
Timothy Loher
Susan Lowerre-Barbieri

Marc Mangel
Unai Markaida
Rodrigo Martins
Philip Matich
Craig Matkin
Francesc Maynou Hernández
Rich McBride
Rick Methot
Erlend Moksness
Henry Mollet
Megan Moore
Enrique Morales-Bojórquez
Kentaro Morita
Andrew Muir
Bruce Mundy
Bob Murphy
Michael Musyl

Joacim Näslund
Atsushi Nanami
Keith Nislow
Cormac Nolan
Jerrold Norton

Derek Ogle
Barry O'Neill
Yoshioki Oozeki
Mauricio Oritz

José Pajuelo
Miquel Palmer
Kevin Piner
Jodi Pirtle
Michael Prager
Steven Purcell

David Richardson
Rick Rideout
Rubén Roa-Ureta
Cara Rodgveller
G. Curtis Roegner
Maria Roldán
Evgeny Romanov

Craig Rose

Yvonne Sadovy de Mitcheson
David Sampson
Bernd Schöne
David Schneider
Amy Schueller
Andrew Seitz
Chugey Sepulveda
Burton Shank
Andrew Shelton
Peter Shelton
Gary Shepherd
Graham Sherwood
Kate Siegfried
Douglas Sigourney
Colin Simpfendorfer
Michael Simpkins
David Smith
Stephen Smith
Dave Somerton
Ingrid Spies
Dale Squires
Duane Stevenson
Ian Stewart
Kevin Stokesbury
Christoph Stransky
James Sulikowski

Brett Taylor
Fabrice Teletchea
Todd Tenbrink
Steven Teo
Grant Thompson
James Thorson
M. Veronica Toral-Granda
Verena Trenkel
Marc Trudel
Robert Trumble
M. Kurtis Trzcinski
Sara Turner Cooper
Victor Tuset

S. Sebastian Uhlmann
Joseph Urban

Jon Vølstad
Dráusio Véras
Jaap van der Meer
Kray Van Kirk
Jeremy Vaudo
Gabriel Vianna

Richard Wahle
John Walter
Jessica Ward
David Welch
Bradley Wetherbee
Rebecca Whitlock
Andreas Winter

Daniel Yeoh
Mary Yoklavich

Yisen Zhong
Mitchell Zischke
Gayle Zydlewski

Fishery Bulletin

Guidelines for authors

Contributions published in *Fishery Bulletin* describe original research in marine fishery science, fishery engineering and economics, as well as the areas of marine environmental and ecological sciences (including modeling). Preference will be given to manuscripts that examine processes and underlying patterns. Descriptive reports, surveys, and observational papers may occasionally be published but should appeal to an audience outside the locale in which the study was conducted.

Although all contributions are subject to peer review, responsibility for the contents of papers rests upon the authors and not on the editor or publisher. *Submission of an article implies that the article is original and is not being considered for publication elsewhere.*

Plagiarism and double publication are considered serious breaches of publication ethics. To verify the originality of the research in papers and to identify possible previous publication, manuscripts may be screened with plagiarism-detection software.

Manuscripts must be written in English; authors whose native language is not English are strongly advised to have their manuscripts checked by English-speaking colleagues before submission.

Once a paper has been accepted for publication, online publication takes approximately 3 weeks.

There is no cost for publication in *Fishery Bulletin*.

Types of manuscripts accepted by the journal

Articles generally range from 20 to 30 double-spaced typed pages (12-point font) and describe an original contribution to fisheries science, engineering, or economics. Tables and figures are not included in this page count, but the number of figures should not exceed one figure for every four pages of text. Articles contain the following divisions: abstract, introduction, methods, results, and discussion.

Short contributions are generally less than 15 double spaced typed pages (12-point font) and, like articles, describe an original contribution to fisheries science. They follow the same format as that for articles: abstract, introduction, results and discussion, but the results and discussion sections may be combined. They are distinguished from full articles in that they report a noteworthy new observation or discovery—such as the first report of a new species, a unique finding, condition, or event that expands our knowledge of fisheries science, engineering or economics—and do not require a lengthy discussion.

Companion articles are presented together and published together as a scientific contribution. Both articles address a closely related topic and may be articles that result from a workshop or conference. They must be submitted to the journal at the same time.

Review articles generally range from 40 to 60 double-spaced typed pages (12-point font) and address a timely topic that is relevant to all aspects of fisheries science. They should be forward thinking and address novel views or interpretations of information that encourage new avenues of research. They can be reviews based on the outcome from thematic workshops, or contributions by groups of authors who want to focus on a particular topic, or a contribution by an individual who chooses to review a research theme of broad interest to the fisheries science community. A review article will include an abstract, but the format of the article per se will be up to the authors. Please contact the Scientific Editor to discuss your ideas regarding a review article before embarking on such a project.

Preparation of manuscript

Title page should include authors' full names, mailing addresses, and the senior author's e-mail address.

Abstract should be limited to 200 words (one-half typed page), state the main scope of the research, and emphasize the authors conclusions and relevant findings. Do not review the methods of the study or list the contents of the paper. Because abstracts are circulated by abstracting agencies, it is important that they represent the research clearly and concisely.

General text must be typed in 12-point Times New Roman font throughout. A brief introduction should convey the broad significance of the paper; the remainder of the paper should be divided into the following sections: Materials and methods, Results, Discussion, and Acknowledgments. Headings within each section must be short, reflect a logical sequence, and follow the rules of subdivision (i.e., there can be no subdivision without at least two subheadings). The entire text should be intelligible to interdisciplinary readers; therefore, all acronyms, abbreviations, and technical terms should be written out in full the first time they are mentioned. Abbreviations should be used sparingly because they are not carried over to indexing databases and slow readability for those readers outside a discipline. They should never be used for the main subject (species, method) of a paper.

For general style, follow the U.S. *Government Printing Office Style Manual* (2008) [available at website] and *Scientific Style and Format: the CSE Manual for Authors, Editors, and Publishers* (2014, 8th ed.) published by the Council of Science Editors. For scientific nomenclature, use the current edition of the American Fisheries Society's *Common and Scientific Names of*

Fishes from the United States, Canada, and Mexico and its companion volumes (*Decapod Crustaceans, Mollusks, Cnidaria and Ctenophora*, and *World Fishes Important to North Americans*). For species not found in the above mentioned AFS publications and for more recent changes in nomenclature, use the Integrated Taxonomic Information System (ITIS) (available at website), or, secondarily, the California Academy of Sciences *Catalog of Fishes* (available at website) for species names not included in ITIS. Common (vernacular) names of species should be lowercase. Citations must be given of taxonomic references used for the identification of specimens. For example, "Fishes were identified according to Collette and Klein-MacPhee (2002); sponges were identified according to Stone et al. (2011)."

Dates should be written as follows: 11 November 2000. Measurements should be expressed in metric units, e.g., 58 metric tons (t); if other units of measurement are used, please make this fact explicit to the reader. Use numerals, not words, to express whole and decimal numbers in the general text, tables, and figure captions (except at the beginning of a sentence). For example: We considered 3 hypotheses. We collected 7 samples in this location. Use American spelling. Refrain from using the shorthand slash (/), an ambiguous symbol, in the general text.

Word usage and grammar that may be useful are the following:

- *Aging* For our journal, the word *aging* is used to mean both age determination and the aging process (senescence). Authors should make clear which meaning is intended where ambiguity may arise.

- *Fish and fishes* For papers on taxonomy and biodiversity, the plural of *fish* is *fishes,* by convention. In all other instances, the plural is *fish.*

  Examples:
  The fishes of Puget Sound [biodiversity is indicated];
  The number of fish caught that season [no emphasis on biodiversity];
  The fish were caught in trawl nets [no emphasis on biodiversity].
  The same logic applies to the use of the words *crab* and *crabs, squid* and *squids,* etc.

- *Sex* For the meaning of male and female, use the word *sex*, not *gender.*

- *Participles* As adjectives, participles must modify a specific noun or pronoun and make sense with that noun or pronoun.

  Incorrect:
  Using the recruitment model, estimates of age-1 recruitment were determined. [Estimates were not using the recruitment model.]

  Correct:
  Using the recruitment model, we determined age-1 estimates of recruitment. [The participle now modifies the word *we,* i.e., those who were using the model.]

  Incorrect:
  Based on the collected data, we concluded that the mortality rate for these fish had increased. [*We* were not based on the collected data.]

  Correct:
  We concluded, on the basis of the collected data, that the mortality rate for these fish had increased. [Eliminate the participle and replace it with the adverbial phrase *on the basis of.*]

Equations and mathematical symbols should be set from a standard mathematical program (MathType) and tool (Equation Editor in MS Word). LaTex is acceptable for more advanced computations. For mathematical symbols in the general text (α, χ^2, π, $\pm$, etc.), use the symbols provided by the MS Word program and italicize all variables, except those variables represented by Greek letters. Do not use photo mode when creating these symbols in the general text and do not cut and paste equations and letters or symbols of variables from a different software program.

Number equations (if there are more than 1) for future reference by scientists; place the number within parentheses at the end of the first line of the equation.

Literature cited section comprises published works and those accepted for publication in peer-reviewed journals (in press). Follow the name and year system for citation format in the "Literature cited" section (that is to say, citations should be listed alphabetically by the authors' last names, and then by year if there is more than one citation with the same authorship. A list of abbreviations for citing journal names can be found at website.

Authors are responsible for the accuracy and completeness of all citations. Literature citation format: Author (last name, followed by first-name initials). Year. Title of article. Abbreviated title of the journal in which it was published. Always include number of pages. For a sequence of citations in the general text, list chronologically: (Smith, 1932: Green. 1947; Smith and Jones, 1985).

Acknowledgments should be no more than 6 lines of text. Only those who have contributed in an outstanding way should be acknowledged by name. For recognition of other persons or groups, use a general term, such as "crew," "observers," "research coordinators," and do not include names with these terms.

Digital object identifier (doi) code ensures that a publication has a permanent location online. Doi code should be included at the end of citations of published litera-

ture. Authors are responsible for submitting accurate doi codes. Faulty codes will be deleted at the page-proof stage.

Cite all software, special equipment, and chemical solutions used in the study within parentheses in the general text: e.g., SAS, vers. 6.03 (SAS Inst., Inc., Cary, NC).

Footnotes are used for all documents that have not been formally peer reviewed and for observations and personal communications. These types of references should be cited sparingly in manuscripts submitted to the journal.

All reference documents, administrative reports, internal reports, progress reports, project reports, contract reports, personal observations, personal communications, unpublished data, manuscripts in review, and council meeting notes are footnoted in 9 pt font and placed at the bottom of the page on which they are first cited. Footnote format is the same as that for formal literature citations. A link to the online source (e.g., [http://www/..... , accessed July 2007.]), or the mailing address of the agency or department holding the document, should be provided so that readers may obtain a copy of the document.

Tables are often overused in scientific papers; it is seldom necessary to present all the data associated with a study. Tables should not be excessive in size and must be cited in numerical order in the text. Headings should be short but ample enough to allow the table to be intelligible on its own.

All abbreviations and unusual symbols must be explained in the table legend. Other incidental comments may be footnoted with italic numeral footnote markers. Use asterisks only to indicate significance in statistical data. Do not type table legends on a separate page; place them above the table data. *Do not submit tables in photo mode.*

- Notate probability with a capital, italic *P*.
- Provide a zero before all decimal points for values less than one (e.g., 0.07).
- Round all values to 2 decimal points.
- Use a comma in numbers of five digits or more (e.g., 13,000 but 3000).

Figures must be cited in numerical order in the text. Graphics should aid in the comprehension of the text, but they should be limited to presenting patterns rather than raw data. Figures should not exceed one figure for every four pages of text and must be labeled with the number of the figure. Place labels **A, B, C,** etc. within the upper left area of graphs and photos. Avoid placing labels vertically (except for the y axis).

Figure legends should explain all symbols and abbreviations seen in the figure and should be double-spaced on a separate page at the end of the manuscript.

Line art and halftone figures should be saved at a resolution of >800 dpi (dots per inch) and >300 dpi, respectively. Color is allowed in figures to show morphological differences among species (i.e., for species identification), to show stain reactions, and to show gradations, such as those of temperature and salinity within maps. Color is discouraged in graphs. For the few instances where color is allowed, the use of color will be determined by the Managing Editor. Figures approved for color should be saved in CMYK format.

All figures must be submitted as either PDF of EPS files.

- Capitalize the first letter of the first word in all labels within figures.
- Do not use overly large font sizes in maps and for axis labels in graphs.
- Do not use bold fonts or bold lines in figures.
- Do not place outline rules around graphs.
- Place a North arrow and label degrees latitude and longitude (e.g., 170°E) in all maps.
- Use symbols, shadings, or patterns (not clip art) in maps and graphs.

Supplementary materials that are considered essential, but are too large or impractical for inclusion in a paper (e.g., metadata, figures, tables, videos, websites), may be provided at the end of an article. These materials are subject to the editorial standards of the journal. A URL to the supplementary material and a brief explanation for including such material should be sent at the time of initial submission of the paper to the journal.

- **Metadata, figures, and tables** should be submitted in standard digital format (Word docx) and should be cited in the general text as (Suppl. Table, Suppl. Fig., etc.).
- **Websites** should be cited as (Suppl. website) in the general text and be made available with doi code (if possible) at the end of the article.
- **Videos** must not be larger than 30 MB to allow a swift technical response for viewing the video. Authors should consider whether a short video uniquely captures what text alone cannot capture for the understanding of a process or behavior under examination in the article. Supply an online link to the location of the video.

Copyright law does not apply to *Fishery Bulletin,* which falls within the public domain. However, if an author reproduces any part of an article from *Fishery Bulletin*, reference to source is considered correct form (e.g., Source: Fish. Bull. 97:105).

Failure to follow these guidelines and failure to correspond with editors in a timely manner will delay publication of a manuscript.

Submission of manuscript

Submit manuscript online at the ScholarOne website. Commerce Department authors should submit papers under a completed NOAA Form 25-700. For further details on electronic submission, please contact the Associate Editor, Kathryn Dennis, at

kathryn.dennis@noaa.gov

When requested, the text and tables should be submitted in Word format. Figures should be sent as separate PDF or EPS files. Send a copy of figures in the original software if conversion to any of these formats yields a degraded version of the figure.

Questions? If you have questions regarding these guidelines, please contact the Managing Editor, Sharyn Matriotti, at

sharyn.matriotti@noaa.gov

Questions regarding manuscripts under review should be addressed to Kathryn Dennis, Associate Editor.

Fishery Bulletin

Subscription form

Superintendent of Documents **Publications** Order Form

*5178

☐ YES, please send me the following publications:

____ Subscriptions to *Fishery Bulletin*
for $32.00 per year ($44.80 foreign)

The total cost of my order is $ _____ . Prices include regular domestic postage and handling and are subject to change.

_____
(Company or Personal Name) (Please type or print)

_____
(Additional address/attention line)

_____
(Street address)

_____
(City, State, ZIP Code)

_____
(Daytime phone including area code)

_____
(Purchase Order No.)

Charge your order. IT'S EASY!

VISA

MasterCard

Please Choose Method of Payment:

☐ Check payable to the Superintendent of Documents
☐ GPO Deposit Account ☐☐☐☐☐☐☐–☐
☐ VISA or MasterCard Account
☐☐☐☐☐☐☐☐☐☐☐☐☐☐☐☐
☐☐☐☐ (Credit card expiration date)

To fax your orders (202) 512-2104

_____
(Authorizing Signature)

Mail to: Superintendent of Documents
P.O. Box 979050, St. Louis, Missouri 63197
Tel. no. (U.S. callers): 866-512-1800
Tel. no. (International callers): 1-202-512-1800

Thank you for your order!

Also available online at
http://bookstore.gpo.gov/actions/GetPublication.do?stocknumber=703-023-00000-2
email: ContactCenter@gpo.gov